UNIVERSITY OF OKLAHOMA

GRADUATE COLLEGE

NEUROCHEMICAL AND IMMUNOHISTOCHEMICAL EFFECTS INDUCED BY THE 1-METHYL-4-PHENYLPYRIDINIUM ANIMAL MODEL OF PARKINSON'S DISEASE: AN *IN VIVO* MICRODIALYSIS INVESTIGATION IN FREELY-MOVING RATS

A Dissertation

SUBMITTED TO THE GRADUATE FACULTY

in partial fulfillment of the requirements for the

degree of

Doctor of Philosophy

By

STEVEN B. FOSTER

Norman, Oklahoma

2003

ProQuest Information and Learning Company
300 North Zeeb Road
P.O. Box 1346
Ann Arbor, MI 48106-1346

NEUROCHEMICAL AND IMMUNOHISTOCHEMICAL EFFECTS INDUCED BY THE 1-METHYL-4-PHENYLPYRIDINIUM ANIMAL MODEL OF PARKINSON'S DISEASE: AN *IN VIVO* MICRODIALYSIS INVESTIGATION IN FREELY-MOVING RATS

A Dissertation APPROVED FOR THE
DEPARTMENT OF CHEMISTRY AND BIOCHEMISTRY

BY

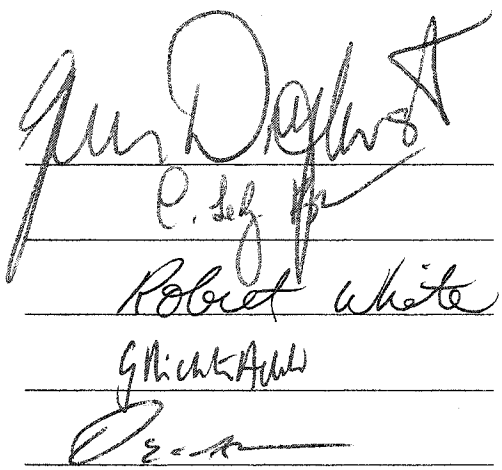

Acknowledgements

"If I have seen further, it is because I have stood on the shoulders of giants." This quote from Sir Issac Newton best describes how I feel about Dr. Glenn Dryhurst. I will forever be grateful for the time we have spent together. Thank you for mentoring me, sharing your knowledge of science and for tolerating me. I could not have chosen a better place to study.

Linda Chapman, my partner and soul mate. All I really need in life is you, plenty of snacks and Sterling. This journey that we both began back in 1994, is soon to come to a conclusion. You are my motivation in life. Maybe now we can have some time to smell the roses.

There are many people in my family that I want to thank. Many of you have seen me through the good and bad times. I love you all. Most importantly my mother Rebecca, my father Stan, my brother Andrew, my daughters Stacy and Tracy, and my mother-in-law Teresa, my uncles Don, Bart and Jerry, my aunts Pat, Gwen, Janice and Gloria.

I want to especially thank Dr. Monika Wrona. Thank you for sharing your knowledge of science and life. Most importantly, thank you for being my friend. My journey has been enriched by your presence.

Many thanks to my Graduate Committee: Professors C. LeRoy Blank, Robert L. White, George B. Richter-Addo, and Donald A. Wilson. Special thanks to Professor Roland E. Lehr who is greatly missed. Many other professors have been important in my time here including Professors Ken Miller, Paul Cook, Ron Halterman and Richard Taylor. I would like to thank the post-docs who shared their experience and wonderful

food Drs. Jilin Han, Hong Li and Xiangrong Jiang. Thanks to Dandan Li for all her care. Hiawang Tang should be acknowledged for help in analyzing dialysate for amino acids.

Many of the people at WOSC, I hold near and dear. I would like to thank Elizabeth Wallace, Mike Tucker, Glyna Olson, Art Jantz, Thad Crosnoe and Randy Cumby for everything all of you did back in those early years.

Without the help of Dean, John and Carl of the Electronics Shop this dissertation would have been more appropriately labeled: "How to Fix Research Equipment." Thank you gentlemen. Many thanks to the Department of Chemistry and Biochemistry Staff: Teresa Hackney, Arlene Crawford, Bobby Collins, Laura Cornell, Susan Lauderbach and Analytical Services. I would like to thank Scott Zerger for taking care of the animals and for being there to listen to me for all these years.

My friends outside the department are very important in my life. They know what unconditional love is about. I am grateful to have friends like these. Thank you Mary Jane Rutherford, Greg Grindle, Justin Lenox, Bruce Lloyd, Phil Gilstrap, Valli Powell, Sue Davis, Paul Willis, Meg Moore and Wendy Galbraith. There are many friends in the department who have been there for my times in the air and on the ground. Thank you Whitney Smith, Karen and Rob Johnson and Gary Smith for your friendship.

Thank God for giving me another chance to do what I always wanted to do.

Finally none of this would have been possible without
the wisdom and love of three guys:
Bill, Bob and Bryce

This is dedicated to those I love:

my partner,

Linda J. Chapman

my mother,

Rebecca A. Foster

my father,

Stanley L. Foster

my brother,

Andrew K. Foster

our buddy,

Sterling

Table of Contents

Chapter Three

The Effects of Antioxidants and Confirmation of L-DOPA

Chapter Five

Microdialysis Study of MPP^+-Induced Alterations in Extracellular Amino Acid Levels

Chapter Six

Immunohistochemistry

List of Tables

List of Figures

Figure **page**

Figure **page**

Figure **page**

Neurochemical

List of Abbreviations

ABC	avidin-biotin-peroxidase complex
aCSF	artificial cerebral spinal fluid
ACV	acivicin
AMPA	α-amino-3-hydroxy-5-methylisoxazole-4-propionic acid
ApN	aminopeptidase N
Asp	aspartate
ATP	adenosine 5'-triphosphate
BSA	bovine serum albumin
BT	benzothiazine
CNS	central nervous system
COMT	catechol-*O*-methyltransferase
Cox-2	cyclooxygenase type 2
CSF	cerebral spinal fluid
Cys	cysteine
5-*S*-Cys-DA	5-*S*-cysteinyldopamine
2,5-di-*S*-Cys-DA	2,5-di-*S*-cysteinyldopamine
CysGly	cysteinylglycine
DA	dopamine
DAB	3,3'-diaminobenzidine
DAQ	dopamine quinone
DAT	dopamine transporter

DDC	L-DOPA decarboxylase
2,3-DHBA	2,3-dihydroxybenzoic acid
2,5-DHBA	2,5-dihydroxybenzoic acid
DHBT	dihydroxybenzothiazine
DOPAC	3,4-dihydroxyphenylacetic acid
DP	dipeptidase
DTT	dithiothreitol
EC	electrochemical detection
EMTs	extraneuronal monoamine transporters
ESI-MS	electrospray ionization mass spectrometry
FBS	fetal bovine serum
GFAP	glia fibrillary acidic protein
GLT-1	glutamate transporter-1
Glu	glutamate
γ-Glu-GSH	γ-glutamylglutathione
Gly	glycine
5-*S*-GS-DA	5-*S*-glutathionyldopamine
2,5-di-*S*-GS-DA	2,5-di-*S*-glutathionyldopamine
2,5,6-tri-*S*-GS-DA	2,5,6-tri-*S*-glutathionyldopamine
5-*S*-GS-DOPAC	5-*S*-glutathionyl-3,4-dihydroxyphenylacetic acid
2,5-di-*S*-GS-DOPAC	2,5-di-*S*- glutathionyl-3,4-dihydroxyphenylacetic acid
GSH	glutathione
GSSG	glutathione disulfide

γ-GT	γ-glutamyl transpeptidase
H_2O_2	hydrogen peroxide
6-HDA	6-hydroxydopamine
5-HIAA	5-hydroxyindole-3-acetic acid
HO·	hydroxyl radical
HPLC	high performance liquid chromatography
5-HT (serotonin)	5-hydroxytryptamine
HVA	homovanillic acid
i.p.	intra-peritoneal
IL-1β	interleukin-1β
iNOS	inducible nitric oxide synthase
α-KGDH	α-ketoglutarate dehydrogenase
L-DOPA	L-3,4-dihydroxyphenylalanine
MA	methamphetamine
MAO	monoamine oxidase
MDMA (ecstasy)	3,4-methylenedioxymethamphetamine
MPP^+	1-methyl-4-phenylpyridinium
MPTP	1-methyl-4-phenyl-1,2,3,6-tetrahydropyridine
MRP-1	multidrug resistance protein-1
mt	mitochondrial
3-MT	3-methoxytyramine
NE	norepinephrine
NGS	normal goat serum

NHS	normal horse serum
3-nitro-Tyr	3-nitrotyrosine
4-nitro-Phe	4-nitrophenylalanine
NMDA	*N*-methyl-D-aspartate
nNOS	neuronal nitric oxide synthase
$NO\cdot$	nitric oxide
$O_2^{-}\cdot$	superoxide
$ONOO^-$	peroxynitrite
PARP	poly(ADP-ribose)polymerase
PBS	phosphate buffered saline
PD	Parkinson's disease
PDA	photodiode array
PDHC	pyruvate dehydrogenase complex
PET	positron emission tomography
PGE_2	prostaglandin E_2
Phe	phenylalanine
PLP	pyridoxal 5'-phosphate
PVP	polyvinylpyrrolidone
RNS	reactive nitrogen species
ROS	reactive oxygen species
SA	salicylate
SCE	saturated calomel electrode
SERT	serotonin transporter

SN_{pc}	substantia nigra pars compacta
SOD	superoxide dismutase
Tau	taurine
TH	tyrosine hydroxylase
TNF-α	tumor necrosis factor-α
TPH	tryptophan hydroxylase
t_R	chromatographic retention time
Tyr	tyrosine
UV-VIS	ultraviolet-visible
VMAT-2	vesicular monoamine transporter-2

Abstract

Parkinson's disease (PD) is a neurodegenerative disorder which afflicts more than 1 million Americans with an estimated 50,000 new diagnoses each year. 1-methyl-4-phenyl-1,2,3,6-tetrahydropyridine (MPTP) causes parkinsonian symptoms in humans, and in animals most faithfully mimics the chemical, pathological and immunohistological features of idiopathic PD. In the nigrostriatal pathway, MPTP evokes selective degeneration of dopamine (DA) neurons in the substantia nigra pars compacta (SN_{pc}). Dopaminergic neurons project their axons into the striatum where MPTP induces a loss of DA and degeneration of dopaminergic terminals. Perfusion of neurotoxic concentrations of 1-methyl-4-phenylpyridinium (MPP^+; the active metabolite of MPTP) into the rat striatum reversibly inhibits mitochondrial (mt) complex I and, hence, causes a transient ATP energy impairment leading to activation of *N*-methyl-D-aspartate (NMDA) receptors, a massive release of DA and a rise in the extracellular concentrations of glutathione (GSH) and cysteine (Cys). Elevated extracellular levels of Cys along with glutamate (Glu) and glycine (Gly) evoked by MPTP/MPP^+ may primarily originate from degradation of GSH by γ-glutamyl transpeptidase (γ-GT) and dipeptidases.

Reactive oxygen species (ROS) and reactive nitrogen species (RNS) have been implicated in MPP^+-induced neurotoxicity, although, whether these ROS/RNS are generated extracellularly and/or intracellular is unknown. Increased extracellular levels of ROS/RNS should react with MPP^+-mediated elevated extracellular concentrations of DA, GSH and Cys to form glutathionyl and cysteinyl conjugates of DA along with characteristic disulfides. Once the MPP^+-induced energy impairment subsides, NMDA receptors should remain activated by elevated concentrations of Glu and, hence, there

should be a continued production of intraneuronal ROS/RNS. Increased ATP production should also mediate membrane repolarization and, hence, DA should be transported back into dopaminergic neurons by the dopamine transporter (DAT) where DA should be oxidized by ROS/RNS to dopamine quinone (DAQ), which is by itself a dopaminergic neurotoxin. However, most of the DAQ could react with translocated Cys forming 5-*S*-cysteinyldopamine. The latter could lead to formation of dihydroxybenzothiazine (DHBT) and benzothiazine (BT) metabolites which have been shown previously to be mitochondrial toxins *in vitro* and, thus result in dopaminergic cell death. Based on the preceding ideas it follows that inhibition of γ-GT (by acivicin; ACV) should afford protection from eventual dopaminergic cell death by inhibiting the degradation of GSH to Glu, Cys and Gly. Thus, as the MPP^+-induced energy impairment subsides Glu should not be elevated sufficiently to continue activation of NMDA receptors and, therefore, elevated intraneuronal production of ROS/RNS would cease. Therefore, the DA transported back into dopamine neurons would not be oxidized and elevated Cys would not be available and, hence, DHBT/BTs should not be formed.

In the present microdialysis study, neurotoxic concentrations of MPP^+ were perfused into rat striatum and dialysate was analyzed. However, extracellular markers of ROS/RNS were not detected in the presence or absence of coperfused ACV. Inhibition of γ-GT was not neuroprotective to DA neurons and had no significant effect on the MPP^+-mediated rise of extracellular concentrations of Glu, Cys and Gly. Immunohisto-chemical studies of the striatum in the area around the probe conducted 24 h after MPP^+ perfusions showed that with increasing concentrations of MPP^+ there was a

corresponding increase in DA terminal damage, loss of astrocytes, formation of reactive microglia and cell death.

Perfusion of MPP^+ evoked the neurotransmitter-like release of L-3,4-dihydroxy-phenylalanine (L-DOPA) which was also detected in dialysate from experiments in which rats received neurotoxic doses of methamphetamine or 3,4-methylenedioxymeth-amphetamine. The antioxidants mannitol and salicylate had no effect on the MPP^+-mediated rise of extracellular concentrations of L-DOPA. Instead, the latter was found to be the result of (*in vivo* not *in vitro*) MPP^+-induced inhibition of L-DOPA decarboxylase (DDC). L-DOPA can mediate Glu release, as well as being an excitotoxin itself. Furthermore, previous studies suggest that treatment of PD symptoms with L-DOPA may exacerbate nigrostriatal dopamine degeneration. Nevertheless, the results from the present study suggest that DDC inhibition with subsequent L-DOPA release may play a role in MPP^+-induced neurotoxicity and, because of the similarities of MPTP/MPP^+-induced neurotoxicity and PD, may be an early event in PD.

Chapter One

Introduction

A. Parkinson's disease

Parkinson's disease (PD) is a neurodegenerative brain disorder which afflicts more than 1 million Americans with an estimated 50,000 new diagnoses each year.[1] In 1817, James Parkinson first described this disorder in his book "An Essay on the Shaking Palsy."[2] In this book Parkinson described the physical manifestations of PD which include tremor, muscular rigidity, bradykinesia and simian posture. The reasons for these physical abnormalities stems from the loss of striatal dopamine (DA) consequent to the degeneration of DA neurons in the substantia nigra pars compacta (SN_{pc}),[3,4] which are essential for motor functions. Dopaminergic neurons located in the SN_{pc} project their axon terminals into the striatum. Clinical signs of PD do not become apparent until approximately 80% of DA has been lost from the striatum.[5,6] A characteristic neuropathological feature of PD is the presence of Lewy bodies in the remaining neurons of the SN_{pc}. Lewy bodies are cytoplasmic inclusions composed of α-synuclein,[7] ubiquitin, neurofilaments[8] and Cu/Zn SOD.[9] The mechanisms which produce Lewy bodies and cause the destruction of dopaminergic neurons in the SN_{pc} are not understood. PD neurodegeneration also affects other neuronal systems (although to a much lesser extent than the loss of DA neurons) as evidenced by reports in PD of decreased levels of 5-hydroxytryptamine (5-HT; serotonin)[3,10,11] and norepinephrine (NE)[12] and degeneration

of cholinergic[13,14] and noradrenergic neurons.[10,15,16] There is no cure for PD, however, treatment with a combination of L-3,4-dihydroxyphenylalanine (L-DOPA; the precursor to DA) and a peripheral dopa decarboxylase (DDC; decarboxylates L-DOPA to DA) inhibitor (e.g., carbidopa) temporarily relieves clinical symptoms. However, this treatment ultimately causes negative side effects including dyskinesias, involuntary motor fluctuations and psychosis.[17,18] Controversy exits that L-DOPA/carbidopa therapy could exacerbate the destruction of SN_{pc} cell death,[19] and indeed, neurodegeneration is not halted by treatment.[20,21] Patients with PD can live for 20 years or more, but the average life span after diagnosis is 12 years. Death rates are approximately 1.6 times greater than normal individuals of the same age,[22] usually resulting from choking, decreased mobility, physical damage from constant falls or from an unrelated illness.[23]

The pathobiochemical changes that are observed in the SN_{pc} of PD individuals include decreased activity of α-ketoglutarate dehydrogenase (α-KGDH)[24] and mitochondrial (mt) complex I[25] but not mt complexes II-IV. Oxidative stress is evident in advanced PD as evidenced by increased oxidation products of lipids,[26] proteins,[27] DNA and RNA.[28] Activities of cytoplasmic and mt superoxide dismutase (SOD) are increased,[29] perhaps implying an effect induced by increased levels of intracellular superoxide ($O_2^{-}\cdot$). Nigral iron levels are increased.[30] There is a massive decrease in the antioxidant glutathione (GSH) without a corresponding increase in glutathione disulfide (GSSG).[30-32] In fact, decreased levels of GGSG have been observed in the cerebral spinal fluid (CSF) of PD patients.[33] $O_2^{-}\cdot$ itself is not considered directly neurotoxic, but is believed to lead to production of tissue damaging hydroxyl radical ($HO\cdot$) by Fenton and/or Haber-Weiss reactions.[34] Additionally, the role of reactive nitrogen species

(RNS) in PD has become apparent with the observation of elevated levels of 3-nitrotyrosine (3-nitro-Tyr) in the proteins that comprise Lewy bodies in surviving SN_{pc} neurons of PD patients.[35] $O_2^{-\cdot}$ can readily react with nitric oxide ($NO\cdot$) to form peroxynitrite ($ONOO^-$) which can decompose at physiological pH to $HO\cdot$.[36] $ONOO^-$ itself is highly reactive and can lead to oxidation and nitration of DNA,[37] lipids[38] and proteins.[39]

Aging is the biggest risk factor for acquiring PD.[20,40] As people age there is resulting compromised brain glucose utilization,[41] decreased mt function[42-44] and energy metabolism[45] and disruption of Ca^{2+} homeostasis.[46-48] The DA cell bodies in the SN_{pc} are characteristically pigmented with dark brown neuromelanin formed from autoxidation[49,50] and/or enzymatic oxidation of DA.[51,52] With normal aging there is a slow loss of the SN_{pc} neurons[53] with the most heavily pigmented neurons dying first. However, the opposite happens in PD where the least pigmented neurons are lost first.[54-56]

Familial PD is rare and genetic studies have produced conflicting observations.[40] However, a genetic predisposition to an environmental toxin may underlie the source of idiopathic PD.[57,58] Along with this, advanced age could potentiate the susceptibility to toxins since impaired xenobiotic metabolism is associated with aging.[59] Numerous epidemiological studies have shown an increase in PD with repeated exposure to environmental toxins.[57,60-63] For example, the insecticides dieldrin and lindane have been found in the SN_{pc} of PD patients,[64,65] and *in vitro* dieldrin is a selective DA neurotoxin. Trichloroethylene[66], hindered amines[67], CN^-[68] and iron[69] have been linked to development of PD or a parkinsonian syndrome, and cause degeneration of nigrostriatal DA neurons in animals.[66,67,70,71] Many of these toxins[72-75] along with the dopaminergic

neurotoxins rotenone,[76] 1-methyl-4-phenyl-1,2,3,6-tetrahydropyridine (MPTP)[77] and methamphetamine (MA)[78] interfere with mt respiration and the vesicular uptake and storage of DA.[79-82]

GSH is the major antioxidant that protects neurons (and all other cells) against oxidative and nitrative stress. Neuronal GSH is maintained by its export from astrocytes,[83-85] and hence, an important function of the latter cells is to protect neurons against oxidative and nitrative stress.[86-88] Recent evidence indicates that multidrug resistance protein-1 (MRP-1) mediates most release of GSH from astrocytes and that these cells are responsible for maintaining intraneuronal GSH.[89] Neurons, however, are unable to import released astrocytic GSH. Rather, extracellular GSH is first degraded by γ-glutamyl transpeptidase (γ-GT), present on the external surface of neurons and glia,[90] forming cysteinylglycine (CysGly) which is then degraded by aminopeptidase N (ApN) to cysteine (Cys) and glycine (Gly).[91] The resultant Cys[92-94] is translocated into neurons where it is the rate-limiting substrate for GSH synthesis.[83,84,95,96] Energy-dependent mechanisms maintain intraneuronal GSH. Thus, energy impairment and depolarization of the neuronal and mt membranes induces release of both cytoplasmic and mt GSH.[97-104] In view of the preceding discussion, it is of interest that not only do nigral levels of GSH fall in PD but the activity of γ-GT is increased.[105] This raises the possibility that the fall of GSH in PD may be the result of its release from SN_{pc} cells[106] in response to an energy impairment and also, because the fall is so large, from surrounding astrocytes, followed by its extracellular degradation by γ-GT/ApN.

The elevation of 5-*S*-cysteinyldopamine (5-*S*-Cys-DA)/DA concentration ratio seen in the SN_{pc} of PD patients[107,108] could be the result of increased levels of Cys

(normally present in the brain at low concentrations) and DA. The increase in Cys suggests a correlation to the decrease in nigral GSH and an increase in γ-GT activity as a result of γ-GT/DP degradation of nigral GSH. Increased intraneuronal $O_2^{-\cdot}$ with resultant $ONOO^-$ generation could oxidize DA to DAQ (without nitration)[109,110] which reacts with Cys to form 5-*S*-Cys-DA[108] (usually a minor DA metabolite).[111]

B. Animal Models of Parkinson's disease

Several animal models of PD have been developed which may mimic the human condition. The ideal model would replicate all the biochemical, histological, clinical and pathological changes seen in humans. However, no one model has thus far been able to do so. Various drugs, environmental toxins and pharmacological agents are administered to animals to replicate these changes. Among these 6-hydroxydopamine (6-HDA), MA, rotenone and MPTP are the most widely employed.[5,112]

6-HDA is a well established neurotoxin with its mode of cellular death probably due to generation of reactive oxygen species (ROS).[112] 6-HDA is unable to cross the blood-brain barrier so it is administered directly to the nigrostriatal tract, SN_{pc} or striatum,[113] where it induces dose-dependent lesions [114] of DA neurons in the SN_{pc} within 24 hours and decreased levels of DA in the striatum in 2-3 days.[114-116] Typically these experiments are conducted in rats where 6-HDA is injected into one side of the brain, inducing dose-dependent asymmetric circling behavior.[117] The unlesioned side serves as a control for tissue studies designed to analyze the 6-HDA-induced damage. These injections lead to reduced levels of GSH and SOD activity,[118] and inhibition of mt

complexes I and IV.[119] The limitations of this model are that it does not produce Lewy bodies and is specific to only dopaminergic neurons.[5,112]

High doses of MA when administered to animals (rodents and non-human primates) serve as a model of PD.[5] Single[120] or multiple injections[121] of MA result in: (1) decreased levels of DA, 3,4-dihydroxyphenylacetic acid (DOPAC), homovanillic (HVA) in the striatum and 5-HT (in the striatum and other areas of the brain);[122] (2) perturbation of amino acid levels, especially, glutamate (Glu) elevation;[123] (3) decreased tyrosine hydroxylase (TH) and tryptophan hydroxylase (TPH) activity;[124] (4) inhibition of monoamine oxidase (MAO);[125] (5) decreased DA[126] and 5-HT uptake;[127] and (6) axonal and terminal dieback of DA[128] and 5-HT neurons.[129] MA administration induces hyperthermia in animals[130] and humans.[131] The limitations of the MA model of PD include: (1) high mortality due to hyperthermia which can be controlled by external cooling if the dose is not too high; (2) animals can be difficult to manage due to drug-induced hyperactivity; and (3) absence of Lewy body formation.

Recently, the pesticide rotenone has been employed to mimic PD in rats.[132] Rotenone is commonly used in vegetable gardens and to eliminate overproduction of fish. Chronic systemic administration of rotenone to rats results in mt complex I inhibition, that is not limited to dopaminergic neurons. However, rotenone-induced degeneration appears to be specific to nigrostriatal dopaminergic neurons. Rotenone also causes selective striatal oxidative damage and produces ubiquitin- and α-synuclein-positive inclusions in nigral cells. In some rats (but not all) physical parkinsonian-like behavior is observed, indicated by hypokinesis, hunched posture and rigidity.[132] However, for several reasons this is still far from replacing MPTP (see later) as the compound that best

mimics PD. The methodology for administration of rotenone is in the early stages of development. Current protocols lead to approximately a 50% death rate and lesions have not been detected in all of the surviving rats. Therefore, quantitative results are questionable especially immunohistological analysis.[112] Additionally, chronic administration of rotenone requires constant supervision, with animals often having to receive food and water manually. Nevertheless, this model does support the idea that idiopathic PD may be related to chronic exposure to environmental toxins.

Currently, administration of MPTP (or its active metabolite 1-methyl-4-phenyl-pyridinium; MPP^+; Figure 1:01) is the most widely employed and characterized animal model of PD.

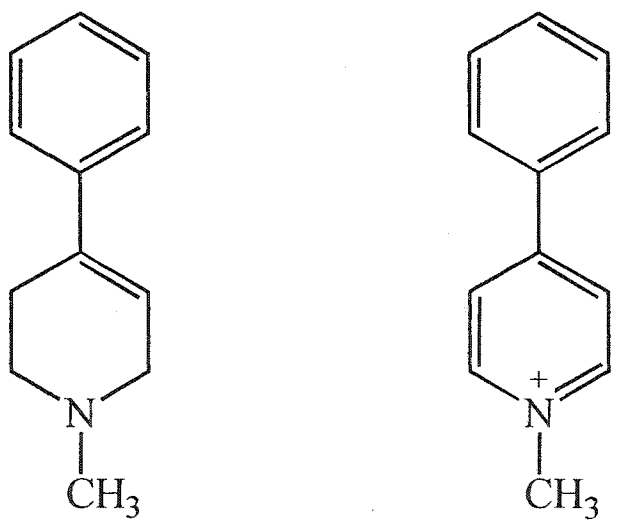

Figure 1:01. 1-Methyl-4-phenyl-1,2,3,6-tetrahydropyridine (MPTP) and its active metabolite 1-methyl-4-phenylpyridinium (MPP^+).

The accidental by-product of an ambitious graduate student's meperidine analog synthesis in 1982,[133] MPTP causes parkinsonian symptoms in humans, and in animals most faithfully mimics the chemical, pathological and immunohistological features of idiopathic PD.[5,112] MPTP evokes selective degeneration of nigrostriatal DA neurons[5,77,134] and a fall of GSH levels without a corresponding increase of GSSG.[135-138] Following MPTP administration to primates, eosinophilic inclusions[139] and α-synuclein aggregates[140] are present in remaining SN_{pc} neurons suggestive of early stage formation of Lewy bodies. The selectivity of MPTP can be traced to its oxidation by MAO-B in astrocytes to MPP^{+}[141] that is transported by the dopamine transporter (DAT)[142] into DA neurons where it is concentrated into mitochondria.[143] MPP^{+} then reversibly[75] inhibits mt complex I[143] and α-KGDH[144] that together with poly(ADP-ribose)polymerase (PARP) activation,[145-148] rapidly depletes adenosine 5'-triphosphate (ATP).[145,149]

For some reason, in rats MPTP is unable to readily cross the blood-brain barrier, and hence little MPP^{+} is formed in the brain. Therefore, in the rat model of PD, the active metabolite of MPTP, MPP^{+}, is perfused directly into the brain. Perfusion of neurotoxic concentrations of MPP^{+} into the rat striatum or SN_{pc} induces a massive instantaneous release of DA[150-152] by mechanisms that include rapid ATP depletion with resultant impairment of membrane ion pumps (Na^{+}/K^{+} and Ca^{2+}ATPases),[153] depolarization,[154] interference with the vesicular storage of DA[79,80] and reversal of the DAT.[155] However, the energy impairment evoked by MPP^{+} is temporary.[138,149] Thus, as the energy impairment begins to subside, increasing ATP production reactivates ATPases which initiate neuron membrane repolarization and the DAT-mediated reuptake of released DA.[156]

Perfusion of relatively high concentrations of MPP^+ into rat brain also evokes a delayed elevation of Glu.[151,157] Since Na^+-channel blockers protect against MPTP/MPP^+ neurotoxicity,[158] without affecting DA release,[159] suggests that Glu transporter reversal and Glu release are key steps in the neurotoxic cascade. All striatal neurons[160,161] and dopaminergic SN_{pc} cells[162-165] express *N*-methyl-D-aspartate (NMDA) and α-amino-3-hydroxy-5-methylisoxazole-4-propionic acid (AMPA) glutamate receptors. Recent studies indicate that AMPA receptor antagonists protect striatal neurons against MPTP/MPP^+-induced neurotoxicity[166] and NMDA receptor antagonists protect SN_{pc} neurons.[167,168] Such results implicate Glu ionotropic receptor activation as a key step in the neurotoxic cascade.

There is also strong evidence implicating elevated $O_2^{-}\cdot$ generation in the neurotoxic cascade leading to DA neurodegeneration evoked by MPTP/MPP^+. For instance, copper/zinc SOD (CuZn-SOD; cytosolic SOD) transgenic mice that overexpress the human gene for CuZn-SOD resulting in increased expression of CuZn-SOD,[169] are resistent to MPTP-induced neurotoxicity.[170] Transgenic mice which overexpress human manganese SOD (Mn-SOD; mitochondrial SOD) also show attenuated neurotoxicity to MPTP.[171] Additionally, MPTP neurotoxicity is potentiated in CuZn-SOD knockout mice.[172]

Activation of nNOS and iNOS with resultant neuronal and glial $NO\cdot$, $O_2^{-}\cdot$ and $ONOO^-$ generation also appear to be key steps in the neurotoxic cascade induced by MPTP/MPP^+.[173] Some of the $O_2^{-}\cdot$ generated by administration of MPTP/MPP^+ reacts with $NO\cdot$ to form $ONOO^-$ which nitrates and inactivates TH, the rate-limiting enzyme in DA synthesis.[173] This is substantiated by several previous studies where MPTP-induced

neurotoxicity was attenuated in neuronal nitric oxide synthase (nNOS) knockout mice,[36,174] inducible (i) NOS knockout mice,[175] and wild-type (normal) mice with inhibition of nNOS by 7-nitroindazole (7-NI).[36,176] In the SN_{pc} the source of NO· is from iNOS which is upregulated in microglia in response to MPTP.[175] In the striatum the principle source of NO· is from nNOS.[36] However, DA neurons do not contain nNOS.[177] Instead, nNOS-positive neurons that colocalize with somatostatin and neuropeptide Y are responsible for MPP^+-mediated NO· production[36,177] and, thus, the NO· must travel through the extracellular fluid in order to enter DA terminals and react with intraneuronal O_2^{-}· to form $ONOO^-$. This suggests that extracellular $ONOO^-$ formation could also occur by reaction of the nNOS-positive neuronal generation of NO· and extracellular O_2^{-}·. Indeed, extracellular O_2^{-}· can be generated by reactive microglia[178] and correspondingly, MPTP/MPP^+-induces activation of microglia.[175,176,179,180] $ONOO^-$-mediated DNA damage with resultant activation of the DNA-repair enzyme PARP contributes to the depletion of intraneuronal ATP evoked by MPTP/MPP^+.[145-148] There is also evidence for MPTP/MPP^+-induced generation of HO·.[181]

DA also appears to be a key participant in the neurotoxic cascade evoked by MPTP/MPP^+, because MPP^+-mediated cell death is substantially potentiated in rat hepatocytes pretreated with DA compared to normal control hepatocytes which do not contain DA.[182] The DAT must also play a critical role in MPTP/MPP^+ neurotoxicity since DA uptake inhibitors are neuroprotective,[183] and mice lacking the DAT are resistant to MPTP-induced neurotoxicity.[184] However, vesicular monoamine transporter-2 (VMAT-2) knockout mice are more susceptible to MPTP neurotoxicity.[185] Furthermore, dopaminergic SN_{pc} cells containing high levels of the DAT mRNA are preferentially

vulnerable to MPTP neurotoxicity.[186] One interpretation of these observations is that DATs potentiate DA neurotoxicity by accumulating intraneuronal MPP^+, whereas the VMAT-2 is neuroprotective by sequestering MPP^+ into vesicles thus attenuating its inhibitory effects on mt complex I.[187] However, in view of the possible role of DA in the neurotoxic cascade, and because MPP^+ impairs its vesicular uptake and storage, an alternative explanation is that the DAT-mediated reuptake of released DA as the energy impairment subsides results in abnormally high cytoplasmic concentrations of DA. Indeed, *in vitro* studies have demonstrated that elevation of cytoplasmic DA levels evoke neurotoxicity.[182] These observations implicate the release of DA during the MPP^+-induced energy impairment, its subsequent DAT-mediated reuptake and elevated cytoplasmic DA levels as the energy impairment subsides as important steps in the neurotoxic cascade evoked by MPTP. This implies that DA is either directly neurotoxic or the precursor of intraneuronal toxins. *In vitro*, DA potentiates neurotoxicity induced by energy impairment and/or Glu receptor activation which can be blocked by GSH or other thiols.[188] This suggests that intraneuronal DA oxidation during a period when intraneuronal GSH levels are reduced and Glu receptors are activated may be a key step in the neurotoxic process. Indeed, a recent study implicates intraneuronal DA oxidation as a key step in the *in vitro* neurotoxicity of MPP^+.[155]

C. Hypothesis

Proposed Neurotoxic Cascade Induced by MPP^+

Based on the background presented above (and much more) the following hypothetical neurotoxic cascade was formulated in this laboratory in 1999. The hypothesis was based on studies conducted in our laboratory as well as an exhaustive analysis of the literature.

The hypothesis (at that time) for the pathogenesis of SN_{pc} cell death in PD, proposed that a neurotoxic cascade is triggered by a large transient impairment of dopaminergic energy metabolism. In the MPTP/MPP^+ model this is caused by the DAT-mediated transport[142] of MPP^+ into dopaminergic neurons where it reversibly[75] inhibits mt complex I[143] and α-KGDH.[144] In individuals susceptible to PD this selective dopaminergic energy impairment could be evoked by exposure to environmental toxins that interfere with mt respiratory enzymes.[72,73,77,189-193] This is so because of both age[20] and genetically-based impairments[194-197] of xenobiotic metabolism[57,60-63] and the low selectivity of the DAT which transports many structurally diverse substances into DA neurons.[76,198] The energy impairment induces a massive release of DA[150-152] and, of equal importance, intraneuronal GSH[97-104] and potentiates NMDA receptor activation[199,200] by basal extracellular levels of Glu.[201,202] The resultant influx of Ca^{2+} through the NMDA receptor channel mediates massive intraneuronal $O_2^{-\cdot}$ generation[203-205] and activates neuronal nNOS[173,176,179,180] with consequent $NO\cdot$[206] and, thence, $ONOO^-$ generation.[207-209] Damage to DNA by $ONOO^-$ activates the repair enzyme PARP[145-148] which potentiates intraneuronal ATP depletion.[145,149]

During the dopaminergic energy impairment, some $ONOO^-$ crosses the neuronal membrane and, by both direct decomposition and release of Fe^{2+} from iron-containing proteins, was proposed to mediate extracellular $HO\cdot$ generation.[210,211] This $HO\cdot$ should oxidize released GSH and DA to radicals which in a cascade of coupling and oxidation reactions form glutathionyl conjugates of DA (and DOPAC) as shown in Figure 1:02.[108,212] DA, DOPAC (Figure 1:03), GSH and Cys (Figure 1:03) can be oxidized by $ONOO^-$, $HO\cdot$ and O_2. A principle function of GSH is as an antioxidant and, thus, oxidation by $ONOO^-$, $HO\cdot$ or O_2 of extracellular GSH and Cys would also be expected to form the corresponding sulfinic and sulfonic acids in addition to disulfides (e.g., Figure 1:04).[213] The oxidation and depletion of extracellular GSH (basal and that released from DA neurons) and Cys was proposed to trigger release of GSH from astrocytes[83-85] in amounts sufficient to scavenge $HO\cdot$, maintain normal basal levels of GSH and Cys, and protect neurons.[86-88,111,214] Extracellular Cys is maintained at basal levels[215] by the γ-GT/ApN-mediated hydrolysis of released astrocytic GSH in, it was hypothesized, reactions that should result in elevated extracellular levels of Glu.

As the neuronal energy impairment begins to subside, the hypothesis proposed that increasing ATP production and Na^+/K^+ and Ca^{2+}ATPase reactivation should initiate the DAT-mediated reuptake of released DA[156] that is oxidized by and hence, scavenges intraneuronal $ONOO^-$, thus blocking extracellular $HO\cdot$ generation and oxidation of GSH, Cys, DA and DOPAC. During this period extracellular levels of Glu are known to rise.[151,157] In addition to formation of Glu by γ-GT-mediated hydrolysis of GSH, this may also occur because MPP^+ (and possibly environmental mt toxins implicated with PD) induce an astrocytic energy impairment which results in reversal of the Glu

transporter (in the nigrostriatal pathway this is the GLT-1 astrocytic Glu transporter).[151,157] The release of Glu may be delayed because extraneuronal monoamine transporters (EMTs) on astrocytes accumulate intracellular MPP^+ and other toxins more slowly than neuronal DATs.[216-218] In order to replenish intraneuronal GSH, released and oxidized during the dopaminergic energy impairment, would necessitate its continued release from astrocytes and its degradation by γ-GT/DP to Cys, Gly and Glu. Extracellular Cys would then be transported into DA neurons where, normally, it is the rate limiting substrate for GSH synthesis.[83,84,95,96]

During the period of recovering but still reduced neuronal ATP production, elevated extracellular Glu (formed by hydrolysis of released GSH by γ-GT and/or by GLT-1 reversal on astrocytes) should continue NMDA receptor activation and intraneuronal generation of $ONOO^-$ that oxidizes DA to DAQ. Some of this DAQ could bind covalently to active site cysteinyl residues of TH, thus evoking irreversible inhibition of this enzyme.[219] The hypothesis also proposed that DAQ might react with translocated Cys forming 5-*S*-Cys-DA which is further oxidized to dihydroxybenzothiazine (DHBT) and benzothiazine (BT) metabolites.[220-223] These cytoplasmic DHBT/BTs have been shown in this laboratory to be accumulated by mitochondria and oxidized at the mt membrane to electrophilic intermediates which bind covalently to active site Cys residues[224-226] of complex I, α-KGDH and pyruvate dehydrogenase complex (PDHC) evoking their irreversible inhibition. Such processes could lead to a fall of nigral GSH, inhibition of mt complex I and α-KGDH, and ultimately, SN_{pc} cell death and PD.

D. Initial Dissertation Purpose

In previous microdialysis experiments conducted in our laboratory, a 30 min perfusion of 2.5 mM MPP^+ invoked a delayed rise of extracellular GSH and Cys (Figure 1:05). In identical experiments with MPP^+ in the presence of a constant perfusion of 1.0 mM acivicin (ACV; and inhibitor of γ-GT), there was an increase in the maximum rise of extracellular GSH and an attenuated rise of extracellular Cys (compared to the experiments conducted in the absence of ACV), implying that extracellular Cys originated from GSH (Figure 1:06).[215] Thus, it was anticipated that a constant perfusion (before, during, and after MPP^+) of ACV contained in the aCSF would inhibit γ-GT, resulting in an attenuated MPP^+-induced efflux of Glu and Gly (compared to experiments when ACV was not coperfused). This would be expected if the hypothesized source of Glu and Gly was from the γ-GT-mediated hydrolysis of GSH. In turn, ACV would be expected to be neuroprotective both by blocking the rise of extracellular Glu (by γ-GT hydrolysis of released astrocytic GSH) and, perhaps, by blocking the rise of Cys and, hence, intraneuronal formation of DHBT/BT endotoxins.

The fundamental intention of the experiments described in Chapter Two was to evaluate the role of γ-GT as proposed in the hypothetical neurotoxic cascade induced by MPP^+. In microdialysis experiments in freely moving rats, when 0.7, 1.3, 2.5 or 10.0 mM MPP^+ was perfused for 30 min, it was expected that glutathionyl and cysteinyl conjugates of DA and DOPAC would be detected (Figure 1:02). Some of the Cys (formed from released GSH by γ-GT and ApN) would enter DA neurons and react with DAQ forming 5-*S*-Cys-DA and eventual DHBT-1 and BT-1/BT-2 formation, which would result in dopaminergic cell death. In these microdialysis experiments various

concentrations of MPP^+ were perfused on day 1. On day 2 (24 hr after day 1 experiments), the same concentration of MPP^+ was again perfused for 30 min. An attenuated release of DA on day 2 has been reported[227] to be proportional to dopaminergic neuronal terminal damage.

In experiments where ACV was perfused before, during and after 30 min perfusions of MPP^+, GSH would remain intact. The extracellular generation of $HO\cdot$ would result in glutathionyl conjugates of DA. Since there would be no (or limited) Cys available to enter DA neurons, the proposed reaction with DAQ would not occur (or would be attenuated), and hence, DA neuron death would not occur as a result of intraneuronal DHBTs/BTs formation. Additionally, ACV was expected to block the degradation of released GSH to Glu (which rises upon MPP^+ perfusion).[157] Hence, ACV should block Glu-mediated excitotoxicity induced by MPP^+. Glu levels would not be sufficiently high to continue activation of NMDA receptors as the energy impairment subsided and, thus, intraneuronal $HO\cdot/ONOO^-$ production would not oxidize DA to DAQ (the latter of which is certainly neurotoxic without conversion to DHBT/BT metabolites).[228] In other words, ACV should afford protection against MPP^+-induced dopaminergic neuronal degeneration by inhibiting γ-GT.

E. Project Description

The results presented in Chapter Two are from experiments conducted in the early stages of this project. As the years have gone by, results from experiments conducted in our laboratory and observations reported in the literature have continued to reshape the initial ideas. As a result, this project constantly changed and branched into different directions in effort to explore newly developed hypotheses. The work presented here is but a small piece of a much larger ongoing and continuously evolving project.

The following work was conducted as presented in the ensuing chapters:

Chapter Two

A. Glutathionyl and cysteinyl conjugates of DA and DOPAC were electrochemically synthesized, isolated by HPLC-UV, and identified by UV and electrospray ionization mass spectrometry (ESI-MS).

B. HPLC-EC method I was developed to monitor DA, 5-HT, their normal metabolites DOPAC, 3-methoxytyramine (3-MT), HVA, 5-hydroxyindole-3-acetic acid (5-HIAA) and glutathionyl and cysteinyl conjugates of DA and DOPAC.

C. Method development was conducted to determine the ideal storage conditions (pH, type of solvent and temperature) of neurochemicals employed in this project.

D. Surgical procedures were conducted to implant guide cannula/dummy probe into rat striatum so that optimum location would be utilized during microdialysis procedures.

E. Employing microdialysis, four different concentrations of MPP^+ (0.7, 1.3, 2.5, 10.0 mM) were perfused for 30 min into the striata of freely-moving rats and dialysate fractions were collected in vials contained in a refrigerated fraction collector. In identical experiments 1.0 mM ACV was perfused 3 hr before, during and after 30 min perfusions of the same concentrations of MPP^+.

F. Twenty-four hr after day 1 experiments an identical microdialysis experiment was performed either with or without 1.0 mM ACV, as appropriate.

G. Alternate dialysate fractions collected from microdialysis experiments were analyzed for DA, 5-HT, DOPAC, 3-MT, 5-HT, 5-HIAA and HVA, and to search for glutathionyl and cysteinyl conjugates of DA and DOPAC employing HPLC-EC method I.

H. ESI-MS experiments were conducted to search for glutathionyl and cysteinyl conjugates of DA and DOPAC and to confirm the identity of putative 2,5,6-tri-*S*-glutathionyldopamine (2,5,6-tri-*S*-GS-DA).

I. HPLC-EC methods II and III were developed in order to provide further support for formation of 2,5,6-tri-*S*-GS-DA and enable more successful ESI-MS detection of neurochemicals in dialysate.

J. HPLC-EC methods I-III were eventually employed to confirm L-(D-)DOPA in dialysate from microdialysis experiments.

Chapter Three

A. Antioxidants salicylate (SA) and mannitol were perfused before, during and after a 30 min perfusion of 10.0 mM MPP^+ into the striatum of freely-moving rats. Dialysate fractions were collected and analyzed employing HPLC-EC method I.

B. HPLC-EC method IV was developed in connection with *in vitro* experiments with active and denatured purified DDC in the presence and absence of MPP^+.

C. Surgical procedures were developed to implant two guide probe/dummy cannulas into striata in both sides of the rat brain.

D. Microdialysis experiments were designed and conducted to evaluate the activity of DDC in rat brain after 30 min perfusion of 10.0 mM MPP^+.

E. HPLC-EC method V was developed in order to analyze DDC activity from rat striatal homogenate after 30 min perfusion of 10.0 mM MPP^+ into the right striata of rats with aCSF being perfused into the left striata.

Chapter Four

A. Microdialysis was conducted on freely-moving rats during experiments where rats received 30 mg/kg (intraperatoneal; i.p.) administration of MA and dialysate analyzed employing HPLC-EC method I.

B. Temperature probes were developed to monitor striatal temperature during microdialysis experiments employing MA and 3,4-methylenedioxymethamphetamine (MDMA; 'ecstasy').

C. *In vitro* experiments were conducted with active and denatured purified DDC in the presence and absence of MA.

D. Microdialysis was conducted on freely-moving rats during experiments where rats received 15 mg/kg (i.p.) administration of MDMA and dialysate analyzed employing HPLC-EC method I.

E. HPLC-UV method I and HPLC-photodiode array (PDA) method I were developed to search for unknown compounds (specifically markers of ROS/RNS) formed during microdialysis experiments with 10.0 mM MPP^+.

Chapter Five

Alternate fractions collected from microdialysis experiments (as described in Chapter Two) were analyzed for the amino acids Glu, Gly, aspartate (Asp) and taurine (Tau) by HPLC-EC method VI.

Chapter Six

A. Microdialysis experiments (as described in Chapter Two) were conducted on another group of animals, except on day 2 brains were fixed and striata of these animals were analyzed immunohistochemically.

B. Methods were developed and conducted to analyze rat striatal tissue for TH-, glial fibrillary acidic protein- (GFAP) and OX-42-immunoreactivity (IR) and Nissl staining.

Chapter One Figures

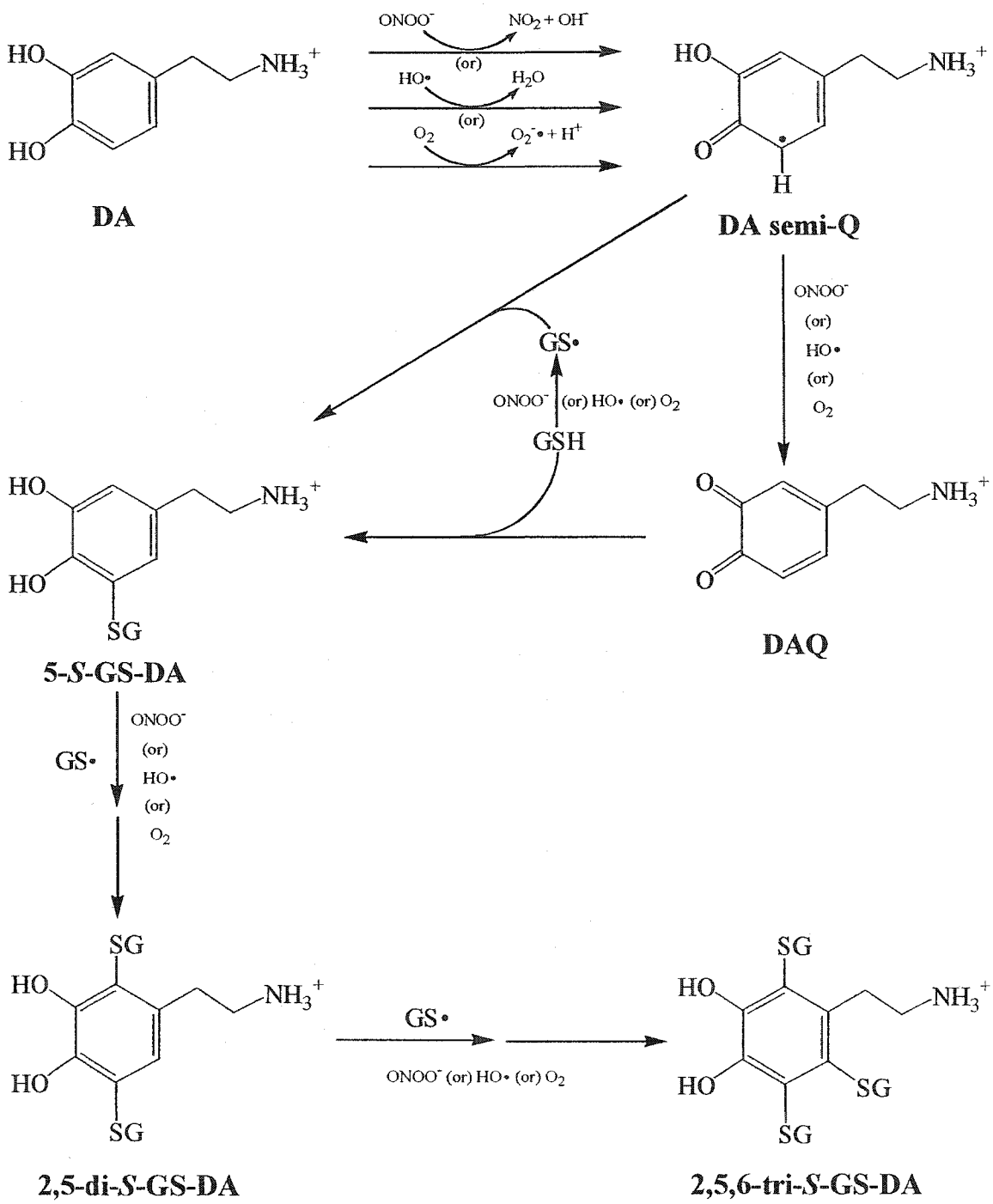

Figure 1:02. Proposed extracellular formation of glutathionyl conjugates of dopamine during the MPP^+-induced energy impairment. Glutathionyl conjugates of DOPAC and cysteinyl conjugates of DA and DOPAC are proposed to be formed by identical schemes.

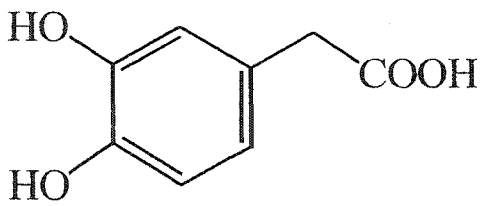

DOPAC
3,4-dihydroxyphenyl-
acetic acid

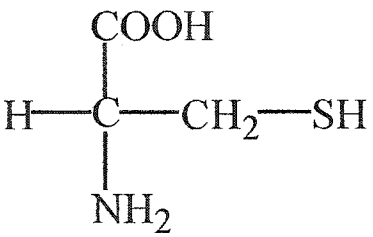

Cys
Cysteine

Figure 1:03. Structures of 3,4-dihydroxyphenyl-acetic acid (DOPAC) and cysteine (Cys).

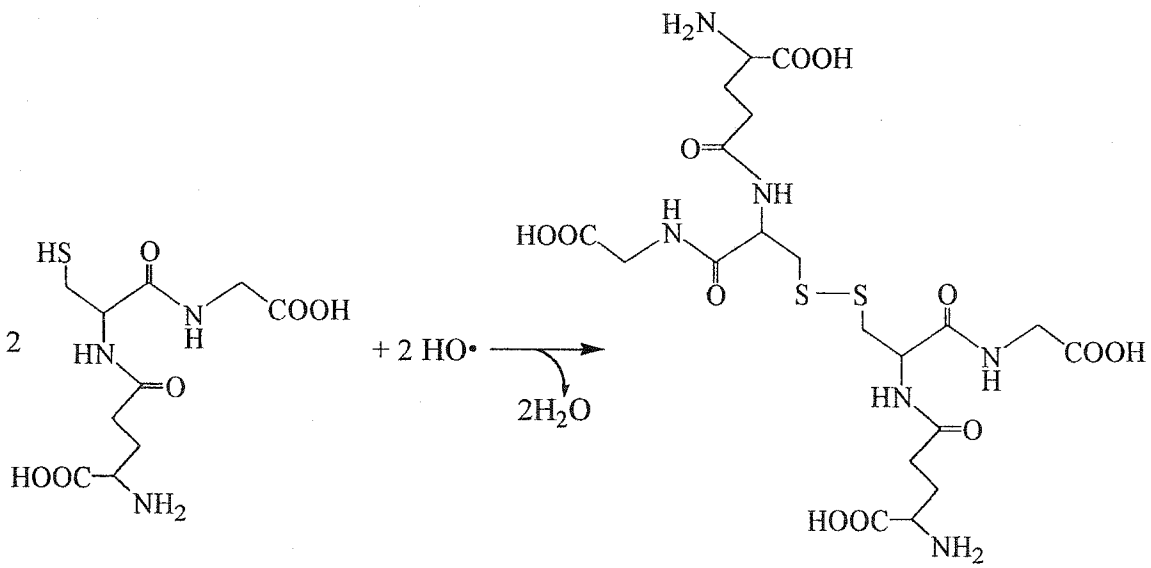

GSH **GSSG**

Figure 1:04. Hydroxyl radical oxidation of glutathione to form glutathione disulfide.

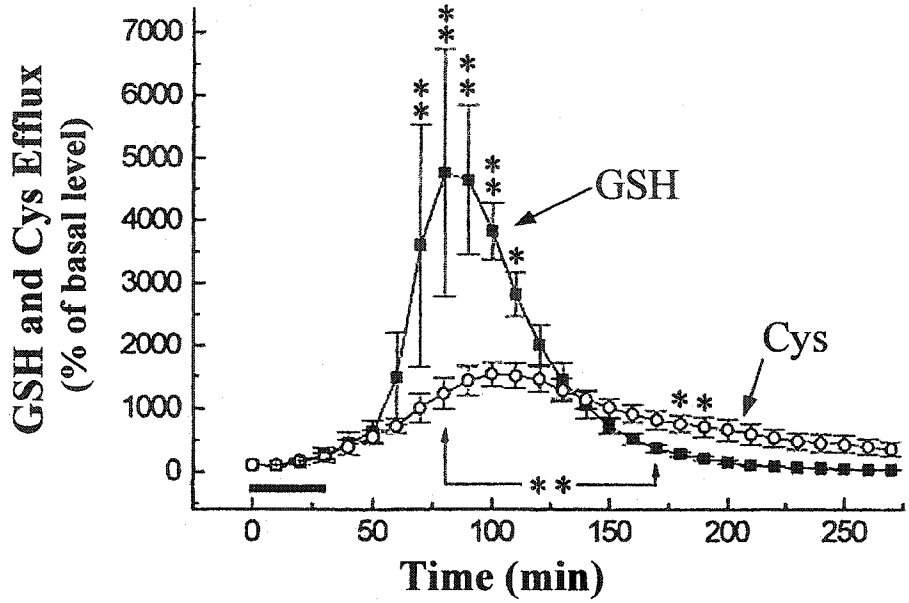

Figure 1:05. Time-dependent effects of a 30 min perfusion of 2.5 mM MPP^+ into rat striatum on microdialysate levels of GSH and Cys. The horizontal bar shows the time during which MPP^+ entered the brain. Data are mean ± SEM percentages of basal GSH and Cys ($n \geq 4$). $*p < 0.05$, $**p < 0.01$.[215]

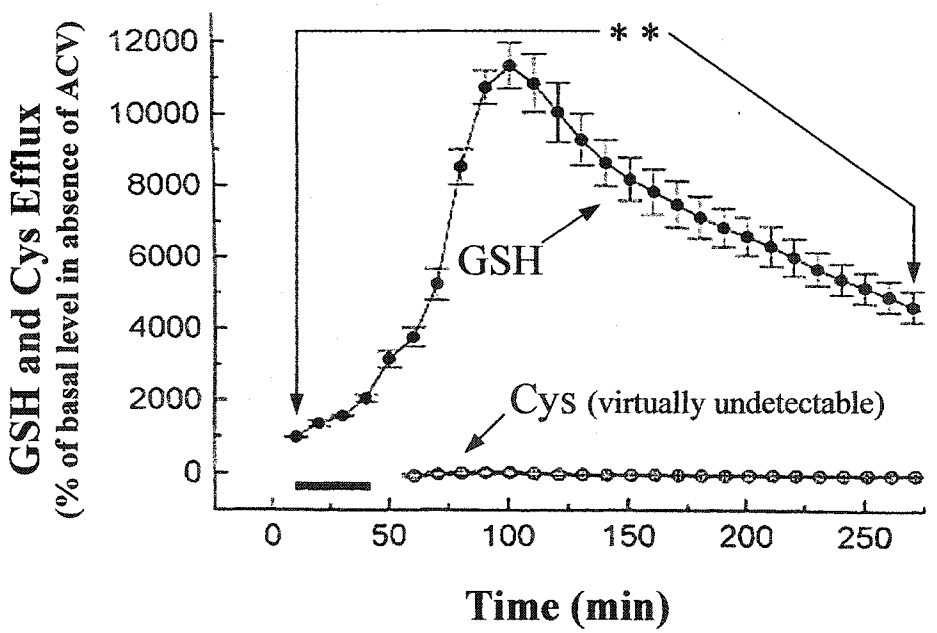

Figure 1:06. Time-dependent effects of a 30 min coperfusion of 2.5 mM MPP^+ and 1.0 mM ACV into rat striatum on microdialysate levels of GSH and Cys. The horizontal bar shows the time during which MPP^+ entered the brain. Data are mean ± SEM percentages of basal GSH and Cys in the absence of ACV coperfusion ($n \geq 4$). $*p < 0.05$, $**p < 0.01$.[215]

Chapter Two

In Vivo Microdialysis in Freely-Moving Rats: Effects of MPP^+ Perfusions

A. Introduction

The fundamental intention of the experiments presented in this chapter was to evaluate some of the predictions of the hypothetical neurotoxic cascade induced by MPP^+ as presented in Chapter One. The glutathionyl and cysteinyl conjugates of DA and DOPAC are not commercially available. Therefore, early stages of this project entailed the controlled potential electrochemical oxidation, isolation and identification of these compounds. In the past, our laboratory has developed methods to synthesize these compounds and numerous other similarly conjugated compounds. Hence, only the procedures (synthesis and isolation) which deviated from the previous descriptions will be presented.

Once these conjugates were isolated and identified, a critical initial aspect of this project involved the development of a suitable HPLC-EC system which would provide adequate separation and optimum throughput of all thirteen compounds of interest (Table 2:01 and Figures 2:01-03). Typical HPLC-EC method development included adjustments to mobile phase composition, flow rate, applied EC potential and constructing standard curves. Standard mixtures were made such that the EC response for each compound produced chromatographic peak heights within 30% of every other

compound. Ideal conditions (e.g. type of acid, pH, length of storage) were developed for the standard solutions and the collected dialysate.

Microdialysis experiments were conducted in which four different concentrations (0.7, 1.3, 2.5, 10.0 mM) of MPP^+ (in the presence and absence of 1.0 mM ACV) were perfused into the striatum of freely moving rats. Analysis of dialysate from these experiments revealed the presence of an unknown compound which initially appeared to be 2,5,6-tri-*S*-GS-DA. This prompted numerous attempts to confirm the identity of this compound. These included ESI-MS (Micromass, Q-TOF; Manchester, U.K) analysis and the development of three additional HPLC-EC methods (II-IV).

B. Experimental

1. Synthesis of Glutathionyl and Cysteinyl Conjugates of DA and DOPAC.

a. Chemicals

DA (hydrochloride salt), DOPAC, GSH (reduced form, free base), and Cys were obtained from Sigma (St. Louis, MO). Trifluoroacetic acid (TFA) was obtained from Acros Organics (Cliffside Park, NJ). Acetonitrile (MeCN, HPLC grade) was obtained from Fisher Scientific (Fair Lawn, NJ). Sodium phosphate dibasic (anhydrous; Na_2HPO_4) was obtained from Mallinckrodt (Paris, KY). Ammonium hydroxide (NH_4OH) and sodium phosphate monobasic ($NaH_2PO_4 \cdot H_2O$) were obtained from EM Science (Gibbstown, NJ). All chemicals were used without further purification. All solutions were prepared with deionized water from a Milli-Q system (Continental Water System, El Paso, TX). Before injection into a preparative HPLC system, all reaction solutions were filtered through a membrane (type HA, pore size 0.45 μm, Millipore Corporation,

Bedford, MA). Phosphate buffer pH 7.4 (μ = 0.2 M) was prepared according to Christian and Purdy.[229]

b. Instrumentation

Controlled potential electrochemical oxidation reactions employed a Brinkman Instruments (Westbury, NJ) model LT 73 potentiostat. The working electrode consisted of six plates of pyrolytic graphite having a total surface area of *ca.* 300 cm^2. The counter electrode was platinum gauze and the reference electrode was a saturated calomel electrode (SCE). The potentials employed for controlled potential electrolyses are referenced to the SCE at ambient temperature (22 ± 2°C). A three-compartment cell was utilized in which the working, counter and reference electrode compartments were separated by a Nafion membrane (type 117, DuPont Co., Wilmington, DE). The working electrode compartment had a capacity of 50 mL. During electrolysis, the solution in the working electrode compartment was continuously stirred with a Teflon-coated magnetic stir bar and nitrogen (N_2) gas was bubbled through the solution.

Preparative HPLC utilized a Gilson (Middleton, WI) binary gradient system equipped with two Gilson model 302 pumps, a manometric module model 802B, a dynamic mixer model 811, a Holochrome UV detector (254 nm) and a Rheodyne (Cotati, CA) model 7125 injector with a 10 mL sample loop. For larger volumes (up to 35 mL) the solution was loaded directly onto the column through one of the HPLC pumps. A preparative reversed-phase column (J. T. Baker, Phillipsburg, NJ; Bakerbond C_{18}, 10 μm, 25.0 x 2.1 cm) protected by a short guard column (50.0 x 0.9 cm) packed with the same stationary phase was employed. For preparative separation, isolation and purification

two binary gradient mobile phase systems were employed. Solvent A was prepared by adding 30 mL of concentrated NH_4OH to 3.97 L of deionized water and adjusting the pH to 2.50 with concentrated TFA. Solvent B was prepared by adding 30 mL of NH_4OH to a solution of 1985 mL of HPLC grade MeCN and 1985 mL of deionized water. The apparent pH of this solvent was then adjusted to 2.50 with concentrated TFA. Solvent C was prepared by adding concentrated TFA to deionized water until the pH was 2.50. Solvent D was prepared by adding concentrated TFA to a solution of 2 L of HPLC grade MeCN and 2 L of deionized water until the apparent pH was 2.50.

HPLC-UV preparative method I was used to monitor the oxidation of DA in the presence of GSH or Cys (and in separate experiments the oxidation of DOPAC in the presence of GSH) and to separate and isolate the products from the reaction mixture. This method utilized solvents A and B with the following gradient: 0-2 min, 100% solvent A; 2-55 min, linear gradient to 30% solvent B; 55-60 min, linear gradient to 100% solvent B; 60-65 min, 100% solvent B; 65-66 min, linear gradient to 100% solvent A; 66-80 min, 100% solvent A. The flow rate was constant at 7.0 mL/min.

HPLC-UV preparative method II was used for additional purification and desalting of the isolated products from HPLC preparative method I. This method utilized the following gradient: 0-2 min, 100% solvent A; 2-35 min, linear gradient to 9% solvent B; 35-40 min, linear gradient to 100% solvent B; 40-45 min, 100% solvent B; 45-46 min, linear gradient to 100% solvent A; 46-60 min, 100% solvent A. The flow rate was constant at 7.0 mL/min.

c. Oxidation reactions, isolation, purification and identification of products

For synthesis of the glutathionyl conjugates of dopamine, DA·HCl (21 mg, 0.11 mmol) and GSH (105 mg, 0.34 mmol) were dissolved in 35 mL of pH 7.4 phosphate buffer (μ = 0.2 M) and electrolyzed for 60 min at a controlled potential of 100 mV. Following filtration, aliquots (10 $\leq$ 35 mL) of the product solution were repeatedly injected into the preparative HPLC system and the components were separated using preparative method I. The components eluted under individual chromatographic peaks were collected separately. The fractions containing 5-*S*-glutathionyldopamine (5-*S*-GS-DA), 2,5-di-*S*-glutathionyldopamine (2,5-di-*S*-GS-DA), and 2,5,6-tri-*S*-GS-DA were freeze-dried and the resulting solid materials, which contained ammonium trifluoroacetate from the HPLC mobile phase (preparative method I), were each dissolved in the minimum volume of deionized water. The pH was adjusted to 2.5 with TFA, desalted and purified using HPLC preparative method II. UV spectra (Hewlett-Packard model 8452A diode array spectrophotometer) and ESI-MS spectra were collected for each compound for proper identification as described in previous reports from this laboratory.[212,221]

For synthesis of the glutathionyl conjugates of DOPAC, GSH (74 mg, 0.24 mmol) and DOPAC (20 mg, 0.12 mmol) were used. For synthesis of the cysteinyl conjugates of dopamine, Cys (27 mg, 0.22 mmol) and DA·HCl (21 mg, 0.11 mmol) were used. The methodology for the electrolysis, isolation, purification and identification of the reaction products followed the procedures used for the glutathionyl conjugates of DA (above). The following products were identified based on UV-visible spectra and ESI-MS spectra[212,221] (see also, Figures 2:01-03).

i. 5-*S*-cysteinyldopamine (5-*S*-Cys-DA)

ii. 2,5-di-*S*-cysteinyldopamine (2,5-di-*S*-Cys-DA)

iii. 5-*S*-glutathionyldopamine (5-*S*-GS-DA)

iv. 2,5-di-*S*-glutathionyldopamine (2,5-bi-*S*-GS-DA)

v. 2,5,6-tri-*S*-glutathionyldopamine (2,5,6-tri-*S*-GS-DA)

vi. 5-*S*-glutathionyl-3,4-dihydroxyphenylacetic acid (5-*S*-GS-DOPAC)

vii. 2,5-di-*S*-glutathionyl-3,4-dihydroxyphenylacetic acid (2,5-di-*S*-GS-DOPAC)

2. Analytical HPLC-EC Method I Development

a. Chemicals

5-HT, 3-MT, 5-HIAA, HVA, sodium 1-octanesulfonic acid (SOS), ethylenediaminetetraacetic acid (EDTA, disodium salt) and citric acid were obtained from Sigma (St. Louis, MO). Methanol (MeOH, HPLC grade), hydrochloric acid (HCl) and perchloric acid ($HClO_4$) were obtained from Fisher Scientific (Fair Lawn, NJ). Diethylamine (DEA) was obtained from Mallinckrodt (Paris, KY). The sources of all other chemicals have been described above.

b. Analytical HPLC Instrumentation

Analytical HPLC-EC method I was originally developed to obtain separation of thirteen compounds: DA and its normal metabolites (DOPAC, 3-MT and HVA), 5-HT and its metabolite 5-HIAA, and glutathionyl and cysteinyl conjugates of DA and DOPAC. This method employed a BAS 200B HPLC system equipped with a BAS Unijet reversed phase microbore column (ODS-18, 100 x 1 mm, 3 μm particle size),

Unijet guard column (ODS-18, 10 x 1 mm, 3 μm particle size) and a glassy carbon electrode (3 mm diameter) set at +750 mV with respect to a Ag/AgCl reference electrode. This system was equipped with a flow splitter so that approximately 10% of the mobile phase traveled through the microbore column and the other 90% through a Phenomenex (Torrence, CA) IB-SIL reversed phase column (OBS-18-BD, 100 x 3.2 mm, 3 μm). ChromGraph® (BAS; version 1.5.01) software was utilized for data collection (Control; version 1.52) and data analysis (Report; version 1.53). For some of the initial method development, standards were manually injected onto column with a Rheodyne (Cotati, CA) 9125 injector equipped with a 5.2 μL sample loop. Eventually, injections were automated using a CMA/200 refrigerated autosampler (4°C) equipped with a CMA/240 online injector and a 5.2 μL sample loop. Standards were placed in 300 μL plastic vials and sealed with Teflon seals.

c. Method Development & Standard Stability

Initial separations were attempted using a mobile phase traditionally used to separate biogenic amines consisting of citric acid, SOS, EDTA, DEA and MeOH and/or MeCN. Despite numerous adjustments to percentages of each of these components, pH and flow rate, this mobile phase proved inadequate for a reasonable separation of all thirteen compounds of interest. After extensive method development of mobile phase conditions the following composition was used: 100 mL MeOH, 10 mL MeCN, 30 mL NH_4OH and 31 mL of TFA were added to 890 mL of deionized water. After filtration (0.45 μm type HA membrane filter, Millipore, Bedford MA) the apparent pH was

adjusted to 2.60 with TFA. The flow rate employed was 40 μL/min. This mobile phase composition and flow rate provided optimum throughput with adequate resolution.

The mobile phase employed had minimal buffering capacity and, hence, it was susceptible to pH drift. Therefore, the pH had to be closely monitored and correspondingly adjusted when appreciable changes (± 0.1) occurred. HPLC-EC method I was designed with a flow splitter, and hence, the only portion of the mobile phase that was recycled is that which did not contain the injected compounds. This design enables the injected compounds to travel through the microbore column and then to waste. Typically, fresh mobile phase was made every month.

Experiments were conducted to determine: (1) the most stable acid for dissolving and storing the standards and (2) the lowest analyte concentration that could be held for approximately six months at -80°C. Various concentrations (1.0-100.0 mM) of either HCl, $HClO_4$, or TFA were used with numerous concentrations (1.0 μM-10.0 mM) of the thirteen compounds. The final conditions were as follows: (1) 0.1 M HCl was used to make all analyte solutions; (2) individual compounds (from anhydrous form) were made into solution at 5.0 mM; (3) after determining each compound's EC response, a mixture of all thirteen compounds was made so that the chromatographic peak height was within *c.a.* 30% of each other; (4) once in solution all samples were stored at -80°C in 1.5 mL plastic vials prior to use but were discarded after 6 months. This mixture of compounds had a concentration range of 0.1-1.0 mM and *c.a.* 20 μL was stored in plastic 1.5 mL Eppendorf microcentrifuge vials. On the day of an experiment, one vial was removed and 15 μL was diluted to (typically) 1500 μL with 0.1 M HCl and used to obtain a standard curve (generated by at least 3 injections of 3 different concentrations). All

standards were held on ice or at 4°C (if in the autosampler) and were discarded at the end of the day. The detection limit ± standard error of the mean (SEM) was calculated as 3 times the peak to peak baseline noise at the corresponding compound's t_R with a 5.2 µL sample loop injection (Table 2:01). In this particular field of microdialysis studies, concentrations are typically reported in efflux units (fmol/min). Microdialysis flow rate was always 1.5 µL/min, so conversion from traditional concentration units to efflux units is straightforward.

Table 2:01. Detection limits (nM or fmol/min; ± SEM, n = 48) with 5.2 µL injection for 13 compound separation (HPLC-EC method I).

Compound	Detection limit ± SEM (nM)	Detection limit ± SEM (fmol/min)
2,5,6-tri-*S*-GS-DA	9.57 ± 2.58	14.35 ± 3.87
DA	4.82 ± 1.53	7.23 ± 2.29
2,5-di-*S*-Cys-DA	15.00 ± 3.64	22.5 ± 5.46
5-*S*-Cys-DA	5.36 ± 1.81	8.04 ± 2.71
DOPAC	5.00 ± 1.58	7.50 ± 2.37
2,5-di-*S*-GS-DA	18.33 ± 4.77	27.50 ± 7.16
5-*S*-GS-DA	8.75 ± 2.98	13.12 ± 4.47
5-HT	3.00 ± 0.95	4.50 ± 1.42
3-MT	4.88 ± 1.54	7.31 ± 2.31
5-HIAA	2.85 ± 0.90	4.28 ± 1.35
5-*S*-GS-DOPAC	11.36 ± 4.34	17.04 ± 6.51
HVA	10.07 ± 3.39	16.07 ± 5.08
2,5-di-*S*-GS-DOPAC	21.17 ± 5.01	31.76 ± 7.52

3. *In Vivo* Microdialysis in Freely Moving Rats

a. Chemicals and drugs

L-DOPA, α-amino-3-chloro-4,5-dihydro-5-isoxazoleacetic acid (ACV) and magnesium chloride hexahydrate ($MgCl_2 \cdot 6H_2O$) were obtained from Sigma (St. Louis, MO). MPP^+ (iodide salt) was purchased from Research Biochemicals International (RBI; Natick, MA). Xylazine was obtained from Miles (Shawnee Mission, KS). Ketamine was purchased from Phoenix Scientific (St. Joseph, MO). Sodium chloride (NaCl) and calcium chloride dihydrate ($CaCl_2 \cdot 2H_2O$) were obtained from Mallinckrodt (Paris, KY). Potassium chloride (KCl) was purchased from J.T.Baker (Phillipsburg, NJ). Ethyl alcohol (EtOH; 200 proof) was obtained from Aaper Alcohol and Chemical Co. (Shelbyville, KY). Ethyl ether and formic acid (88%) were obtained from Fisher Scientific (Fair Lawn, NJ). The sources of all other chemicals have been described previously.

b. Animals

Adult male albino Sprague-Dawley rats (Harlan Sprague-Dawley, Madison, WI) weighing 330-350 g were used. After arrival they were allowed one week to become equilibrated to new surroundings while housed in cages with bedding (Sani Chips®; P.J. Murphy Forest Products, Montville, NJ) in groups of two or three with free access to food (Lab Diet® #5008 Formulab Diet; PMI® Nutrition International, LLC; Brentwood, MO) and water with a 12 hour light-dark cycle. After one week, rats were brought into the laboratory during the day to become accustomed to the smell, noises and handling.

c. Surgery

Animals were lightly anesthetized with ethyl ether (in a desiccator) to facilitate the initial injections of surgical anesthesic (ketamine, 85.72 mg/kg; *ca.* 290 μL) and analgesic (xylazine, 5.72mg/kg; *ca.* 195 μL). Approximately ten minutes after initial anesthesic/analgesic, animals were given a pinch (with tweezers) on one of the muscles in either hind leg to insure complete unconsciousness (lack of response). During surgery animals received additional doses (if necessary) of anesthesic/analgesic at 67% of the original dose, i.e., 57.15 mg/kg (*ca.* 193 μL) of ketamine and 3.83 mg/kg (*ca.* 130 μL) of xylazine. Animals were placed in a stereotaxic instrument (Lab Standard™, Stoelting, Wood Dale, IL) with the nose bar positioned 3.3 mm below the interaural line. Sterile eye lubricant (Moisture Eyes™ PM; Bausch and Lomb, Rochester, NY) was applied to the animal's eyes for protection. The scalp was trimmed of excess hair and sterilized with 70% EtOH. A midsagital incision was made with a surgical scalpel and the skull was exposed. Bone trapenization was made with an electric drill handpiece system (XL-30W; Osada Electric Co., LTD, Tokyo, Japan) using a surgical trephine drill bit (BAS). Proper placement was relative to bregma and identified according to Paxinos and Watson.[230] Three smaller trapenizations were made in the area around the initial location and cranial screws (Plastics One, Roanoke, VA) were secured (1 mm depth below surface of skull) in these 3 locations. Dura was cut with a sterile needle (Precision Glide® 26 G ½; Becton Dickinson and Co., Franklin Lakes, NJ). The microdialysis probe guide/dummy cannula (12-type, CMA) was implanted into the initial hole location, using the coordinates: 2.8 mm lateral and 0.5 mm anterior to bregma with the tip positioned 3.4 mm below dura.

The probe guide/dummy cannula was secured to the skull and the three screws with cranioplastic cement (Plastics One).

Once the cranioplastic cement hardened, the incision was closed with 2-4 sutures using monofilament polyglyconate synthetic absorbable sterile surgical suture (Maxon 5-0, 17 mm; Davis + Geck, Danbury, CT). A collar (Bar-Lok® Cable Ties; Avery Dennison, Framingham, MA; obtained from CMA) was fastened around the animal's neck. The animal was then placed in a paper towel-lined cage on a heating pad (low temperature setting) and allowed to recover from the anesthesia/analgesia. Once conscious, each animal was transferred to its own cage with bedding, food and water and were left undisturbed for 1-2 days. Two to three days before actual microdialysis experiments, animals were placed in a bedding-lined 40 cm diameter Plexiglas bowl seated on a BAS Raturn. The animal's collar was attached to a tether (with the ability to move freely) and were given free access to food and water. This equilibration period allowed the animals additional opportunity to become familiar with the microdialysis experimental conditions.

d. Microdialysis

On the day of experiments using MPP^+, a microdialysis probe (CMA 12, 4 mm membrane) was placed in a solution of 1.0 μM DA (dissolved in 1.0 mM HCl) and perfused with artificial cerebral spinal fluid (aCSF; 147.0 mM NaCl, 2.7 mM KCl, 1.2 mM $CaCl_2$, and 0.85 mM $MgCl_2$ in deionized water in the presence or absense of 1.0 mM ACV, as appropriate) at a flow rate of 1.5 μL/min using a CMA 100 microinfusion pump and a gastight 1000 μL syringe (Bee Stinger, model MD-0100: BAS). Dialysate was

perfused through lengths of BAS Teflon and PEEK tubing (0.65 mm O.D. x 0.12 mm I.D.) and collected in 300 μL plastic vials in a CMA 170 refrigerated (4°C) microfraction collector. To determine probe recovery, six vials were collected for 10 min each (15 μL) and the last 3 collections were analyzed by HPLC-EC method I. Additionally, at least 3 separate injections of the original 1.0 μM DA (in 1.0 mM HCl) were analyzed by HPLC-EC method I. The perfusate chromatograms were compared to the standard DA chromatograms and a recovery percentage was calculated. If the recovery for DA was < 20%, the probe was discarded. Typically, probes were found to be within the acceptable DA recovery range (i.e., ≥ 20%) for 2-3 experiments. At regular intervals over the course of these microdialysis experiments, the probe recovery for all 13 compounds was determined. Since this procedure required a much longer time period and more importantly, was not necessary to determine probe recovery efficiency, it was conducted only on a weekly basis.

Once satisfactory probe recovery had been achieved, the dummy probe was removed from the guide cannula (in the animal) and replaced by the microdialysis probe with the tip positioned 7.4 mm below dura. Throughout microdialysis experiments rats were attached to a tether in a bedding-lined BAS Raturn and, therefore, were able to move freely, and had free access to food and water. In these experiments, the first and alternate fractions were used for amino acid analysis (Chapter Five), and the second and succeeding alternate fractions for analysis of biogenic amines and possible glutathionyl and cysteinyl conjugates of DA and DOPAC. For analysis of DA, 5-HT, their metabolites and possible glutathionyl and cysteinyl conjugates of DA and DOPAC, the dialysate was collected in the microfraction collector in which the second vial and

alternating vials contained a volume of 0.2 M HCl equivalent to one-fourth the total volume. For example, if the collection time was 5 min (7.5 μL) the vial would originally contain 2.5 μL of 0.2 M HCl. The vials that were used to collecte dialysate for amino acid analysis did not contain any pre-added solution. The dialysate fractions destined for amino acid analysis were capped with a septum and frozen (-80°C) immediately after completion of the microdialysis experiment.

Basal dialysate levels of DA, 5-HT and their metabolites were determined in fractions collected over 15 min intervals (22.5 μL). After analysis of these dialysates gave at least three consecutive constant basal levels of these neurochemicals (*ca.* 3 h; e.g., ± 10 % for DOPAC), a BAS Uniswitch Syringe Selector switched the perfusion solution to aCSF containing MPP^+ (0.7, 1.3, 2.5 or 10.0 mM) with or without 1.0 mM ACV for 30 min after which the perfusate was switched back to aCSF alone or aCSF plus 1.0 mM ACV. Upon initiation of MPP^+ perfusion, dialysate samples were collected at 5 min intervals (7.5 μL) for 3 h and subsequently at 10 min intervals (15 μL) for at least another 3 h. In all these studies, an identical microdialysis experiment was carried out on the same animal 24 h after the initial experiment. The concentration and length of perfusion of ACV was based on previous microdialysis investigations conducted in our laboratory[215] where a 3 h perfusion of 1.0 mM ACV was found to fully inhibit γ-GT based on two results: (1) extracellular Cys levels became undetectable (< 0.08 μM) after about 1 h of a constant pefusion of 1.0 mM ACV; and (2) during the perfusion of 1.0 mM ACV extracellular GSH levels rose for about 3 h.

At the conclusion of each day's microdialysis procedures, in vitro DA probe recovery was carried out to insure that the probe had functioned properly throughout the

experiment. All tubing was thoroughly rinsed with deionized water for 12 h in order to remove all traces of salts and other chemicals. After the day 1 microdialysis experiment, animals were removed from the Raturn and returned to individual cages. Following day 2 experiments, animals were sacrificed and correct placement of probes was verified as described by Santiago et al.[231]

e. HPLC-EC

HPLC-EC method I was automated and was the primary system used throughout the entire project to analyze dialysate fractions for DA, 5-HT, their normal metabolites and to search for glutathionyl and cysteinyl conjugates of DA and DOPAC. Vials containing dialysate fractions were capped with a septum and loaded into a refrigerated (4°C) autosampler. Neurochemical concentrations (expressed as efflux in fmol/min) were determined based on calibration curves obtained with standard mixtures of known compounds. At the beginning of each day's chromatographic analysis, standard mixtures (3 different concentrations, 3 times each) were injected to check calibration curves. During the course of autoinjection of dialysate fractions, standard mixtures were injected as every fifth sample to monitor and correct for possible chromatographic drift and detector response deviations. Using this method, the following basal neurochemical levels were measured (fmol/min ± SEM; n = 32): L-DOPA (8 ± 6), DA (28 ± 12), DOPAC (3468 ± 1159), 5-HIAA (1864 ± 270), and HVA (2211 ± 489). Basal levels of 5-HT and 3-MT were at or below their detection limits, 5 and 7 fmol/min, respectively.

HPLC-EC analytical methods II-IV all employed a BAS PM-80 pump, a LC-4C amperometric detector with a glassy carbon detector electrode (3 mm diameter) and a

DA-5 data acquisition system. HPLC-EC method II used a Rheodyne 9125 injector with a 5.0 μL sample loop. The glassy carbon detector electrode was set at +750 mV vs. a Ag/AgCl reference electrode. A BAS Unijet microbore column (ODS-18, 100 x 1 mm, particle size 3 μm) was used. The mobile phase was prepared by adding 50 mL MeOH, 20 mL NH_4OH and 21 mL TFA to 950 mL of deionized water. After filtration, the apparent pH was adjusted to 2.50 with additional TFA. The flow rate was 30 μL/min.

HPLC-EC method III used a Rheodyne 7125 injector and a 20.0 μL sample loop. The glassy carbon detector was set at +850 mV vs. Ag/AgCl reference electrode. This system was equipped with a Phenomenex (Torrence, CA) IB-SIL reversed phase column (OBS-18-BD, 100 x 3.2 mm, 3 μm). The mobile phase was 5% (v/v) MeOH in deionized water adjusted to pH 2.80 with formic acid. The flow rate was 0.3 mL/min.

HPLC-EC analytical system IV used a Rheodyne 9125 injector and a 5.0 μL sample loop. The glassy carbon detector electrode was set at +850 mV vs. Ag/AgCl reference electrode. This system was equipped with a BAS unijet reversed phase microbore column (ODS-18, 110 x 1 mm, 3 μm) and a Unijet guard column (ODS-18, 10 x 1 mm, 3 μm). The mobile phase was prepared by adding 0.85 mL DEA, 59.2 mg SOS, 187 mg Na_2EDTA dihydrate and 21 g citric acid monohydrate to 970 mL of deionized water. After filtration, the pH of this solution was adjusted to 2.40 with $HClO_4$ and then 30 mL of MeCN added. The flow rate was 72 μL/min.

f. Calculations and Statistics

Neurochemical concentrations measured in microdialysis experiments are expressed as efflux in fmol/min ± SEM based on at least four replicate experiments. The

effects of MPP^+ on neurochemical levels compared efflux data before, during and after perfusion using one-way ANOVA followed by Dunnet's post hoc test. A p-value < 0.05 was taken as significant. GraphPad Prism™ (version 2.01, GraphPad Software; San Diego, CA) was used for efflux plots and statistical calculations.

C. Results

1. Effects of MPP^+ Perfusion on Dialysate Levels of DA, 5-HT and Metabolites

A chromatogram of a standard mixture of DA, 5-HT, their normal metabolites together with 5-*S*-, 2,5-di-*S*- and 2,5,6-tri-*S*-GS-DA, 5-*S*- and 2,5-di-*S*-GS-DOPAC and 5-*S*- and 2,5-di-*S*-Cys-DA is shown in Figure 2:04A. A representative chromatogram of a rat striatal dialysate collected immediately prior to perfusion of MPP^+ (Figure 2:04B) shows peaks corresponding to basal levels of DA, DOPAC, 5-HIAA and HVA. Perfusion of MPP^+ evoked a massive increase of dialysate levels of DA and other characteristic changes in the concentrations of its metabolites. However, MPP^+ also evoked the appearance of a compound in dialysates having a t_R of 3.66 min (Figure 2:04C) identical to the t_R of 2,5,6-tri-*S*-GS-DA. However, several factors tended to argue against the likelyhood that this peak was in fact due to 2,5,6-tri-*S*-GS-DA. For example, peaks corresponding to 5-*S*- and 2,5-di-*S*-GS-DA (Figure 1:02), obligatory precursors of 2,5,6-tri-*S*-GS-DA when DA is oxidized in the presence of GSH,[212] were never observed in chromatograms of striatal dialysate samples collected during or after perfusions of MPP^+ (0.7-10.0 mM). Similarly, peaks corresponding to cysteinyl conjugates of DA were never detected in dialysates. Such conjugates would be expected when perfusions were conducted in the absence of ACV both as a consequence of the oxidation of

released DA in the presence of Cys[221] and as a result of the degradation of extracellular glutathionyl conjugates of DA by the action of γ-GT and ApN.[232]

2. Detection of an Unknown Compound and Identification Experiments

The acquisition of a new Micromass Q-TOF ESI-MS prompted numerous efforts to determine the identity of the unknown peak employing ESI-MS with direct injection, HPLC-MS and nanospray sample introduction. Previous studies have been conducted in which the identity of similar unknown compounds had been determined by this method.[146,233-235] Other investigators have reported detection limits for similar compounds that were in the approximate concentration range of putative 2,5,6-tri-*S*-GS-DA.[236-238] Initial studies conducted with standards of 2,5,6-tri-*S*-GS-DA provided disappointing detection limits for the MS detector that were certainly above the suspected concentration of the unknown compound present in dialysate.

Experiments were conducted to identify the unknown compound by reducing the solvent volume in order to increase the concentration of putative 2,5,6-tri-*S*-GS-DA. Microdialysis fractions that contained the highest concentrations of this unknown were autoinjected onto HPLC-EC method I and the solution eluted under its chromatographic peak was collected and held at 4°C until at least 6 samples had been collected. The collected samples were pooled in 1.5 mL microcentrifuge vials and centrifuged (14,000 x g, 4°C) until the solvent volume was reduced to approximately 5 μL. The sample was then introduced into the ESI-MS, usually with nanospray delivery. These experiments were unsuccessful at confirming the identity of putative 2,5,6-tri-*S*-GS-DA.

Further literature research provided clues that the HPLC-EC method I mobile phase was interfering with the ESI-MS signal, principally the high concentration of TFA which at elevated levels supresses ionization. Accordingly, additional HPLC-EC methods were designed to eliminate this problem by employing mobile phases with a lower level of TFA (HPLC-EC method II) and a method that eliminated TFA from the mobile phase employing only formic acid and deionized water as the mobile phase (HPLC-EC method III). Dialysate collected from microdialysis experiments where MPP^+ was perfused was analyzed employing HPLC-EC methods II and III. Results from these experiments failed to confirm the identity of the unknown compound as 2,5,6-tri-*S*-GS-DA (Table 2:02). Employing HPLC-EC methods II-IV the unknown compound present in dialystae from MPP^+-perfused rats, did not have the same t_R as 2,5,6-tri-*S*-GS-DA and did not coelute with added 2,5,6-tri-*S*-GS-DA (Table 2:02). Instead employing HPLC-EC methods I-IV the unknown compound present in dialysate from MPP^+-perfused rats had the same t_R as L-DOPA* and coeluted with added L-DOPA (Table 2:02). Despite reducing and eliminating HPLC mobile phase interferents, additional ESI-MS experiments failed to confirm the identity of this compound as L-(D-)DOPA, probably because of the high salt content of aCSF/CSF which are easily ionized by ESI.

* Unequivocal proof that extracellular L-DOPA is formed is provided in Chapter Three (pg. 106 and Figure 3:17, pg. 125).

Table 2:02. Chromatographic retention times for DA, 2,5,6-tri-*S*-GS-DA, L-DOPA and the compound present in rat striatal dialysates in response to perfusion of MPP^{+a}

HPLC-EC method[b]	retention time (min)[c]			
	DA	2,5,6-tris-*S*-GS-DA	L-DOPA	dialysate compound
I	4.02	3.66	3.66	3.66
II	4.58	9.09	4.97	4.99
III	3.74	4.23	3.41	3.43
IV	5.25	4.09	3.90	3.90

[a]Dialysate samples were collected between 15-20 min (5 min collection time, 7.5 μL) following 30 min perfusion of 10.0 mM MPP^+ dissolved in aCSF.
[b]Experimental conditions for HPLC-EC methods I-IV are provided in *Experimental*.
[c]Data are mean of at least 3 replicate measurements.

3. Extracellular effects of various concentrations of MPP^+ with and without ACV on day 1 and day 2.

Previous microdialysis studies with MPP^+[152,227,239-241] have shown that a significantly reduced efflux of DA in response to MPP^+ perfusion on day 2 compared to that on day 1 provides a reliable indication that the day 1 perfusion causes neurotoxic damage to dopaminergic terminals.[227] However, in many of these previous experiments the dialysate collection time was ≥ 10 min and the day 2 concentration of MPP^+ was greater than that received on day 1. In the present study the dialysate collection time was 5 min which provided a more detailed temporal profile of extracellular neurochemical changes evoked by MPP^+. Additionally, the day 2 concentration of MPP^+ was the same

as that perfused on day 1. The idea was that as MPP^+ is perfused into the striatum it will travel a certain distance from the probe. Therefore, perfusion of the same concentration of MPP^+ on day 2 as that received on day 1 would affect approximately the same area of the striatum as the identical concentration of MPP^+ did on day 1.

The time-dependent effects evoked by 30 min perfusions of MPP^+ (0.7-10.0 mM) on day 1 into the rat striatum on dialysate neurochemical levels are presented in Figures 2:05-60. Thus, MPP^+ evoked an almost instantaneous dose-dependent efflux of DA that, after attaining maximal values, declined back towards basal levels (Figures 2:13-20). Perfusion of MPP^+ also evoked an almost immediate decrease of dialysate concentrations of DOPAC (Figures 2:21-28) and HVA (Figures 2:53-60), an effect that persisted for many hours after the perfusion was discontinued, presumably the result of the inhibition of MAO-A and -B by MPP^+.[242] Dialysate levels of 3-MT increased when MPP^+ perfusions were initiated but then declined when the perfusions were discontinued (Figures 2:37-44). However, both during and after MPP^+ perfusion, dialysate concentrations of 3-MT remained significantly elevated above virtually undetectable basal levels indicating a shift of DA metabolism from the MAO-B pathway, inhibited by MPP^+, to that catalyzed by catechol-*O*-methyltransferase (COMT). Perfusion of MPP^+ on day 1 evoked a delayed increase of dialysate levels of L-DOPA (Figures 2:05-12). As with DA, this rise of extracellular L-DOPA was only transient. Perfusion of MPP^+ on day 1 also evoked an almost immediate but transient efflux of 5-HT (2:29-36), although much smaller than that of DA (Figures 2:13-20), and a profound but persistent decrease of dialysate levels of 5-HIAA (Figures 2:45-52), presumably caused by inhibition of MAO.

Perfusion of MPP^+ (0.7-10.0 mM) on day 2 resulted in a greatly attenuated release of DA (Figures 2:13-20) and L-DOPA (Figures 2:05-12), compared to day 1. For 5-HT (Figures 2:29-36) and 3-MT (Figures 2:37-44) this same day 2 effect was apparent except when 0.7 mM MPP^+ had been perfused (in the absence of ACV) on day 1, which resulted in a day 2 release for both 5-HT (Figure 2:29) and 3-MT (Figure 2:37) that was virtually identical to the day 1 release. Prior to MPP^+ perfusion on day 2, dialysate concentrations of DOPAC (Figures 2:21-28) and HVA (Figures 2:53-60) were attenuated in inverse proportion to the concentration of MPP^+ perfused on day 1. For 5-HIAA the day 2 attenuated basal levels was not apparent until MPP^+ concentrations were $\geq$ 2.5 mM (Figures 2:49-52). These effects are consistent with neurotoxic damage to dopaminergic and serotonergic systems in the striatum by MPP^+ perfusion on day 1.[227]

Using the preceding 2-day experimental paradigm it was possible that physical damage caused by insertion of the microdialysis probe on day 1 might have affected the MPP^+-mediated release of DA on day 2. This was investigated by perfusing aCSF alone on day 1 followed by MPP^+ (2.5 mM; 30 min) on day 2 and comparing the DA release and other neurochemical changes on day 2 to those observed when MPP^+ (2.5 mM) was perfused on day 1. The results presented in Table 2:03 indicated that the neurochemical effects evoked by MPP^+ perfusion on day 2, aCSF alone having been perfused on day 1, were indistinguishable from those evoked by MPP^+ perfusion on day 1. These results indicate that there was no significant dopaminergic or serotonergic terminal damage caused by probe insertion on day 1 that influenced any of the neurochemicals levels induced by day 2 perfusion of MPP^+.

Table 2:03. Maximum extracellular neurochemical changes evoked by perfusion of MPP^+ (2.5 mM; 30 min) into the awake rat striatum on day 1 and on day 2 after perfusion of aCSF alone on day 1.

Neurochemical	Maximal Neurochemical Concentration[a] (fmol/min) for:	
	Day 1 perfusion[b] of MPP^+	Day 2 perfusion[b] of MPP^+ one day after aCSF perfusion
L-DOPA	327 ± 111	341 ± 119
DA	6766 ± 2031	6886 ± 2043
DOPAC	3713 ± 1478	3521 ± 1646
5-HT	198 ± 69	179 ± 36
3-MT	600 ± 109	685 ± 115
5-HIAA	1904 ± 255	1842 ± 340
HVA	2092 ± 683	2257 ± 715

[a]Measured at time of maximal release.
[b]Data are mean ± SEM (n = 4).

Perfusion of increasing concentrations of MPP^+ (0.7-10.0 mM) into the striatum on day 1 caused correspondingly increased maximal releases of L-DOPA, DA, 5-HT and 3-MT (Figures 2:61-64, 67-70 and Table 2:04). However, the larger the release of L-DOPA, DA, 5-HT and 3-MT on day 1 the smaller their release caused by the day 2 perfusion of MPP^+ (Figures 2:61-64, 67-70 and Table 2:04). Additionally, the day 2 basal levels of DOPAC (Figures 2:65, 66), HVA (Figures 2:71, 72) and 5-HIAA (Figures 2:73, 74), which were usually the maximum efflux for these compounds, were

increasingly attenuated proportional to increasing concentrations of MPP^+ perfused on day 1 (Table 2:04). These observations suggested that the severity of dopaminergic and serotonergic damage increases with increasing concentration of MPP^+ perfused on day 1. For L-DOPA (Figures 2:11, 12) and DA (Figures 2:19, 20), there was no detectable release on day 2 when 10.0 mM MPP^+ had been perfused on day 1. Coinciding with this observation, on day 2, after 10.0 mM perfusions of MPP^+ on day 1, metabolites of DA, DOPAC (Figures 2:27, 28) and 3-MT (Figures 2:43, 44), were undetectable. For 5-HT when this same concentration of MPP^+ (10.0 mM) had been perfused on day 1, there was still a detectable release on day 2 (although minimal; Figures 2:35, 36) with an increase from basal levels of 5-HIAA (Figures 2:51, 52) occurring after 5-HT release. In microdialysis experiments where 1.0 mM ACV was constantly perfused (3 h before, during and after MPP^+), the maximum efflux and the time-dependent behavior of L-DOPA, DA, DOPAC, 3-MT, 5-HT, 5-HIAA and HVA evoked by a 30 min perfusion of MPP^+ (0.7-10.0 mM) did not significantly differ from experiments conducted in the absence of ACV (Table 2:04).

Table 2:04. Maximum extracellular neurochemical concentrations (fmol/min) of L-DOPA, DA, DOPAC, 5-HT, 3-MT, 5-HIAA and HVA evoked by perfusion of MPP^+ on day 1 and day 2 in the absence and presence of ACV (mean ± SEM, n = 4).

		Absence of ACV		Presence of ACV	
Biogenic Amine	**MPP^+ [mM]**	**Day 1**	**Day 2**	**Day 1**	**Day 2**
L-DOPA	0.0	8 ± 6^c	8 ± 4^c	7 ± 2^c	7 ± 5^c
	0.7	95 ± 32 (*)	31 ± 11 (*,#)	269 ± 60 (**,++)	27 ± 14 (*,##)
	1.3	292 ± 97 (**, x)	31 ± 17 (*,#)	388 ± 188 (**)	2 ± 5 (#)
	2.5	327 ± 111 (**)	8 ± 5 (x,#)	503 ± 185 (**)	9 ± 6^c (##)
	10.0	606 ± 108 (***,x)	6 ± 10 $(21,0,5,0)^b$ (##)	752 ± 220 (**)	5 ± 4^c $(0,6,4,10)^b$ (##)
DA	0.0	26 ± 15^c	12 ± 12^c	25 ± 13^c	7 ± 3^c
	0.7	2459 ± 496 (**)	1482 ± 190 (***,#)	3920 ± 424 (**,++)	1317 ± 200 (***,##)
	1.3	6165 ± 1533 (***,x)	598 ± 330 (*,xx,##)	6143 ± 1320 (**,x)	375 ± 197 (*,xx,##)
	2.5	6766 ± 2031 (***)	393 ± 240 (*,##)	6492 ± 1384 (**)	72 ± 52 (##)
	10.0	8596 ± 1268 (***)	0^a (x,###)	8792 ± 1396 (***)	0^a (###)
DOPAC	0.0	3468 ± 223^c	3380 ± 137^c	2905 ± 273^c	2854 ± 400^c
	0.7	3275 ± 941^c	1200 ± 490^c (**,##)	2850 ± 1041^c	1002 ± 241^c (**,#)
	1.3	3933 ± 1231^c	1566 ± 823^c (*,#)	2935 ± 1672^c	572 ± 530^c (***,##)
	2.5	3713 ± 1478^c	256 ± 106^c (***,##)	3429 ± 1962^c	228 ± 125^c (***,#)
	10.0	4246 ± 677	16 ± 11 $(19,21,24,0)^b$ (***,x,##)	4869 ± 592 (**)	22 ± 26 $(0,34,0,52)^b$ (***,x,###)

5-HT	0.0	4 ± 4^{c} $(0,0,9,5)^{b}$	4 ± 4^{c} $(0,0,8,6)^{b}$	4 ± 5^{c} $(0,7,9,0)^{b}$	3 ± 3^{c} $(0,5,6,0)^{b}$
	0.7	52 ± 11 (**)	51 ± 8 (***)	96 ± 13 (***,++)	35 ± 11 (**,##)
	1.3	162 ± 45 (**,x)	86 ± 26 (**,x,#)	184 ± 58 (**,x)	41 ± 19 (*,#,+)
	2.5	198 ± 69 (**)	54 ± 8 (***,#)	208 ± 103 (*)	31 ± 9 (**,#,+)
	10.0	324 ± 110 (**,x)	43 ± 69 $(9,146,0,7)^{b}$ (##)	256 ± 63 (**)	8 ± 10 $(0,19,0,15)^{b}$ (x,##)
3-MT	0.0	2 ± 4^{c} $(0,0,7,0)^{b}$	2 ± 4^{c} $(7,0,0,0)^{b}$	4 ± 5^{c} $(0,9,0,8)^{b}$	4 ± 4^{c} $(0,0,7,7)^{b}$
	0.7	183 ± 54 (**)	116 ± 33 (**)	250 ± 50 (**)	80 ± 39 (*,##)
	1.3	555 ± 133 (**,xx)	217 ± 86 (*,##)	514 ± 109 (**,xx)	134 ± 84 (*,##)
	2.5	600 ± 109 (**)	113 ± 52 (*,###)	614 ± 92 (***)	124 ± 65 (*,###)
	10.0	676 ± 311 (*)	0^{a} (x,##)	578 ± 218 (**)	0^{a} (x,##)
5-HIAA	0.0	1989 ± 455^{c}	1953 ± 424^{c}	1612 ± 235^{c}	1625 ± 300^{c}
	0.7	1722 ± 108^{c}	1469 ± 342^{c}	1846 ± 210^{c}	1568 ± 304^{c}
	1.3	1852 ± 273^{c}	1780 ± 549^{c}	1944 ± 236^{c}	1498 ± 803^{c}
	2.5	1904 ± 255^{c}	940 ± 366^{c} (**,##)	1734 ± 364^{c}	1144 ± 368^{c} (*,#)
	10.0	2708 ± 340 (*,xx)	394 ± 306 (***,x,###)	2469 ± 354	367 ± 428 $(0,796,0,672)^{b}$ (**,x,###)
HVA	0.0	2064 ± 530^{c}	2209 ± 359^{c}	2293 ± 434^{c}	2076 ± 447^{c}
	0.7	2350 ± 259^{c}	1183 ± 332^{c} (**,##)	2095 ± 436^{c}	732 ± 271^{c} (**,##,+)
	1.3	2402 ± 672^{c}	1195 ± 561^{c} (*,#)	2239 ± 810^{c}	634 ± 437^{c} (**,#)
	2.5	2092 ± 683^{c}	592 ± 217^{c} (***,#)	2048 ± 765^{c}	321 ± 153^{c} (**,#,+)
	10.0	1994 ± 260^{c}	12 ± 8^{c} $(0,14,17,17)^{b}$ (***,xx,###)	2434 ± 230^{c}	13 ± 16^{c} $(0,19,0,33)^{b}$ (***,x,###)

[a] = no release was observed with any animal.
[b] = release values for each animal perfused on day 1 or day 2.
[c] = maximum efflux was the basal level.
(*) = significant difference vs. basal level.
(x) = significant difference vs. the previously lower MPP^+ concentration perfused.
(#) = significant difference between day 2 and day 1.
(+) = significant difference between the presence and absence of ACV.
$^1p < 0.05$, $^2p < 0.01$, $^3p < 0.001$.

The maximum release of L-DOPA on day 1 when 0.7 mM MPP^+ was perfused in the presence of ACV was approximately three times that of experiments where 0.7 mM MPP^+ was perfused in the absence of ACV ($p < 0.01$; Figures 2:61, 62, Table 2:04). However, at all other concentrations of perfused MPP^+ there was no difference between L-DOPA dialysate levels in the presence or absence of ACV on day 1 or 2. The maximum release on day 1 of L-DOPA in the absence of ACV significantly increased ($p < 0.05$) when the concentration of perfused MPP^+ was increased from 0.7 mM to 1.3 mM, and from 2.5 mM to 10.0 mM ($p < 0.05$), but not from 1.3 mM to 2.5 mM. When MPP^+ was perfused in the presence of ACV there was no statistical difference observed in the maximum efflux of L-DOPA on day 1 with increasing concentrations of MPP^+. Nevertheless, while statsistically non-significant, there was still an apparent increase in the mean maximum efflux of L-DOPA by MPP^+ in the presence of ACV. Day 2 maximum efflux levels of L-DOPA were attenuated proportional to the concentration of MPP^+ perfused on day 1 for all concentrations of perfused MPP^+ in the presence and absence of ACV.

The maximum release of DA on day 1 when 0.7 mM MPP^+ was perfused in the presence of ACV was approximately 1.5 times ($p < 0.01$) that of experiments where 0.7

mM MPP^+ was perfused in the absence of ACV (Figures 2:63, 64, Table 2:04). However, the day 2 release did not differ statistically when 0.7 mM MPP^+ was perfused in the absence or presence of ACV. At all other concentrations of perfused MPP^+ there was no difference between DA release in the presence or absence of ACV on day 1 or 2. In the absence and presence of ACV, the only time there was a statistical significant increase ($p < 0.05$) in the maximum efflux of DA on day 1 (comparing the effect of increasing concentrations of perfused MPP^+) was when the concentration of perfused MPP^+ was increased from 0.7 to 1.3 mM. Day 2 maximum efflux levels were attenuated proportional to the concentration of MPP^+ perfused on day 1 for all concentrations of perfused MPP^+ in the presence and absence of ACV. There appears to be a trend (although not statistically significant) that coperfusion of ACV potentiated the MPP^+-induced dopaminergic damage indicated by attenuated maximum DA efflux levels on day 2.

Dialysate levels of DOPAC on day 1 immediately decreased from basal levels during perfusion of all concentrations of MPP^+ (Figures 2:21-28). There was no difference in the maximum efflux (Figures 2:65, 66, Table 2:04) nor the time dependent behavior (Figures 2:21-28) for DOPAC on day 1 or day 2 when MPP^+ was perfused in the presence or the absence of ACV. However, when 10.0 mM MPP^+ was perfused in the presence of ACV, there was an immediate rise in the concentration of DOPAC (2 times basal level; $p < 0.01$) occurring for 10 min, which was soon followed by its rapid decline (Figure 2:28). This same behavior was observed when 10.0 mM MPP^+ was perfused in the absence of ACV, but to a lesser extent (Figure 2:27). At all concentrations of MPP^+ perfused (in the presence and absence of ACV), day 2 basal levels of DOPAC

were significantly attenuated compared to day 1 (Figures 2:21-26), being attenuated proportional to the concentration of MPP^+ perfused on day 1 (Figures 2:65, 66, Table 2:04). When 10.0 mM MPP^+ was perfused on day 1, there was virtually no detectable basal concentration of DOPAC on day 2 in the presence and absence of ACV (Figures 2:27, 28, 65, 66, Table 2:04).

The maximum release of 5-HT on day 1 when 0.7 mM MPP^+ was perfused in the presence of ACV was approximately two times that of experiments where 0.7 mM MPP^+ was perfused in the absence of ACV ($p < 0.01$; Figures 2:29, 30, Table 2:04). However, at all other concentrations of perfused MPP^+ there was no difference between 5-HT dialysate levels in the presence or absence of 5-HT on day 1 or 2 (Figures 2:67, 68, Table 2:04). Day 2 maximum efflux of 5-HT was significantly lower in the presence of ACV compared to the absence of ACV at all concentrations of perfused MPP^+. In the absence of ACV, 0.7 mM MPP^+ evoked the same release of 5-HT on day 2 as on day 1. When 1.3 mM MPP^+ was perfused in the absence of ACV on day 2, the maximum efflux was approximately one half that evoked by identical concentration of MPP^+ perfused on day 1. It appears, therefore, that ACV may potentiate the serotonergic neurotoxicity invoked by MPP^+ as evidenced by the attenuated release of 5-HT on day 2 (compared to 5-HT released in response to perfusion of MPP^+ in the absence of ACV).

There was no difference in the maximum efflux (Figures 2:69, 70, Table 2:04) or the time dependent behavior (Figures 2:37-44) of 3-MT on day 1 or day 2 when MPP^+ was perfused in the presence of ACV or the absence of ACV. Increasing concentrations of perfused MPP^+ above 1.3 mM did not result in a corresponding increase in the maximum efflux of 3-MT on day 1. When 0.7 mM MPP^+ was perfused, day 2 maximum

efflux levels were 60% and 40% of day 1 levels in the absence and presence of ACV, respectively. When 10.0 mM MPP^+ was perfused on day 1, 3-MT was not detected prior to, during or after the day 2 perfusion (Figures 2:43, 44, 69, 70, Table 2:04).

The maximum efflux (usually basal levels; Figures 2:71, 72) and the time dependent behavior (Figures 2:45-52) of 5-HIAA (on day 1 and day 2) were not significantly different when MPP^+ was perfused in the presence or absence of ACV. At all concentrations of MPP^+ perfused, there was a decrease in basal levels of 5-HIAA on day 1 and day 2 immediately induced by perfusion of MPP^+ (Figures 2:45-52). Day 2 basal levels were the same as those on day 1 at concentrations of MPP^+ perfused $\leq$ 1.3 mM in the absence of ACV and $\leq$ 2.5 mM in the presence of ACV (Figures 2:71, 72, Table 2:04).

Day 1 basal levels of HVA decreased at increasing rates in proportion to increased concentration of MPP^+ perfused in the presence and absence of ACV (Figures 2:53-60). On day 1 there was no difference in the maximum efflux of HVA induced by MPP^+ in the presence compared to in the absence of ACV (Figures 2:73, 74, Table 2:04). At all concentrations of MPP^+ day 2 basal levels were attenuated in inverse proportion to the concentration of MPP^+ (in the presence or absence of ACV) perfused on day 1.

D. Discussion

The initial steps in the neurotoxic mechanism evoked by MPP^+ are believed to involve its rapid DAT-mediated uptake into dopaminergic neurons,[142] where it is concentrated into mitochondria[143] and inhibits mt complex I.[243] The resultant energy impairment, depolarization,[154] interference by MPP^+ with the vesicular storage of DA[79] and reversal of the DAT[155] all contribute to the massive almost instantaneous release of DA (Figures 2:13-20). However, the transport process that concentrates MPP^+ into mitochondria is energy dependent.[143] Thus, when dopaminergic mitochondria become severely de-energized, MPP^+ is presumably released into the cytoplasm and then transported out of these neurons by the reversed DAT. MPP^+ therefore should, and indeed does,[75] induce only a transient neuronal energy impairment. As the MPP^+-induced energy impairment subsides, increasing ATP production would be expected to initiate repolarization of the neuronal membrane which in turn would return the reversed DAT to its normal function with the resultant uptake of released DA.[156] Such a sequence is consistent with the massive release of DA evoked by MPP^+ perfusion followed by the fall of extracellular DA concentrations when the perfusion is discontinued (Figures 2:13-20). That the latter effect is probably indicative of the DAT-mediated reuptake rather than metabolism of released DA is supported by the observation that as extracellular DA concentrations fall, so also do those of its metabolites DOPAC (Figures 2:21-28), 3-MT (Figures 2:37-44) and HVA (figures 2:53-60).

The experimental microdialysis results presented earlier, indicate that perfusion of ≥ 0.7 mM MPP^+ on day 1 induces an efflux of DA on day 2 that is inversely proportional to the concentration perfused on day 1 (Figures 2:63, 64). This indicates that perfusion of

≥ 0.7 mM MPP^+ for 30 min on day 1 evokes neurotoxic damage to dopaminergic terminals as demonstrated by Santiago et al.[227] and in observations presented in Chapter Six. The decreased release of 5-HT in response to perfusion of ≥ 1.3 mM MPP^+ on day 2 compared to day 1 (Figures 2:67, 68) suggests that at higher concentrations, MPP^+ is also a serotonergic neurotoxin as proposed by others.[244]

Perfusion of MPP^+ evokes the appearance of a compound in dialysates having a t_R identical to that of 2,5,6-tri-*S*-GS-DA using HPLC-EC method I (Figure 2:04). Attempts to provide additional confirmation of the identity of this compound using ESI-MS were unsuccessful probably due to interference from the high salt content of the aCSF. Accordingly, additional chromatographic methods were developed (HPLC-EC methods II-IV), which unequivocally revealed that this compound was not 2,5,6-tri-*S*-GS-DA. Instead these HPLC methods along with HPLC-EC method I strongly support the conclusion that this compound is L-DOPA on the basis of matching t_R and by co-elution of the unknown with L-DOPA (Table 2:02).

Neither cysteinyl nor glutathionyl conjugates of DA or DOPAC were detected in rat brain dialysates in response to MPP^+ perfusions. There was virtually no major difference in the concentrations of L-DOPA, DA, DOPAC, 5-HT, 3-MT, 5-HIAA, or HVA as a result of MPP^+ perfusions in the presence or absence of ACV (Figure 2:61-74). It was initially hypothesized that ACV would be neuroprotective by inhibiting the γ-GT degradation of GSH to Glu, and hence, excitotoxicity via overstimulation of NMDA/AMPA receptors. However, if anything, ACV appeared to potentiate the apparent dopaminergic and serotonergic damage induced by MPP^+ (Figures 2:63, 64, 2:67, 68 respectively).

Thus, the role of γ-GT may not be as important as initially believed. Apparent dopaminergic neurotoxicity occurred with or without inhibition of γ-GT. However, the neurotoxicity may occur by different mechanisms. When γ-GT is not inhibited the proposed intracellular generation of 5-*S*-Cys-DA leading to neurotoxic DHBT/BT species may still occur. When γ-GT is inhibited, there appears to be no (or limited) Cys^{215} available for import into DA neurons as the energy impairment subsides. However, since ACV had no effect on the rise of extracellular Glu (results presented in Chapter Five), NMDA receptors would continue to be activated and, thus, there would be continued intraneuronal production of $O_2^{-\cdot}$, $HO\cdot$ and $ONOO^-$. Hence, as DA re-enters neurons it will be oxidized to DAQ, which is itself a mt toxin that uncouples respiration, induces mt swelling and opens the permeability transition pore,[228] in addition to irreversibly inhibiting TH.

E. Conclusion

At no time during perfusion of MPP^+ (both, with and without ACV) were glutathionyl or cysteinyl conjugates of DA or DOPAC (or disulfides such as GSSG and cystine)[245] detected by HPLC in striatal dialysates. The presence of such compounds would be expected if MPP^+ mediates extracellular generation of $HO\cdot$ and/or $ONOO^-$ which should oxidize released DA, GSH and Cys. These observations (and those presented in the following chapter) suggest that MPP^+ does not mediate significant production of extracellular $HO\cdot$ and/or $ONOO^-$. Coperfusion of MPP^+ with ACV was not neuroprotective and had no significant effect on extracellular concentrations of DA, 5-HT and their metabolites. However, an unknown compound present in rat striatal dialysate collected during perfusions of (0.7-10.0 mM) MPP^+, initially thought to be 2,5,6-tri-*S*-GS-DA has been identified as L-DOPA.* The validity of this identity was based on the unknown peak in dialysates exhibiting the same t_R and co-migrating with added L-DOPA using HPLC-EC methods I-IV (Table 2:02). This is the first report of a MPP^+-induced transmitter-like release of L-DOPA.

* Unequivocal proof that extracellular L-DOPA is formed is provided in Chapter Three (pg. 106 and Figure 3:17, pg. 125).

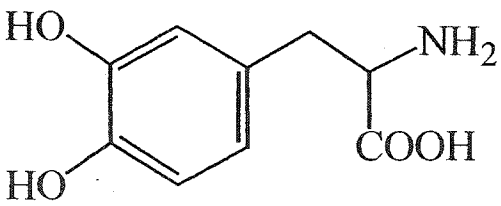

L-DOPA
L-3,4-dihydroxy-
phenylalanine

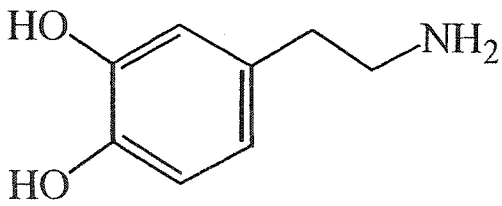

DA
dopamine

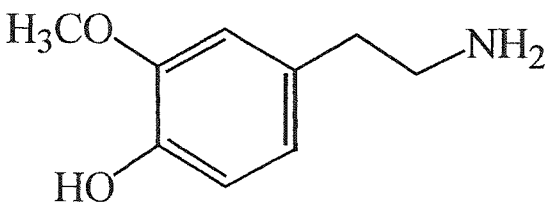

3-MT
3-methoxytyramine

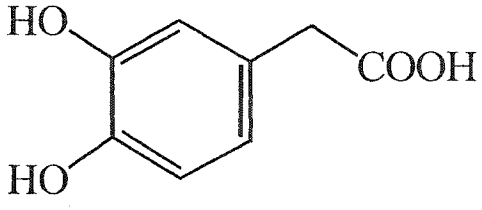

DOPAC
3,4-dihydroxyphenyl-
acetic acid

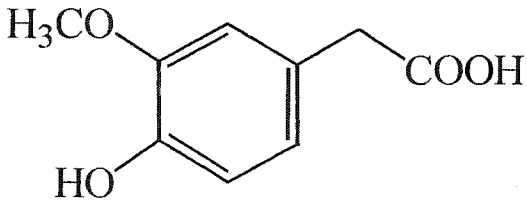

HVA
homovanillic acid

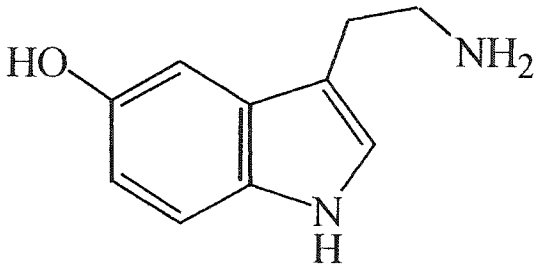

5-HT
5-hydroxytryptamine

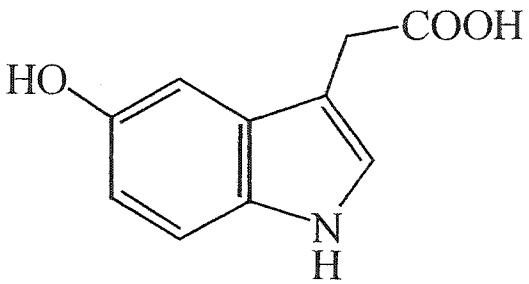

5-HIAA
5-hydroxyindole-3-acetic acid

Figure 2:01. L-DOPA, DA, 5-HT and their normal metabolites, 3-MT, DOPAC, HVA and 5-HIAA

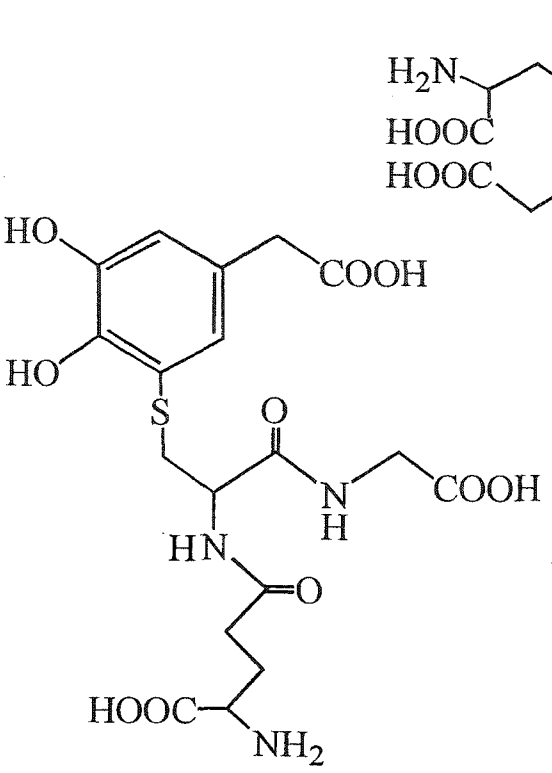

5-*S*-GS-DOPAC
5-*S*-glutathionyl-DOPAC

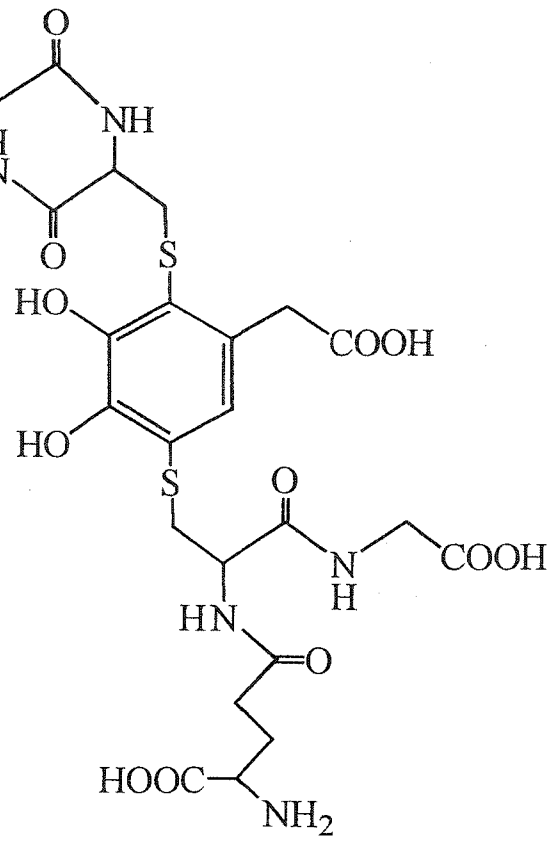

2,5-di-*S*-GS-DOPAC
2,5-di-*S*-glutathionyl-DOPAC

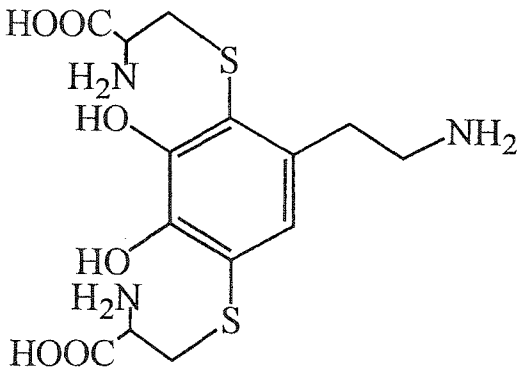

2,5-di-*S*-Cys-DA
2,5-di-*S*-cysteinyldopamine

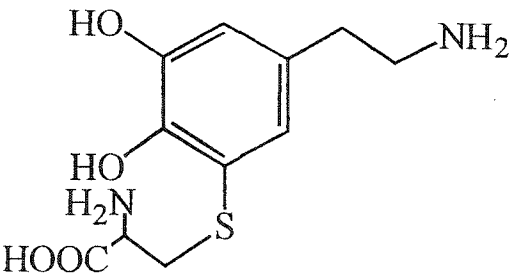

5-*S*-Cys-DA
5-*S*-cysteinyldopamine

Figure 2:02. Glutathionyl conjugates of DOPAC and cysteinyl conjugates of DA were synthesized by controlled potential electrochemical oxidation, isolated by preparative HPLC-UV, and identified by UV spectra and ESI-MS.

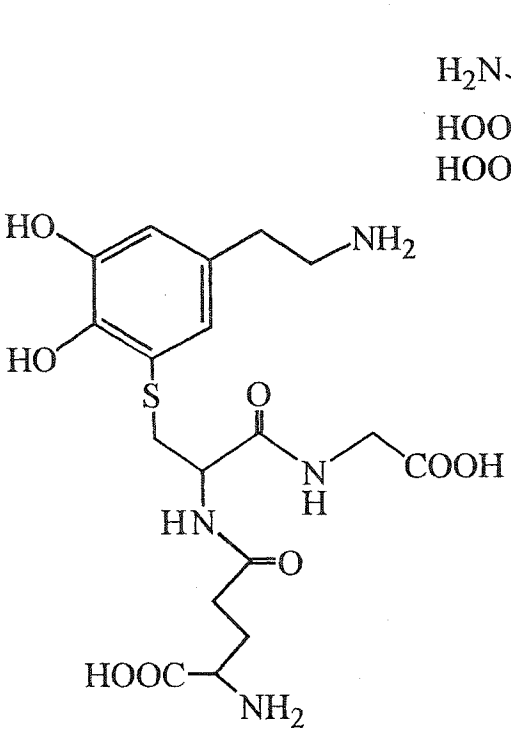

5-*S*-GS-DA
5-*S*-glutathionyl-dopamine

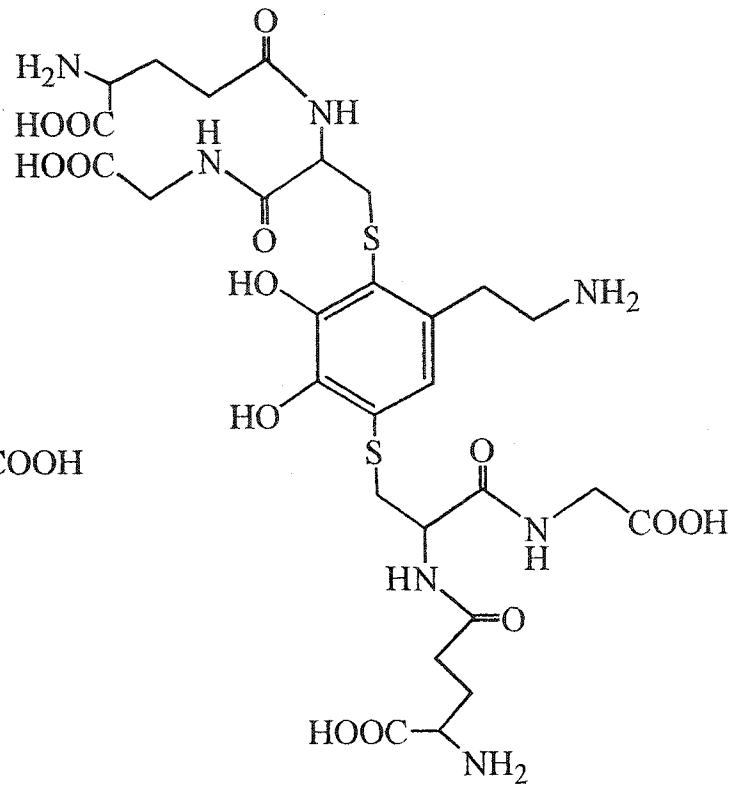

2,5-di-*S*-GS-DA
2,5-di-*S*-glutathionyl-dopamine

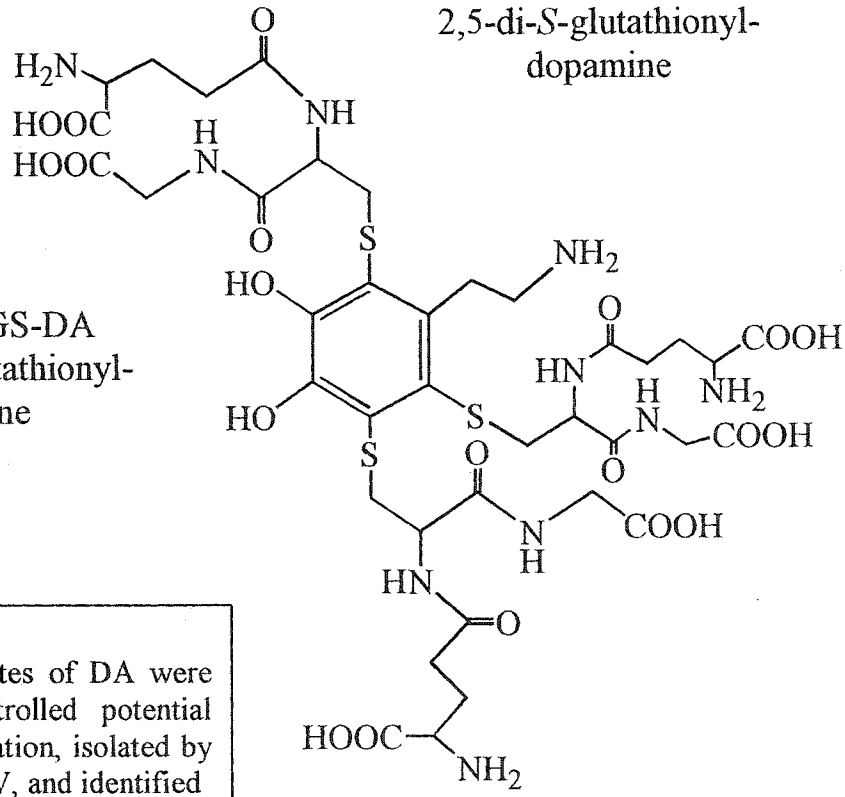

2,5,6-tri-*S*-GS-DA
2,5,6-tri-*S*-glutathionyl-dopamine

Figure 2:03.
Glutathionyl conjugates of DA were synthesized by controlled potential electrochemical oxidation, isolated by preparative HPLC-UV, and identified by UV spectra and ESI-MS.

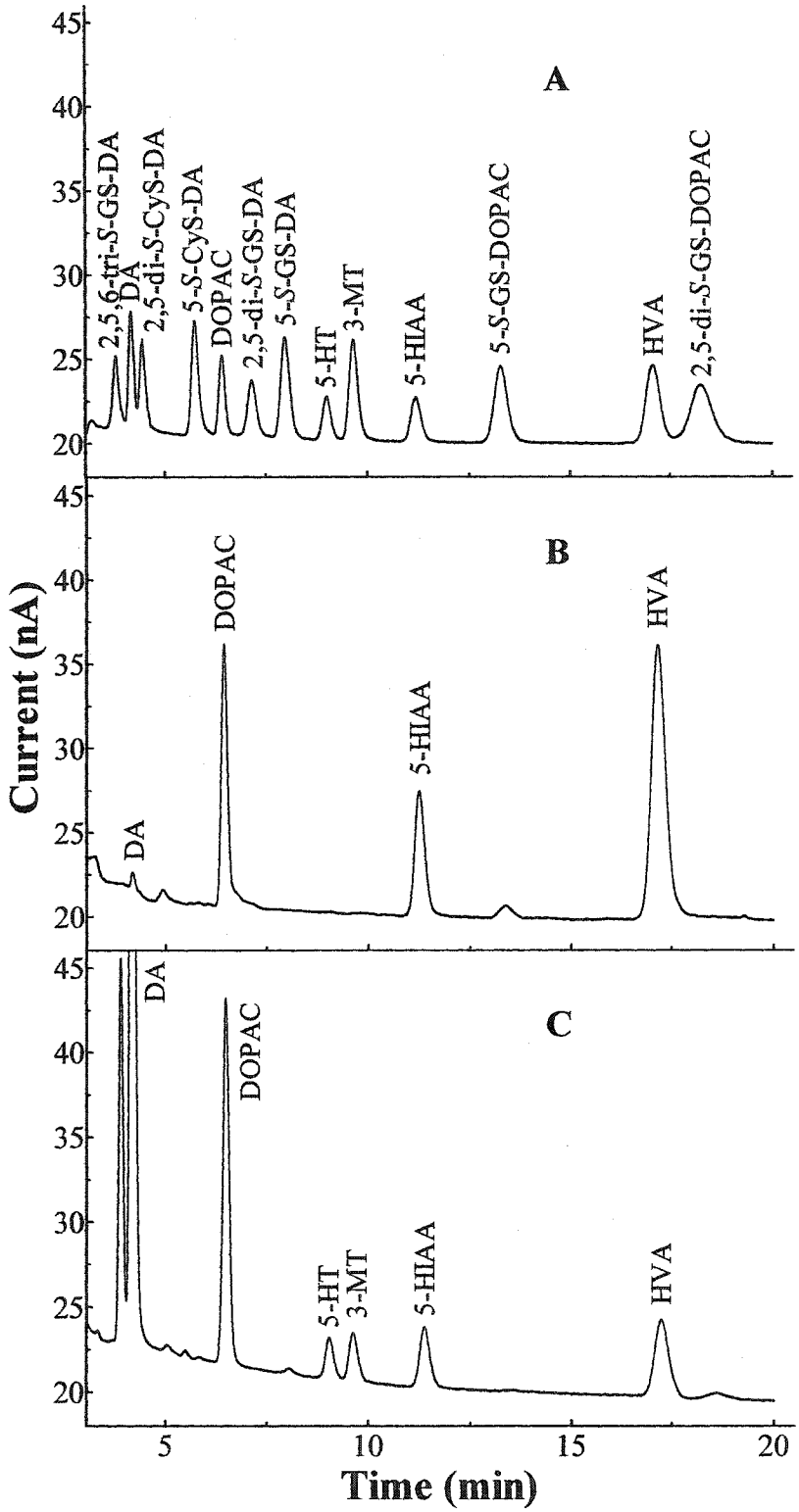

Figure 2:04. HPLC-EC chromatograms (method I) of: (A) standard mixture of DA, 5-HT, their metabolites and glutathionyl and cysteinyl conjugates of DA and DOPAC; (B) rat striatal dialysate collected prior to MPP^+ perfusion; and (C) rat striatal dialysate collected from 15 to 20 min after a 2.5 mM MPP^+ perfusion was terminated.

Chapter Two Figures

Figures 2:05-2:60. Time-dependent effects of a 30 min perfusion of MPP^+ (0.7 - 10.0 mM) in the absence and presence of continuous perfusion of 1.0 mM ACV into rat striatum on dialysate levels of L-DOPA, DA, DOPAC, 5-HT, 3-MT, 5-HIAA and HVA on day 1 and an identical perfusion on day 2. Horizontal black bar shows period during which MPP^+ entered the brain. $^*p < 0.05$; $^{**}p < 0.01$ compared to basal levels measured on day 1 or day 2. $^{\#}p < 0.05$ when basal dialysate concentration on day 2 was compared to day 1. Data are mean ± SEM (n = 4).

Figures 2:61-2:74. Maximum efflux of L-DOPA, DA, DOPAC, 5-HT, 3-MT, 5-HIAA and HVA evoked by 30 min perfusions of MPP^+ (0.0-10.0 mM) in the absence and presence of continuous perfusion of 1.0 mM ACV into the awake striatum on day 1 and day 2. A significant difference between L-DOPA, DA, DOPAC, 5-HT, 3-MT, 5-HIAA and HVA efflux versus basal efflux is indicated by $^*p < 0.05$; $^{**}p < 0.01$; $^{***}p < 0.001$. A significant difference between L-DOPA, DA, DOPAC, 5-HT, 3-MT, 5-HIAA and HVA efflux on day 1 or day 2 compared to that evoked by the immediate lower concentration is indicated by $^{x}p < 0.05$; $^{xx}p < 0.01$. A significant difference between the day 2 and day 1 efflux is indicated by $^{\#}p < 0.05$; $^{\#\#}p < 0.01$; $^{\#\#\#}p < 0.001$. A significant difference between L-DOPA, DA, DOPAC, 5-HT, 3-MT, 5-HIAA and HVA efflux on day 1 or day 2 when 1.0 mM ACV was perfused before, during and after (0.0-10.0 mM) MPP^+ versus to identical perfusion in the absence of ACV is indicated by $^{+}p < 0.05$; $^{++}p < 0.01$. Data are mean ± SEM (n = 4).

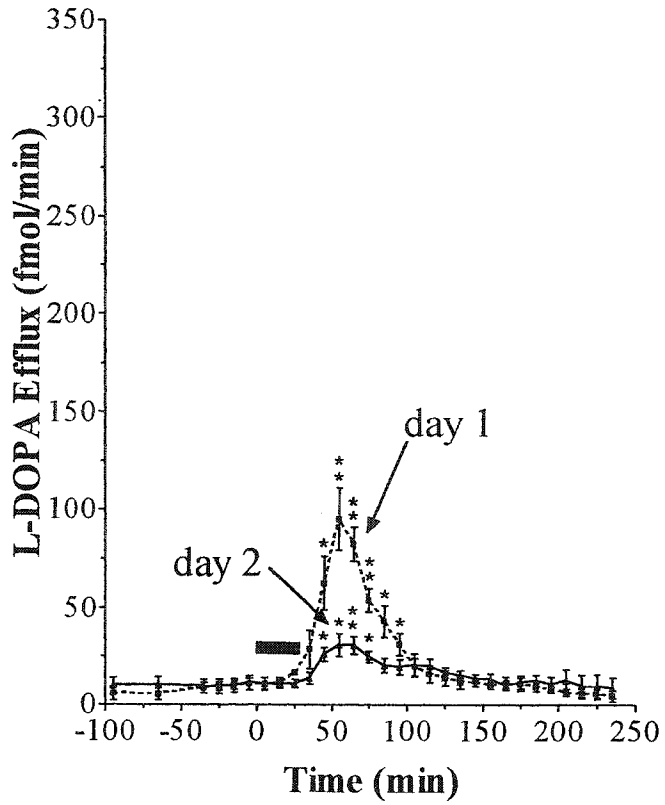

Figure 2:05.
0.7 mM MPP^+;
L-DOPA Efflux (fmol/min)
vs. Time (min), n = 4.

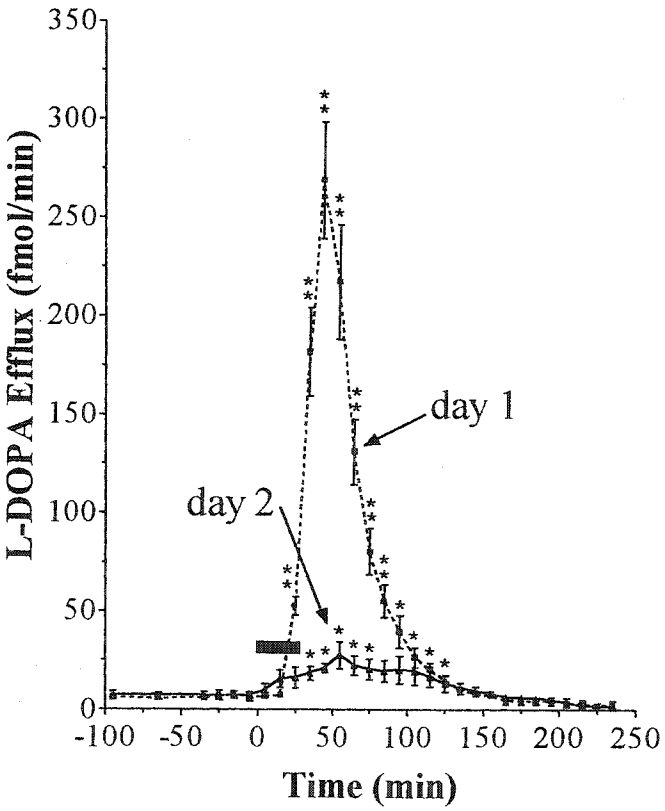

Figure 2:06.
0.7 mM MPP^+ with
1.0 mM ACV;
L-DOPA Efflux (fmol/min)
vs. Time (min), n = 4.

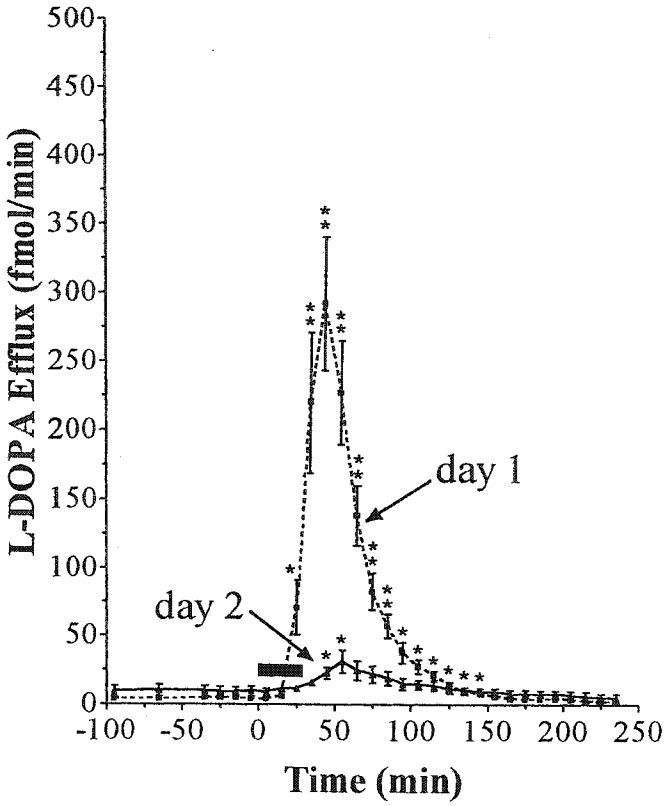

Figure 2:07.
1.3 mM MPP^+;
L-DOPA Efflux (fmol/min)
vs. Time (min), n = 4.

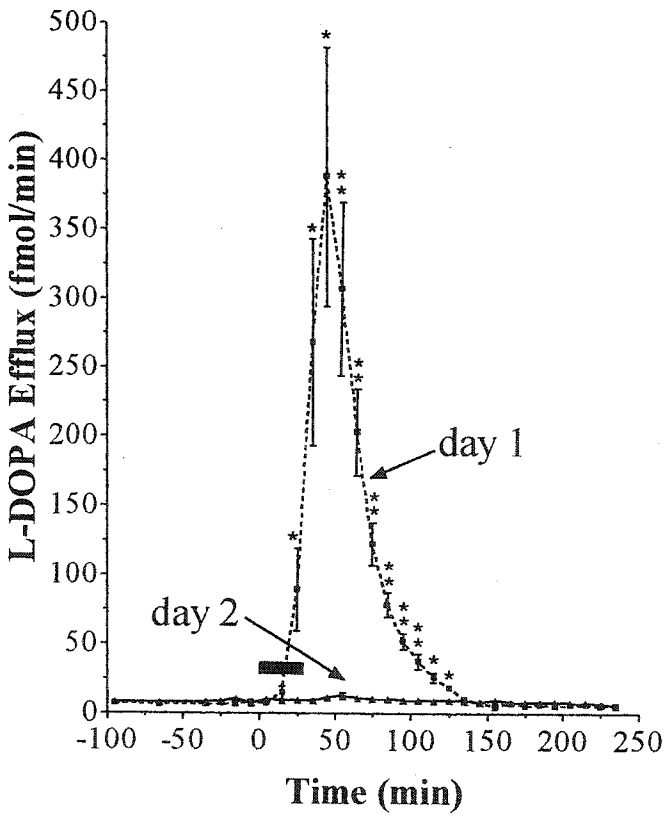

Figure 2:08.
1.3 mM MPP^+ with
1.0 mM ACV;
L-DOPA Efflux (fmol/min)
vs. Time (min), n = 4.

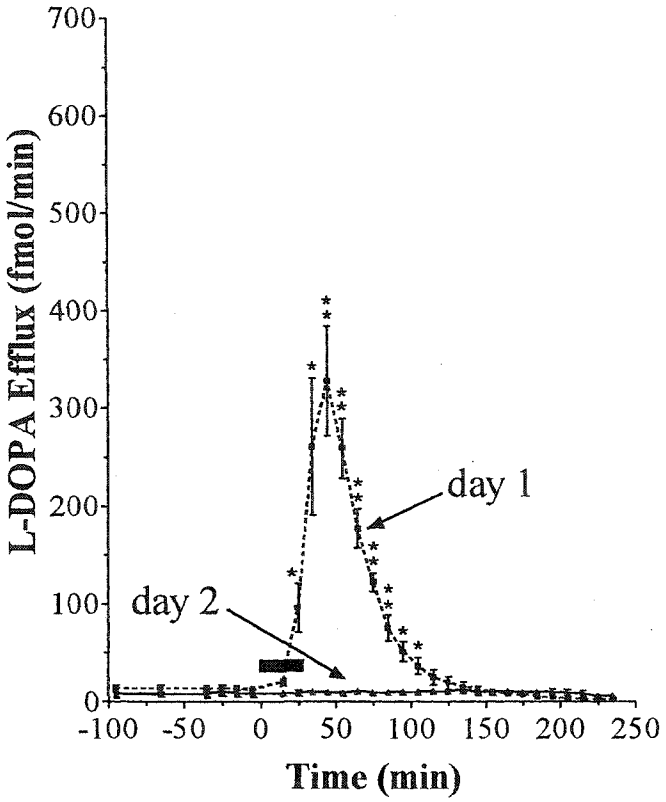

Figure 2:09.
2.5 mM MPP^+;
L-DOPA Efflux (fmol/min)
vs. Time (min), n = 4.

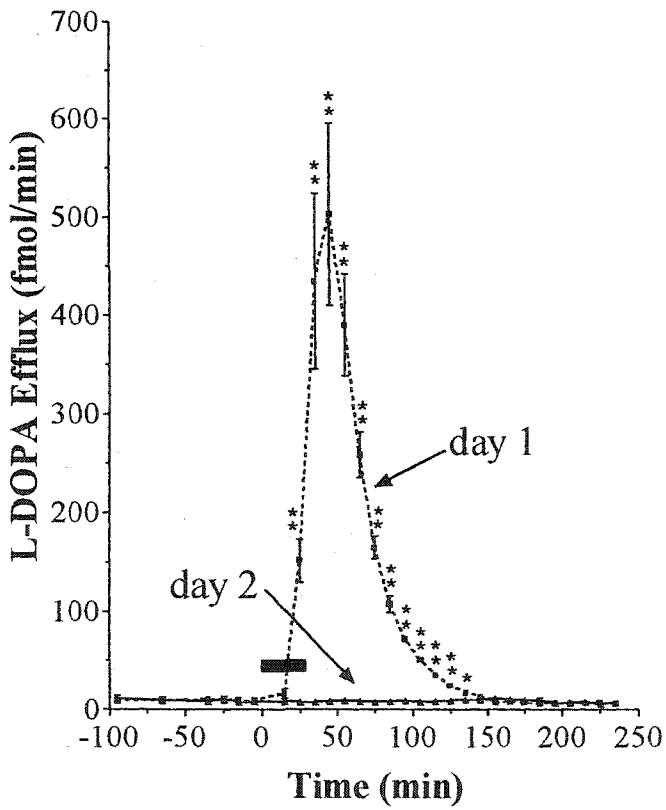

Figure 2:10.
2.5 mM MPP^+ with
1.0 mM ACV;
L-DOPA Efflux (fmol/min)
vs. Time (min), n = 4.

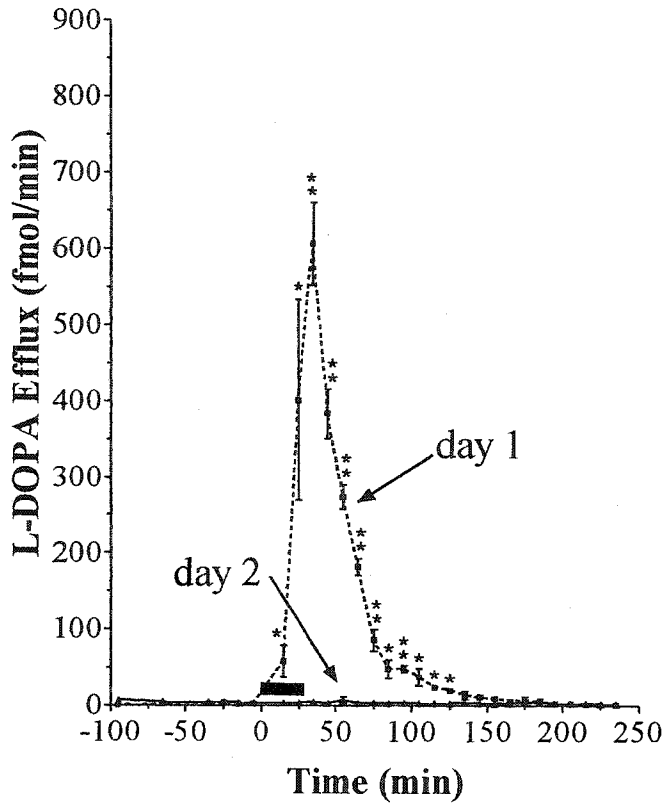

Figure 2:11.
10.0 mM MPP^+;
L-DOPA Efflux (fmol/min)
vs. Time (min), n = 4.

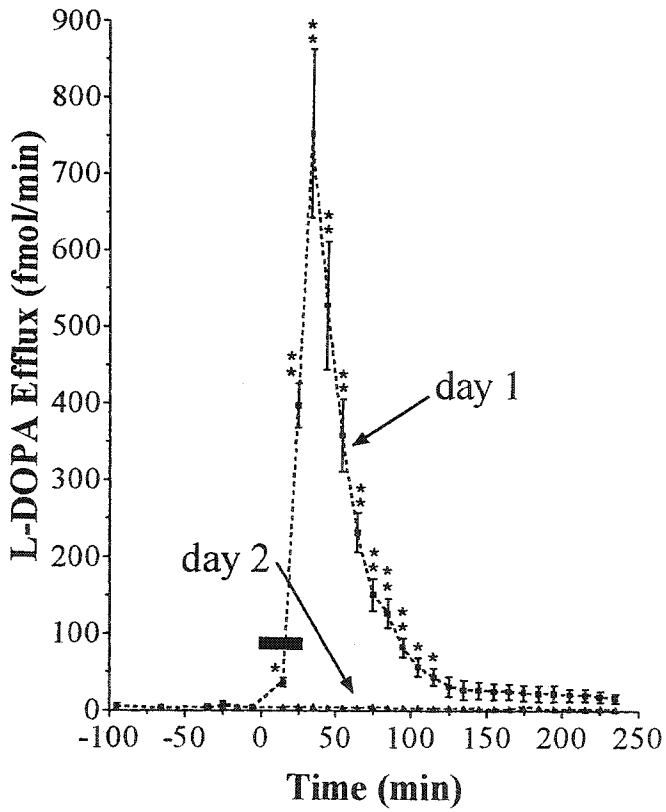

Figure 2:12.
10.0 mM MPP^+ with
1.0 mM ACV;
L-DOPA Efflux (fmol/min)
vs. Time (min), n = 4.

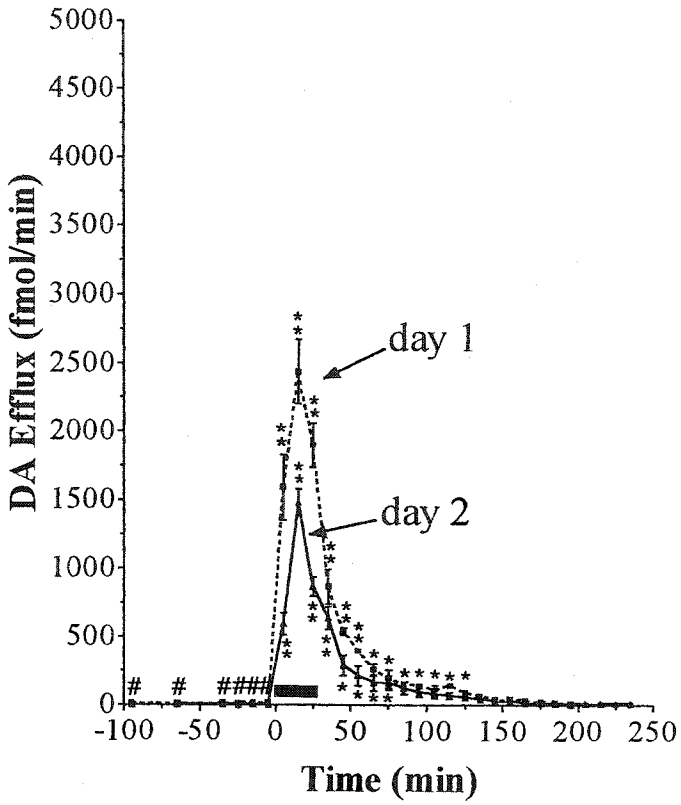

Figure 2:13.
0.7 mM MPP^+;
DA Efflux (fmol/min)
vs. Time (min), n = 4.

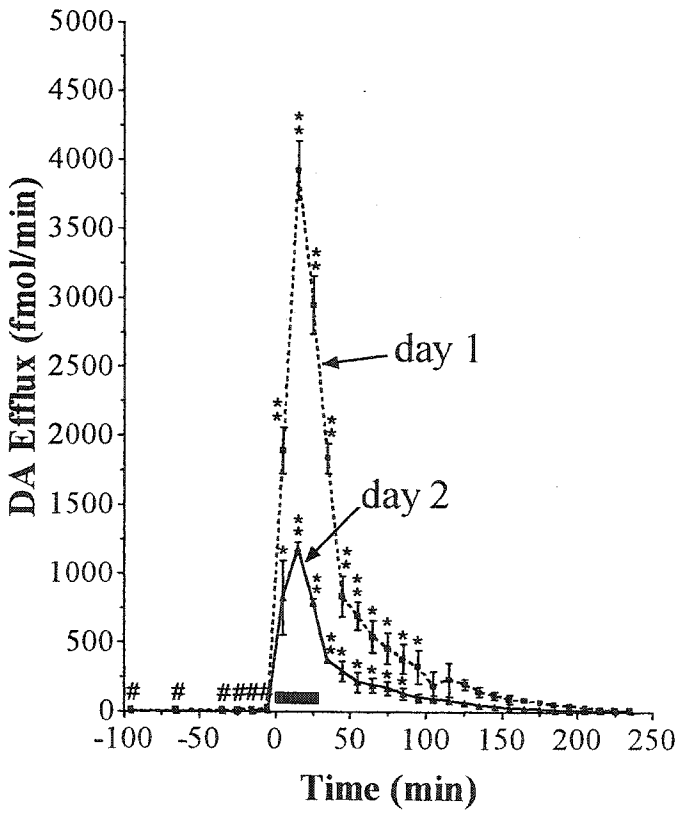

Figure 2:14.
0.7 mM MPP^+ with
1.0 mM ACV;
DA Efflux (fmol/min)
vs. Time (min), n = 4.

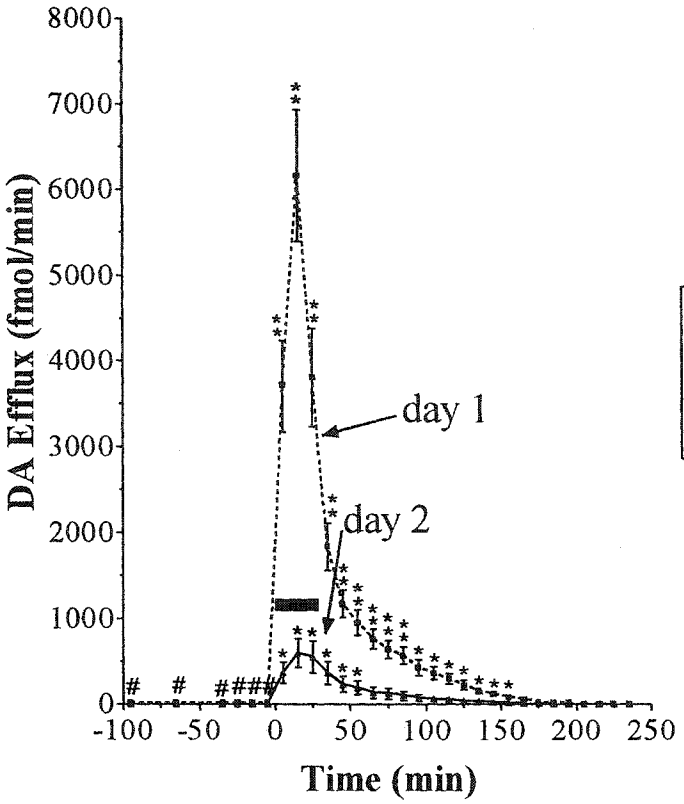

Figure 2:15.
1.3 mM MPP^+;
DA Efflux (fmol/min)
vs. Time (min), n = 4.

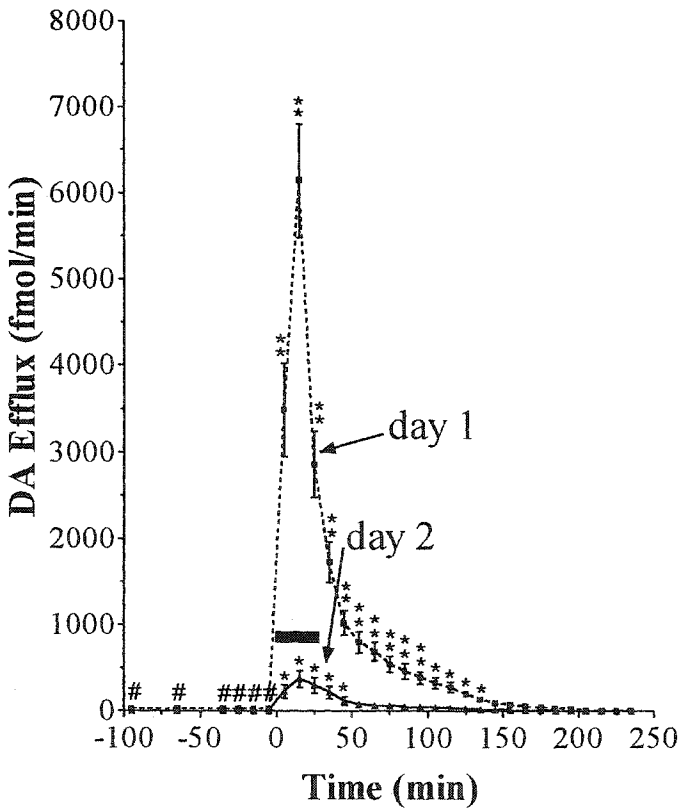

Figure 2:16.
1.3 mM MPP^+ with
1.0 mM ACV;
DA Efflux (fmol/min)
vs. Time (min), n = 4.

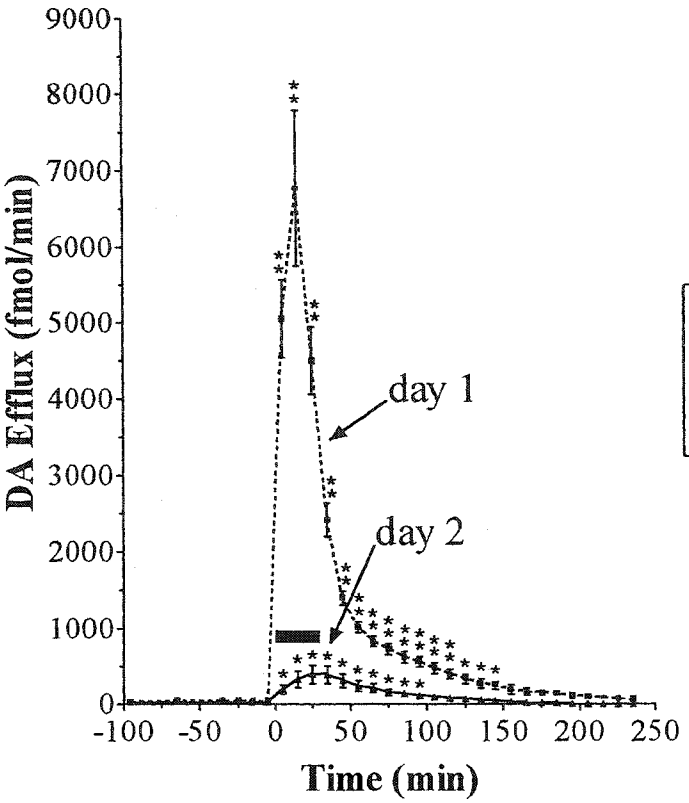

Figure 2:17.
2.5 mM MPP^+;
DA Efflux (fmol/min)
vs. Time (min), n = 4.

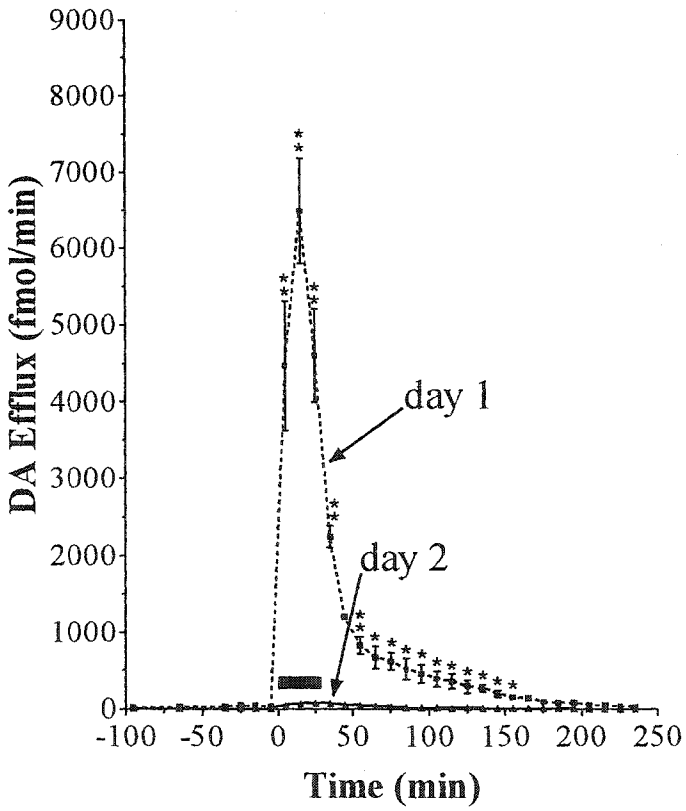

Figure 2:18.
2.5 mM MPP^+ with
1.0 mM ACV;
DA Efflux (fmol/min)
vs. Time (min), n = 4.

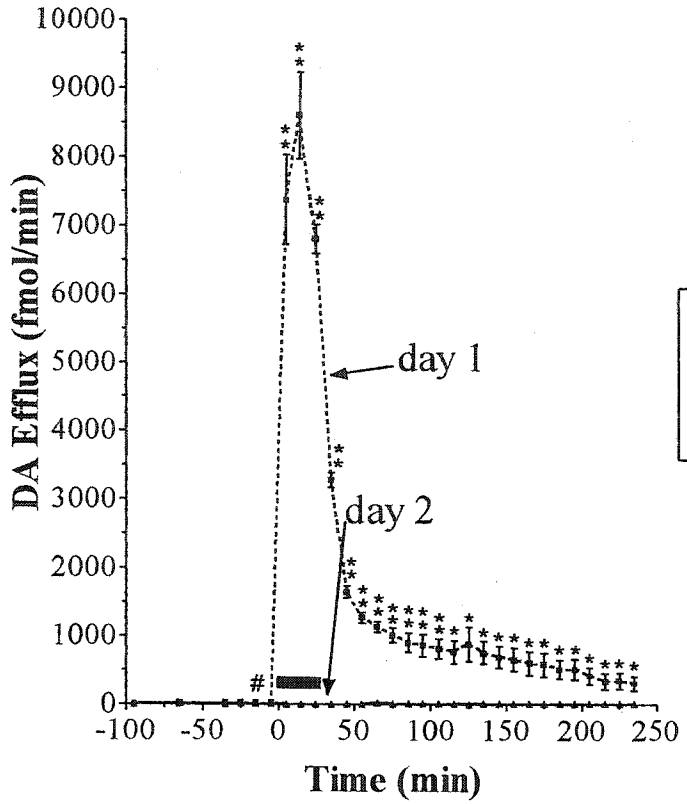

Figure 2:19.
10.0 mM MPP^+;
DA Efflux (fmol/min)
vs. Time (min), n = 4.

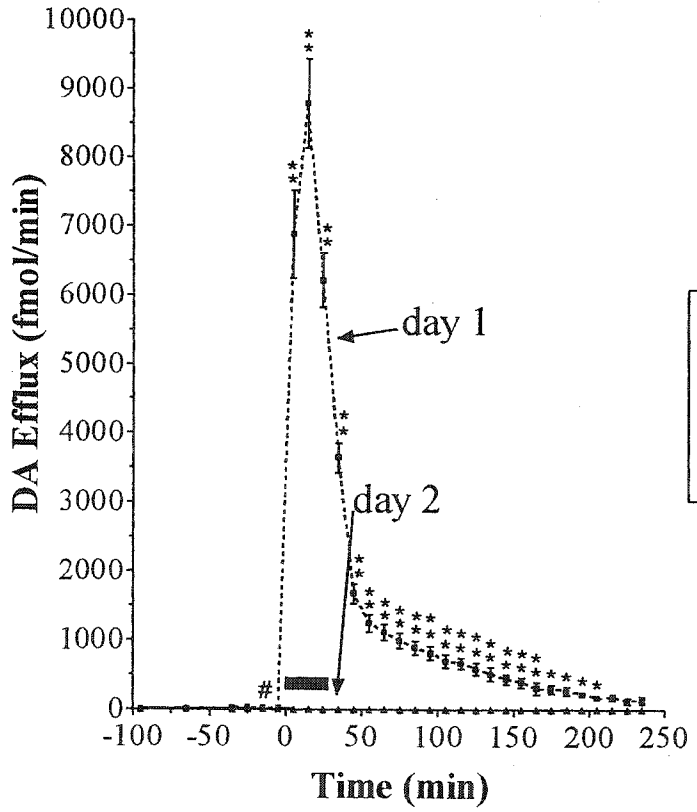

Figure 2:20.
10.0 mM MPP^+ with
1.0 mM ACV;
DA Efflux (fmol/min)
vs. Time (min), n = 4.

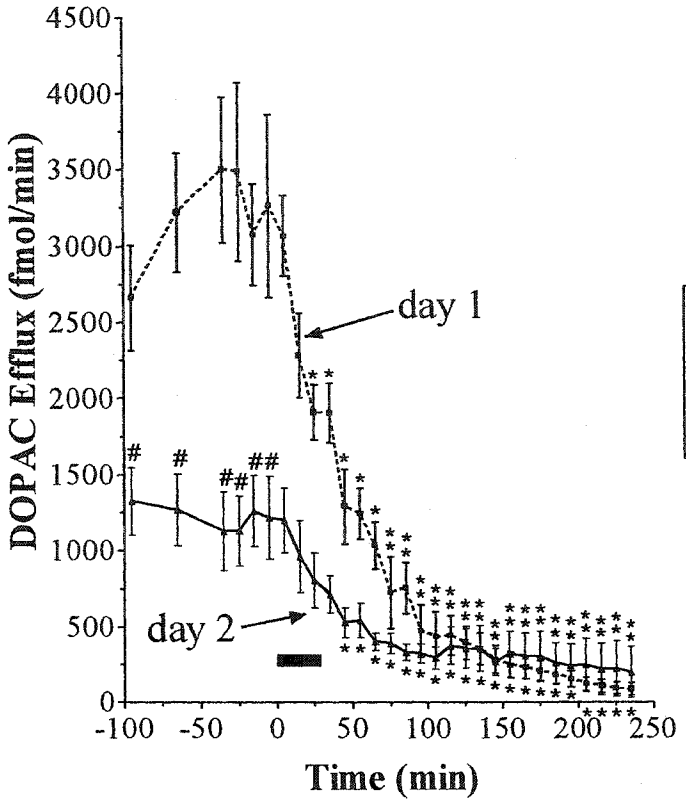

Figure 2:21.
0.7 mM MPP^+;
DOPAC Efflux (fmol/min)
vs. Time (min), n = 4.

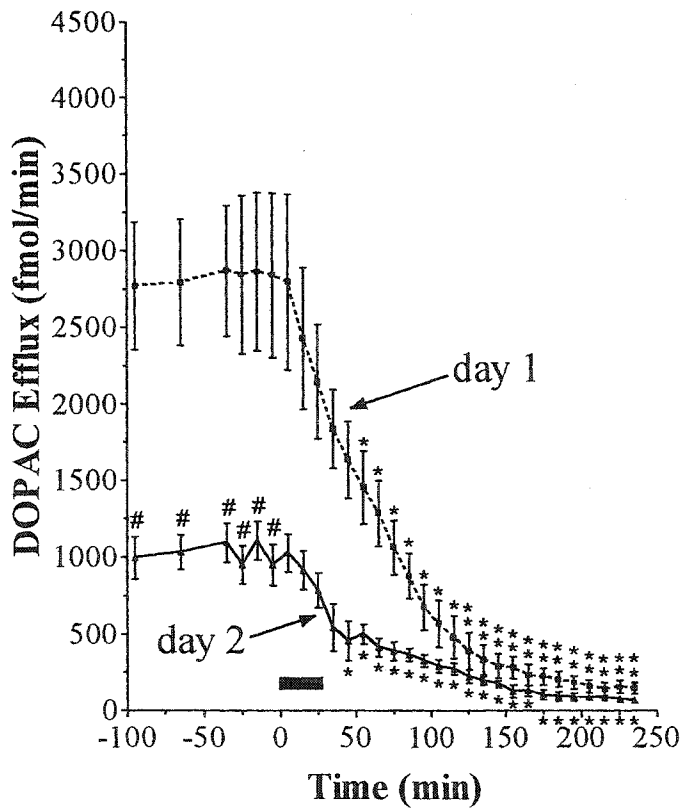

Figure 2:22.
0.7 mM MPP^+ with
1.0 mM ACV;
DOPAC Efflux (fmol/min)
vs. Time (min), n = 4.

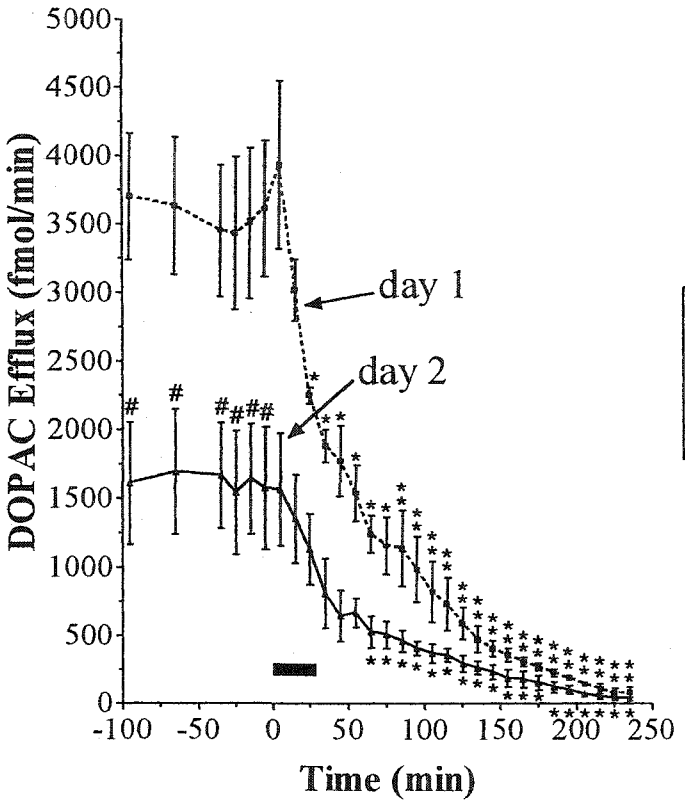

Figure 2:23.
1.3 mM MPP^+;
DOPAC Efflux (fmol/min)
vs. Time (min), n = 4.

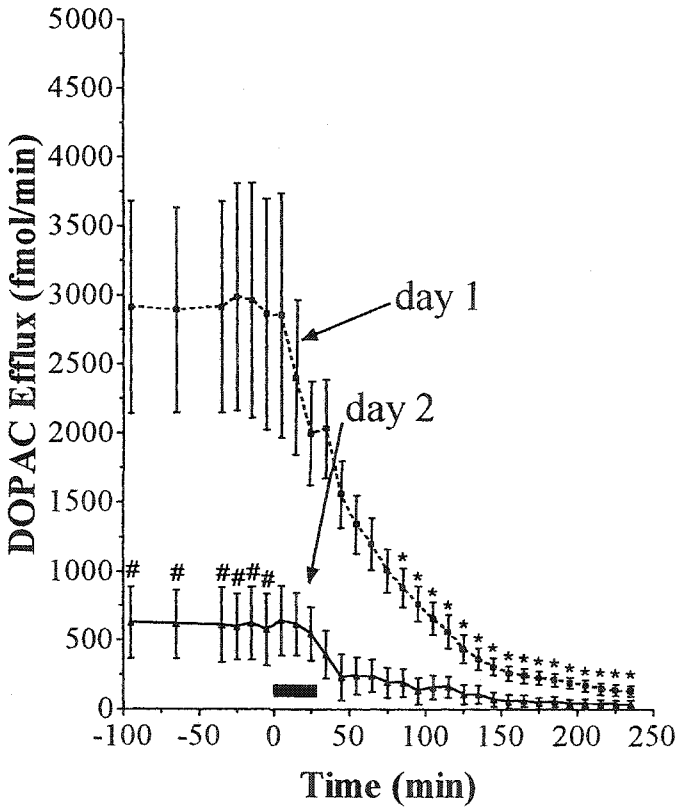

Figure 2:24.
1.3 mM MPP^+ with
1.0 mM ACV;
DOPAC Efflux (fmol/min)
vs. Time (min), n = 4.

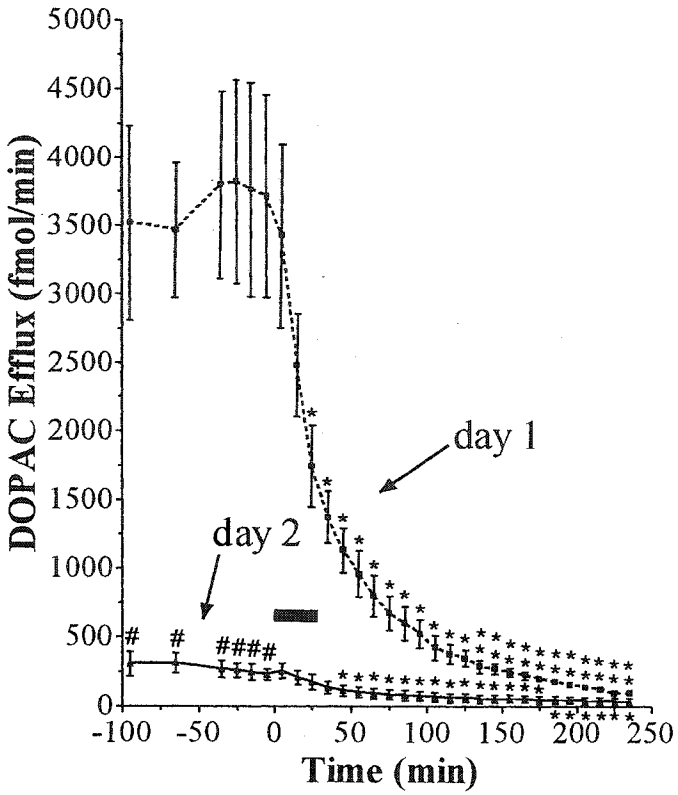

Figure 2:25.
2.5 mM MPP^+;
DOPAC Efflux (fmol/min)
vs. Time (min), n = 4.

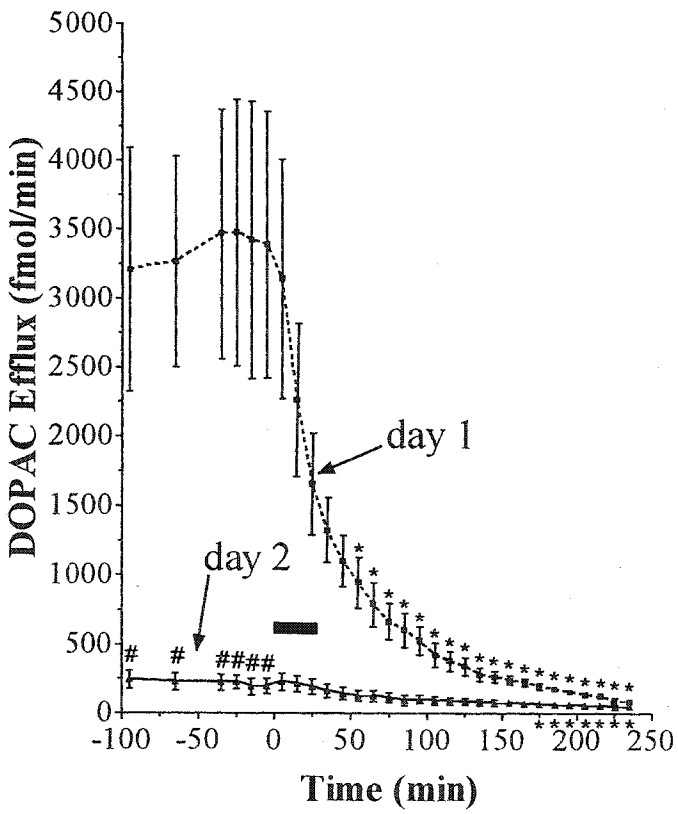

Figure 2:26.
2.5 mM MPP^+ with
1.0 mM ACV;
DOPAC Efflux (fmol/min)
vs. Time (min), n = 4.

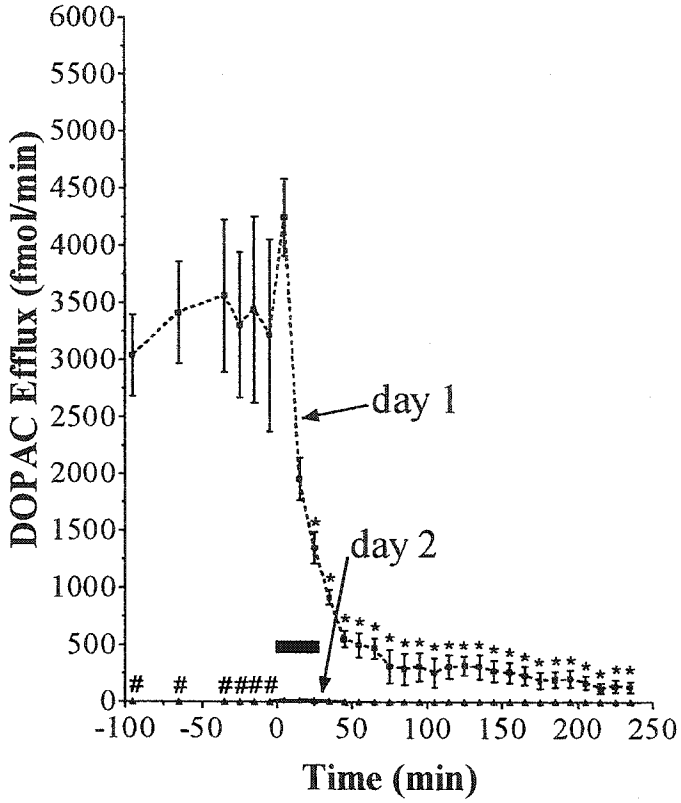

Figure 2:27.
10.0 mM MPP^+;
DOPAC Efflux (fmol/min)
vs. Time (min), n = 4.

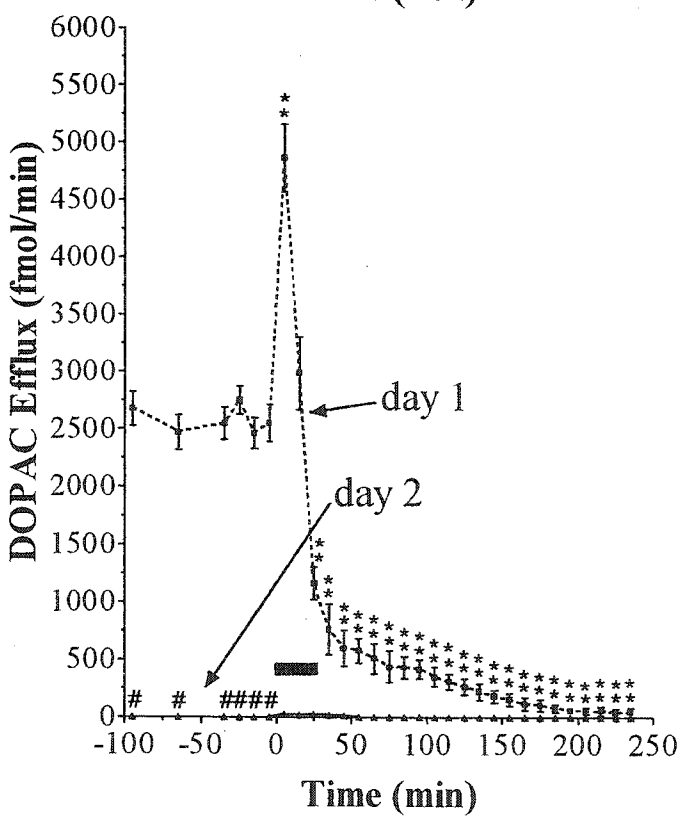

Figure 2:28.
10.0 mM MPP^+ with
1.0 mM ACV;
DOPAC Efflux (fmol/min)
vs. Time (min), n = 4.

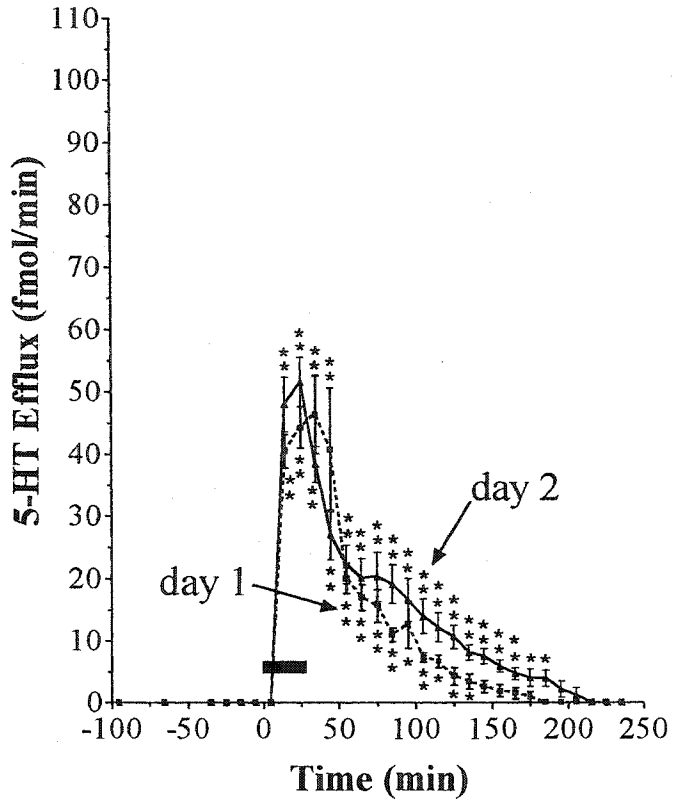

Figure 2:29.
0.7 mM MPP^+;
5-HT Efflux (fmol/min)
vs. Time (min), n = 4.

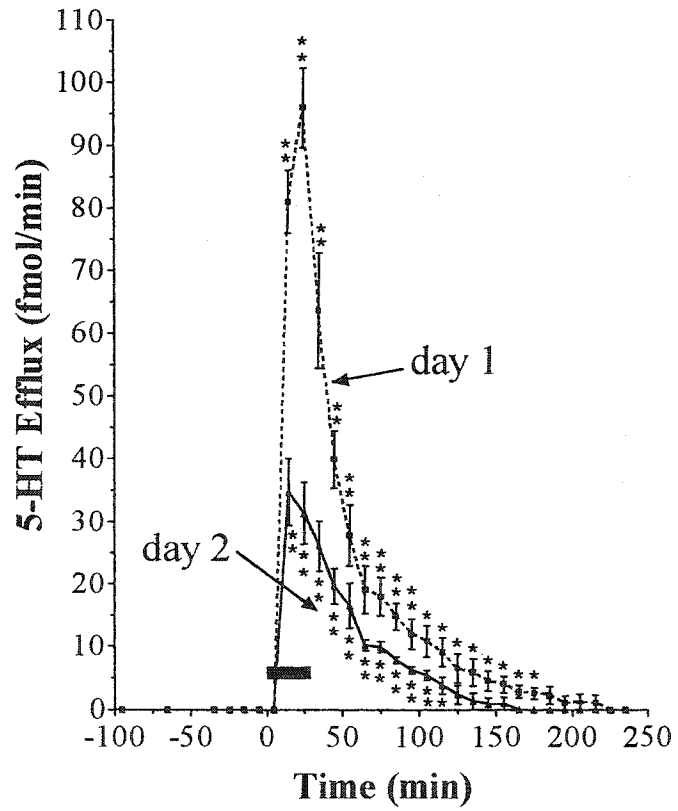

Figure 2:30.
0.7 mM MPP^+ with
1.0 mM ACV;
5-HT Efflux (fmol/min)
vs. Time (min), n = 4.

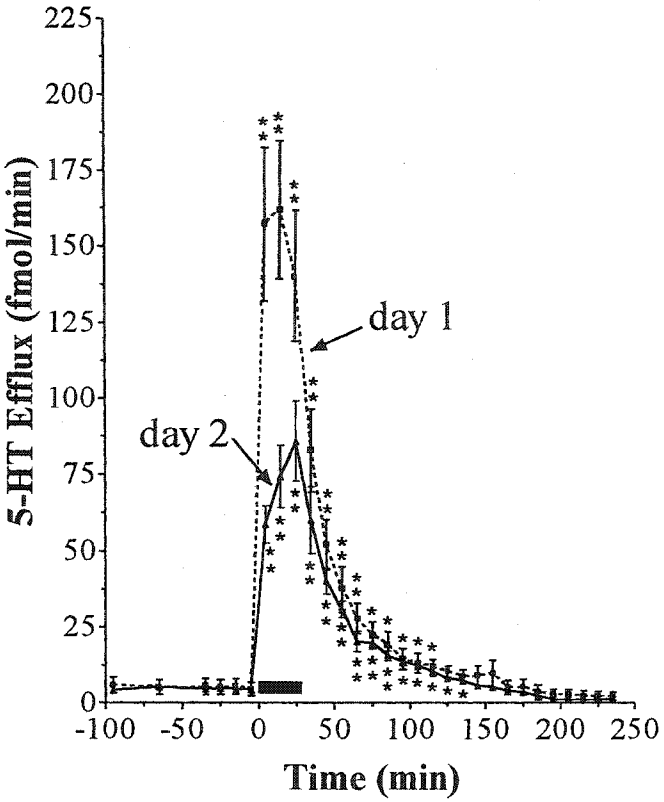

Figure 2:31.
1.3 mM MPP^+;
5-HT Efflux (fmol/min)
vs. Time (min), n = 4.

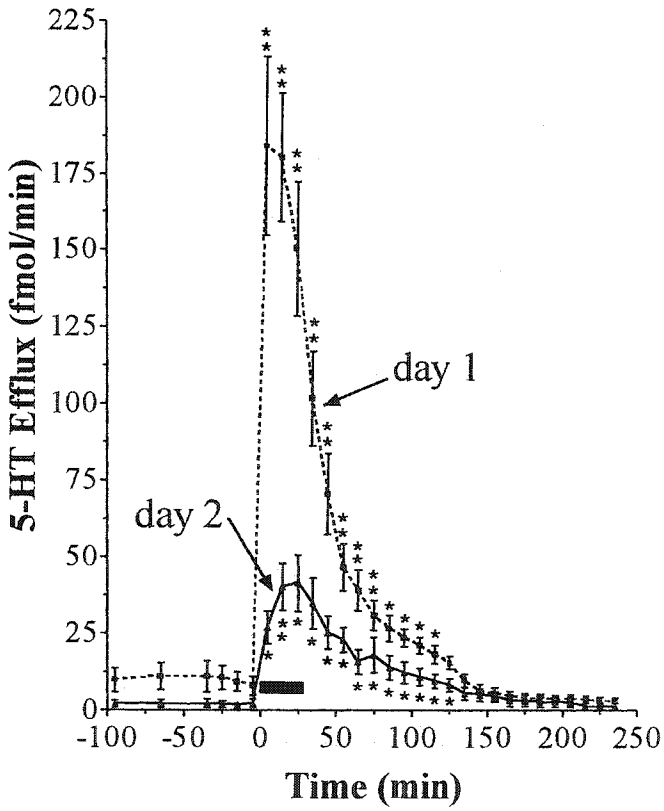

Figure 2:32.
1.3 mM MPP^+ with
1.0 mM ACV;
5-HT Efflux (fmol/min)
vs. Time (min), n = 4.

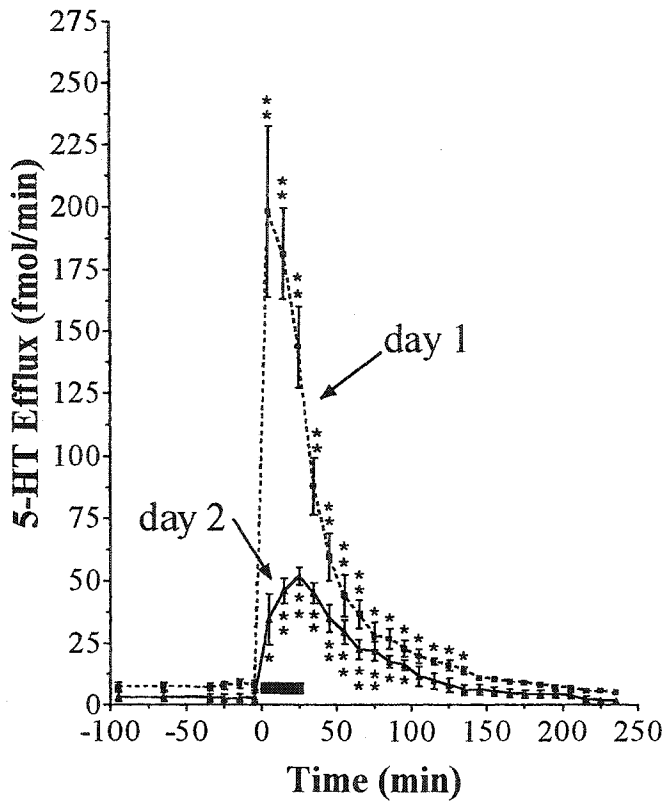

Figure 2:33.
2.5 mM MPP^+;
5-HT Efflux (fmol/min)
vs. Time (min), n = 4.

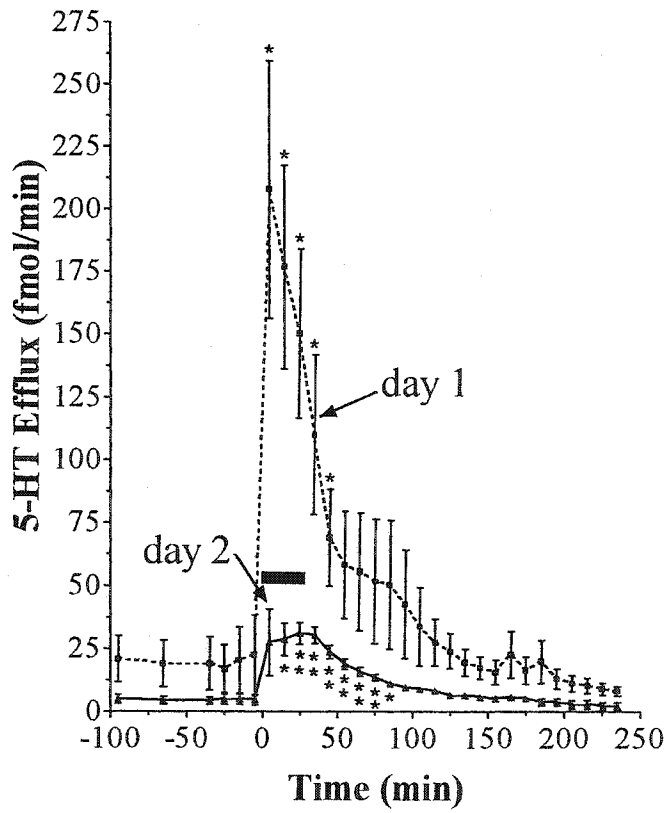

Figure 2:34.
2.5 mM MPP^+ with
1.0 mM ACV;
5-HT Efflux (fmol/min)
vs. Time (min), n = 4.

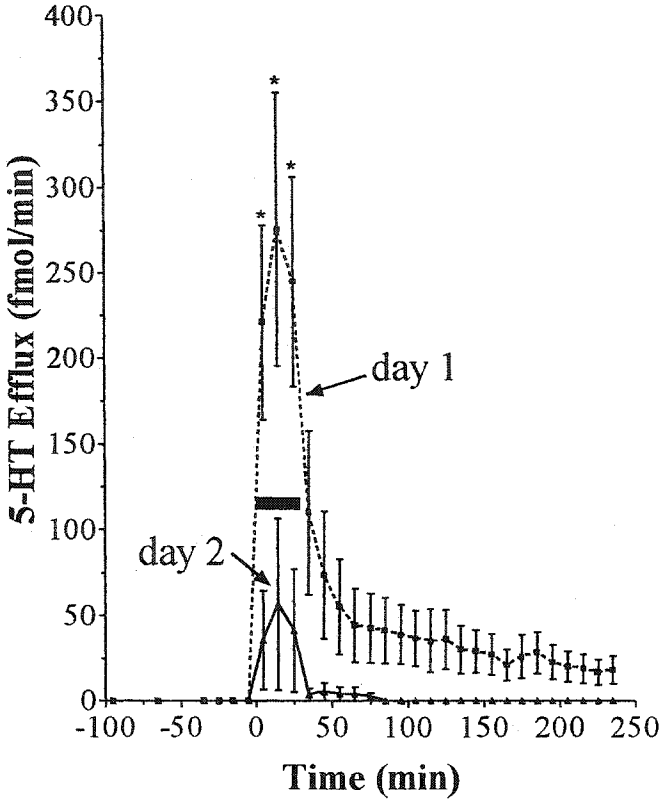

Figure 2:35.
10.0 mM MPP^+;
5-HT Efflux (fmol/min)
vs. Time (min), n = 4.

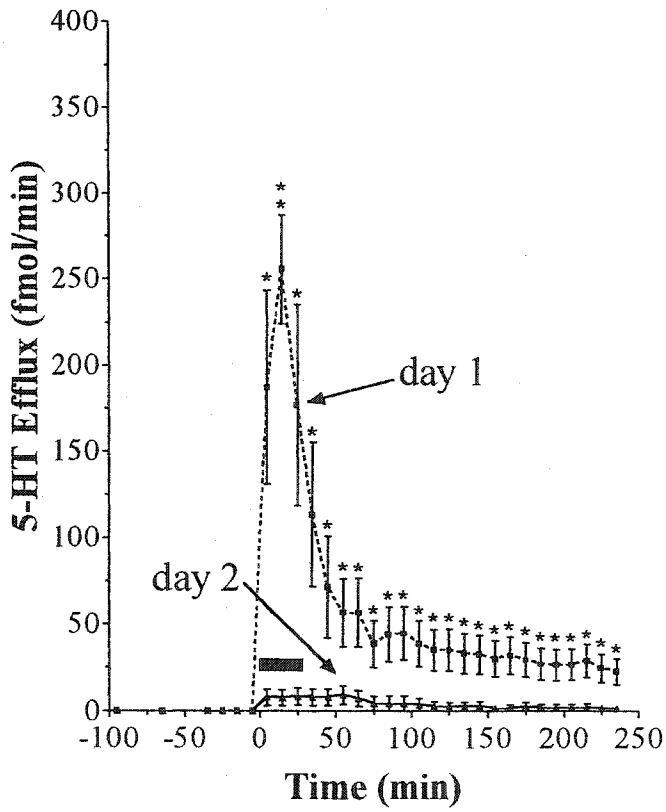

Figure 2:36.
10.0 mM MPP^+ with
1.0 mM ACV;
5-HT Efflux (fmol/min)
vs. Time (min), n = 4.

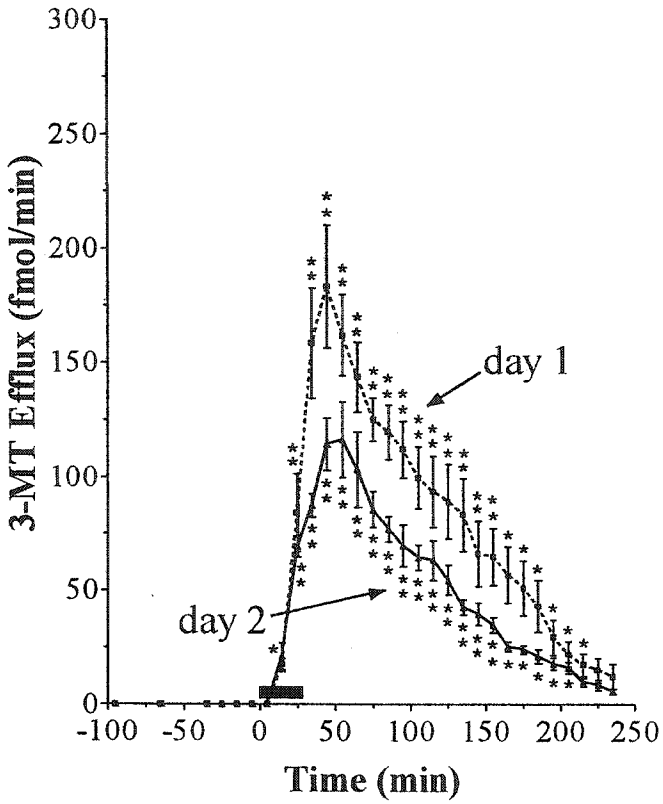

Figure 2:37.
0.7 mM MPP^+;
3-MT Efflux (fmol/min)
vs. Time (min), n = 4.

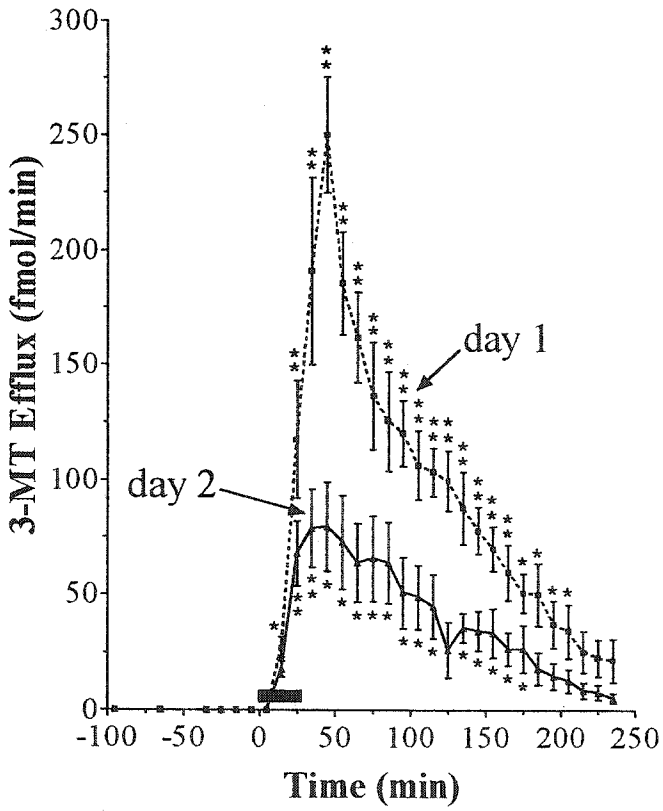

Figure 2:38.
0.7 mM MPP^+ with
1.0 mM ACV;
3-MT Efflux (fmol/min)
vs. Time (min), n = 4.

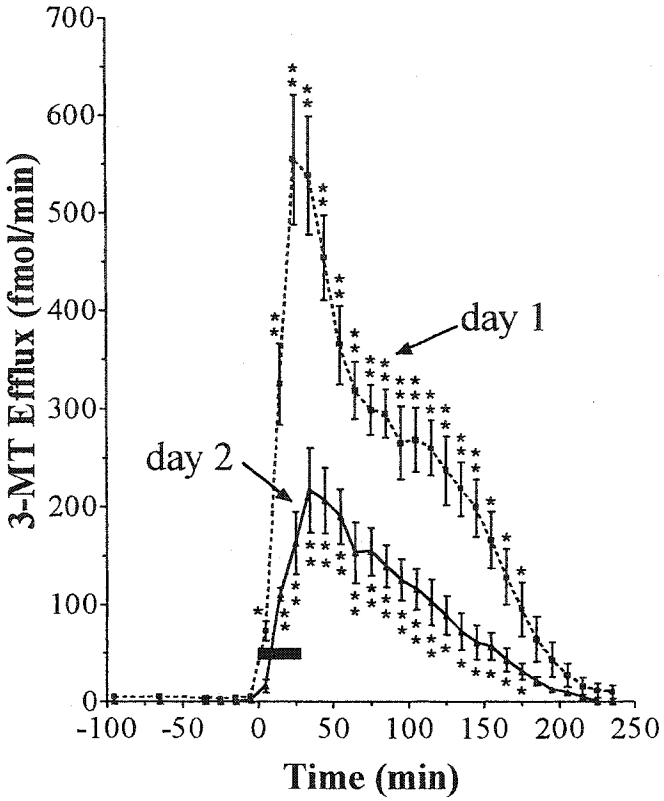

Figure 2:39.
1.3 mM MPP^+;
3-MT Efflux (fmol/min)
vs. Time (min), n = 4.

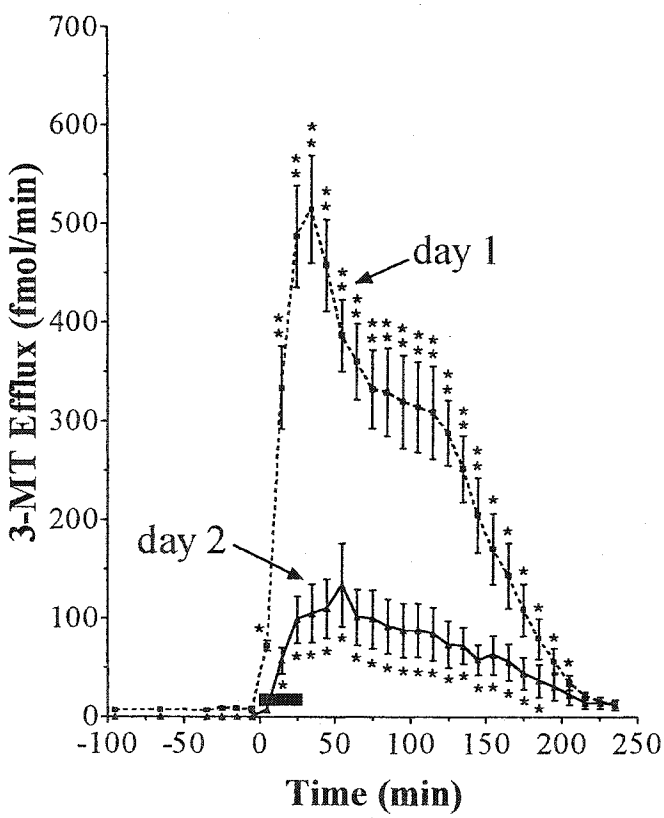

Figure 2:40.
1.3 mM MPP^+ with
1.0 mM ACV;
3-MT Efflux (fmol/min)
vs. Time (min), n = 4.

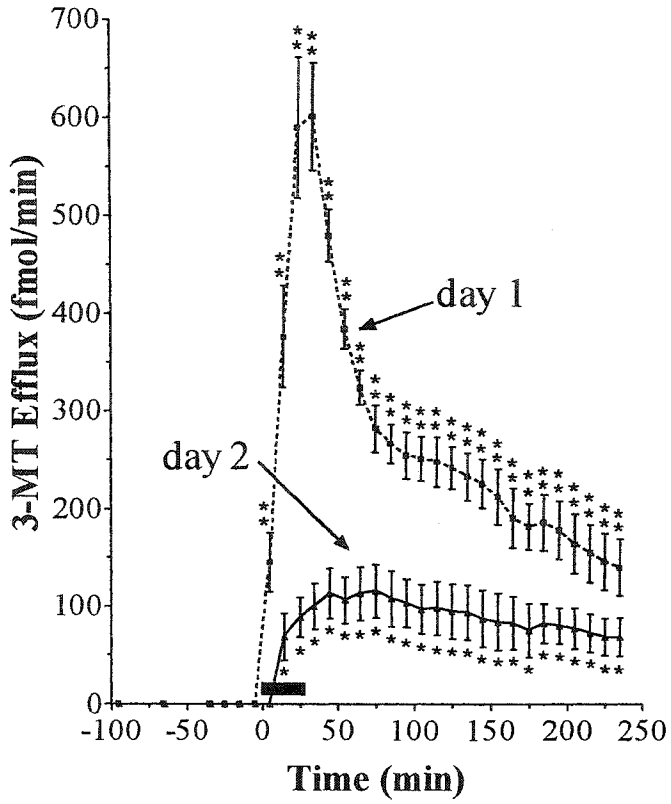

Figure 2:41.
2.5 mM MPP^+;
3-MT Efflux (fmol/min)
vs. Time (min), n = 4.

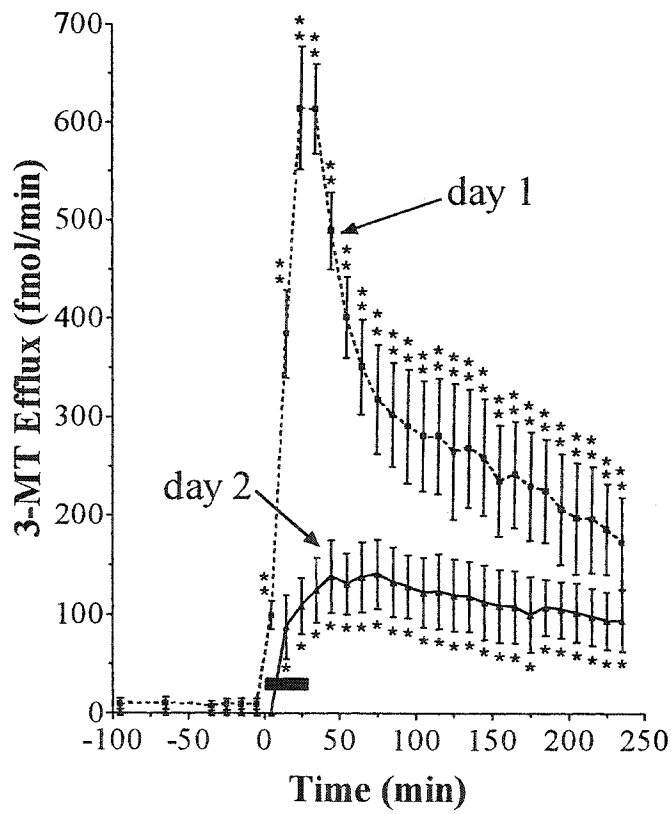

Figure 2:42
2.5 mM MPP^+ with
1.0 mM ACV;
3-MT Efflux (fmol/min)
vs. Time (min), n = 4.

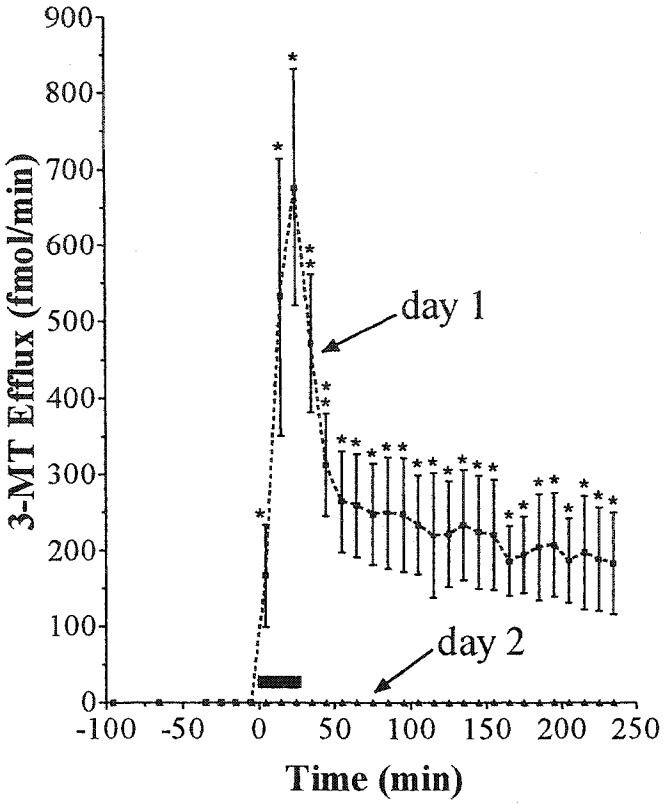

Figure 2:43.
10.0 mM MPP^+;
3-MT Efflux (fmol/min)
vs. Time (min), n = 4.

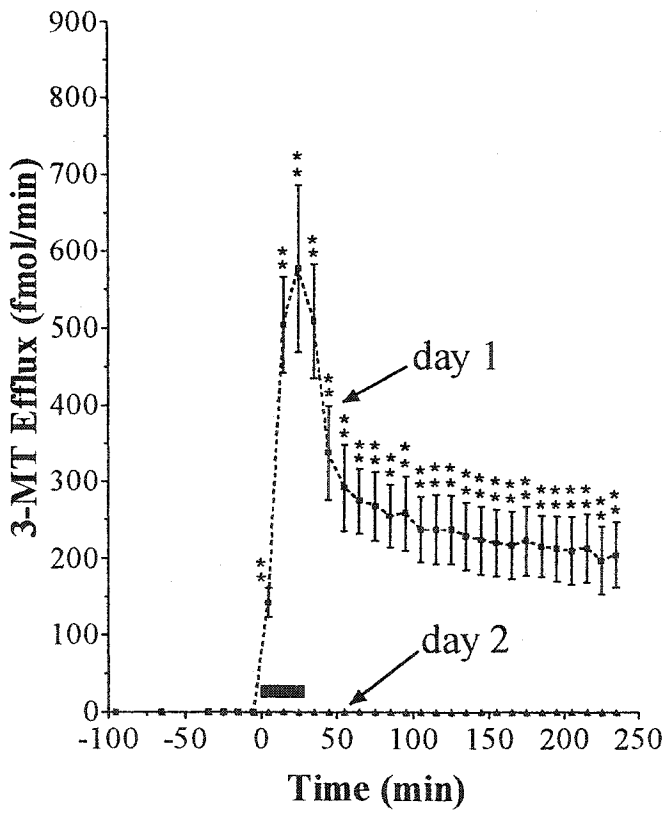

Figure 2:44.
10.0 mM MPP^+ with
1.0 mM ACV;
3-MT Efflux (fmol/min)
vs. Time (min), n = 4.

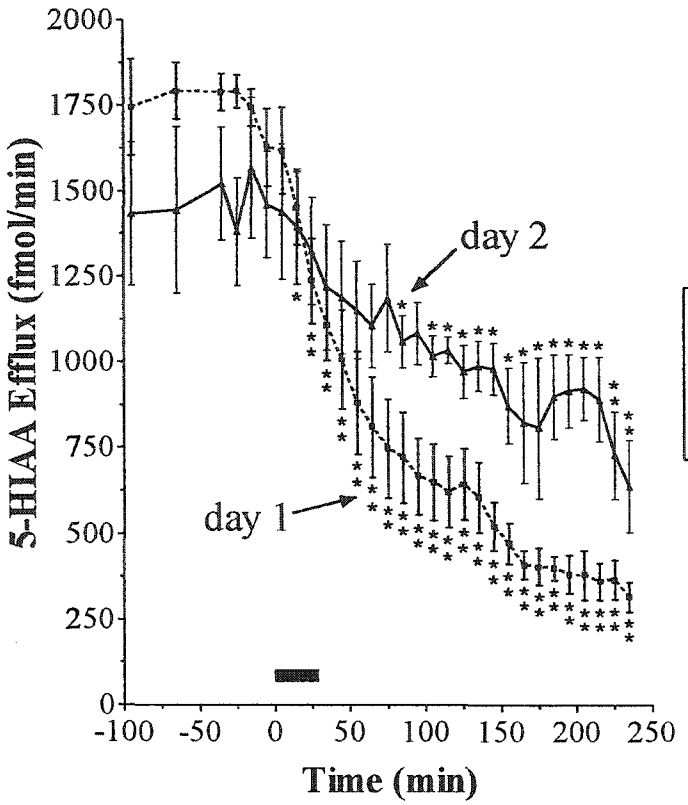

Figure 2:45.
0.7 mM MPP^+;
5-HIAA Efflux (fmol/min)
vs. Time (min), n = 4.

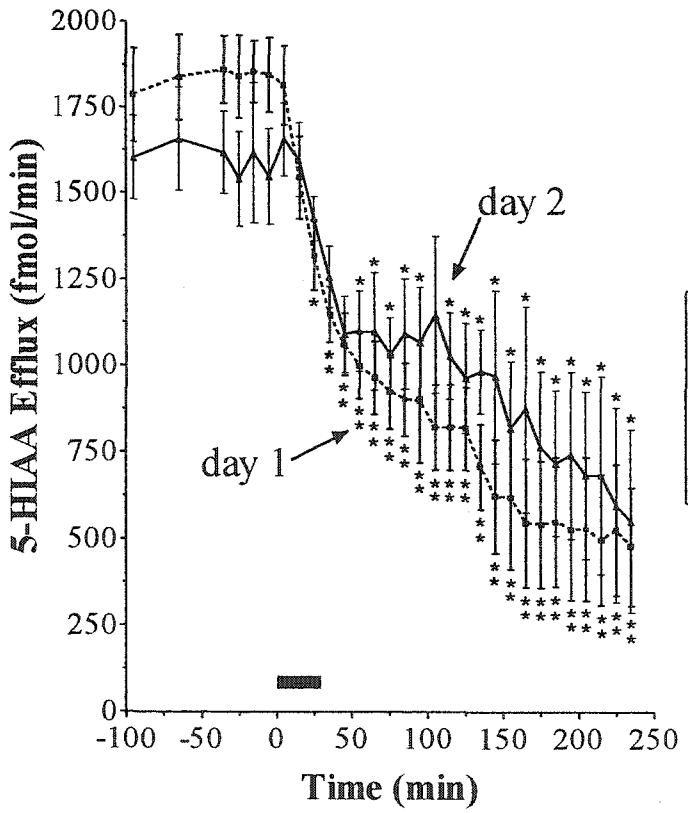

Figure 2:46.
0.7 mM MPP^+ with
1.0 mM ACV;
5-HIAA Efflux (fmol/min)
vs. Time (min), n = 4.

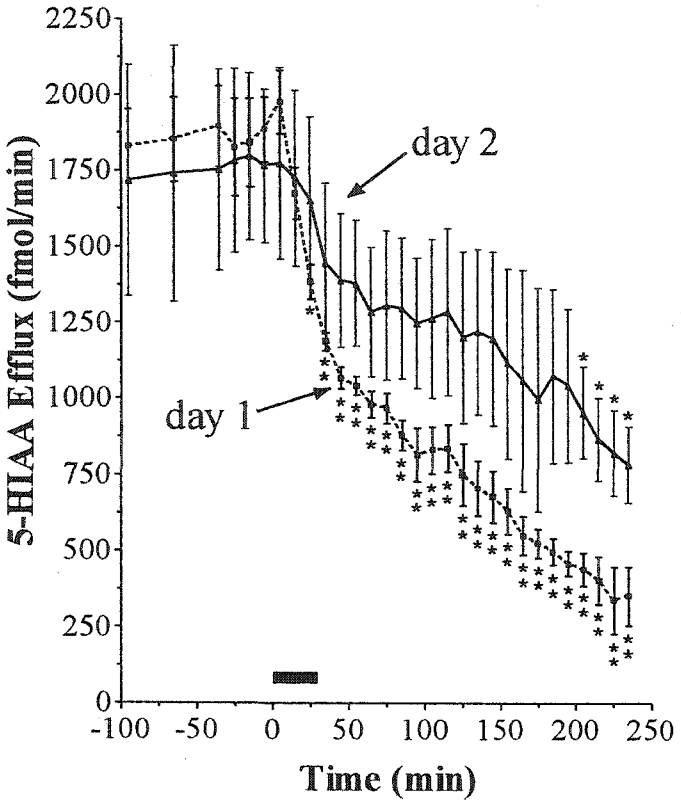

Figure 2:47.
1.3 mM MPP^+;
5-HIAA Efflux (fmol/min)
vs. Time (min), n = 4.

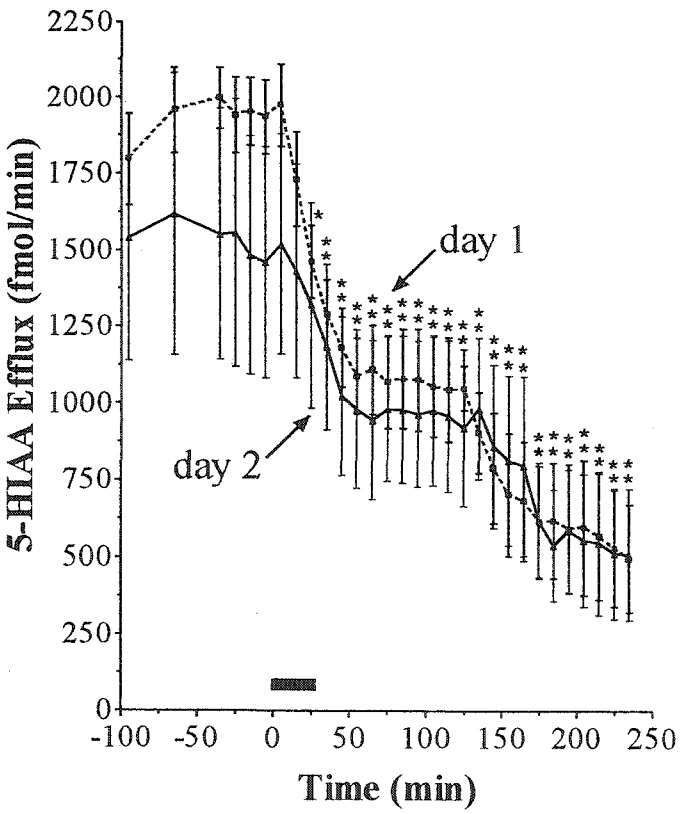

Figure 2:48.
1.3 mM MPP^+ with
1.0 mM ACV;
5-HIAA Efflux (fmol/min)
vs. Time (min), n = 4.

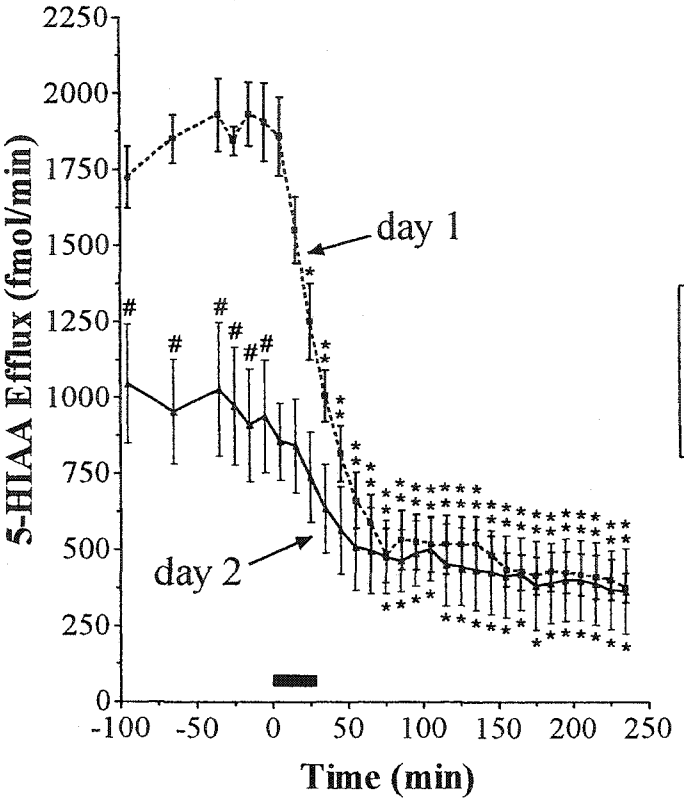

Figure 2:49.
2.5 mM MPP^+;
5-HIAA Efflux (fmol/min)
vs. Time (min), n = 4.

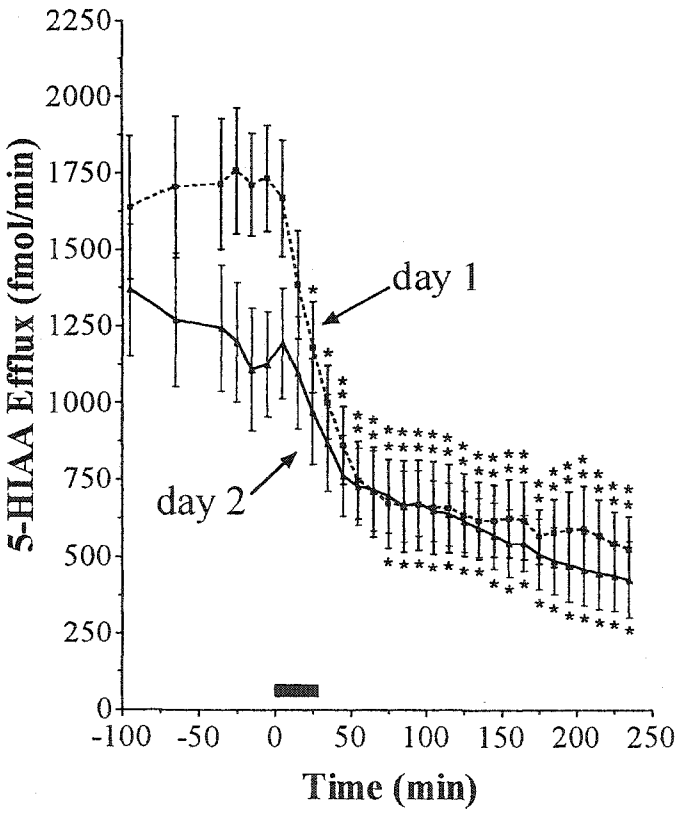

Figure 2:50.
2.5 mM MPP^+ with
1.0 mM ACV;
5-HIAA Efflux (fmol/min)
vs. Time (min), n = 4.

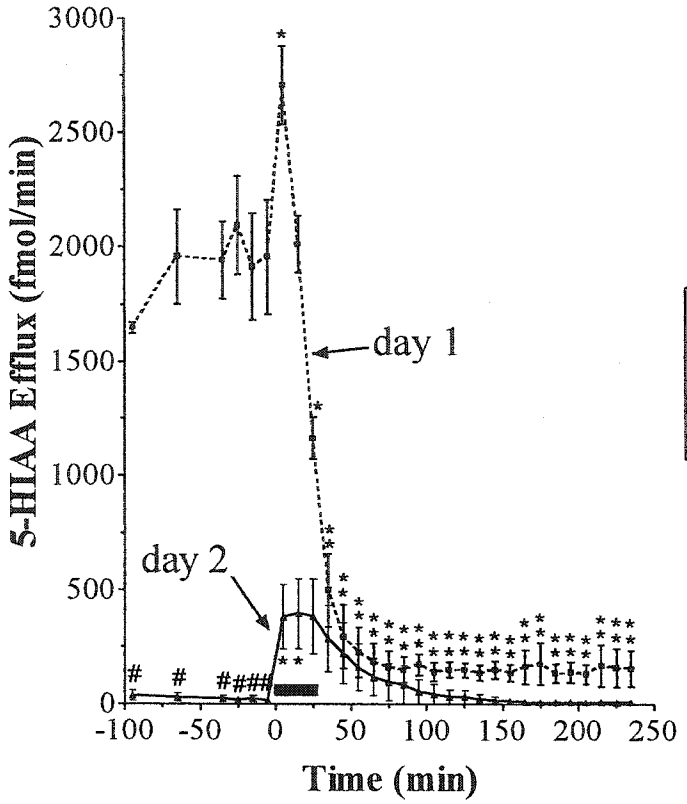

Figure 2:51.
10.0 mM MPP^+;
5-HIAA Efflux (fmol/min)
vs. Time (min), n = 4.

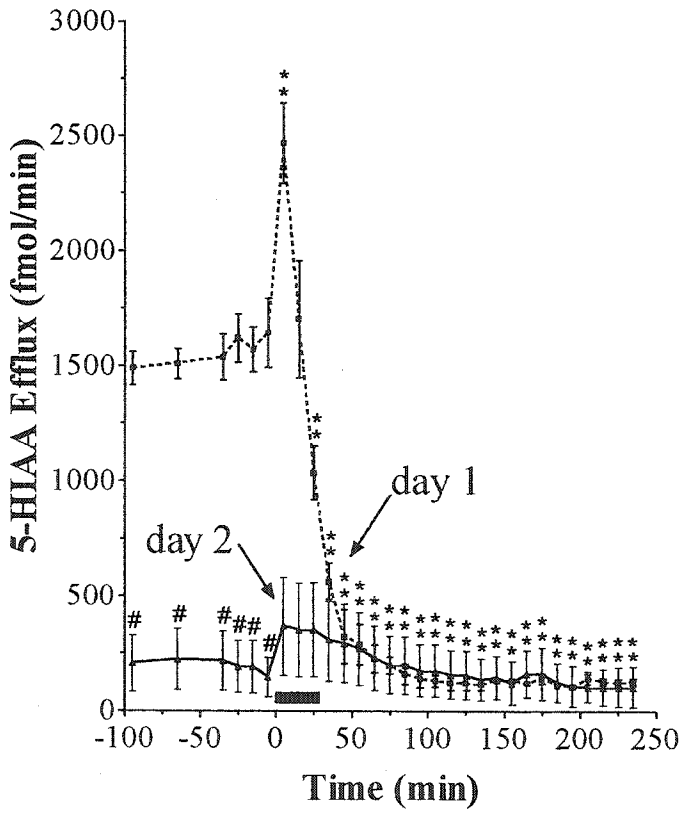

Figure 2:52.
10.0 mM MPP^+ with
1.0 mM ACV;
5-HIAA Efflux (fmol/min)
vs. Time (min), n = 4.

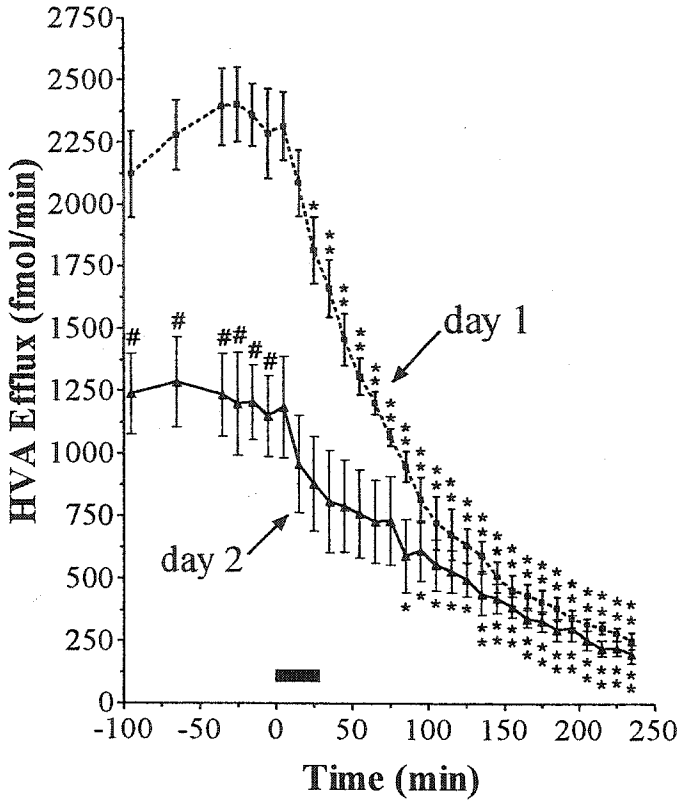

Figure 2:53.
0.7 mM MPP^+;
HVA Efflux (fmol/min)
vs. Time (min), n = 4.

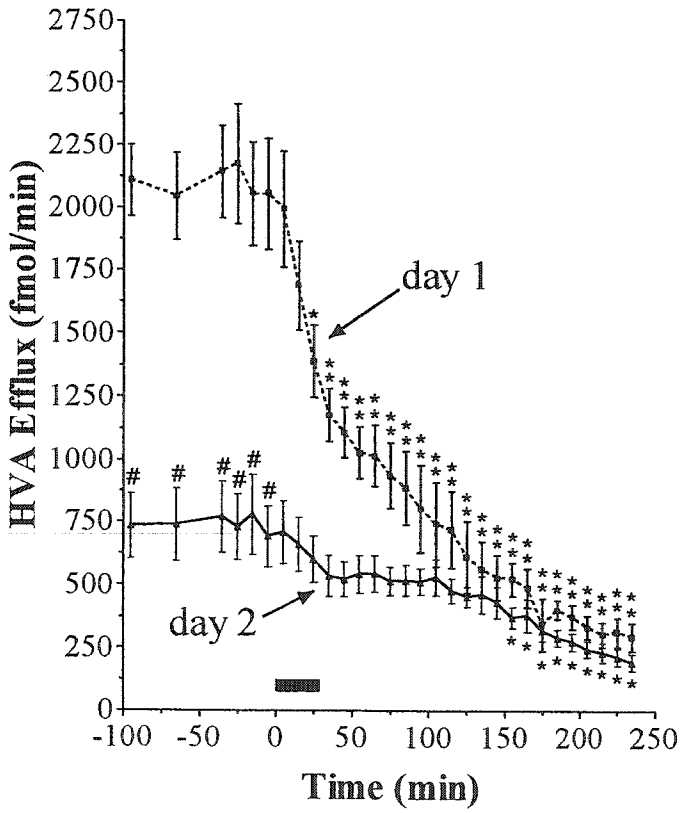

Figure 2:54.
0.7 mM MPP^+ with
1.0 mM ACV;
HVA Efflux (fmol/min)
vs. Time (min), n = 4.

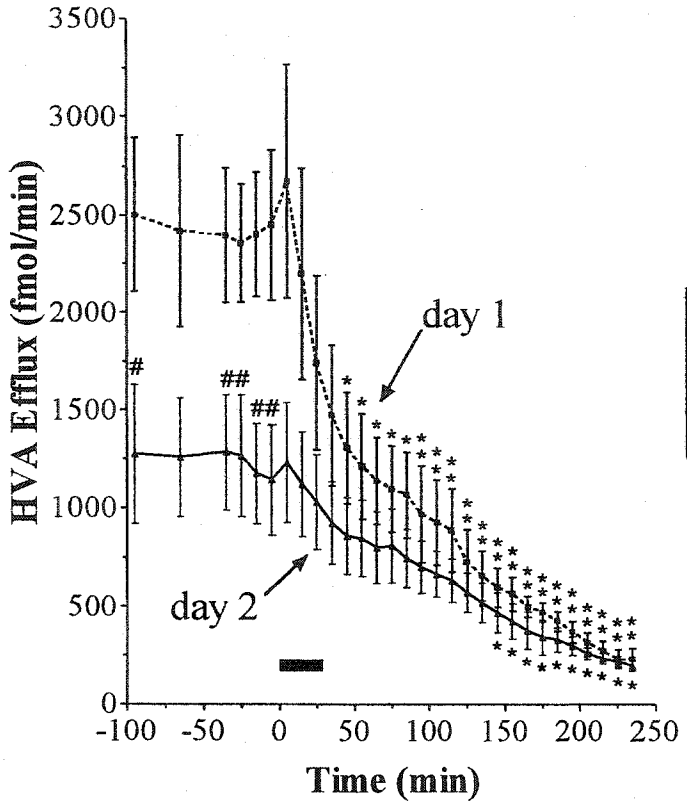

Figure 2:55.
1.3 mM MPP^+;
HVA Efflux (fmol/min)
vs. Time (min), n = 4.

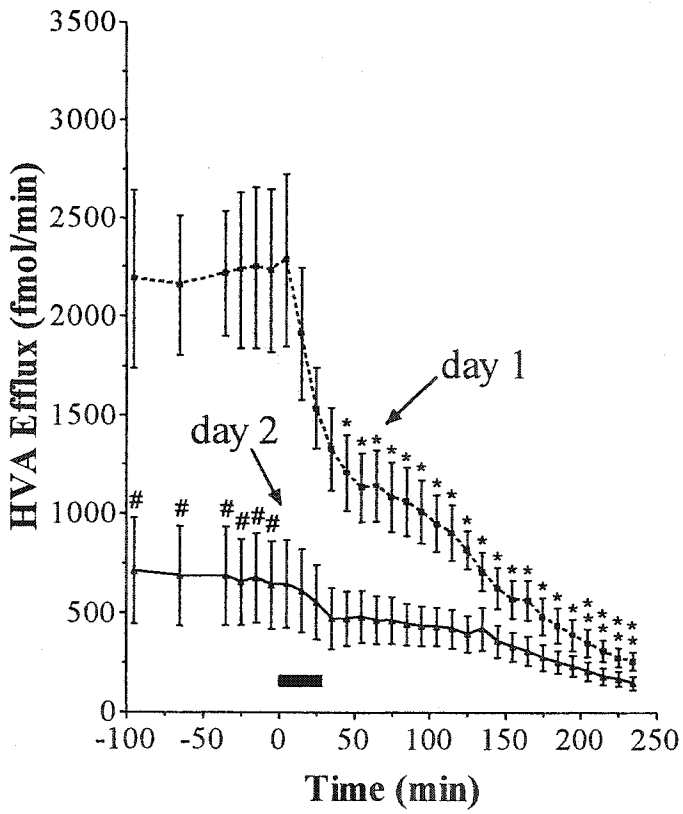

Figure 2:56.
1.3 mM MPP^+ with
1.0 mM ACV;
HVA Efflux (fmol/min)
vs. Time (min), n = 4.

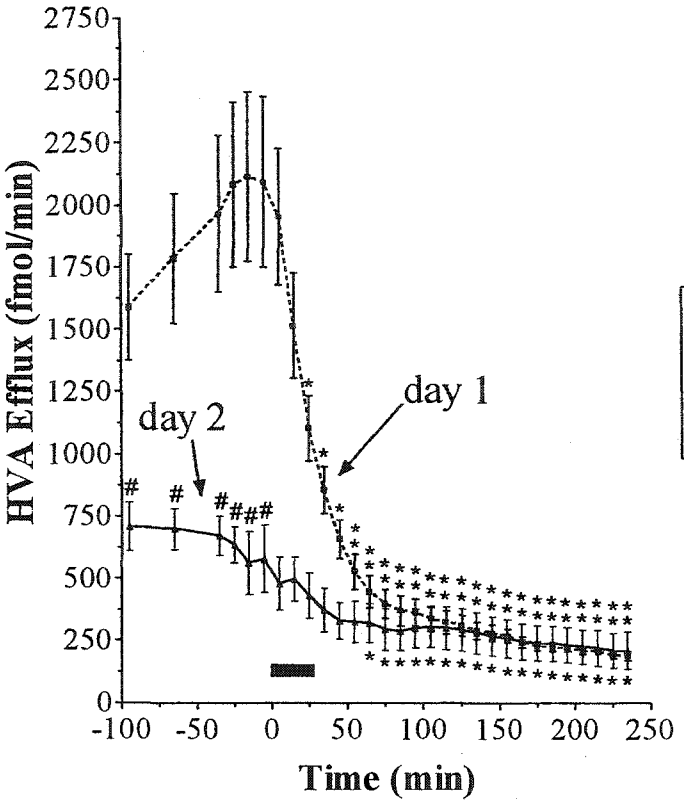

Figure 2:57.
2.5 mM MPP^+;
HVA Efflux (fmol/min)
vs. Time (min), n = 4.

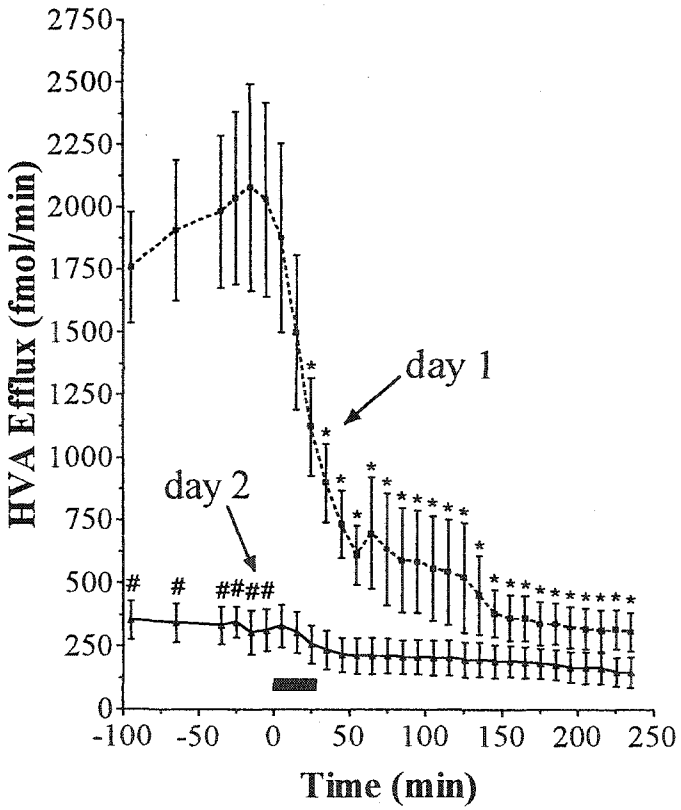

Figure 2:58.
2.5 mM MPP^+ with
1.0 mM ACV;
HVA Efflux (fmol/min)
vs. Time (min), n = 4.

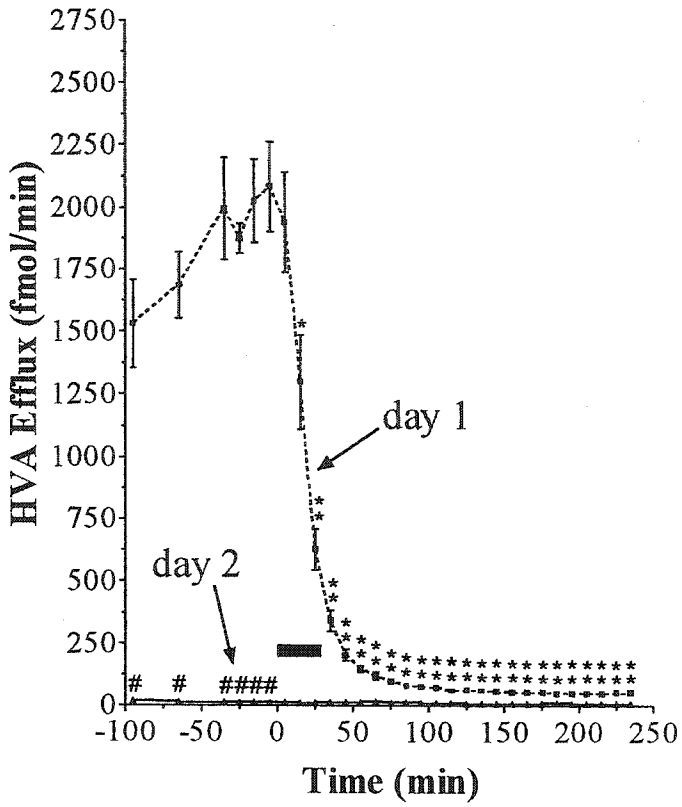

Figure 2:59.
10.0 mM MPP^+;
HVA Efflux (fmol/min)
vs. Time (min), n = 4.

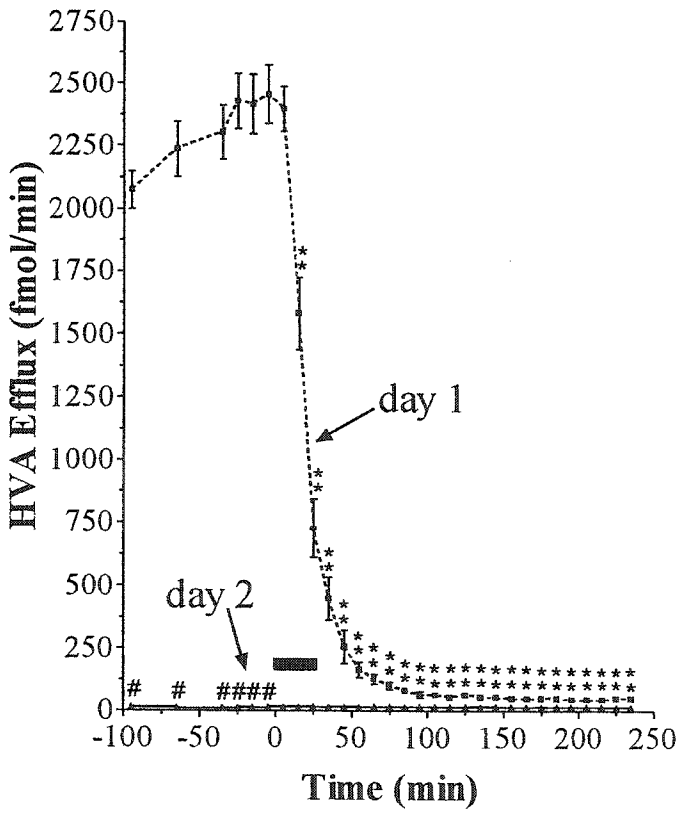

Figure 2:60.
10.0 mM MPP^+ with
1.0 mM ACV;
HVA Efflux (fmol/min)
vs. Time (min), n = 4.

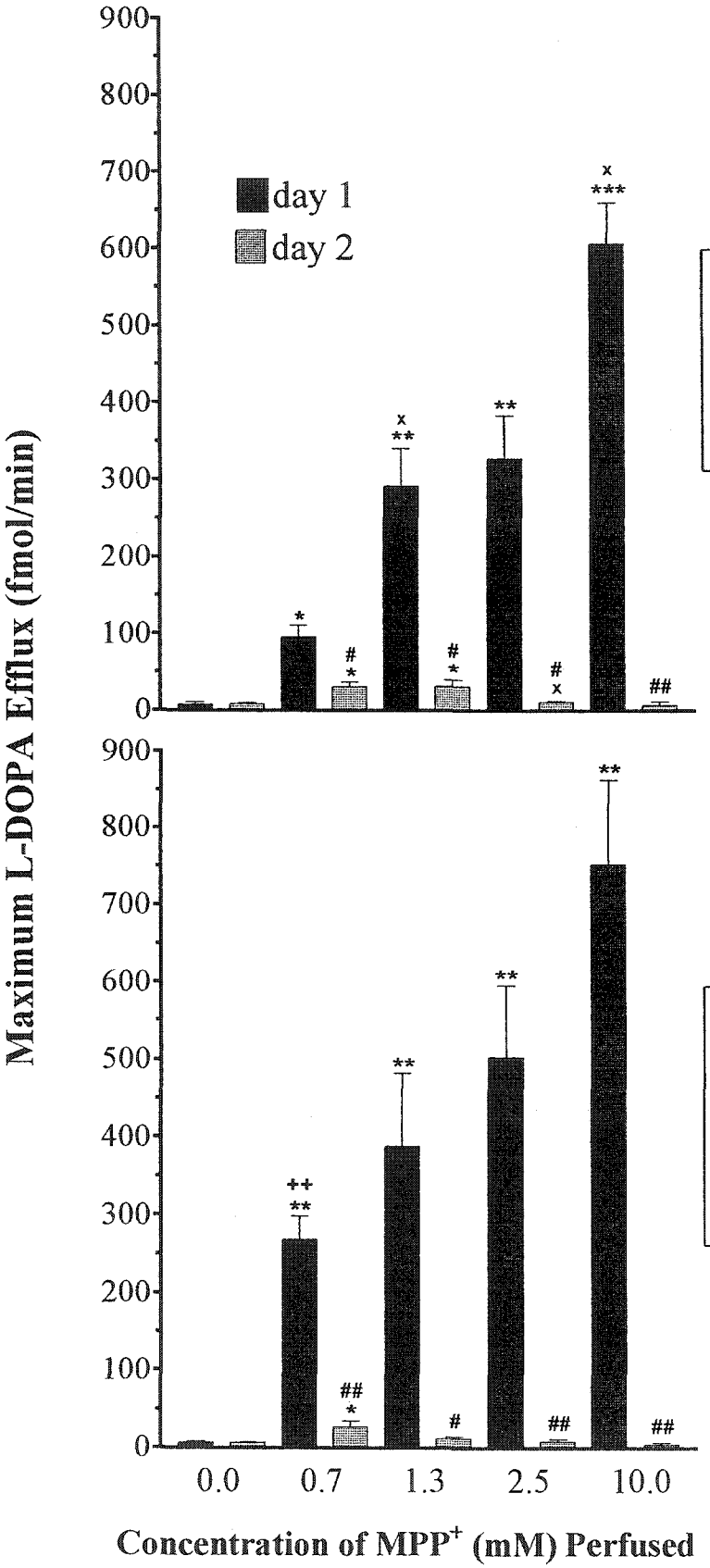

Figure 2:61.
L-DOPA maximum efflux (fmol/min) at each MPP^+ concentration perfused, n = 4 for each concentration

Figure 2:62.
L-DOPA maximum efflux (fmol/min) at each MPP^+ concentration perfused with 1.0 mM ACV, n = 4 for each concentration

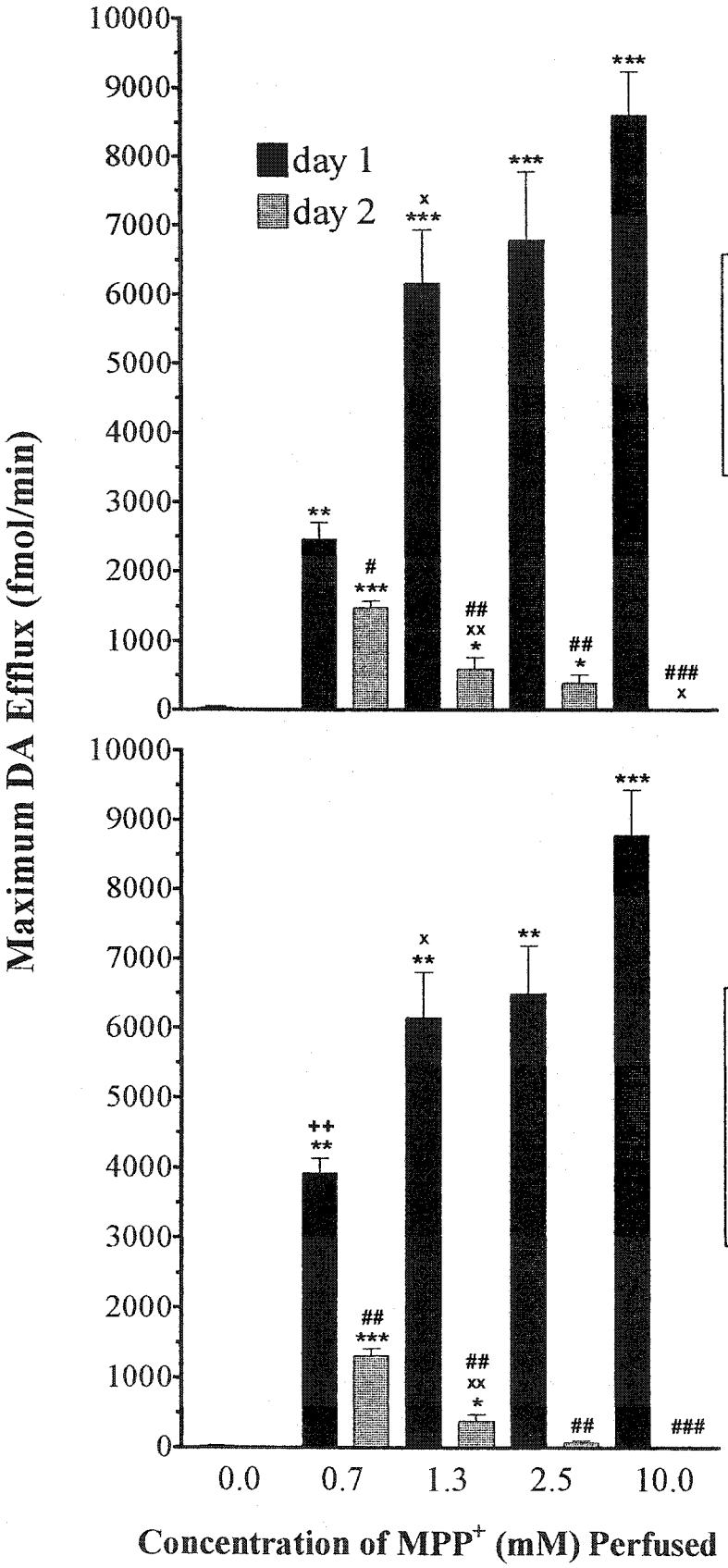

Figure 2:63.
DA maximum efflux (fmol/min) at each MPP^+ concentration perfused, n = 4 for each concentration

Figure 2:64.
DA maximum efflux (fmol/min) at each MPP^+ concentration perfused with 1.0 mM ACV, n = 4 for each concentration

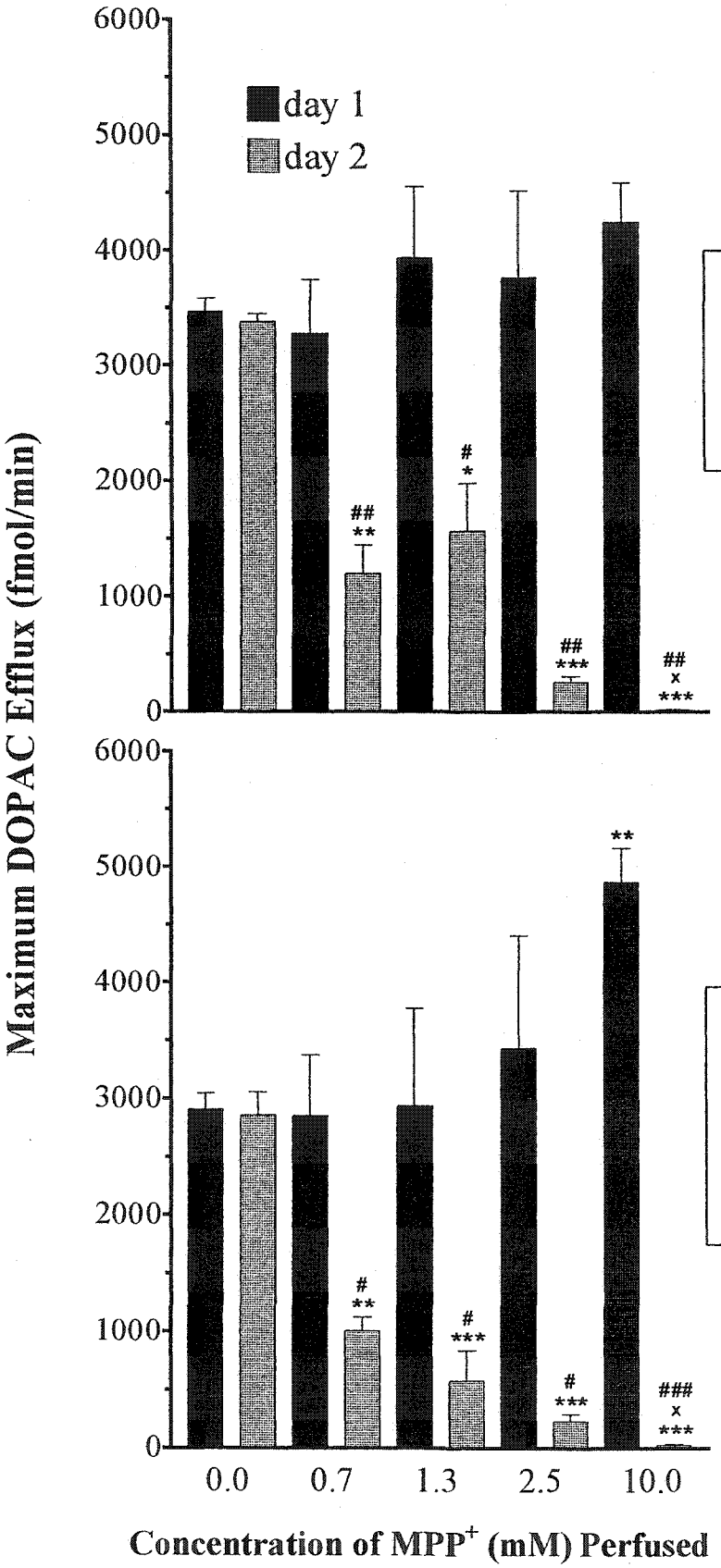

Figure 2:65.
DOPAC maximum efflux (fmol/min) at each MPP^+ concentration perfused, n = 4 for each concentration

Figure 2:66.
DOPAC maximum efflux (fmol/min) at each MPP^+ concentration perfused with 1.0 mM ACV, n = 4 for each concentration

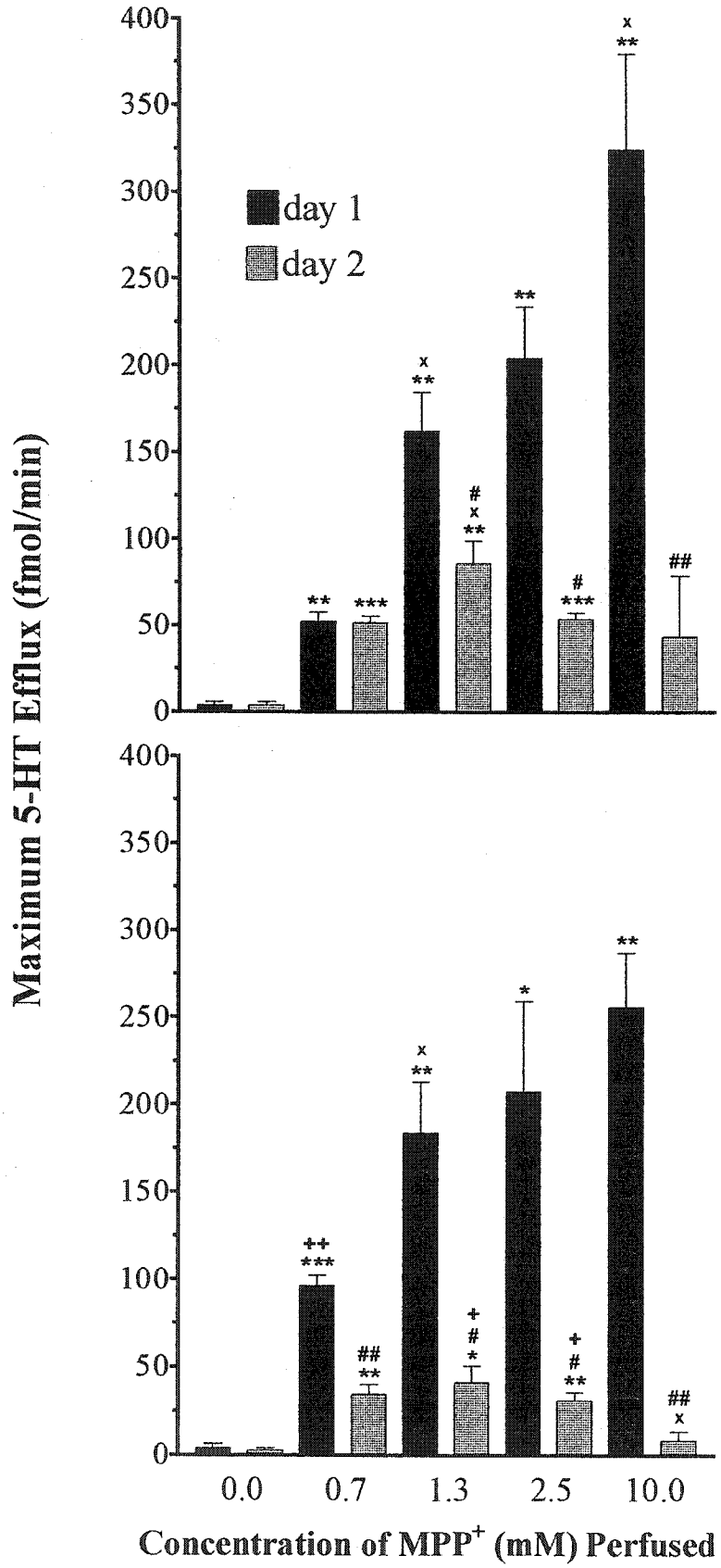

Figure 2:67.
5-HT maximum efflux (fmol/min) at each MPP^+ concentration perfused, n = 4 for each concentration

Figure 2:68.
5-HT maximum efflux (fmol/min) at each MPP^+ concentration perfused with 1.0 mM ACV, n = 4 for each concentration

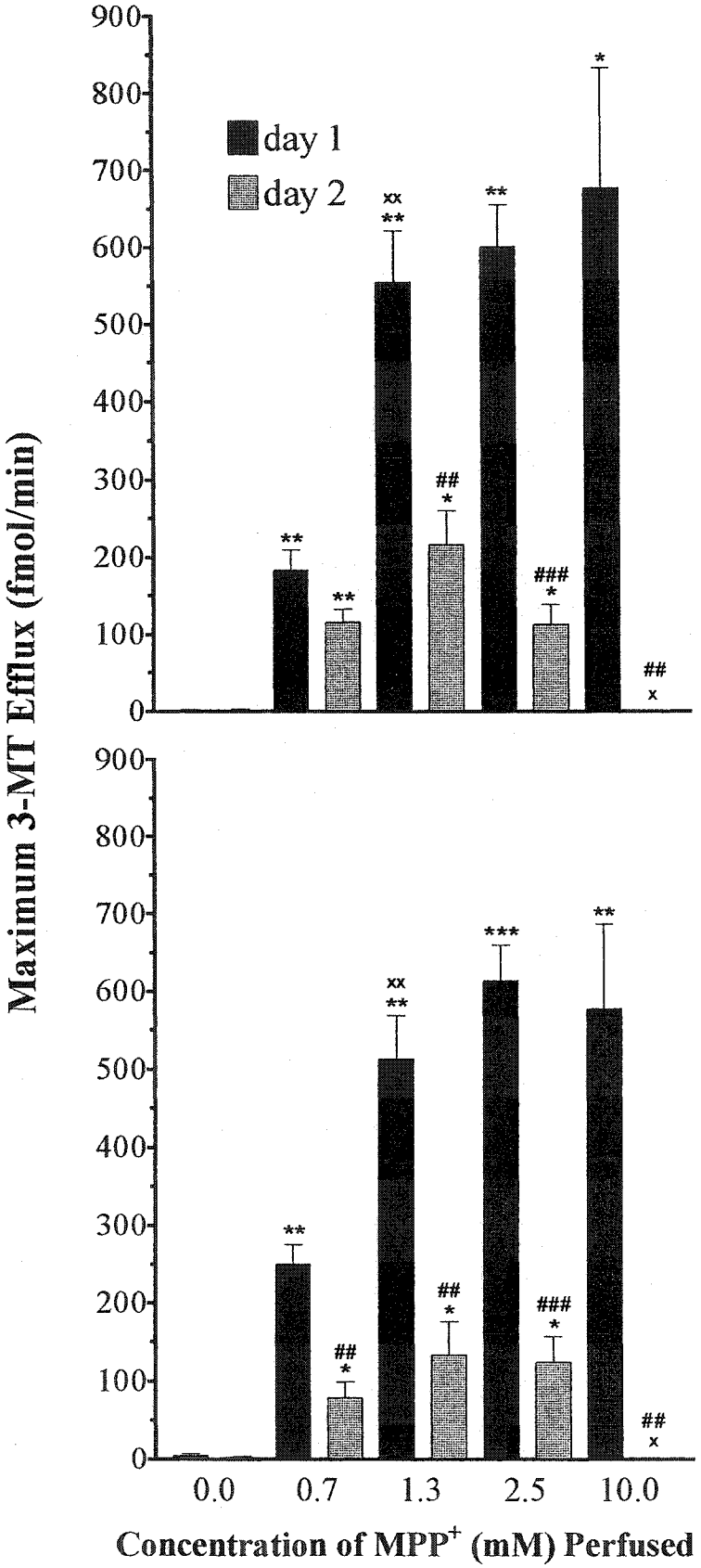

Figure 2:69.
3-MT maximum efflux (fmol/min) at each MPP^+ concentration perfused, n = 4 for each concentration

Figure 2:70.
3-MT maximum efflux (fmol/min) at each MPP^+ concentration perfused with 1.0 mM ACV, n = 4 for each concentration

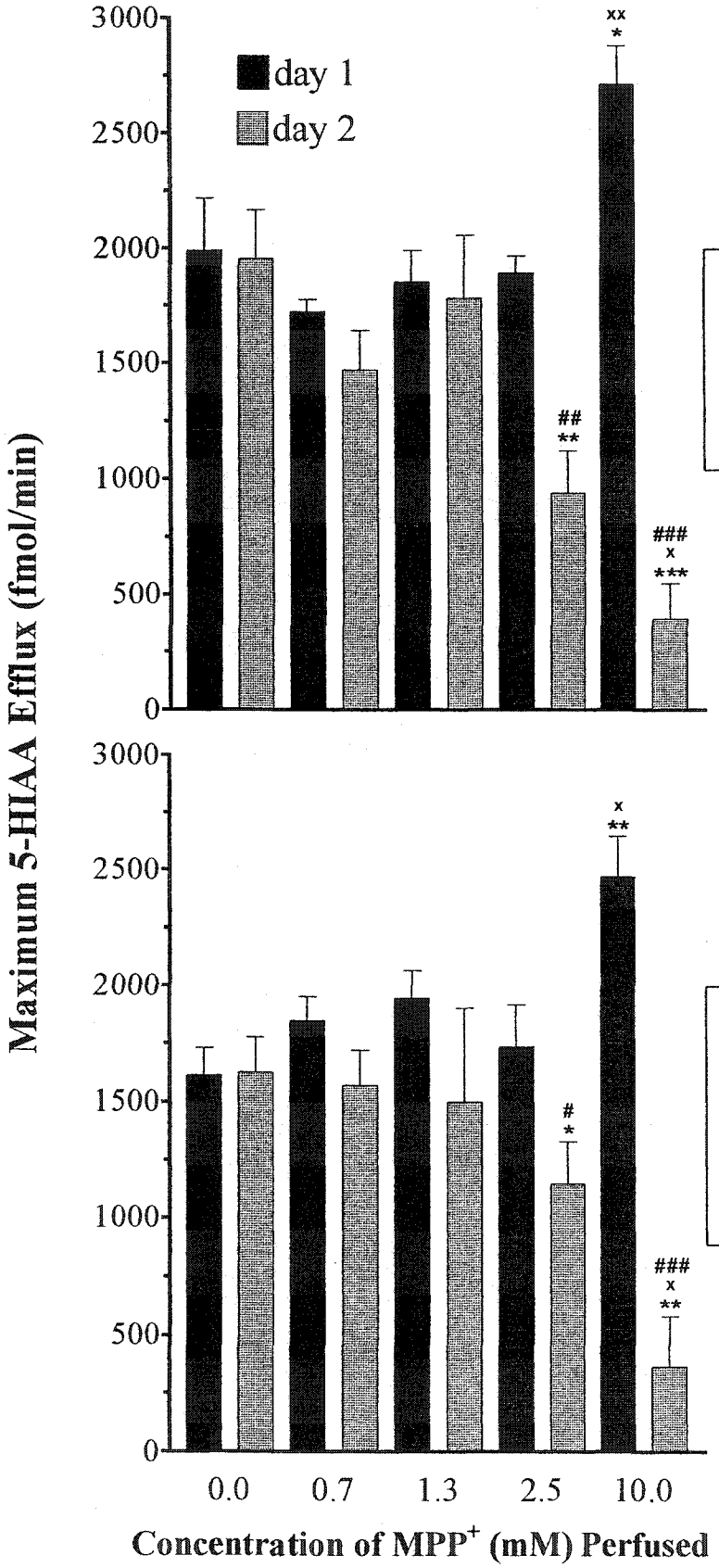

Figure 2:71.
5-HIAA maximum efflux (fmol/min) at each MPP^+ concentration perfused, n = 4 for each concentration

Figure 2:72.
5-HIAA maximum efflux (fmol/min) at each MPP^+ concentration perfused with 1.0 mM ACV, n = 4 for each concentration

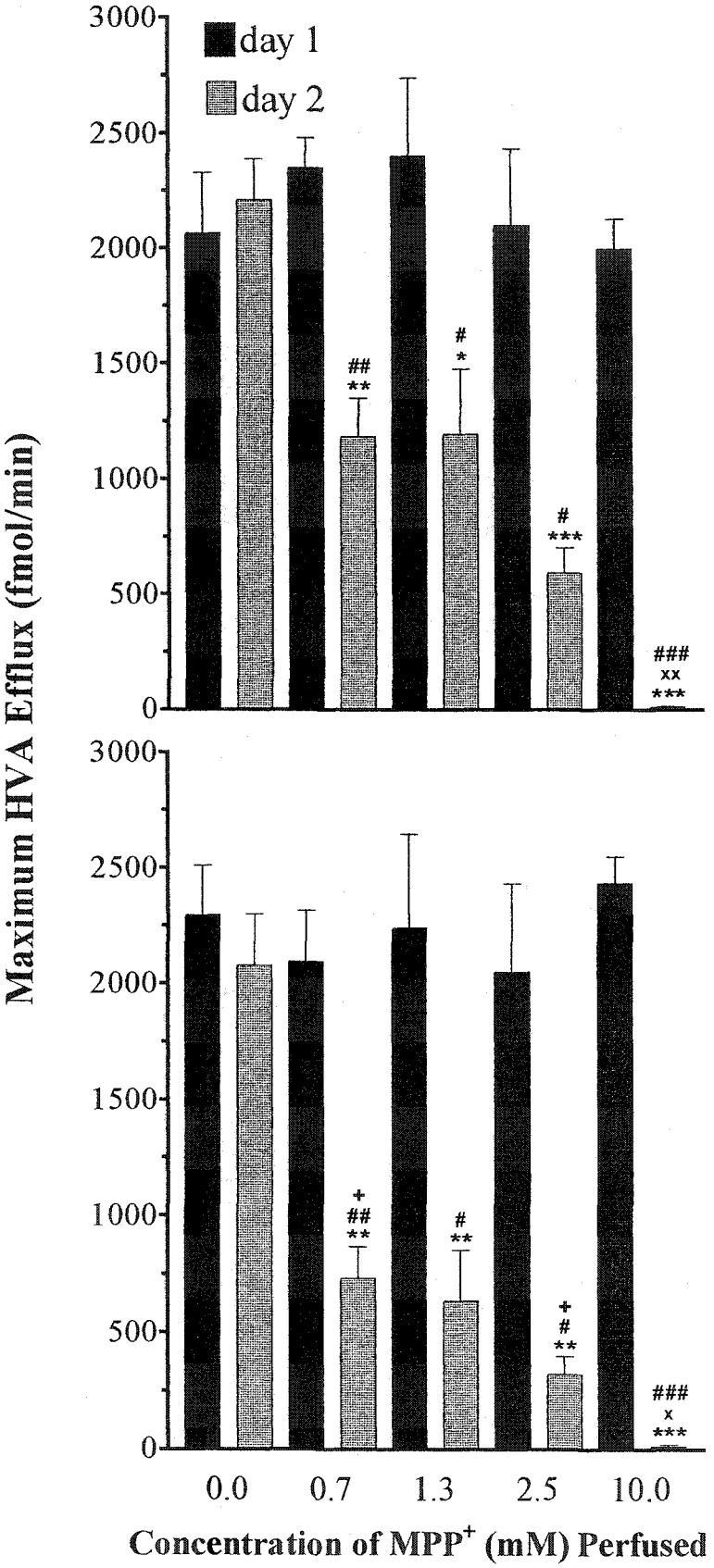

Figure 2:73.
HVA maximum efflux (fmol/min) at each MPP^+ concentration perfused, n = 4 for each concentration

Figure 2:74.
HVA maximum efflux (fmol/min) at each MPP^+ concentration perfused with 1.0 mM ACV, n = 4 for each concentration

Chapter Three

The Effects of Antioxidants and Confirmation of L-DOPA

A. Introduction

From the results in the previous chapter a compound was detected, which by use of several HPLC-EC analysis methods, appeared to be L-DOPA. Normally, tyrosine (Tyr; the precursor of L-DOPA) is hydroxylated by the enzyme TH to form L-DOPA. However, L-DOPA could arise from MPP^+-mediated generation of $HO\cdot$[239] and/or $ONOO^-$[240,241] with resultant non-enzymatic hydroxylation of Tyr. Accordingly, microdialysis experiments were carried out in which the antioxidants SA and mannitol (both $HO\cdot$ scavengers) were perfused before, during and after a 30 min perfusion of 10.0 mM MPP^+.

In vitro and *ex vivo* studies of DDC activity were conducted to provide unequivocal evidence for the identity of putative L-DOPA observed by HPLC analysis in microdialysis experiments. DDC is the enzyme which decarboxylates L-DOPA to form DA. Additionally, analysis of results from the antioxidant studies led to investigations to explore the possibility that the neurotransmitter-like release of L-DOPA was a result of MPP^+-mediated inhibition of DDC.

B. Experimental

1. Chemicals

Dithiothreitol (DTT), ascorbic acid, 3,4-dihydroxybenzylamine, aluminum oxide, mannitol, SA (sodium salt), TRIS [(hydroxymethyl)aminomethane-hydrochroride (TRIS·HCl)], sucrose, β-mercaptoethanol, *N*-methyl-*N*-propargylbenzylamine (pargyline), pyridoxal 5'-phosphate (PLP), 2,5-dihydroxybenzoic acid (2,5-DHBA) and 2,3-DHBA were obtained from Sigma. Acetic acid was obtained from Fisher Scientific (Fair Lawn, NJ). Purified DDC was a generous gift from Professor Carla Borri-Voltattorni (University of Perugia, Italy). The sources of all other chemicals have been described previously.

2. HPLC-EC

HPLC-EC methods I and IV were described in Chapter Two. HPLC-EC method V used a Rheodyne 7125 injector with a 20.0 μL sample loop. The glassy carbon detector electrode was set at +850 mV *vs.* a Ag/AgCl reference electrode. A Phenomenex IB-SIL column (ODS-18-BD, 100 x 3.2 mm, 3 μm) was used. The mobile phase was prepared by adding 0.85 mL DEA, 59.2 mg SOS, 187 mg Na_2EDTA dihydrate and 21.0 g citric acid monohydrate to 970 mL of deionized water. After filtration, the pH of this solution was adjusted to 2.40 with $HClO_4$ and then 30 mL of MeCN and 15 mL of MeOH were added. The flow rate was 0.35 mL/min. For all chromatography, mobile phases were degassed by stirring under vacuum for approximately 30 min prior to use. HPLC-EC method I was used to analyze dialysate from microdialysis experiments with

SA and mannitol. HPLC-EC methods IV and V were employed in assays for the activity of purified DDC and the activity of this enzyme in rat brain tissue samples.

3. Microdialysis with SA or Mannitol

Microdialysis conditions were basically the same as those described in Chapter Two. However, in the SA and mannitol experiments, aCSF containing SA (2.5 mM) or mannitol (100 mM) was perfused 3 h prior to, during and after perfusion of 10.0 mM MPP^+.

4. Enzymatic Confirmation of L-DOPA in Dialysates

Dialysate fractions (7.5 μL) from rat brains collected during the period when maximal concentrations of putative L-DOPA were formed in response to perfusion of MPP^+ were collected in vials maintained at 4°C which contained 0.75 μL of 4.3 mM ascorbic acid. Dialysate from 4 rats were then pooled (170 μL) and 14.5 μL of 1 M Tris-HCl buffer (pH 7.3) was added to give a final pH of 7.2. One fraction (74 μL) was incubated with a solution containing purified DDC (6.0 μL of 50 mM potassium phosphate buffer pH 6.8 containing 0.1 mM DTT and 3 μg of DDC protein) for 20 min at 20°C. A second 74 μL fraction was incubated with a solution containing heat denatured DDC (30 min at 100°C) under otherwise identical conditions. Reactions were terminated after 20 min by addition of 8.0 μL of 9.1 M $HClO_4$ solution. The resulting solutions were treated with 160 μL of 0.75 M Tris-HCl buffer (pH 8.8) containing 0.43 mM ascorbic acid to give a final pH of 7.2, and then 10.0 ± 0.2 mg of alumina was added. Vials were then placed in a Vortex Test Tube Mixer (model K-500-4, Scientific Industries, Bohemia,

New York) and shaken at the high speed setting for 10 min, then centrifuged at 12,000 x g for 10 min and the supernatant discarded. The alumina was washed three times with 360 μL of deionized water using the same procedure. After the final wash, catechols adsorbed on the alumina were eluted by adding 30 μL of a solution of 0.5 M acetic acid and 0.4 M HCl in deionized water, then placed in the Vortex Test Tube Mixer and shaken at the high speed setting for 10 min. After centrifugation (12,000 x g, 5 min), aliquots (5.0 μL) of the supernatants from experimentals (dialysate incubated with DDC) and controls (dialysate incubated with heat denatured DDC) were analyzed for concentrations of L-DOPA, DA and DOPAC using HPLC-EC method IV.

Based on experiments in which rat brain dialysate samples were replaced by aCSF containing 0.43 mM ascorbic acid, 1.71 μM DA, 0.63 μM L-DOPA and 0.63 μM DOPAC and carried through the entire procedure described above, the recoveries (n = 16) of DA, L-DOPA and DOPAC from alumina were 77 ± 6, 72 ± 5 and 63 ± 5%, respectively. In additional experiments it was found that these recoveries were not affected by the inclusion of 10.0 mM MPP^+ in the original aCSF solution.

5. Assay for the Activity of Purified DDC

An in vitro procedure was employed to assay the activity of purified DDC and the effect of MPP^+ on this activity. The assay solution contained a DDC-saturating concentration of L-DOPA (1.5 mM), DOPAC (1.0 μM, internal standard) and ascorbic acid (0.43 mM) dissolved in 917 μL of aCSF and 75.5 μL of 0.75 M Tris-HCl buffer (pH 7.8) to give a final pH of 7.2. Reactions were initiated by addition of 37.5 μg of DDC protein or heat-denatured (30 min, 100°C) DDC protein in 7.5 μL of 50 mM potassium

phosphate buffer (pH 6.8) containing 0.1 mM DTT. Aliquots (75 μL) were removed from the reaction mixture immediately after addition of DDC protein and then at 5 min intervals and added to 7.5 μL of ice-cold 9.1 M $HClO_4$ solution to terminate the reaction. Vials containing these solutions were centrifuged (14,000 x g, 20 min, 4°C) and aliquots (5 μL) of the supernatants analyzed for concentrations of L-DOPA, DA and DOPAC using HPLC method IV. The effect of MPP^+ on the activity of DDC was studied by including 15.0 mM MPP^+ in the initial assay solution. Control experiments included: (1) the above reaction mixtures (with and without MPP^+) with the exclusion of L-DOPA and/or DA in the reaction mixture, and (2) delayed addition of L-DOPA and/or DA until 10 min after the reaction was initiated. The activity of DDC was expressed as nmol DA formed/μg protein/min.

6. Effect of MPP^+ on Rat Striatal DDC Activity

In order to assess the effect of MPP^+ perfusion on the activity of DDC in vivo, microdialysis probes were implanted in the right and left striata of rats. On the day of the experiment, aCSF was perfused (1.5 μL/min) into the left and right striatum for *ca.* 3 h until HPLC analysis (method I) of dialysates (collected at 15 min intervals) gave at least 3 consecutive constant basal levels of DA, 5-HT and their metabolites. At this point the right striatum was perfused for 30 min with aCSF containing 10.0 mM MPP^+, the left striatum being perfused with aCSF alone. The perfusate into the right striatum was then changed back to aCSF, which was perfused at all times into the left striatum. After 10 min, perfusions were terminated, microdialysis probes removed and rats killed by decapitation. Brains were removed and placed in an ice-cold BAS coronal brain matrix

apparatus and a 2 mm coronal slice made 0.75 mm posterior and 0.75 mm anterior to the two microdialysis probe tracks (0.5 mm diameter). The slice was then placed on an ice-cold glass plate and a 2 x 4 mm area of striatal tissue centered around each microdialysis probe track was excised with a punch (constructed in this laboratory).

The activity of striatal DDC was measured under saturating conditions with respect to L-DOPA using a modification of the method described by Hadjiconstantinou et al.[246] Briefly, excised tissue was weighed (16.0 ± 0.6 mg, n = 6) and homogenized in ice-cold 0.25 M sucrose (1.0 mg tissue/7.0 μL sucrose solution). A 10 μL sample of the homogenate was then diluted to 40 μL with ice-cold 0.25 M sucrose and 10 μL of this solution was added to 200 μL of the assay mixture and incubated for 20 min at 37°C. The assay mixture consisted of 50 mM sodium phoshate buffer (pH 7.2) containing 0.1 mM Na_2EDTA, 0.17 mM ascorbic acid, 1.0 mM β-mercaptoethanol, 0.1 mM pargyline, 0.01 mM PLP and 0.2 mM L-DOPA. The reaction was terminated by adding 21 μL of ice-cold 9.1 M $HClO_4$ solution containing 410 pmol of 3,4-dihydroxybenzylamine (internal standard; final concentration 1.77 μM). The pH of this solution was adjusted to 8.0 by addition of 450 μL of 0.75 M Tris-HCl (pH 8.8) containing 0.43 mM ascorbic acid. Aluminum oxide (10.0 ± 0.2 mg) was then added to the resulting solutions, contained in 1.5 mL polypropylene microcentrifuge tubes, in order to adsorb catechols. The reaction vials were placed in a Vortex Test Tube Mixer and shaken at the high speed setting for 10 min and then centrifuged for 3 min at 12,000 x g and the supernatants discarded. The alumina was washed 3 times with 300 μL of water using the same procedure. After the final wash, compounds adsorbed on the alumina were eluted by adding 30 μL of a solution of 0.5 M acetic acid and 0.4 M HCl, shaking for 10 min and

centrifuging for 5 min at 12,000 x g. Aliquots (20 μL) of the supernatant were then analyzed for the concentration of DA using HPLC method V. The extraction recoveries for DA and 3,4-dihydroxybenzylamine from alumina were 74 ± 4% and 69 ± 5%, respectively. Total protein in excised tissue was determined using the Coomassie Plus Protein Assay Reagent Kit (Pierce, Rockford, IL) using bovine serum albumin as the standard.

C. Results

1. Effects of Antioxidants on MPP^+-Induced Extracellular Chemistry and Neurotoxicity

Coperfusion of SA (2.5 mM) and MPP^+ (10.0 mM) into the rat striatum resulted in the appearance of 2,3-DHBA (Figure 3:08) indicative of extracellular and/or intracellular HO· and/or peroxynitrite generation.[241] However, the appearance of 2,3-DHBA in dialysates was delayed such that it was first detected when the perfusion of MPP^+ was discontinued (Figure 3:08). Furthermore, 2,3-DHBA appeared in dialysates later than L-DOPA and as extracellular DA levels were decreasing (Figures 3:01, 02, respectively). 2,5-DHBA was also formed. However, 2,5-DHBA is not exclusively formed by HO· scavenging by SA. Hydroxylation of SA can occur by cytochrome P450 and microsomal enzymes forming 2,5-DHBA.[247] Therefore, since 2,5-DHBA is not an unequivocal marker of the non-enzymatic hydroxylation of SA, results bearing on this compound are not included. Perfusion of 10.0 mM MPP^+ on day 1 evoked virtually the same release of DA, L-DOPA, 3-MT and 5-HT (Table 3:01) and the same time-dependent behavior of DOPAC, 5-HIAA and HVA in the presence of SA (Figures 3:03,

06, 07) as in its absence (Table 3:01 and Figures 2:27, 51, 59). SA also failed to provide any protection against the apparent dopaminergic and serotonergic neurotoxicity of MPP^+ based on the fact that the day 2 perfusion resulted in greatly attenuated release of DA, L-DOPA, 3-MT and 5-HT and attenuated basal levels of DOPAC, 5-HIAA and HVA (Table 3:01 and Figures 3:01-07).

Table 3:01. Effect of Salicylate and Mannitol on the Maximal Release of DA, L-DOPA, 5-HT and 3-MT on Day 1 and Day 2 Evoked by Perfusion of 10.0 mM MPP^+ for 30 min into the Striata of Awake Rats.

Antioxidant [a] (concentration)	day	maximal release (fmol/min) of [b] DA	L-DOPA	5-HT	3-MT
0	1	8596 ± 1268	606 ± 108	324 ± 110	676 ± 311
	2	0***[c]	6 ± 10** (21,0,5,0)[d]	43 ± 69* (9,146,0,7)[d]	0*[c]
salicylate (2.5 mM)	1	8273 ± 1524	643 ± 111	316 ± 78	628 ± 80
	2	3 ± 5** (0,0,9)[d]	2 ± 3* (0,0,6)[d]	6 ± 6* (8,0,11)[d]	0**[c]
mannitol (100 mM)	1	8841 ± 892	723 ± 200	283 ± 53	672 ± 148
	2	0***[c]	5 ± 6* (0,5,11)[d]	7 ± 6* (11,0,10)[d]	0*[c]

[a]Salicylate or mannitol dissolved in aCSF at the indicated concentration were perfused for *ca.* 3h before MPP^+ perfusion, during and for several hours after this perfusion.
[b]Data are mean ± SEM ($n \geq 3$) for release on day 1.
[c]No release was observed with any animal.
[d]Release values for each animal perfused on day 2.

A significant difference between the day 1 and day 2 release is indicated by $*p < 0.05$, $**p < 0.01$, $***p < 0.001$.

A high concentration of mannitol (100 mM), which is believed to act exclusively as an extracellular antioxidant,[248] also failed to affect the release of DA, L-DOPA, 3-MT and 5-HT and the behavior of DOPAC, 5-HIAA and HVA in response to a 30 min perfusion of MPP^+ on day 1. Mannitol coperfusion did not attenuate the apparent dopaminergic and serotonergic neurotoxicity of MPP^+, based on a greatly reduced release of DA, L-DOPA, 3-MT and 5-HT and attenuated basal levels of DOPAC, 5-HIAA and HVA on day 2 (Table 3:01 and Figures 3:09-15). Therefore, the marked elevation of extracellular L-DOPA in the rat striatum evoked by MPP^+ (Table 3:01), appeared to be unrelated to the non-enzymatic hydroxylation of L-tyrosine by $HO\cdot$ or $ONOO^-$ (Table 3:01 and Figures 3:01,09). This, in turn, suggested that perfusion of MPP^+ may mediate the *in vivo* inhibition of DDC.

2. Effects of DDC on Putative L-DOPA

Dialysate containing putative L-DOPA was incubated with purified DDC at pH 6.8 for 20 min and the resultant solution was then treated with alumina to extract catechols. After washing the alumina, catechols were desorbed with acid and the eluents analyzed by HPLC-EC method IV. When carried through such a procedure but using heat-denatured DDC, such eluents exhibited chromatographic peaks for DA and DOPAC in addition to a peak at the same retention time as L-DOPA (Figure 3:17A). However, when the dialysate was incubated with active DDC, chromatograms showed that the L-DOPA peak was quantitatively transformed into DA (Figure 3:17B). These same experiments were conducted using authentic DA, L-DOPA and DOPAC in aCSF (Figure 3:18).

3. Effects of MPP^+ on the Activity of DDC *In Vitro* and *In Vivo*

The activity of purified DDC measured at pH 7.2 in the presence of a saturating concentration of L-DOPA was 5.6 ± 0.4 nmol DA formed/μg protein/min (n = 12). Heat denatured DDC was completely unable to convert L-DOPA into DA. When L-DOPA was not added to the incubation mixture until 10 min after the reaction was initiated with active DDC, there was no difference in the measured activity of DDC. In experiments where L-DOPA and DOPAC were incubated in the absence of active enzyme or with heat denatured enzyme, there was no formation of DA. When 15.0 mM MPP^+ was included with L-DOPA in the assay solution, the measured activity of purified DDC was 5.3 ± 0.6 nmol DA formed/μg protein/min (n = 12). In experiments when: (1) 15.0 mM MPP^+ was not added until 10 min after the incubation mixture had been started, and (2) 15.0 mM MPP^+ was incubated with L-DOPA then 10 min later the active DDC was added, there was no difference in the measured activity of DDC. These results indicate that, *in vitro*: (1) MPP^+ has no effect on the activity of DDC, (2) In the absence of DDC, L-DOPA does not spontaneously form DA.

The possibility that DDC might be inhibited *in vivo*, was explored by terminating microdialysis experiments 10 min after a 30 min perfusion of 10.0 mM MPP^+ into the right striatum of rats had been discontinued. This time corresponded to the point when extracellular concentrations of L-DOPA were highest (Figure 2:11). Tissue in the vicinity of the microdialysis probe was then excised and, after homogenization, assayed for the activity of DDC. Control tissue was excised from the vicinity of an identical microdialysis probe, positioned in the left striatum, that was perfused with aCSF alone. Both left and right striatal tissue was assayed for total protein. The activity of the DDC

in the striatal tissue perfused with MPP^+ was 0.36 ± 0.04 nmol DA formed/mg total protein/20 min (n = 3) which was significantly ($p < 0.001$) lower than that in control tissue, 0.86 ± 0.04 nmol DA formed/mg total protein/20 min (Figure 3:16).

D. Discussion

HPLC analyses of striatal dialysate samples when high concentrations of mannitol were perfused (before, during and after 10.0 mM MPP^+) revealed that this HO· scavenger failed to attenuate either L-DOPA formation (Figure 3:09 and Table 3:01) or the apparent dopaminergic (Figure 3:10) and serotonergic (Figure 3:12) neurotoxicity induced by MPP^+ (Table 3:01). These observations with mannitol, which probably acts exclusively as an extracellular antioxidant,[248] suggests that L-DOPA is not formed by the non-enzymatic hydroxylation of Tyr by extracellular HO· and/or $ONOO^-$. Additionally, (from results presented and discussed in Chapter Two), HPLC analyses of striatal dialysate samples collected both during MPP^+ perfusion and after its termination were unable to detect the presence of glutathionyl or cysteinyl conjugates of DA or DOPAC. The presence of such compounds would be expected if MPP^+ mediates extracellular generation of HO· and/or $ONOO^-$, which should oxidize released DA, GSH and Cys.[124] These observations suggest that MPP^+ does not mediate significant fluxes of extracellular HO· or $ONOO^-$.

SA failed to attenuate MPP^+-mediated formation of L-DOPA (Table 3:01 and Figure 3:01). Since SA is probably both an intracellular and extracellular HO· scavenger, these results suggest that HO· and/or $ONOO^-$ (if generated intracellularly) do not hydroxylate Tyr to form L-DOPA. However, 2,3-DHBA is formed by the MPP^+-induced

hydroxylation of SA (Figure 3:08) which has been previously shown to be an indication of $HO^{\cdot}$[239] and/or $ONOO^-$ production.[240,241] The DA released by MPP^+ could autoxidize and lead to formation of $O_2^{-\cdot}$, H_2O_2 and hence $HO^{\cdot}$, which could then hydroxylate SA to form 2,3-DHBA. However, 2,3-DHBA formation is delayed (Figure 3:08) and does not appear until DA levels have significantly declined (Figure 3:02). In previous studies in our laboratory[124] the extracellular rise of GSH is delayed similar to 2,3-DHBA. Therefore, this suggests that generation of $HO^{\cdot}$/$ONOO^-$ may occur intraneuronally and, hence, the hydroxylation of SA to 2,3-DHBA occurs intraneuronally but not until GSH is released from neurons. SA also failed to attenuate the apparent dopaminergic and serotonergic neurotoxicity induced by MPP^+ (Table 3:01 and Figures 3:02, 04).

L-DOPA first appears in dialysates toward the end of a 30 min perfusion of 10.0 mM MPP^+ and attains peak concentrations approximately 10 min after the perfusion is discontinued (Figure 3:01, 09 and 2:11). At the latter time the activity of DDC in striatal tissue in the vicinity of the microdialysis probe is significantly decreased (Figure 3:16). A previous microdialysis study[249] has shown that perfusion of high concentrations of MPP^+ into the rat striatum causes only a gradual decrease of TH activity which reached approximately 70% of control activity after 3 h, but without significant effect on TH protein content. Thus, the MPP^+-mediated inhibition of DDC appears to occur more rapidly than the inhibition of TH, neither effect being directly related to the degeneration of dopaminergic terminals which almost certainly occurs much later. These observations suggest that during and immediately after MPP^+ perfusion, TH continues to hydroxylate Tyr but conversion of the resulting L-DOPA to DA is blocked because of the more rapid inhibition of DDC.

DDC is a fairly non-selective enzyme found in neuronal and non-neuronal tissues. The molecular mass of DDC is approximately 50 kDa and the enzyme requires PLP as a co-factor. Previous studies on the effect of MPTP/MPP^+ on DDC[250-252] are limited. This seems extraordinary, since: (1) the most common form of PD treatment in humans includes a peripheral DDC inhibitor to aid in replacement of central DA derived from peripherally administered L-DOPA,[253] (2) DDC is the only enzyme which produces DA from L-DOPA,[254] and (3) it has been suggested that poorly modulated or oscillating DDC activity in remaining DA neurons of PD patients may be responsible for the on-off fluctuations which occur with long-term replacement therapy.[255] In MPTP-treated monkeys, the activity of DDC was found to be reduced and this reduction was proportional to the loss of striatal dopamine levels. The latter study also found a correlated loss of DDC activity between *in vivo* as measured by positron emission tomography (PET) at 3 months post MPTP administration and *ex vivo* striatal tissue analysis of the same monkeys 4 months post MPTP treatment.[250] Several studies have observed MPP^+-induced reductions of DDC activity which include: (1) PC12 cells 3 and 6 days after addition of MPP^+,[251] (2) experiments *in vitro* where MPP^+ was added to rat whole brain homogenates and analyzed after an incubation period of 15 min at 37°C,[252] and perhaps most significantly (3) in PET studies of PD patients when compared to age-matched control subjects.[256] There appear to be no previous reports of experiments designed to determine the activity of DDC in experiments similar to those described here.

The rapid inhibition of DDC is not caused directly by MPP^+ which, *in vitro*, has no effect on the activity of the purified enzyme. However, there are several indirect mechanisms that might contribute to this rapid inhibition of DDC. For example, MPP^+

mediates intraneuronal generation of many reactive species that might rapidly inhibit DDC. One such species is $ONOO^-$ which appears to contribute to the MPP^+-induced inhibition of TH by nitrating tyrosine residues.[173,257,258] DDC may similarly be susceptible to $ONOO^-$-mediated inhibition since it contains 15 Tyr residues,[259] at least one of which is essential for catalytic activity.[260] It may also be of relevance that the rise of extracellular L-DOPA evoked by MPP^+ perfusion (Figures 3:01, 09 and 2:11) occurs at a time when extracellular DA is rapidly declining from its peak concentrations (Figures 3:02, 10 and 2:19) presumably from the DAT-mediated reuptake of DA into dopaminergic terminals. Thus, intraneuronal O_2^{-}·[170] or $ONOO^-$,[173] both implicated in the neurotoxic mechanism evoked by MPP^+, could oxidize such DA to DAQ.[108,109] Indeed, *in vitro* studies have implicated intraneuronal oxidation of DA in the dopaminergic neurotoxicity of MPP^+.[155] DAQ could potentially inhibit DDC by covalent attachment to one or more of its 12 cysteinyl residues.[259] Indeed, *in vitro*, DAQ inhibits a number of enzymes by such a mechanism.[219,261]

The significance of the neurotransmitter-like release of L-DOPA seen in these microdialysis studies remains to be determined. Interestingly, L-DOPA in combination with carbidopa is the predominant form of PD treatment.[19,262] In 1961, Hornykiewicz and Birkmayer reported dramatic motor function improvements in patients with PD for several hours after i.v. L-DOPA administration.[263] Several years later in 1967, Cotzias showed that high-dose oral L-DOPA administration resulted in a sustained reduction of PD symptoms.[264] However, even then researchers noted apparent side effects including frequent involunatry movements (dyskinesias), motor fluctuations and mental hallucinations.[265] By 1975, α-methyldopahydrazine (carbidopa) was commercially

available and administered in combination with L-DOPA.[262] Together, they reduced some of the other side effects of mono-L-DOPA therapy including nausea and anorexia.[266] Nevertheless, as current treatment stands today most PD patients will eventually develop dyskinesias, motor fluctuations and mental aberrations. With long-term treatment the benefits of L-DOPA/carbidopa treatment are often outweighed by the side-effects.[17,18] Throughout these past forty years there have been many who believe that L-DOPA treatment may potentiate the damage to dopaminergic neurons.[19] Indeed, L-DOPA therapy does not halt the progression of DA neuronal death.[20,21,267]

Until recently L-DOPA was thought to be simply an inert amino acid which acts as a substrate for DA synthesis.[268] However, recent studies now suggest that L-DOPA may have neurotransmitter characteristics and may yet reach legitimate neurotransmitter status.[269] Several observations support the possibility that L-DOPA may be a neurotransmitter. For example, electrical stimulation and high K^+ concentrations stimulate Ca^{2+}-dependent L-DOPA release from the cytoplasm of catecholaminergic neurons possibly by excitation-secretion coupling mechanisms.[270] Several studies suggest that there may even be L-DOPA neurons[271] and receptors.[272]

Excitotoxicity and generation of reactive oxygen species are the two mechanisms by which L-DOPA is proposed by many investigators to be neurotoxic.[19] L-DOPA can act as an excitotoxin, with approximately one-half the potency of Glu, through its interaction with AMPA[273] receptors. The latter receptors appear to play a role in the striatal dopaminergic neurotoxicity evoked by MPP^+.[166] Micromolar concentrations of L-DOPA have also been reported to mediate Glu release in the rat striatum with resultant delayed neuronal death.[274,275]

Several studies have shown increased levels of 2,3-DHBA after long-term administration of L-DOPA.[276,277] In one of these studies pre-administration of 6-HDA potentiated the production of HO·.[276] These observations suggest that chronic L-DOPA treatment enhances HO· production and that this HO· production may be elevated in the DA-comprimised brain. Long-term administration of L-DOPA causes a significant reversible inhibition of complex I in rat brain, which can be prevented by antioxidants and, thus, another indication of oxidative stress.[278] Interestingly, MPTP/MPP^+ administration also induces reversible inhibition of complex I.[243] Another common observation in many of these investigations with long-term administration of L-DOPA is that GSH is usually neuroprotective. These observations may be significant, because in the PD brain, GSH levels are decreased[30-32] and mt complex I activity is decreased.[279-281]

Overall *in vitro* evidence points to L-DOPA being a neurotoxin.[19,273,274,276,278,282,283] However, *in vivo* studies in animals and normal humans have not found degeneration of nigrostriatal dopamine neurons to occur with chronic treatment of L-DOPA.[284-287] In one *in vivo* study in rats that were pretreated with 6-HDA chronic L-DOPA administration caused a loss of DA neurons not in the SN_{pc}, but in the ventral tegmental area ipsilateral to the 6-HDA administration.[288] The Early versus Late Levodopa (ELLDOPA) clinical drug trial in humans was recently concluded in 2003.[289] This clinical study selected 360 early diagnosed (≤ 2 years) PD patients with minimal clinical symptoms who had previously been treated with ≤ 14 days of L-DOPA/carbidopa or DA agonists. The PD patients received various doses of L-DOPA/carbidopa or placebo for 40 weeks, followed by a 2 week period of no medication.[290] The clinical signs of PD were monitored before, during and after by physicians using the Unified Parkinson's

Disease Rating Scale (UPDRS). The preliminary results[289] suggest that L-DOPA/ carbidopa treatment (after the 2 week period of no medication) did not exacerbate clinical symptoms of PD. However, a subset of 135 of those in the ELLDOPA trial underwent single photon emission tomography neuroimaging studies using 2-β-carbomethoxy-3-β-(4'-iodophenyl)tropane (β-CIT) which binds to the DAT and is used in neuroimaging as a marker of DA neurons. Preliminary results from these neuroimaging studies may suggest that L-DOPA/carbidopa treatment exacerbates degeneration of nigrostrital DA nerve terminals.[289] A thorough final analysis of the results from the ELLDOPA study have yet to be published and the verdict on L-DOPA/carbidopa treatment remains controversial.

E. Conclusion

Perfusion of the antioxidants mannitol and SA (before, during and after a 30 min perfusion of 10.0 mM MPP^+) failed to attenuate formation of L-DOPA, indicating that L-DOPA is not formed by the non-enzymatic hydroxylation of Tyr. Additionally, these antioxidants failed to significantly attenuate the apparent dopaminergic and serotonergic neurotoxicity induced by perfusion of 10.0 mM MPP^+ (as indicated by attenuated day 2 release of DA and 5-HT compared to day 1). 2,3-DHBA (indicative of $HO\cdot$ and/or $ONOO^-$ hydroxylation of SA) was observed, but not until (1) DA levels had fallen, (2) L-DOPA release was observed (3) GSH release was observed.[215] Therefore, hydroxylation of $HO\cdot$ and/or $ONOO^-$ appear to occur intracellularly but only after GSH has been released.

Perhaps the most interesting results were observed from experiments in which DDC activity was significantly decreased 10 min after a 30 min perfusion of 10.0 mM MPP^+ had been discontinued. *In vitro*, MPP^+ did not inhibit DDC. To the best of our knowledge this is the first report that *in vivo* MPP^+ induces the rapid inhibition of DDC with resultant neurotransmitter-like release of L-DOPA in the rat striatum. The reason for this inhibition remains to be determined.

Chapter Three Figures.

Figures 3:01-08. Effect of constant perfusion (3 hr before, during and after) of 2.5 mM SA on the time dependent effects of a 30 min perfusion of 10.0 mM MPP^+ into awake rat striatum on dialysate levels of L-DOPA, DA, DOPAC, 5-HT, 3-MT, 5-HIAA, HVA and 2,3-DHBA on day 1 and an identical perfusion on day 2. Horizontal black bar shows the period during which MPP^+ entered the brain. $*p < 0.05$; $**p < 0.01$ compared to basal levels measured on day 1 or day 2. $^{\#}p < 0.05$ when basal dialysate concentration on day 2 was compared to basal dialysate concentration on day 1. Data are mean ± SEM (n = 4).

Figures 3:09-15. Effect of constant perfusion (3 hr before, during and after) of 100 mM mannitol on the time dependent effects of a 30 min perfusion of 10.0 mM MPP^+ into awake rat striatum on dialysate levels of L-DOPA, DA, DOPAC, 5-HT, 3-MT, 5-HIAA and HVA on day 1 and an identical perfusion on day 2. Horizontal black bar shows the period during which MPP^+ entered the brain. $*p < 0.05$; $**p < 0.01$ compared to basal levels measured on day 1 or day 2. $^{\#}p < 0.05$ when basal dialysate concentration on day 2 was compared to basal dialysate concentration on day 1. Data are mean ± SEM (n = 4).

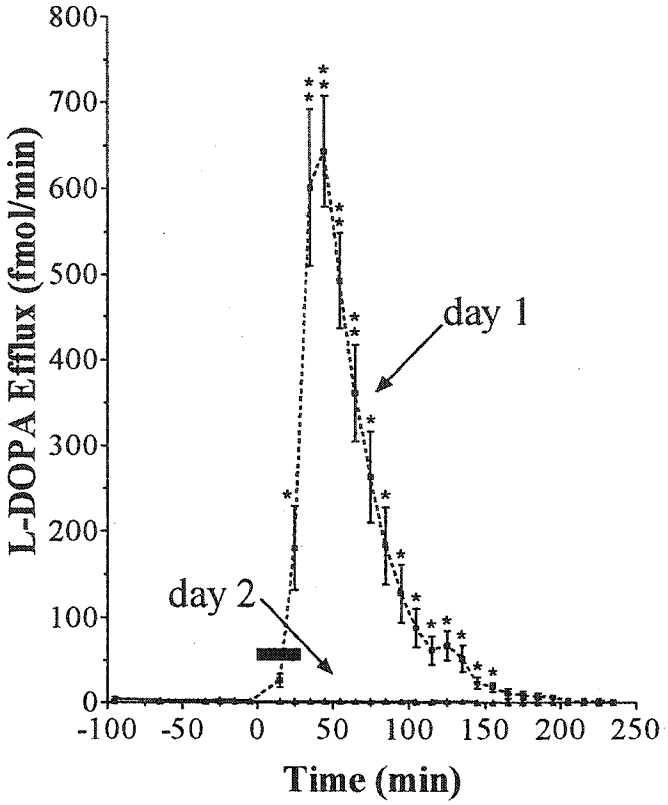

Figure 3:01.
10.0 mM MPP^+ with
2.5 mM Salicylate;
L-DOPA Efflux (fmol/min)
vs. Time (min), n = 4.

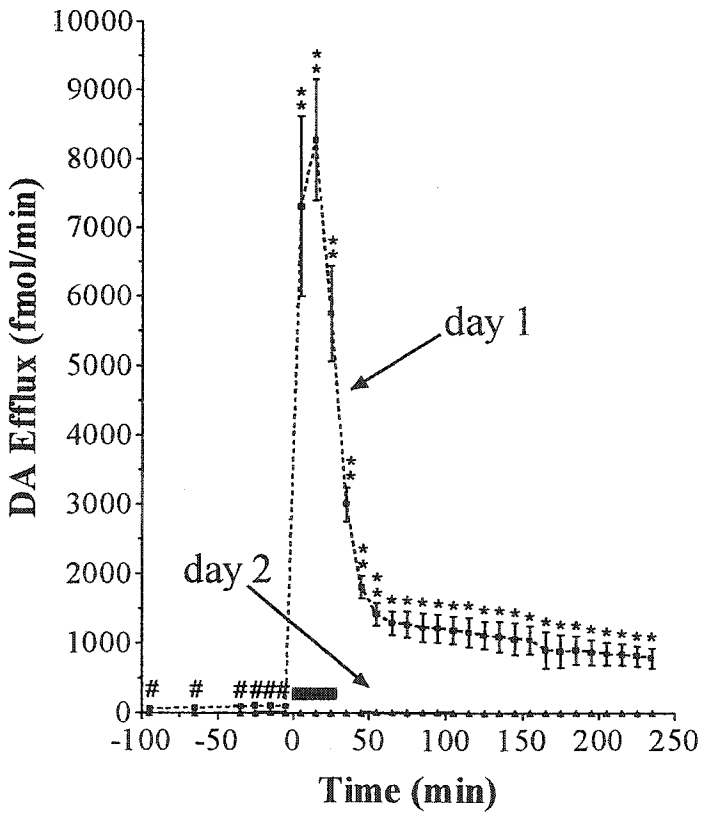

Figure 3:02.
10.0 mM MPP^+ with
2.5 mM Salicylate;
DA Efflux (fmol/min)
vs. Time (min), n = 4.

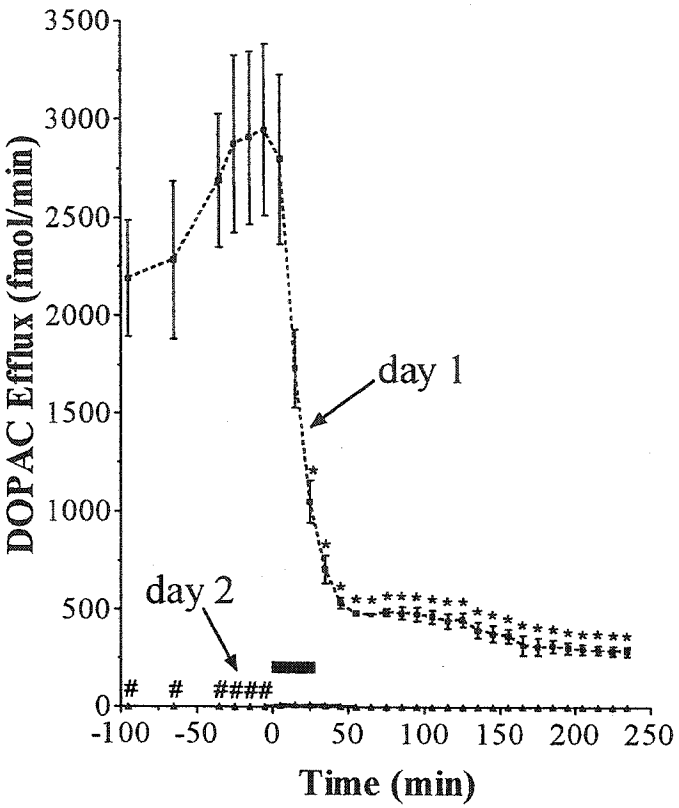

Figure 3:03.
10.0 mM MPP^+ with
2.5 mM Salicylate;
DOPAC Efflux (fmol/min)
vs. Time (min), n = 4.

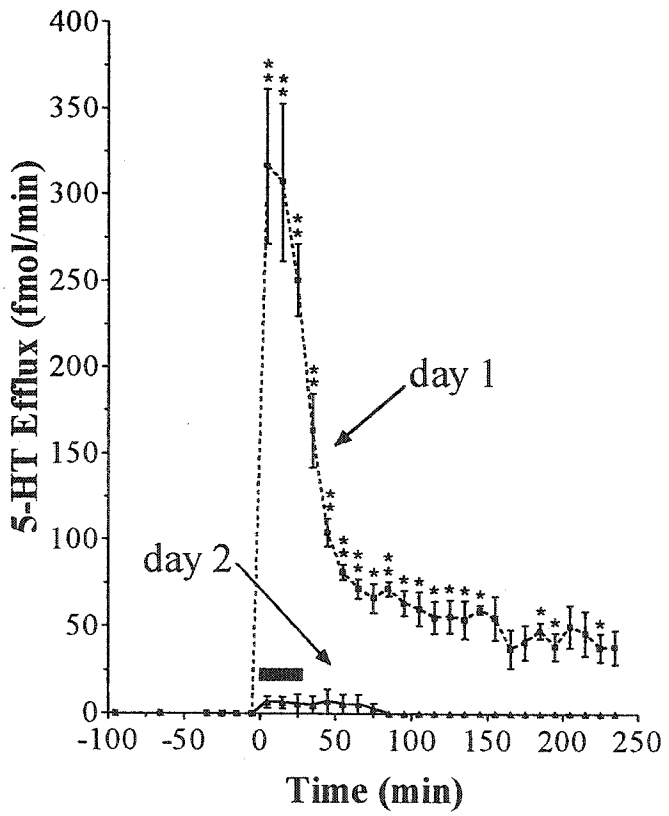

Figure 3:04.
10.0 mM MPP^+ with
2.5 mM Salicylate;
5-HT Efflux (fmol/min)
vs. Time (min), n = 4.

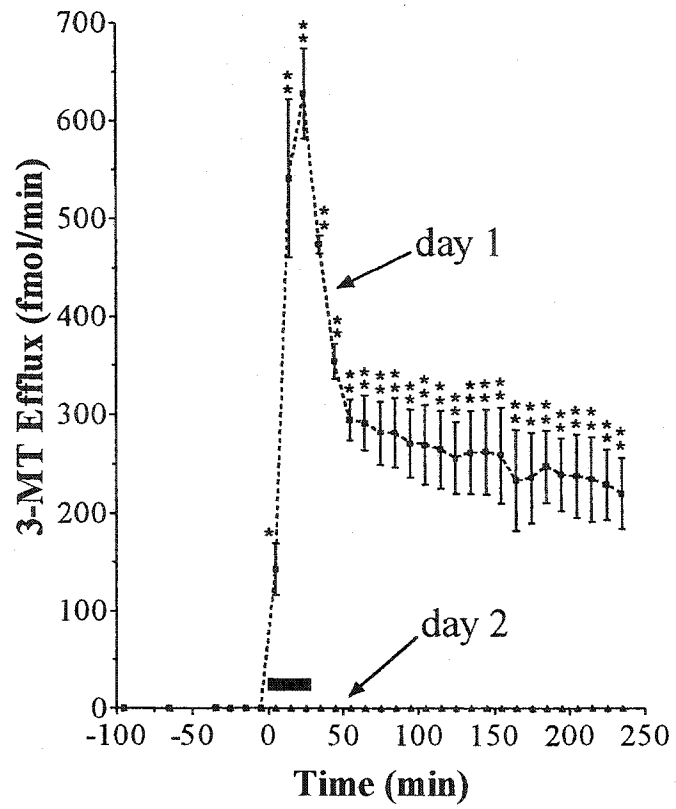

Figure 3:05.
10.0 mM MPP^+ with
2.5 mM Salicylate;
3-MT Efflux (fmol/min)
vs. Time (min), n = 4.

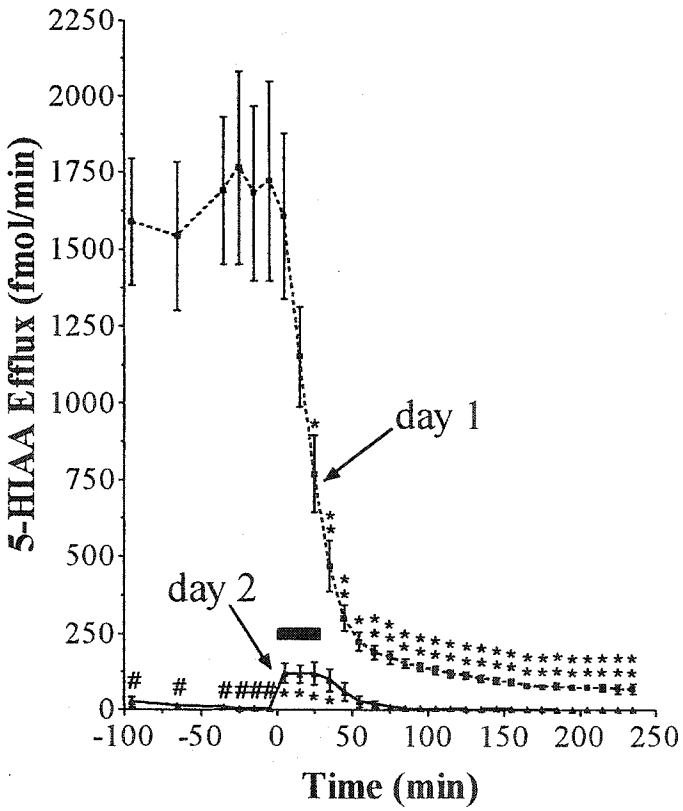

Figure 3:06.
10.0 mM MPP^+ with
2.5 mM Salicylate;
5-HIAA Efflux (fmol/min)
vs. Time (min), n = 4.

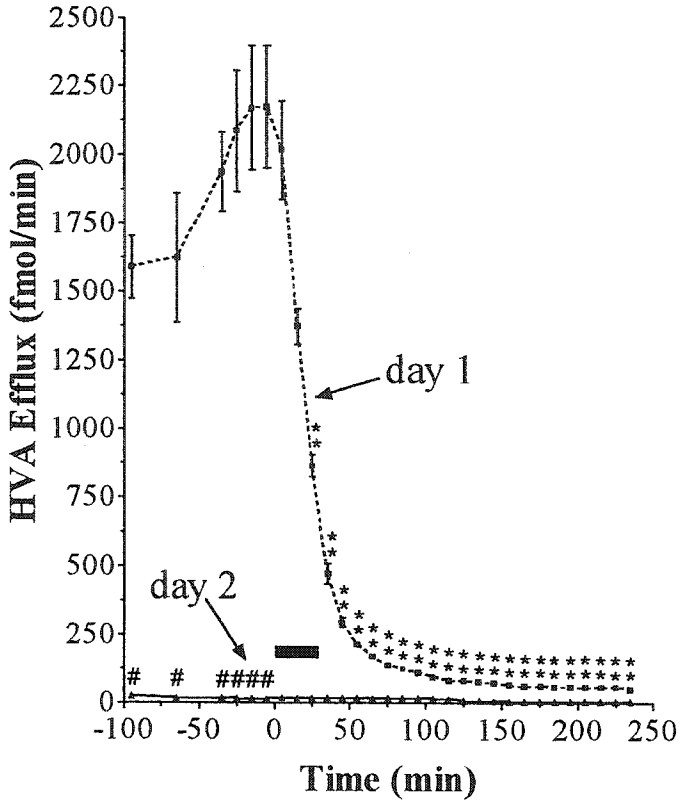

Figure 3:07.
10.0 mM MPP^+ with
2.5 mM Salicylate;
HVA Efflux (fmol/min)
vs. Time (min), n = 4.

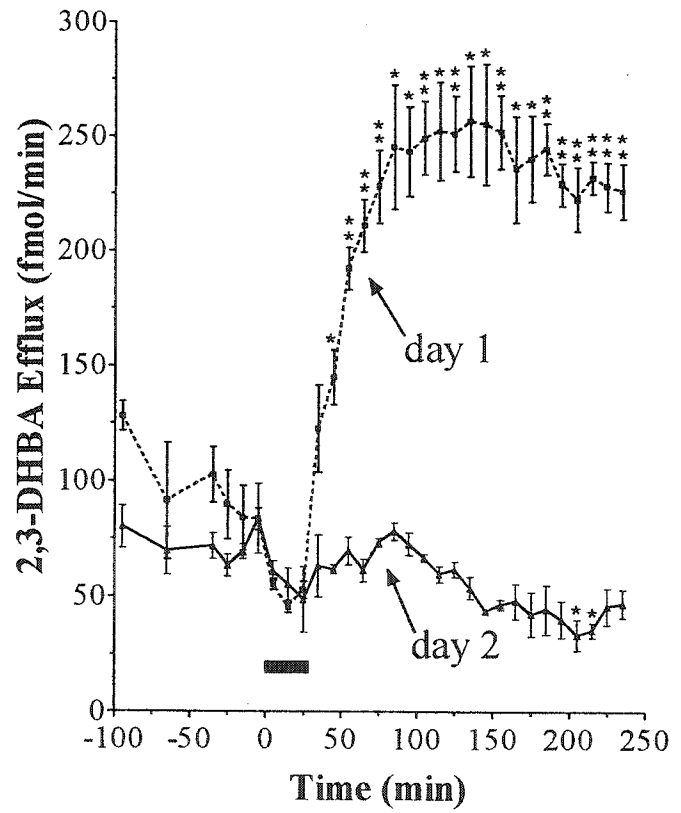

Figure 3:08.
10.0 mM MPP^+ with
2.5 mM Salicylate;
2,3-DHBA Efflux (fmol/min)
vs. Time (min), n = 4.

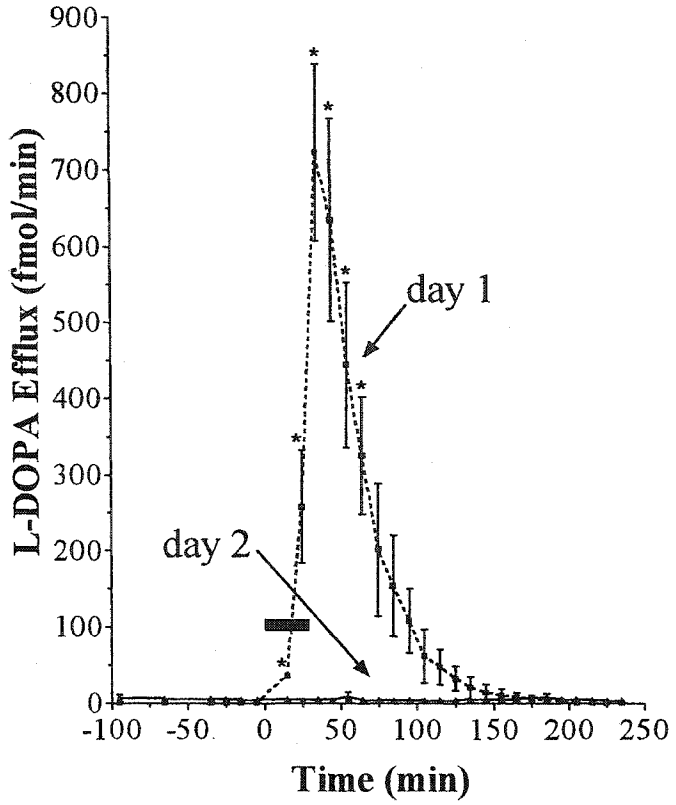

Figure 3:09.
10.0 mM MPP^+ with
100 mM Mannitol;
L-DOPA Efflux (fmol/min)
vs. Time (min), n = 4.

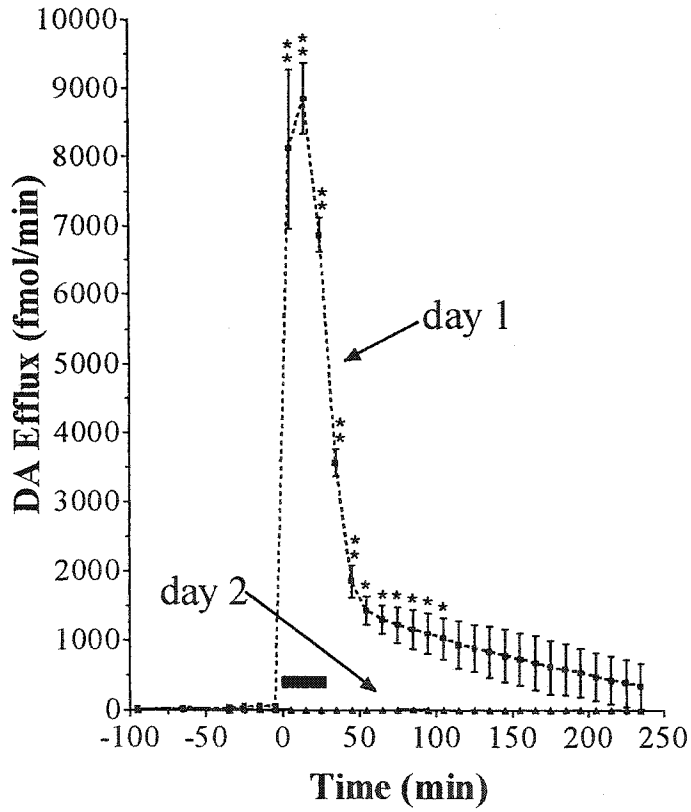

Figure 3:10.
10.0 mM MPP^+ with
100 mM Mannitol;
DA Efflux (fmol/min)
vs. Time (min), n = 4.

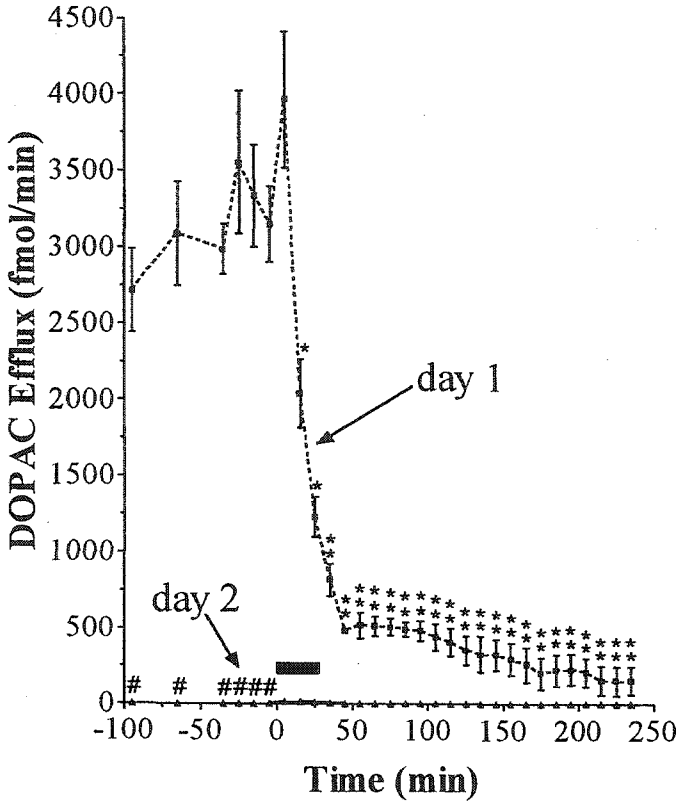

Figure 3:11.
10.0 mM MPP^+ with
100 mM Mannitol;
DOPAC Efflux (fmol/min)
vs. Time (min), n = 4.

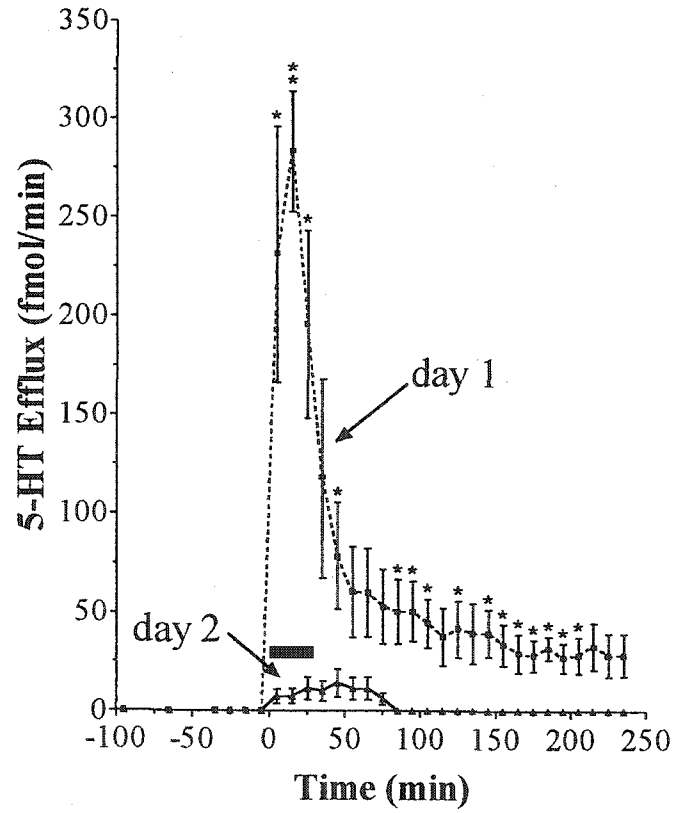

Figure 3:12.
10.0 mM MPP^+ with
100 mM Mannitol;
5-HT Efflux (fmol/min)
vs. Time (min), n = 4.

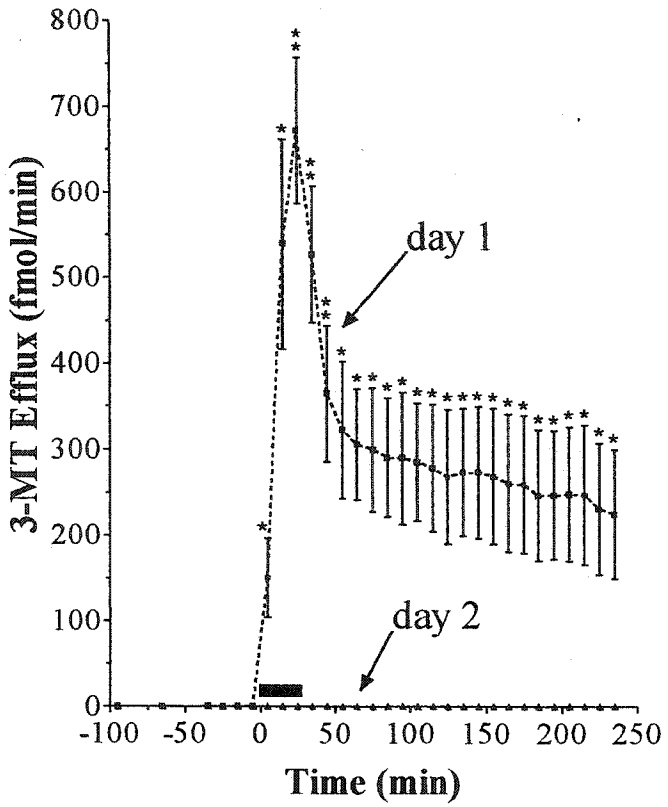

Figure 3:13.
10.0 mM MPP^+ with
100 mM Mannitol;
3-MT Efflux (fmol/min)
vs. Time (min), n = 4.

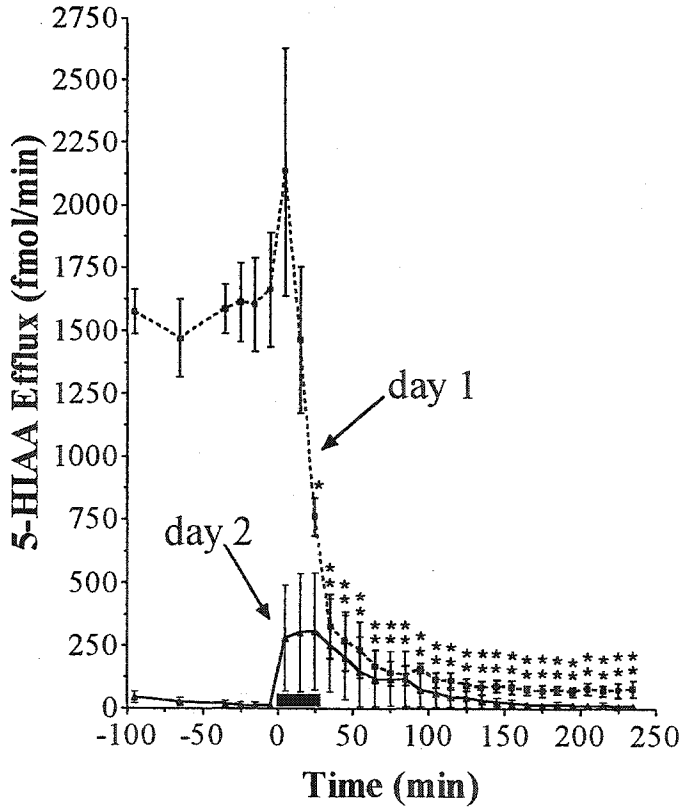

Figure 3:14.
10.0 mM MPP^+ with
100 mM Mannitol;
5-HIAA Efflux (fmol/min)
vs. Time (min), n = 4.

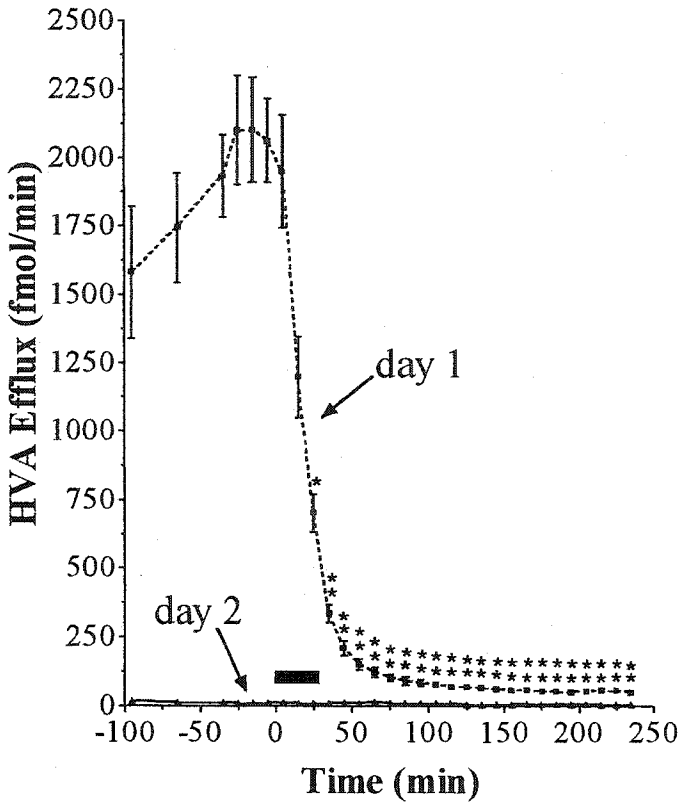

Figure 3:15.
10.0 mM MPP^+ with 100 mM Mannitol; HVA Efflux (fmol/min) vs. Time (min), n = 4.

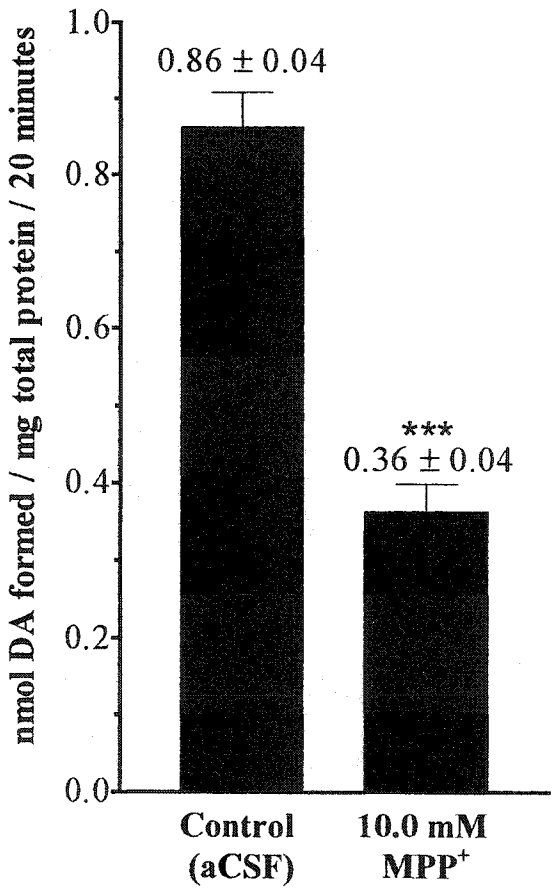

Figure 3:16.
Effect of perfusion of MPP^+ (10 mM) into the right striatum of awake rat on the activity of DDC. MPP^+ dissolved in aCSF was perfused for 30 min after which the perfusate was switched to aCSF alone for 10 min. Animals were then sacrificed and tissue in the vicinity of the microdialysis probe excized and assayed for DDC activity. Control tissue was obtained by perfusing aCSF alone into the left striatum of the same rat. Data are mean ± SEM (n = 3). $***p < 0.001$.

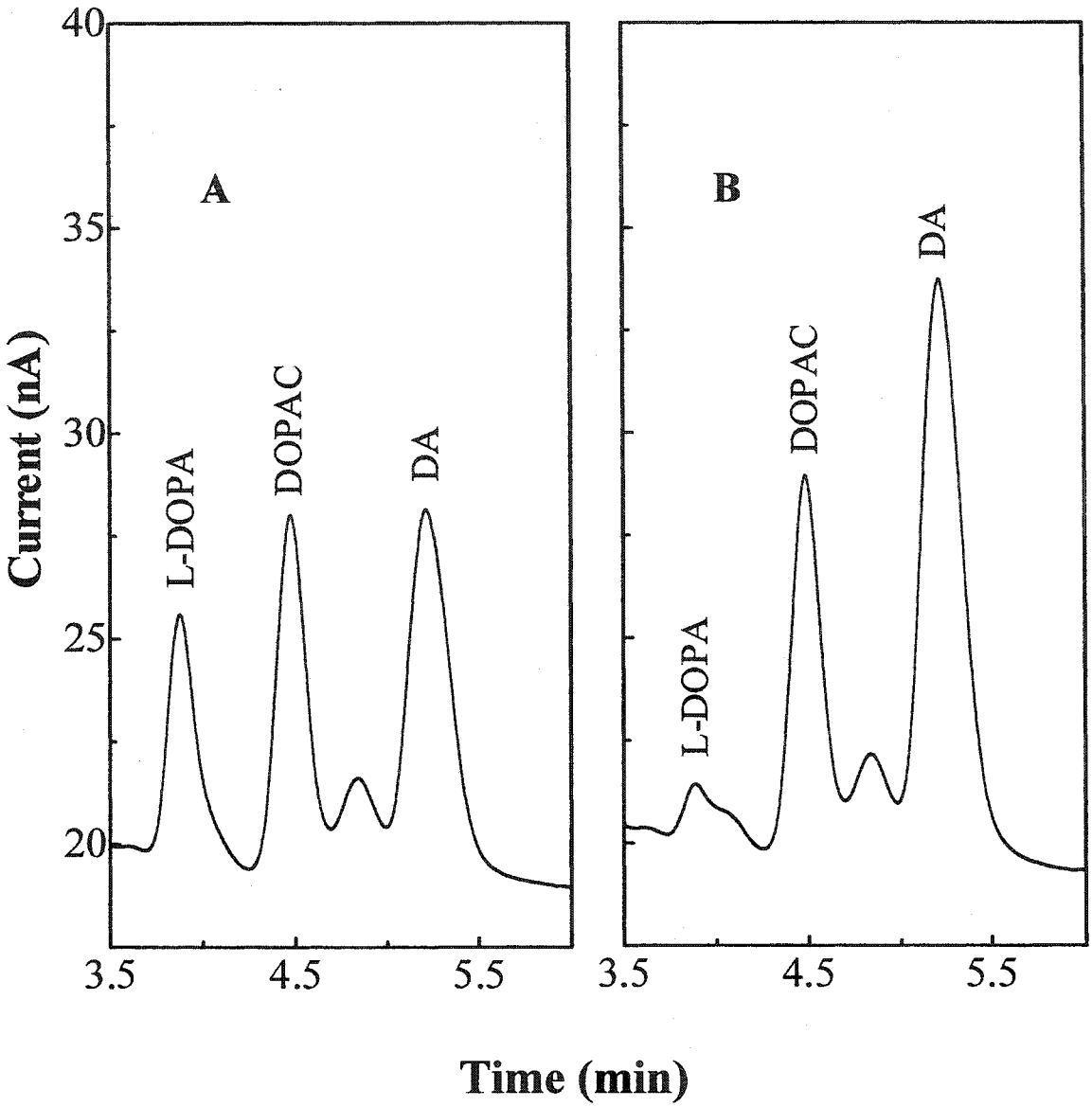

Figure 3:17. HPLC-EC chromatograms of pooled dialysates from 4 rats collected for 26 min after a 30 min perfusion of 10.0 mM MPP^+ was terminated (A) One fraction of this dialysate was incubated for 20 min at pH 6.8 with heat denatured DDC. Then catechols were extracted by adsorption onto alumina. After washing alumina, catechols were acid eluted and an aliquot (5.0 μL) of the eluent was analyzed by HPLC-EC method IV. (B) A second identical fraction of the dialysate was carried through the same procedure as (A) except active purified DDC was employed.

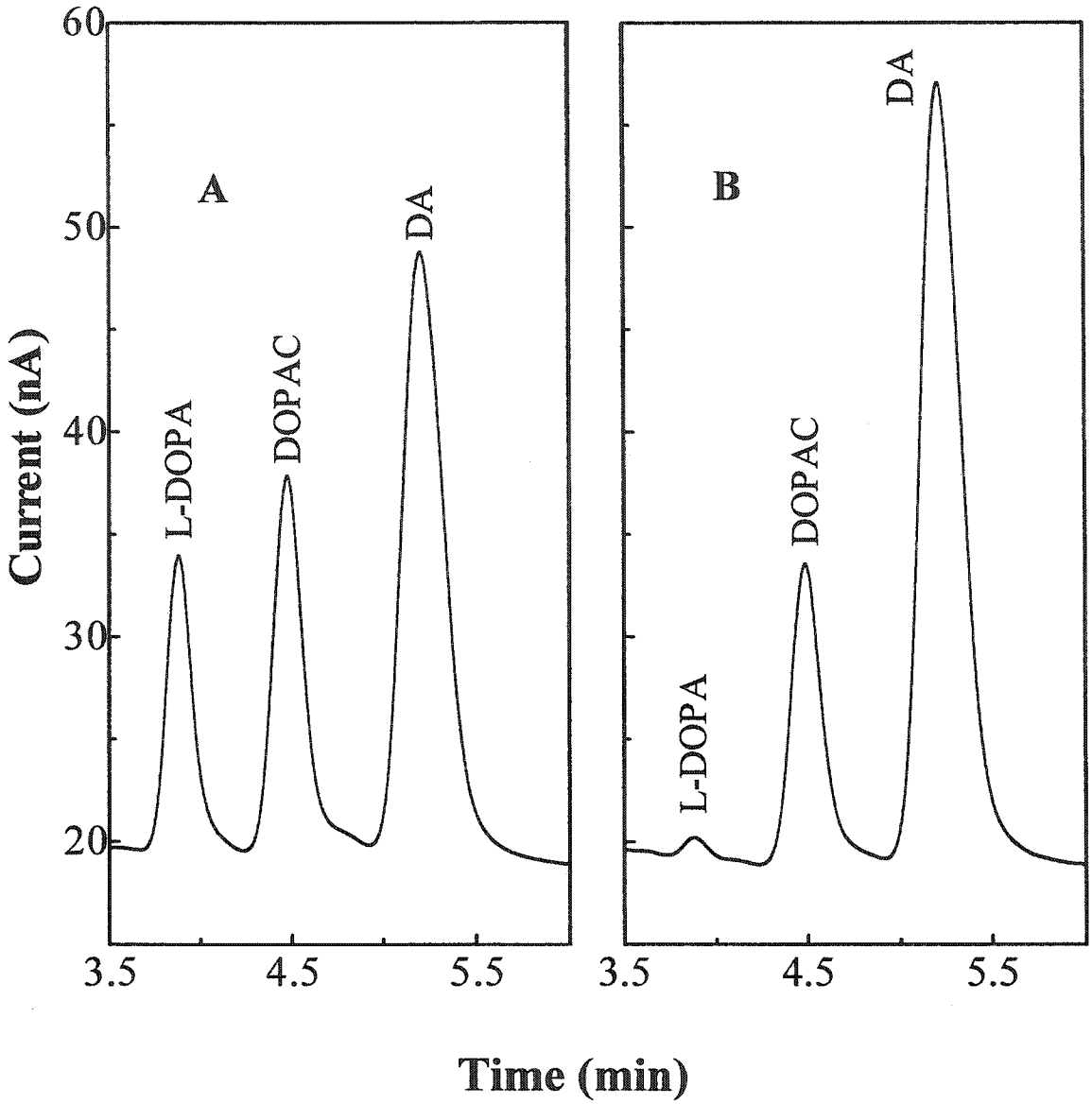

Figure 3:18. HPLC-EC chromatograms of L-DOPA, DOPAC, and DA standard mixture. (A) Standard mixture was incubated for 20 min at pH 6.8 with heat denatured DDC. Then catechols were extracted by adsorption onto alumina. After washing alumina, catechols were acid eluted and an aliquot (5.0 μL) of the eluent was analyzed by HPLC-EC method IV. (B) A second identical standard mixture was carried through the same procedure as (A) except active purified DDC was employed.

Chapter Four

Analysis of Other Animal Models of Neurodegeneration & Parkinson's Disease and Markers of Reactive Oxygen and Nitrogen Species

A. Introduction

1. General

In the work described in previous chapters, perfusions of ≥ 0.7 mM MPP^+ evoked a significant, but transient release of L-DOPA. Furthermore, it was found that at the time of maximum L-DOPA efflux, DDC was significantly inhibited. Another animal model of PD,[5] MA was administered to rats in microdialysis experiments similar to those previously described with MPP^+. The mechanisms of neurotoxicity and resulting effects of MA administration are very similar to those induced by MPP^+. The reasoning behind this was to ascertain if the formation of L-DOPA was limited to the MPP^+, and therefore, not necessarily relevant to PD in humans. Once the results of the MA studies were analyzed, revealing neurotransmitter-like release of L-DOPA, MDMA was administered in similar microdialysis experiments. MDMA differs from MA and MPP^+, in that in rats and most other species it is a selective serotonin neurotoxin,[291] and therefore, not necessarily considered an animal model of PD. However, many of the same factors that appear to be involved in the neurotoxicity mediated by MA and MPP^+ are also involved in MDMA-mediated neurotoxicity. The reasoning here was to determine if L-DOPA release occurred in a rat model that is much less toxic to dopaminergic neurons. One of

the differences between MPP^+/MA neurotoxicity and MDMA is the latter does not lead to dopaminergic cell death in rats except at very high doses.[292] Both of these series of experiments employing MA and MDMA were preliminary, consequently, in-depth descriptions of previous reports and possible mechanisms of neurotoxicity will not be presented. However, several reviews are available.[293-296]

In additional preliminary studies, dialysate from rats perfused with 10.0 mM MPP^+, was analyzed for possible extracellular markers of ROS and RNS. Both ROS and RNS have been implicated in the mechanisms of neurotoxicity induced by MPP^+,[239,241,297] MA,[298,299] and MDMA,[300] and probably play a critical role in the pathogenesis of PD.[301] Extensive analysis was not conducted in this area either. Nevertheless, inclusion of this work certainly is appropriate, for the results, though minor, may provide some further insights into the mechanism of MPP^+-induced neurotoxicity.

2. Methamphetamine

MA was first synthesized in 1919 by a Japanese chemist (Ogata) who was working on developing a replacement for the decreasing supply of naturally-occurring ephedrine which was used to treat asthmatics. Ogata produced D-phenylisopropyl-methylamine which became known as MA. Both MA and amphetamine in the 1940's were prescribed for the treatment of various disorders including sinus problems, fatigue (especially for WWII soldiers) and schizophrenia. By 1970, MA was classified as a schedule II drug and, therefore, as a potentially potentially dangerous and addictive substance. Over the past ten years, MA has become one of the most frequently used drugs of abuse, especially in the mid-western United States where chemicals for its

synthesis (liquid ammonia, sodium, ephedrine and tetrahydrofuran) are readily available.[302]

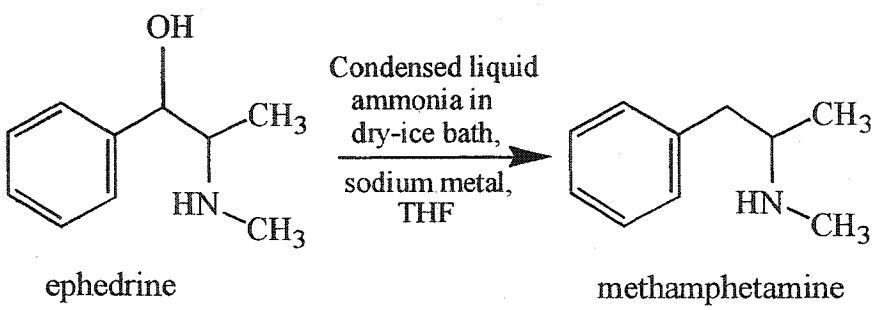

Figure 4:01. "Street" synthesis of methamphetamine.

Unfortunate for drug abusers, but fortunate for those studying neurodegeneration, MA is another drug which, when administered to animals (rodents and non-human primates), serves as a model of PD.[5] Single[120] or multiple injections[121] of MA result in: (1) decreased levels of DA, DOPAC, HVA (in the striatum) and 5-HT (in the striatum and additional areas of the brain);[122] (2) perturbation of amino acids (especially Glu elevation);[123] (3) decreased TH and THP activity;[124] (4) inhibition of MAO;[125] (5) decreased DA[126] and 5-HT uptake;[127] and (6) axonal and terminal dieback of DA[128] and 5-HT neurons.[129]

MA administration induces a 2-3°C temperature increase in animals[130] and humans.[131] The explanation for the MA-induced hyperthermia remains speculative and controversial. The primary purposes of these MA microdialysis experiments were to: (1) observe if there was release of L-DOPA, (2) look for formation of unknown compounds, (3) monitor the extracellular concentrations of DA, 5-HT and their metabolites, and (4)

monitor hyperthermia and possibly correlate the temperature changes to chemical changes.

3. MDMA

MDMA ('ecstasy') has been a popular drug of abuse for the past 20 years, and is a common recreational drug at many dance clubs and all-night rave parties.[303] However, MDMA, a phenethylamine structurally related to MA, is another drug used to study specifically, serotonergic neurotoxicity in rats and other species and dopaminergic neurodegeneration in mice.[291]

Figure 4:02.
'ecstasy';
3,4-methylenedioxy-
methamphetamine

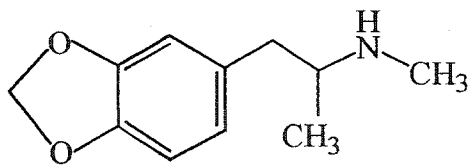

Single[292] or repeated doses[304] of MDMA in rats cause characteristic changes (similar to MPP^+ and MA) in 5-HT, and to a lesser extent in DA.[305-307] MDMA induces 5-HT axon terminal damage (as seen by immunohistochemistry),[308] attenuates 5-HT[309] and DA uptake[310] and causes long-term decreases in 5-HT and 5-HIAA content in rats[305] and non-human primates.[311]

Similar to MA, administration of MDMA evokes a 2-3°C rise in body and brain temperature.[312] Interestingly, in mice, the effects of MDMA administration are quite different. MDMA does not cause 5-HT neurotoxicity in mice, instead, is a dopaminergic neurotoxin.[313] That is, in mice, after administration of MDMA there is long-term damage to DA terminals, decreased levels of DA and DOPAC, yet the serotonergic system recovers after a period of seven days without evidence of 5-HT neurotoxicity.[314] Many

aspects of the mechanisms of MDMA neurotoxicity also remain to be determined. The purpose of MDMA microdialysis experiments was to: (1) observe if there was release of L-DOPA, (2) look for formation of unknown compounds, (3) measure the extracellular concentrations of DA, 5-HT and their metabolites, and (4) monitor hyperthermia.

4. Reactive Nitrogen and Oxygen Species (RNS and ROS)

a. HPLC -UV & -Photo Diode Array

HPLC-EC was employed to analyze dialysate samples in the vast majority of all experiments conducted in this entire project. However, EC detection proved to be unacceptable for analysis of possible markers of extracellular RNS and ROS generation evoked by MPP^+ and the other neurotoxins. For example, to obtain a reasonable detection limit for standard 3-nitro-Tyr, potentials around +1.3 V (vs. a Ag/AgCl reference electrode) were necessary. However, at this potential, the selectivity of oxidation was lost and a large number of unknown endogenous compounds contained in rat brain dialysate respond, making identifications and efficient separations virtually impossible. Previous analysis of 3-nitro-Tyr with EC detection has been conducted. In these reports, compounds were detected employing coulometric[315] and multiple ($\geq$ 8) electrode[316] techniques. HPLC-EC employed in this laboratory is strictly amperometric with single or dual electrodes. HPLC -UV and -PDA methods were developed, providing extremely low detection limits. The HPLC-PDA system was particularly exciting for numerous reasons. One of these being that compounds detected in dialysate could not only be identified based upon t_R and co-elution with added standard but in addition,

characteristic UV spectra can be collected and correlated with the UV spectra of standard compounds.

b. 3-nitro-Tyr and 4-nitrophenylalanine (4-nitro-Phe)

ROS and RNS probably play pivotal roles in the neurotoxicity triggered by MPP^+,[5,317] MA[298,299] and MDMA[300] and in PD.[301] $O_2^{-}\cdot$ is one such ROS, which by itself is not highly reactive.[34] However, under conditions of impaired ATP-production (e.g. MPP^+-induced),[149] NMDA receptors can be activated by normal basal levels of Glu, resulting in an influx of Ca^{2+}.[201] This influx of Ca^{2+} leads to not only production of $O_2^{-}\cdot$,[170] but activation of nNOS, resulting in NO·, $ONOO^-$ and HO· formation.[207,318] $ONOO^-$ and HO· are highly reactive and can directly cause neurotoxic effects. Over-production of $O_2^{-}\cdot$ can promote HO· generation through Fenton chemistry and the metal catalyzed Haber-Weiss reaction by reducing transition metals (especially, iron) and dismuting to form H_2O_2.[34]

$$M^{n^+} + O_2^-\cdot \rightarrow M^{n^+-1} + O_2 \qquad \textbf{Reaction 4:01.}$$

$$2\,O_2^-\cdot \underset{2H^+}{\overset{SOD}{\rightarrow}} O_2 + H_2O_2 \qquad \textbf{Reaction 4:02.}$$

$$M^{n^+-1} + H_2O_2 \rightarrow M^{n+} + HO\cdot + HO^- \qquad \textbf{Reaction 4:03.}$$

The significance of these reactions are exemplified by elevated levels of nonheme iron in the SN_{pc} of PD patients.[30]

$O_2^{-\cdot}$ also reacts at the diffusion limit with NO· to produce $ONOO^-$.

$$O_2^- \cdot + NO \cdot \rightarrow ONOO^- \qquad \textbf{Reaction 4:04.}$$

$ONOO^-$ is able to nitrate both free Tyr (*in vitro*) and protein-bound Tyr residues to form 3-nitro-Tyr.[257] Elevated levels of protein-bound 3-nitro-Tyr have been found in autopsied PD brains.[35] Protein bound 3-nitro-Tyr has been detected in the brains of MPTP/MPP^+-treated animals.[257] $ONOO^-$ can also nitrate Phe to form 4-nitro-Phe. HO· and/or $ONOO^-$ can also hydroxylate Phe to form *o*-, *m*- and *p*-Tyr.[319]

B. Experimental

1. Drugs and Chemicals

S(+)-MA (hydrochloride salt) was obtained from Research Biochemicals International (RBI, Natick, MA). S(+)-MDMA (hydrochloride salt), 3-nitro-Tyr, 4-nitro-Phe, DL-3-(2-hydroxyphenyl)alanine (*o*-tyrosine; *o*-Tyr), and DL-3-(3-hydroxyphenyl)-alanine (*m*-tyrosine; *m*-Tyr) were obtained from Sigma (St. Louis, MO). Sodium Chloride Injection (0.9%) USP (Saline) was obtained from Rhone Merieux (Athens, GA). Phosphoric acid was obtained from Mallinckrodt (Paris, KY). Potassium phosphate monohydrate (KH_2PO_4) was obtained from EM Science (Gibbstown, NJ). The sources of all other drugs and chemicals have been described previously.

2. Animals

Animal surgical procedures described in Chapter Two were followed for experiments when MPP^+ was perfused. For experiments when MA and MDMA were administered, guide cannula were stereotaxically implanted into both the right and left striata as described in Chapter Three. On the day of the experiment, the guide cannula in the right striatum was replaced by a CMA 12 (4 mm tip) probe with the tip positioned 7.4 mm below dura. The left guide cannula was replaced with a Teflon-coated copper/constantan temperature probe (Type T, Physitemp Instruments, Clifton, NJ) with the tip positioned 7.4 mm below dura. Brain temperature was monitored using a Physitemp Thermalert TH-8.

3. Microdialysis Procedure to Monitor Biogenic Amines and Possible Markers of ROS and RNS.

Microdialysis procedures to determine biogenic amines and markers of ROS/RNS using MPP^+ were identical to those described in Chapter Two. However, in microdialysis experiments designed to search for *o*-and *m*-Tyr, 3-nitro-Tyr and 4-nitro-Phe, dialysate vials did not contain any pre-added HCl, which may lead to decomposition of nitrite to form $NO\cdot$ at $pH \leq 3$.[320,321] HPLC (-UV and -PDA) analysis often required larger volumes of dialysate (than the 7.5 μL collected) in order to achieve required detection limits and, hence, when necessary collected fractions were pooled.

For experiments with MA or MDMA, aCSF was perfused via a microdialysis probe into the right striatum. MA and MDMA solutions were prepared in sterile saline ≤ 15 min before administration. MA (30 mg free base/kg, *ca.* 450 μL, i.p.) or MDMA (15

mg free base/kg, *ca.* 450 μL, i.p.) were administered at a time when the concentration of DA, 5-HT and their metabolites in dialysate samples had reached constant basal levels. During microdialysis experiments the brain temperature was recorded every 15 min during collection of basal levels and every 5 min after administration of MA or MDMA. After MA or MDMA administration, two plastic bags containing crushed ice were placed in the bottom of the Raturn bowl when the brain temperature of rats reached 41.5°C. This ice was removed when the brain temperature had declined to 40.0°C. Plastic sheets of bubble-wrap packing material were employed to cover the top of the Raturn bowl in order to keep animals contained within the bowl and reduce damage to the microdialysis tubing and temperature probes due to excessive MA- and MDMA-induced hyperactivity.

4. *In vitro* experiments with DDC and MA

In experiments to determine the effect of MA on DDC activity *in vitro*, 15.0 mM MA (free base final concentration) was included in the assay mixture. The details of this procedure are explained in the Experimental Section of Chapter Three where MPP^+ was employed.

5. HPLC

a. EC Detection for MA and MDMA Experiments

HPLC-EC method I (described in Chapter Two) was employed for microdialysis experiments with MA or MDMA.

b. UV and PDA detection methods for analysis of L-DOPA, DA, 5-HT, their normal metabolites, *o* and *m*-Tyr, 3-nitro-Tyr, and 4-nitro-Phe.

HPLC-UV method I was used to analyze dialysate fractions for DA, 5-HT, their normal metabolites, *o*- and *m*-Tyr, 3-nitro-Tyr and 4-nitro-Tyr, and to continue the search for glutathionyl and cysteinyl conjugates of DA and DOPAC. This method employed a BAS 200B HPLC system equipped with a Phenomenex IB-SIL column (ODS-18-BD, 100 x 3.2 mm, 3 μm), a Rheodyne 7125 injector with a 20.0 μL sample loop and a BAS model UV-116AUV-VIS dual detector set at λ_1 = 280 nm and λ_2 = 365 nm. The mobile phase was prepared by adding 0.85 mL DEA, 59.2 mg SOS, 187 mg Na_2EDTA dihydrate and 21.0 g citric acid monohydrate to 970 mL of deionized water. After filtration, the pH of this solution was adjusted to 2.40 with $HClO_4$ (*ca.* 9.1 N) and then 30 mL of MeCN and 15 mL of MeOH were added. The flow rate was 0.40 mL/min. For all chromatography, mobile phases were degassed by stirring under vacuum for approximately 30 min prior to use.

HPLC-PDA method I was also used to analyze dialysate fractions for DA, 5-HT, their normal metabolites, *o*- and *m*-Tyr, 3-nitro-Tyr and 4-nitro-Tyr, and to search for glutathionyl and cysteinyl conjugates of DA and DOPAC. This method employed a Dionex (Houston, TX) P680A LPG Low Pressure Quaternary Gradient Analytical Pump System and an integrated online degasser equipped with a Phenomenex Nucleosil reversed phase column (ODS-18-BD, 250 x 4 mm, 120 Å, 5 μm particle size), Phenomenex guard column (ODS-18, 4 x 3 mm, 120 Å, 5 μm particle size), a Dionex model 585 column oven (set at 40°C) and a Dionex UVD 340U UV-Vis photodiode. The PDA detector was set to monitor four wavelengths (216, 225, 276, and 356 nm) and the

photodiode scan range was from 200-600 nm. Vials containing dialysate fractions were loaded into a Dionex ASI-100T refrigerated autosampler (4°C) equipped with an in-line variable volume injector. Injection volumes were typically 30.0 μL. The mobile phase was prepared by adding 6.80 g KH_2PO_4 and 80 mL MeOH to 920 mL of deionized water. After filtration, the apparent pH of this solution was adjusted to 3.15 with phosphoric acid. The flow rate was 0.8 mL/min.

C. Results

1. Effects of MA on dialysate levels of L-DOPA, DA, 5-HT and their normal metabolites

A single 30 mg/kg, i.p. dose of MA, previously shown to be neurotoxic in rats,[120,122] induced significant hyperthermia (Figure 4:03) and an almost immediate release of DA (Figure 4:05). The maximum release of DA was approximately one-fourth that induced by perfusion of 0.7 mM MPP^+ (Table 4:01). MA also induced a rise of L-DOPA (Figure 4:04), the maximum release being approximately one-third that caused by perfusion of 0.7 mM MPP^+ (Table 4:01). Injection of MA induced a fall of dialysate levels of DOPAC, an immediate rise of 5-HT and delayed rise of 3-MT, then a time-dependent decline of the latter two (Figures 4:06-08, respectively) with temporal profiles similar to those evoked by MPP^+. However, the maximum 5-HT release was 3 times larger than that caused by perfusion of 0.7 mM MPP^+. Interestingly, dialysate levels of 5-HIAA (Figure 4:09) and HVA (Figure 4:10) did not change greatly from basal levels following MA injection. HPLC-EC (method I) analysis of rat striatal dialysates after administration of MA did not detect the presence of glutathionyl or cysteinyl conjugates

of DA or DOPAC. *In vitro* studies revealed that MA (15.0 mM) had no effect on DDC activity.

Table 4:01. Effect of MA, MDMA and MPP^+ on the maximal release of DA, L-DOPA and 5-HT. Data are mean ± SEM (n ≥ 4) for release.

Drug Administered	Maximal release (fmol/min) of:			
	DA	L-DOPA	5-HT	$^{DA}/_{5\text{-}HT}$ ratio
MA (30 mg/kg; i.p.)	938 ± 331	35 ± 15	150 ± 76	6.2
MDMA (15 mg/kg; i.p.)	274 ± 100	19 ± 4	97 ± 49	2.8
MPP^+ 0.7 mM (30 min perfusion)	3920 ± 449	96 ± 32	47 ± 13	83.4

2. Effect of MDMA on dialysate levels of L-DOPA, DA, 5-HT and their normal metabolites

The results from experiments employing MDMA were similar to those from perfusion of MPP^+ and administration of MA. A single 15 mg/kg, i.p. dose of MDMA, previously, shown to be neurotoxic in rats,[292] induced significant hyperthermia (Figure 4:11) and relatively small release of DA (Figure 4:13). The maximum release of DA was approximately one-third that caused by administration of MA (Table 4:01). DA release was delayed, (compared to MA and MPP^+ experiments) reaching peak levels 55 min after MDMA administration (Figure 4:13). MDMA also induced a rise of

extracellular L-DOPA (Figure 4:12), the maximum release being approximately one-half that caused by administration of MA (Table 4:01). Injection of MDMA induced a fall of dialysate levels of DOPAC, an immediate rise of 5-HT and delayed rise of 3-MT, then a time-dependent decline of the latter two (Figures 4:14-16, respectively). However, the maximum 5-HT release by MDMA was twice that caused by perfusion of 0.7 mM MPP^+ (Table 4:01). As with MA, dialysate levels of 5-HIAA and HVA did not change greatly from basal levels, following MDMA injection (Figures 4:17, 18). HPLC-EC (method I) analysis of rat striatal dialysates after administration of MDMA did not detect the presence of glutathionyl or cysteinyl conjugates of DA or DOPAC.

An additional experiment was conducted to confirm that L-DOPA was present in dialysates from MDMA-treated rats. A chromatogram of a standard mixture of DA, 5-HT and their normal metabolites is shown in Figure 4:19A. Dialysate collected between 55-110 min post-MDMA administration (period when putative L-DOPA peak was at its maximum) was pooled and one-half was analyzed using HPLC-EC method I, as depicted in Figure 4:19B. The chromatogram shown in Figure 4:19C is from the remaining dialysate, in which standard L-DOPA was added to approximately double the putative L-DOPA peak. These figures indicate putative L-DOPA co-eluted with standard L-DOPA and the peak height was increased proportional to the amount of added standard L-DOPA.

3. HPLC (-UV) & (-PDA) search for possible extracellular markers of RNS/ROS: *o*-and *m*-Tyr, 3-nitro-Tyr, 4-nitro-Phe.

It has been shown and proposed that elevated ROS and RNS are generated during experiments with MPTP/MPP^+.[5,257,317] Possible extracellular markers of ROS and RNS generation may include *o*- and *m*-Tyr, 3-nitro-Tyr and 4-nitro-Phe.[319] Microdialysis experiments were conducted in which 10.0 mM MPP^+ was perfused into the striatum of freely moving rats. Initial work was conducted employing HPLC-UV method I. It was eventually determined that the detection limits (3 times peak-to-peak noise) for *o*- and *m*-Tyr, 3-nitro-Tyr and 4-nitro-Phe were probably not acceptable. With a 20.0 μL sample loop, nanomolar detection limits (mean ± SEM; n = 16) employing HPLC-UV method I were as follows: *m*-Tyr (145 ± 13), *o*-Tyr (230 ± 13), 3-nitro-Tyr (187 ± 14), and 4-nitro-Phe (143 ± 11). However, HPLC-PDA has been employed in a recent study and 3-5 nM (30 μL sample volume) detection limits were reported for *o*- and *m*-Tyr, 3-nitro-Tyr and 4-nitro-Phe.[319] In studies presented here, using HPLC-PDA method I, detection limits for *o*- and *m*-Tyr, 3-nitro-Tyr and 4-nitro-Phe were *ca.* 30-52 nM with a 30.0 μL sample volume. The detection limits (3 times peak-to-peak noise; nM ± SEM; n = 16) at maximum absorption λ (nm) for each compound were as follows: *m*-Tyr (45.6 ± 6.9), *o*-Tyr (48.6 ± 7.3), 3-nitro-Tyr (30.6 ± 3.6) all three at λ = 216 nm, and 4-nitro-Phe (51.8 ± 8.4 at λ = 265 nm). However, at no time before, during or after perfusion of MPP^+ were hydroxylation or nitration products of Tyr or Phe detected in dialysate collected from rats perfused with MPP^+. This is not an indication these previous reports[319] may be incorrect. It merely indicates that at the detection limits available with HPLC (-UV method I and -PDA method I) *o*- and *m*-Tyr, 3-nitro-Tyr and 4-nitro-Phe were not detected.

D. Discussion

Elevation of extracellular L-DOPA is not specific to MPP^+ since both MA (another dopaminergic neurotoxin)[5] and MDMA (a serotonergic neurotoxin in rats),[291] also evoke a similar effect (Figures 4:04, 12, respectively). *In vivo* studies on the activity of DDC following MA or MDMA administration were not carried out. However, it seems reasonable to propose a similar inhibition occurs during the period of L-DOPA release evoked by MA and MDMA. The levels of DA and L-DOPA efflux mediated by MA and MDMA are greatly attenuated compared to those induced by minimally neurotoxic concentrations of MPP^+, and thus, the DDC inhibition is not proposed to be as extensive. An obstacle to determining the in vivo activity of DDC in the MA and MDMA experiments, is that unlike the MPP^+-perfused animals, MA and MDMA administration evokes extreme behavioral modifications, making animal handling extremely difficult. In fact, these experiments usually required constant observation and intervention to insure that the microdialysis tubing and probe did not become damaged from the hyperactivity induced by MA- and/or MDMA. Measuring DDC activity at the time of maximum L-DOPA release happens to correspond to the time of maximum hyperactivity.

The attenuated release of DA by both MA and MDMA (Table 4:01), compared to that mediated by a minimally neurotoxic dose (0.7 mM) MPP^+ is probably a result of DAT inhibition.[322] The MA- and MDMA-induced maximum efflux ratios of $^{DA}/_{5\text{-}HT}$ are greatly attenuated compared to this same ratio induced by MPP^+. MA is proposed to enter neurons through the DAT, and if inhibited, DA release (through the reversed DAT) into the extracellular fluid, would be subsequently decreased. To the best of our

knowledge, there have been no reports of MPTP/MPP^+-induced DAT inhibition. MDMA is a substrate for the serotonin transporter (SERT) but not the DAT. MDMA enters DA neurons by passive diffussion, a much slower process. Indeed, support for MDMA as a selective serotonergic neurotoxin is shown by the delayed maximum release of DA (compared to both MA and MPP^+ experiments; Figures 4:05 and 2:19, respectively), which does not occur until 55 min after MDMA administration (Figure 4:13), and 40 min after 5-HT maximal release (Figure 4:15). This indicates that MDMA enters serotonergic neurons before and more efficiently than dopaminergic neurons. Additionally, the $^{DA}/_{5\text{-HT}}$ ratio induced by MDMA is one-half that induced by MA (Table 4:01), therefore, it follows that the MDMA-induced $^{5\text{-HT}}/_{DA}$ ratio is twice that induced by MA. The increased $^{5\text{-HT}}/_{DA}$ ratio induced by MDMA (compared to MA) is another indication of the selectivity of MDMA for the serotonin transporter.

Similar hyperthermic responses were observed in both MA and MDMA treated animals. In initial investigations, animals were unable to survive the entire length of the experiment when they did not receive intervention (with ice) to halt hyperthermia. A crucial aspect of these studies was employing bags of ice to modulate the temperature of the rats. The possible explanation for MA/MDMA induced hyperthermia and its relevance remain speculative. Despite decades of MA and MDMA research, until recently, the role of hyperthermia had been virtually ignored.

E. Conclusion

The experiments with MA and MDMA indicate L-DOPA formation/release is not limited to the MPP^+ model of PD. This is significant for several reasons: (1) L-DOPA can act as an excitotoxin by interaction with AMPA receptors,[273] (2) Glu release can be mediated by micromolar concentrations of L-DOPA with subsequent delayed neuronal death,[274,275] (3) the neurotransmitter-like release of L-DOPA may occur in PD, and (4) perhaps most significant, L-DOPA administration is the most common form of treatment for PD and this treatment is suspected of exacerbating nigrostriatal neurodegeneration.[19,290] Indeed, the extracellular rise of L-DOPA mediated by MPP^+, MA and MDMA suggests that L-DOPA may be an early event in idiopathic PD.

Nevertheless, MPTP/MPP^+, MA and MDMA -induced neurotoxicity have well established similarities and the neurotransmitter-like release of L-DOPA is certainly an important addition. The implications of these findings remain to be determined, yet, may at least prove beneficial in determining the source and mechanism for the formation/release of L-DOPA and could provide insight into the mechanisms involved in the damage induced by these neurotoxins.

Chapter Four Figures.

Figures 4:03-4:10. Time-dependent effects of administration of 30 mg/kg (i.p.) MA on rat striatal brain temperature and striatal dialysate levels of L-DOPA, DA, DOPAC, 5-HT, 3-MT, 5-HIAA and HVA. Horizontal black bar shows the period during which MPP^+ entered the brain. $*p < 0.05$; $**p < 0.01$ compared to basal levels. Data are mean ± SEM (n = 6).

Figures 4:11-4:18. Time-dependent effects of administration of 15 mg/kg (i.p.) MDMA on rat striatal brain temperature and striatal dialysate levels of L-DOPA, DA, DOPAC, 5-HT, 3-MT, 5-HIAA and HVA. Horizontal black bar shows the period during which MPP^+ entered the brain. $*p < 0.05$; $**p < 0.01$ compared to basal levels. Data are mean ± SEM (n = 4).

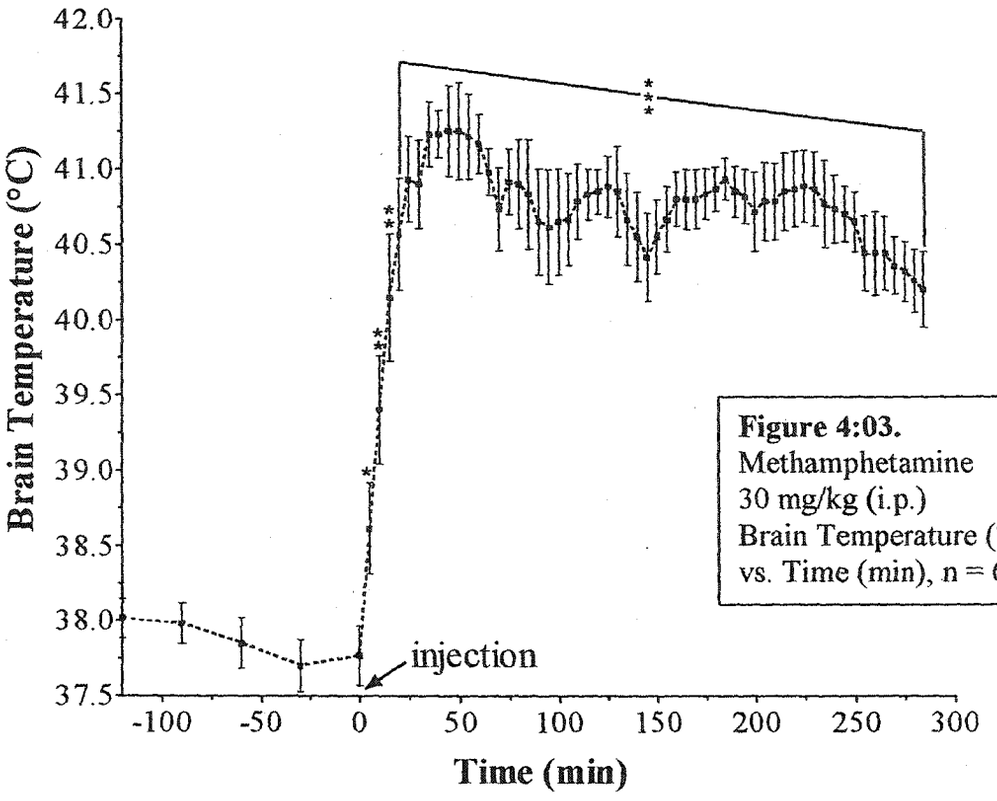

Figure 4:03.
Methamphetamine
30 mg/kg (i.p.)
Brain Temperature (°C)
vs. Time (min), n = 6

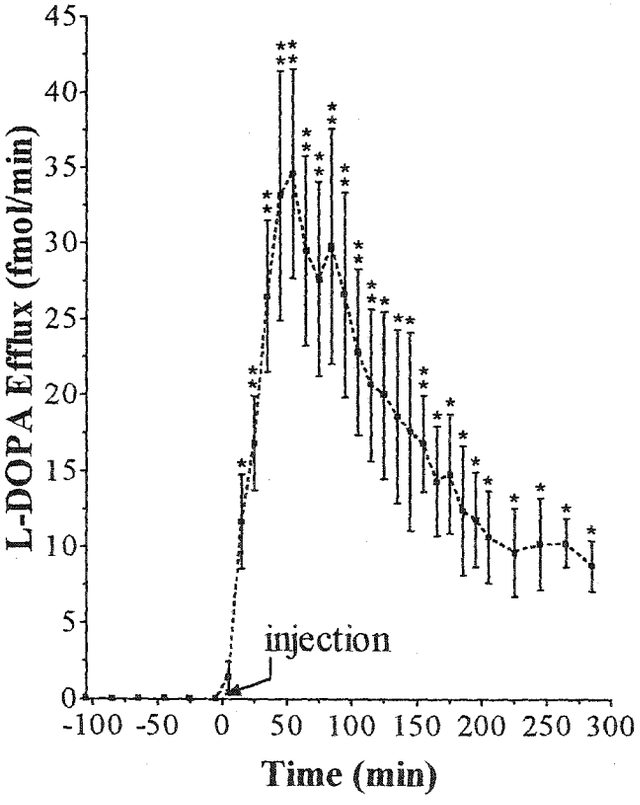

Figure 4:04.
Methamphetamine
30 mg/kg (i.p.);
L-DOPA Efflux (fmol/min)
vs. Time (min), n = 6.

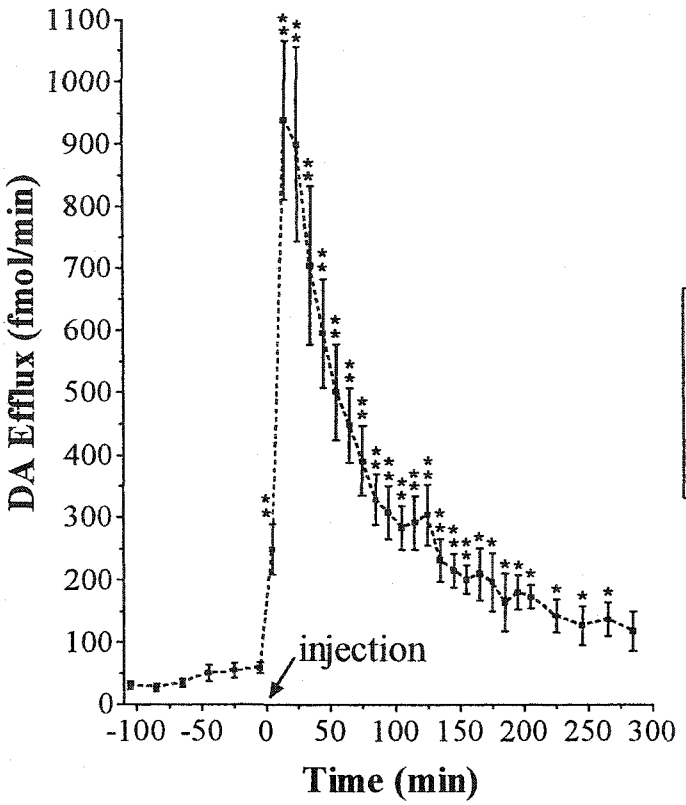

Figure 4:05.
Methamphetamine
30 mg/kg (i.p.);
DA Efflux (fmol/min)
vs. Time (min), n = 6.

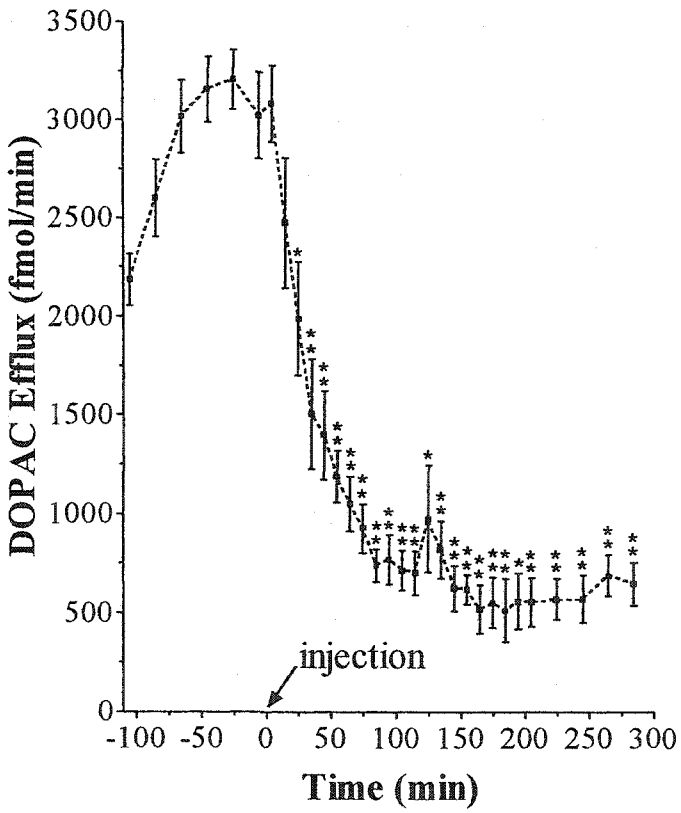

Figure 4:06.
Methamphetamine
30 mg/kg (i.p.);
DOPAC Efflux (fmol/min)
vs. Time (min), n = 6.

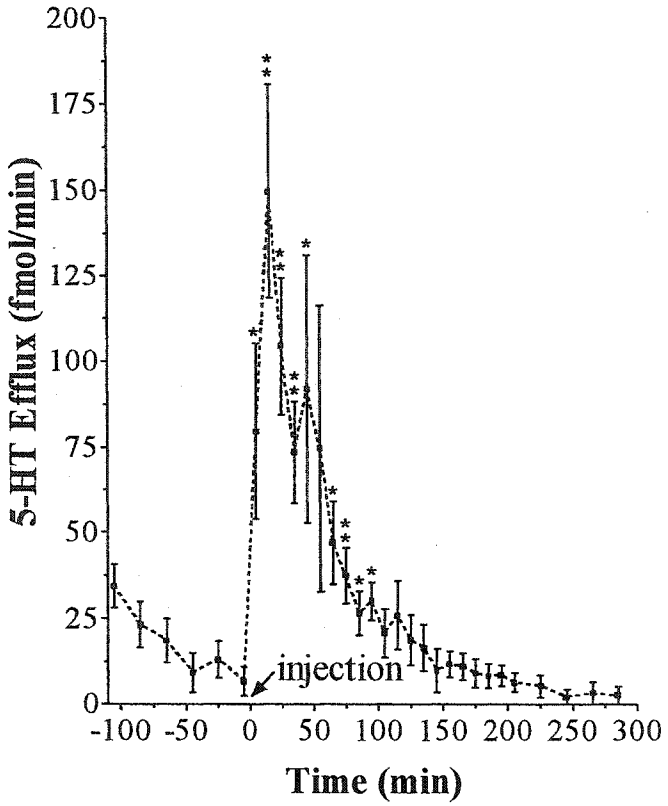

Figure 4:07.
Methamphetamine
30 mg/kg (i.p.);
5-HT Efflux (fmol/min)
vs. Time (min), n = 6.

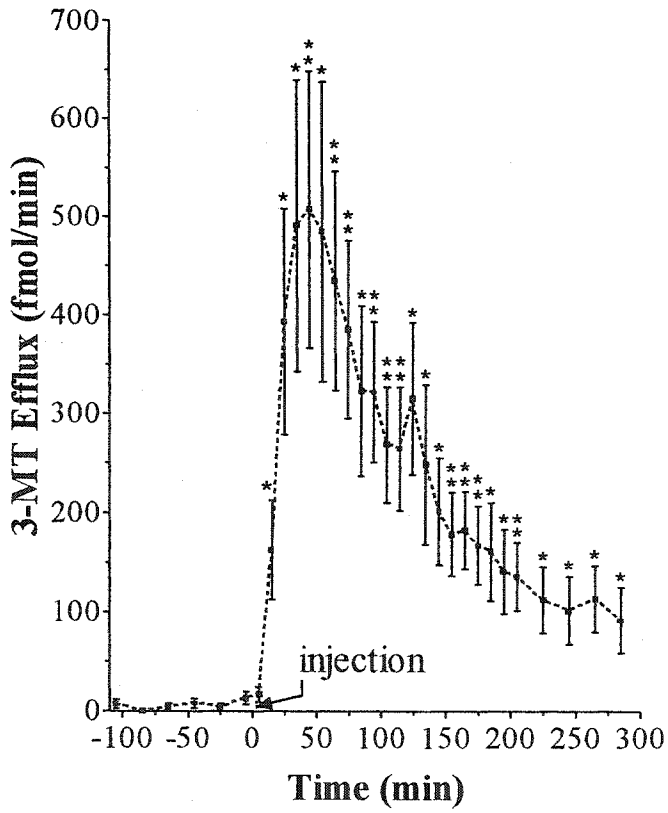

Figure 4:08.
Methamphetamine
30 mg/kg (i.p.);
3-MT Efflux (fmol/min)
vs. Time (min), n = 6.

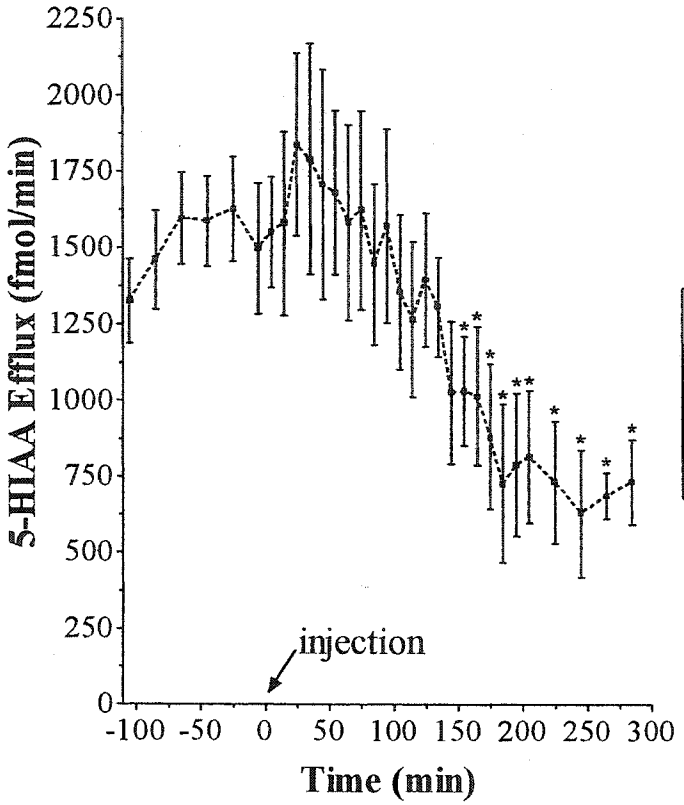

Figure 4:09.
Methamphetamine
30 mg/kg (i.p.);
5-HIAA Efflux (fmol/min)
vs. Time (min), n = 6.

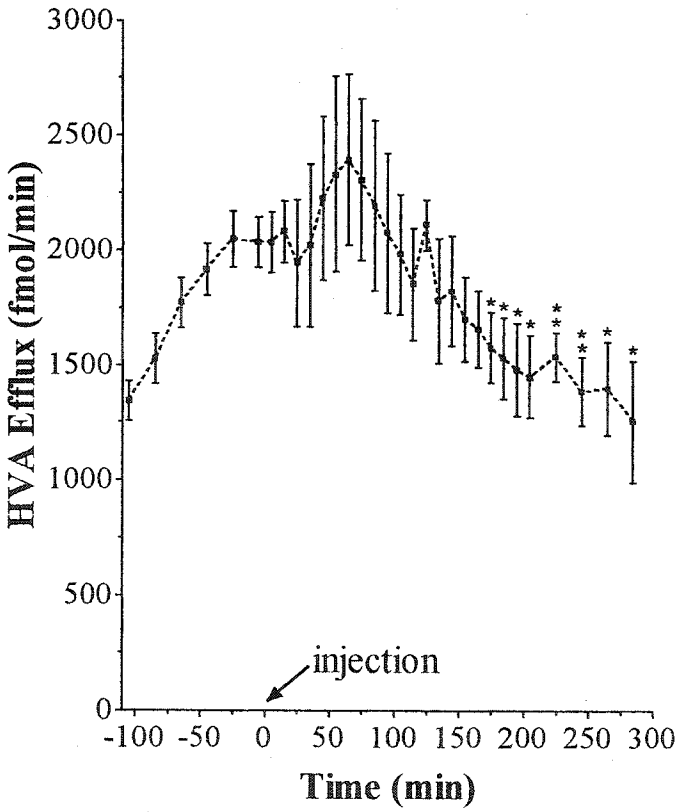

Figure 4:10.
Methamphetamine
30 mg/kg (i.p.);
HVA Efflux (fmol/min)
vs. Time (min), n = 6.

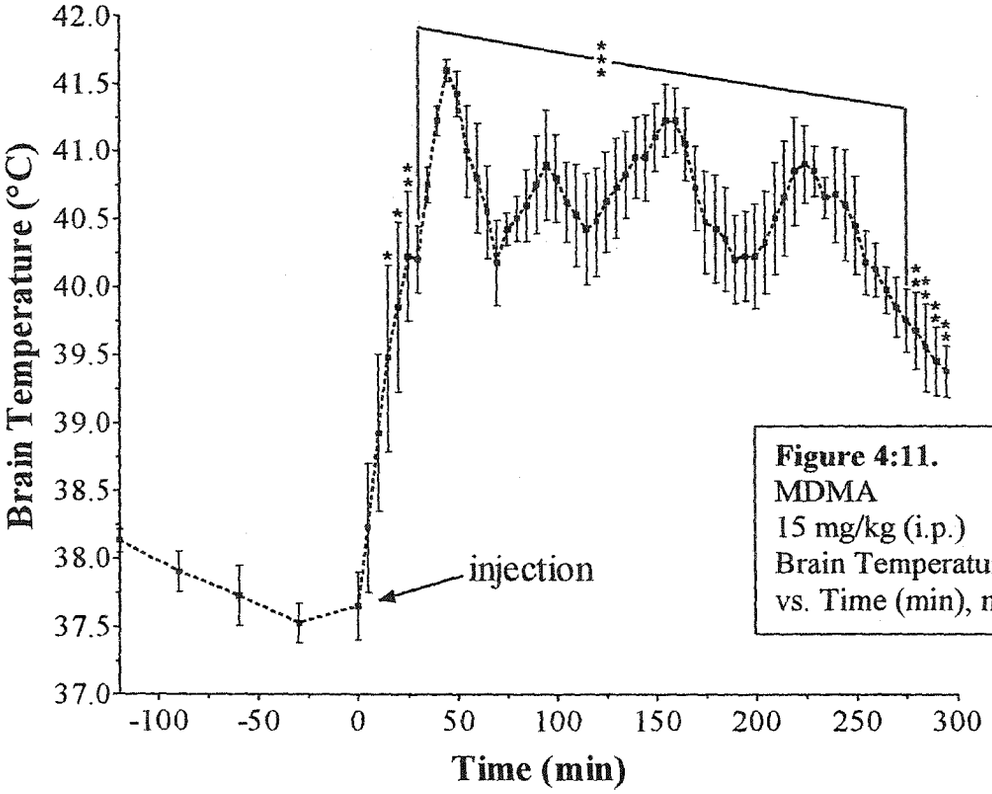

Figure 4:11.
MDMA
15 mg/kg (i.p.)
Brain Temperature (°C)
vs. Time (min), n = 4

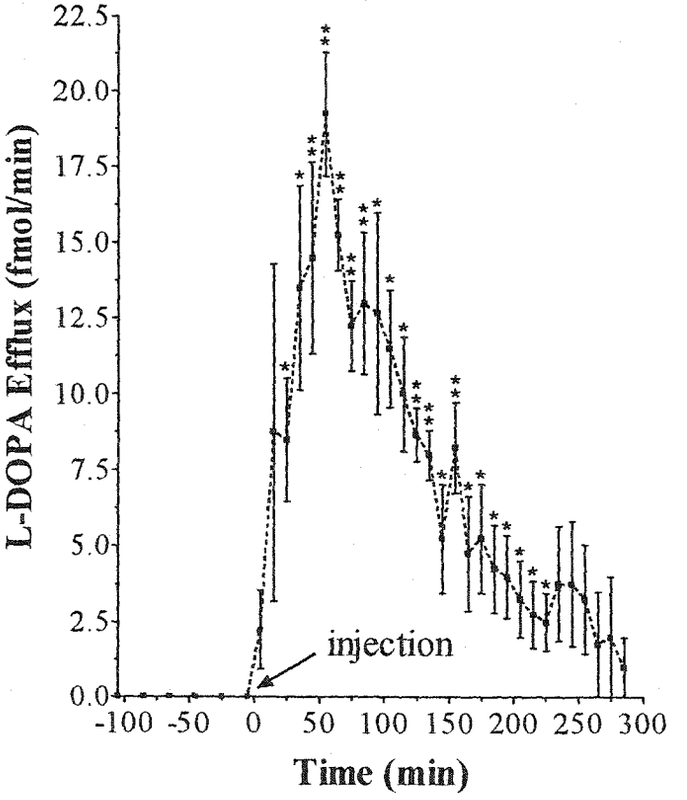

Figure 4:12.
MDMA
15 mg/kg (i.p.);
L-DOPA Efflux (fmol/min)
vs. Time (min), n = 4.

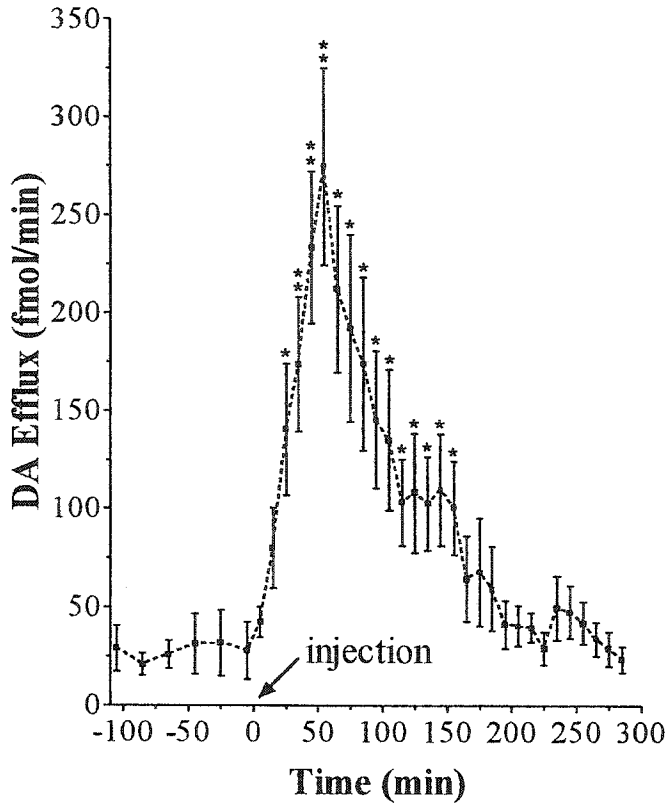

Figure 4:13.
MDMA
15 mg/kg (i.p.);
DA Efflux (fmol/min)
vs. Time (min), n = 4.

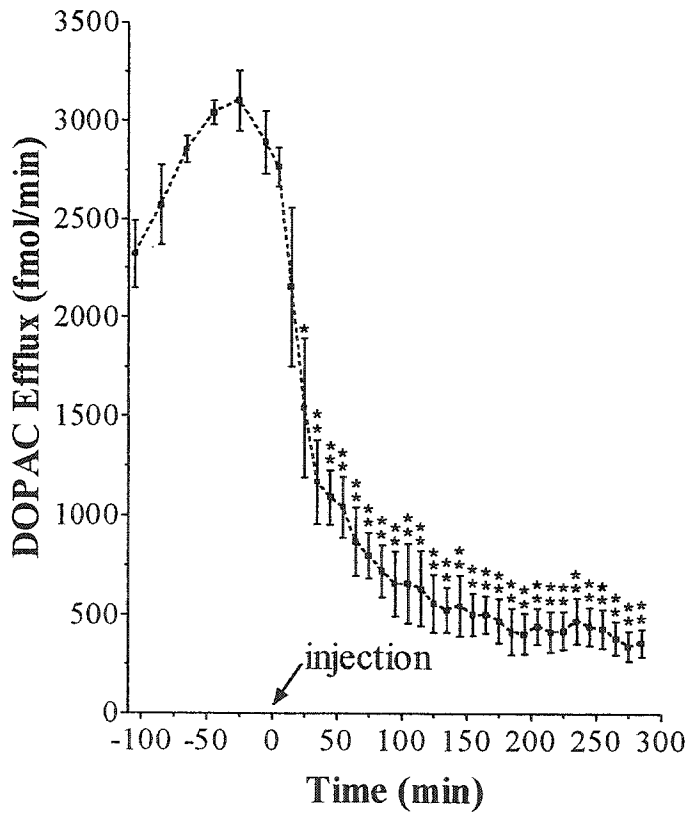

Figure 4:14.
MDMA
15 mg/kg (i.p.);
DOPAC Efflux (fmol/min)
vs. Time (min), n = 4.

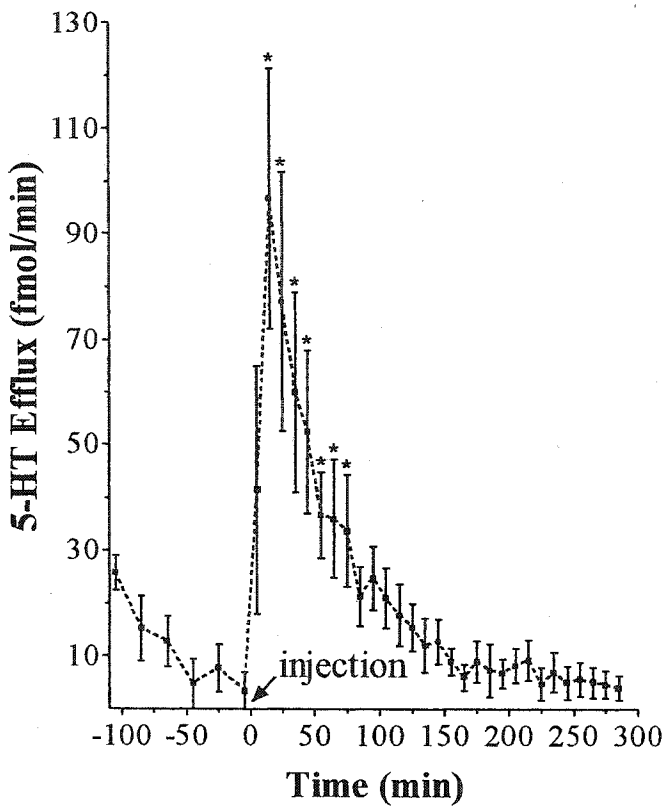

Figure 4:15.
MDMA
15 mg/kg (i.p.);
5-HT Efflux (fmol/min)
vs. Time (min), n = 4.

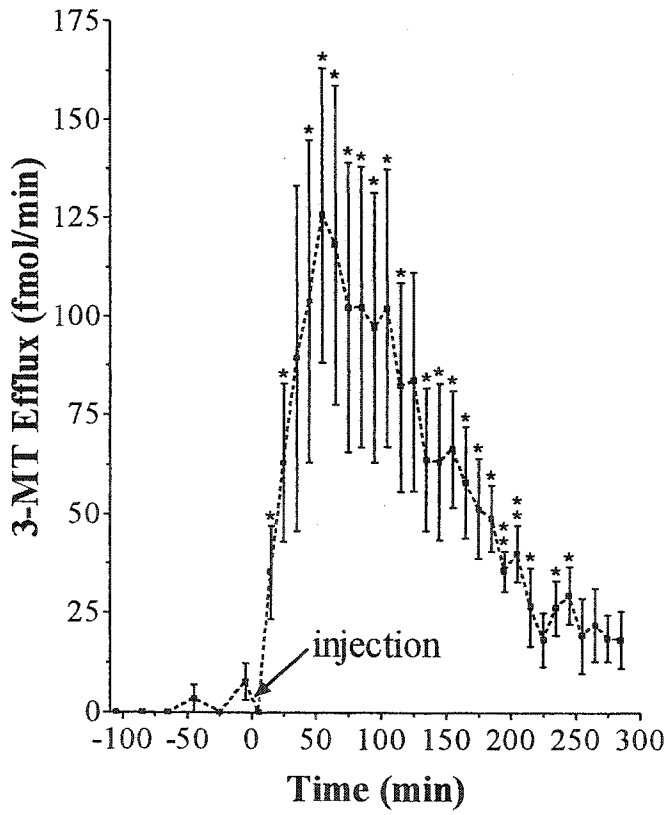

Figure 4:16.
MDMA
15 mg/kg (i.p.);
3-MT Efflux (fmol/min)
vs. Time (min), n = 4.

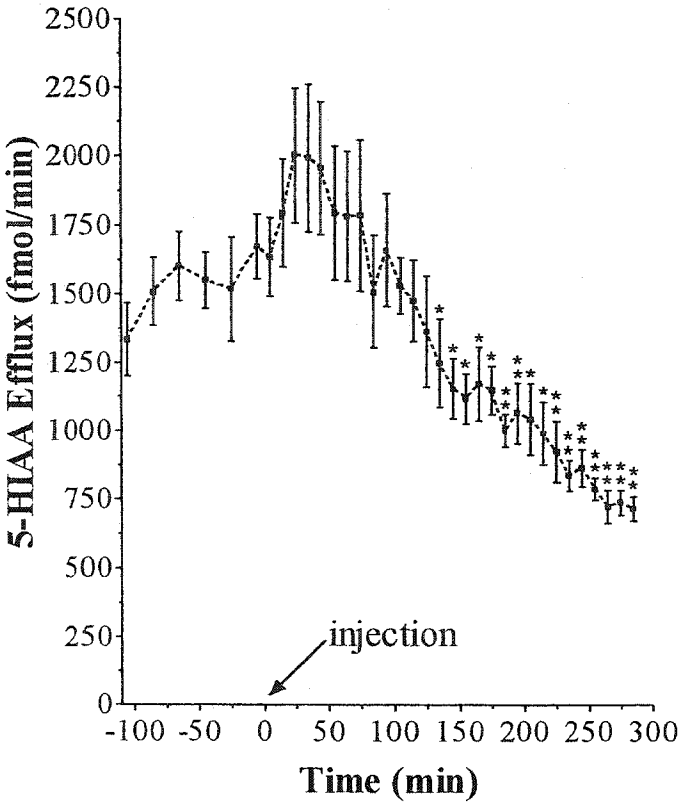

Figure 4:17.
MDMA
15 mg/kg (i.p.);
5-HIAA Efflux (fmol/min)
vs. Time (min), n = 4.

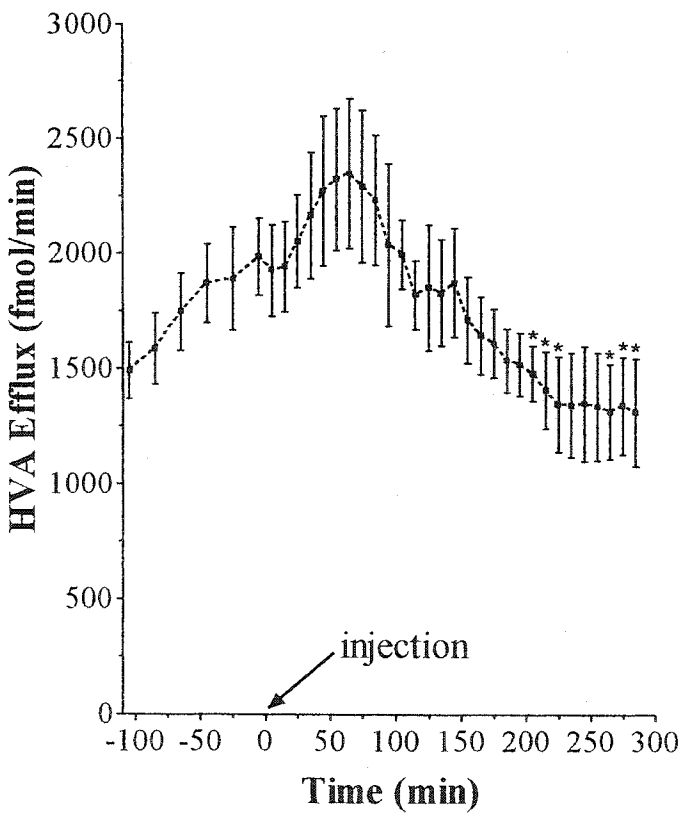

Figure 4:18.
MDMA
15 mg/kg (i.p.);
HVA Efflux (fmol/min)
vs. Time (min), n = 4.

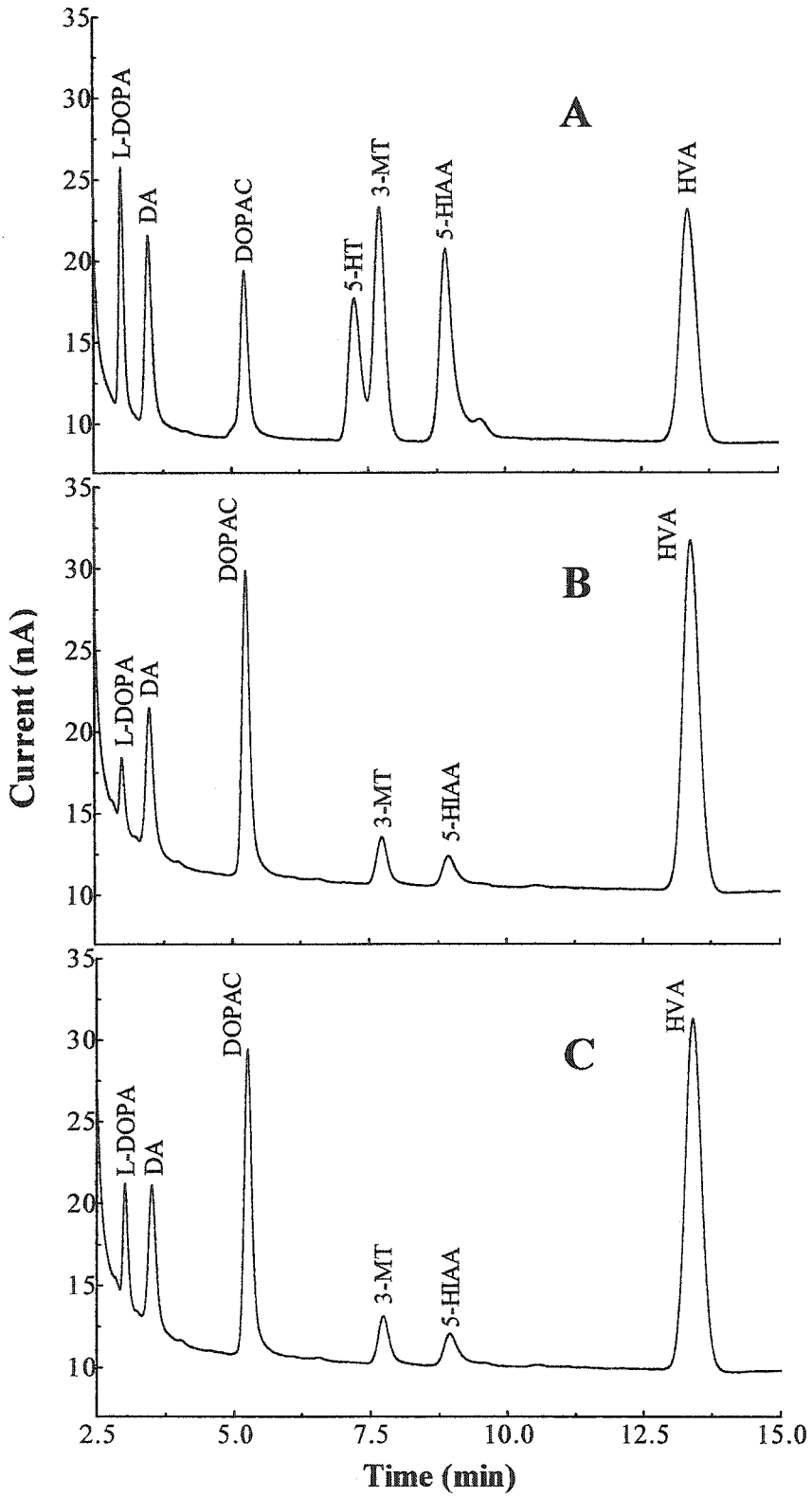

Figure 4:19. HPLC-EC chromatograms of (A) standard mixture of DA, 5-HT and their metabolites; (B) rat striatal dialysate collected 60-110 min after administration of MDMA; and, (C) dialysate identical to B with added standard L-DOPA.

Chapter Five

Microdialysis Study of MPP^+-Induced Alterations in Extracellular Amino Acid Levels

A. Introduction

The function and characteristics of amino acids in PD and animal models of PD (MPTP/MPP^+ and MA) has been investigated in only a few previous studies.[323-326] The analysis of GSH and Cys in dialysate from rats perfused with various concentrations of MPP^+ (in the presence and absence of ACV) have been discussed in Chapters One and Two. In this section experiments are presented which examined effects of perfused MPP^+ on extracellular concentrations of Glu, Asp, Gly and Tau (Figure 5:01) employing microdialysis in freely-moving rats and the effects of ACV on the extracellular amino acid levels. A rise of extracellular Glu has been implicated in the dopaminergic neurotoxicity of MPTP/MPP^+[157] and MA.[123,172] However, the source of this Glu is unknown and the effects of those neurotoxins on other amino acids has not been studied. One possibility is that the γ-GT/ApN-mediated degradation of released GSH might result in the rise of extracellular Glu induced by MPTP/MPP^+ and MA.

Initial studies were designed especially to monitor the efflux of Glu and Gly to ascertain whether γ-GT hydrolyzed released GSH. In previous microdialysis experiments conducted in our laboratory, a 30 min perfusion of 2.5 mM MPP^+ invoked a delayed rise of extracellular GSH and Cys. In identical experiments with MPP^+ in the presence of a

constant perfusion of 1.0 mM ACV, there was an increase in the maximum rise of extracellular GSH and an attenuated rise of extracellular Cys (compared to the experiments conducted in the absence of ACV), suggesting Cys originated from GSH.[215] Thus, it was anticipated that a constant perfusion (before, during, and after MPP^+) of ACV contained in the aCSF would inhibit γ-GT, resulting in an attenuated MPP^+-induced efflux of Glu and Gly (compared to experiments when ACV was not coperfused). This would be expected if the hypothesized source of Glu and Gly was from the γ-GT-mediated hydrolysis of GSH.

Glu and Asp exert their physiological effects by acting on various receptors in the central nervous system (CNS). Two major classifications of receptors are the ionotropic (further divided into NMDA, AMPA/kainate), and the metabotropic receptors. However, Asp does not activate AMPA/kainate receptors. While the roles of all of these receptors (in relation to neurodegeneration) have been studied (with a recent surge of interest in Glu metabotropic receptor function),[327-329] the NMDA receptor has been most extensively investigated. The NMDA receptor contains a Glu and a Gly binding site, both required for activation (co-agonists). However, at normal physiological conditions Mg^{2+} blocks the calcium channel of the NMDA receptor. Under conditions where the membrane is depolarized (e.g., inhibition of mitochondrial complex 1 activity resulting in decreased ATP production induced by perfusions of MPP^+) the Mg^{2+} blockade is removed and the binding of Gly and Glu (or Asp) activates the NMDA receptor and induces Ca^{2+} (and Na^+) influx. The release of Mg^{2+} is really a graded process, the greater the depolarization (loss of membrane potential) the more Mg^{2+} is released and, hence, the lower the concentration of Glu required to cause activation. The Ca^{2+} influx is believed to be one

of the primary factors leading to neuronal death by mechanisms addressed in the discussion below. Therefore, many studies have employed numerous agonists and antagonists of the NMDA receptor (and the other "Glu" receptors) to provide insights into the neurotoxicity of MPP^+ (and MA) and to explore the possibility of neuroprotective strategies for idiopathic PD in humans.[330,331]

Decreased levels of Tau have been observed in CSF of PD patients,[326,332] and hence, the investigations presented here, were designed to monitor changes in dialysate concentrations of Tau. Additionally, hyperosmolarity due to an influx of Na^+ and maybe MPP^+ could result in the release of Tau (along with Glu and Asp) from astrocytes. While there have been fairly limited studies concerning Tau, its functional roles may be as an osmoregulator, inhibitory neuromodulator, antioxidant and membrane stabilizer.[333]

B. Experimental

1. Chemicals and Drugs

L-Glutamic acid (Glu), L-aspartic acid (Asp), L-glycine (Gly), Tau and *N,N*-dimethylacetamide were obtained from Sigma (St. Louis, MO). A microbore amino acid analysis reagent kit (CF-2102) was obtained from BAS. This kit contained: (1) diluent A (borate/methanol buffer, pH 8.8); (2) diluent B (methanol); (3) reagent A (a mixture of *o*-phthalaldehyde, boric acid, 2-methyl-2-propanethiol and NaOH); (4) reagent B (iodoacetamide); and (5) a 2.5 mM stock solution of 20 amino acids dissolved in 0.1 M HCl containing L-alanine (Ala), 4-aminobutyric acid (GABA), L-arginine (Arg), L-asparagine (Asn), L-glutamine (Gln), L-histidine (His), L-isoleucine (Ile), L-leucine (Leu), L-lysine (Lys), L-methionine (Met), L-phenylalanine (Phe), L-serine (Ser), L-

threonine (Thr), L-tryptophan (Trp), L-tyrosine (Tyr), L-valine (Val), Glu, Asp, Gly and Tau. This kit was stored at -20°C. The sources of all other chemicals have been described previously.

2. Animals and Surgery

Details of rats and surgical procedures were described in Chapter Two. For all microdialysis experiments conducted to analyze amino acids, only one guide cannula was surgically implanted into rats. Hence, microdialysis experiments were conducted in one side of the striatum.

3. Microdialysis

On the day of experiments using MPP^+, a microdialysis probe (CMA 12, 4 mm membrane) was placed in a solution of Glu, Asp, Gly and Tau (each at 2.5 μM dissolved in 10 mM HCl) and perfused with aCSF at a flow rate of 1.5 μL/min using a CMA 100 microinfusion pump and gastight 1000 μL syringe (Bee Stinger, model MD-0100; BAS). Dialysate was perfused through lengths of BAS Teflon and/or PEEK tubing (0.65 mm O.D. x 0.12 mm I.D.) and collected in CMA 300 μL plastic vials in a CMA 170 refrigerated (4°C) microfraction collector. To determine probe recovery, six vials were collected for 10 min each (15 μL) and the last 3 collections were analyzed by HPLC-EC method VI. At least 3 separate aliquots of the original amino acid mixture were also analyzed by HPLC-EC method VI. Chromatograms of the recovered dialysate amino acid fractions were compared to the standard amino acid chromatograms and a recovery percentage was calculated. Typical probe recoveries were calculated as percentage of

standard ± SEM, n = 30: Glu (20.8 ± 4.0), Asp (28.0 ± 5.6), Gly (29.8 ± 4.4) and Tau (26.5 ± 6.1). These recoveries were correlated to the DA recovery discussed in Chapter Two. After establishing a probe recovery relationship between DA and these amino acids (approximately n = 30), amino acid probe recovery was no longer conducted before and after every experiment. Instead, that a probe recovery was satisfactory was based on the DA recovery percentage, since this required a much shorter time for determination. Acceptable DA recoveries were from 20-27 %, corresponding to acceptable amino acid probe recoveries. Typically, probes were found to be within the acceptable DA recovery range for 2-3 experiments.

Once an acceptable probe recovery had been achieved, the dummy probe was removed from the guide cannula (in the animal) and replaced by the microdialysis probe with the tip positioned 7.4 mm below dura. Throughout microdialysis experiments, rats were attached to a tether in a bedding-lined BAS Raturn, were able to move freely, and had free access to food and water. In these experiments the first and alternate fractions collected were used for amino acid analysis and the other fractions being analyzed for biogenic amines and possible glutathionyl and cysteinyl conjugates of DA and DOPAC (as described in Chapter Two). Dialysate samples destined for amino acid analysis were capped with septa and frozen (-80°C) immediately after the microdialysis experiment.

Basal dialysate levels of Glu, Asp, Gly and Tau were determined in fractions collected at 15 min intervals (22.5 μL). After analysis of these dialysates gave at least three consecutive constant (basal) levels of these amino acids (*ca.* 3 h; e.g., ± 10 % for Glu), a BAS Uniswitch Syringe Selector switched the perfusion solution to aCSF containing MPP^+ (0.7, 1.3, 2.5 or 10.0 mM) for 30 min after which the perfusate was

switched back to aCSF alone. Upon initiation of MPP^+ perfusion, dialysate samples were collected at 5 min intervals (7.5 μL) for 3 h and subsequently at 10 min intervals (15 μL) for at least another 3 h. In all these studies, an identical microdialysis experiment was carried out on the same animal 24 h after the initial experiment. In an identical series of experiments, 1.0 mM ACV was included in the aCSF (and the aCSF with the four different millimolar concentrations of MPP^+) and, hence, was perfused throughout the entire microdialysis procedure, on day 1 and 2.

At the conclusion of each day's microdialysis procedures, *in vitro* DA probe recovery was carried out to insure that the probe had functioned properly throughout the experiment. All tubing was thoroughly rinsed with deionized water for 12 h in order to remove all traces of salts and other chemicals. Upon completion of the day 1 microdialysis experiment, animals were removed from the Raturn and returned to individual cages. Following day 2 experiments, animals were sacrificed and correct placement of probes was verified as described by Santiago et al.[231]

4. HPLC-EC

HPLC-EC method VI was originally developed to obtain separation of a twenty amino acid standard mixture (BAS). However, many of these amino acids are not detectable in dialysate or were of no interest in our experiments. This method employed a BAS 200B HPLC system equipped with a BAS Unijet reversed phase microbore column (ODS-8, 100 x 1 mm, 3 μm particle size), Unijet guard column (ODS-8, 10 x 1 mm, 3 μm particle size) and dual glassy carbon detector electrodes (both 3 mm diameter) set in parallel at +750 mV with respect to a Ag/AgCl reference electrode. This system

was equipped with a flow splitter where approximately 10% of the mobile phase traveled through the microbore column and the other 90% through a Phenomenex (Torrence, CA) IB-SIL reversed phase column (OBS-18-BD, 100 x 3.2 mm, 3 μm). ChromGraph® (BAS; version 1.5.01) software was utilized for data collection (Control ®; version 1.52) and data analysis (Report ®; version 1.53).

Electrochemical detection of derivatized amino acid standards and dialysate fractions was automated using a CMA/200 refrigerated autosampler (4°C) equipped with a CMA/240 online injector and a 5.2 μL sample loop. Standards and dialysate fractions were adjusted to pH 10.0 with 1.0 M NaOH and loaded into the autosampler. The derivatization procedure was also automated and utilized Reagent A and Reagent B of the BAS amino acid kit (with one mL of Diluent B added to Reagent B) both kept in the refrigerated autosampler during analysis. Once removed from the -20°C storage freezer, Reagents A and B were employed for no more than 7 days. The autosampler was programmed such that the derivatization procedure occurred immediately prior to sample injection. For derivatization, three μL of Reagent A was added to 7.5 μL of dialysate (or standard) and mixed twice for 20 seconds each. Three μL of Reagent B was added and mixed twice for 2 min each, then injected onto column.

Amino acid concentrations (expressed as efflux in fmol/min) were determined based on calibration curves obtained with standard mixtures of known compounds. At the beginning of each day, standard mixtures (3 different concentrations, 3 times each) were injected to check calibration curves. During the course of autoinjection of dialysate fractions, standard mixtures were injected as every fifth sample to monitor and correct for possible derivatization errors, chromatographic drift and detector response deviations.

For analysis of dialysate and amino acid standards a binary gradient mobile phase system was employed. Solvent A was prepared by adding 160 mL of *N,N*-dimethylacetamide and 270 mL of MeOH to 570 mL of 0.1 M sodium acetate buffer (pH 6.8, containing 40 mg/L Na_2EDTA). Solvent B was prepared by adding 400 mL of *N,N*-dimethylacetamide and 450 mL of MeOH to 150 mL of 0.1 M sodium acetate buffer (pH 6.8, containing 40 mg/L Na_2EDTA). After filtration (0.45 μm type HA membrane filter, Millipore, Bedford MA) both solvents were degassed under vacuum for approximately one hour. During analysis, solvents were constantly degassed by a BAS Vacuum Degasser (model LC-26B). The following binary gradient was employed: 0-20 min, 100% solvent A; 20-21 min, linear gradient to 5% solvent B; 21-30 min, 5% solvent B; 30-31 min, linear gradient to 100% solvent B; 31-47 min, 100% solvent B; 47-49 min, linear gradient to 100% solvent A; 49-59 min, 100% solvent A. The flow rate was constant at 70 μL/min.

C. Results

HPLC-EC method VI was used to analyze rat striatal dialysate samples for the effect of MPP^+ perfusion (with and without ACV) on the concentrations of Glu, Asp, Gly and Tau. A chromatogram of a standard mixture of 20 amino acids (including the four listed above) is shown in Figure 5:02A. A representative chromatogram of a rat striatal dialysate collected immediately prior to perfusion of MPP^+ (Figure 5:02B) shows peaks corresponding to basal levels of Glu, Gly and Tau. Various concentrations of MPP^+ (0.7, 1.3, 2.5 and 10.0 mM) were perfused for 30 min into the striata of awake rats on day 1 and dialysate levels of Glu, Asp, Gly and Tau were measured using HPLC-EC method

VI. Twenty-four hours later (day 2), an identical microdialysis experiment was carried out on the same animal. In additional experiments, 1.0 mM ACV was coperfused 3 h before, during and after perfusion of identical concentrations of MPP^+ on day 1 and day 2.

Perfusion of MPP^+ ($\geq$ 2.5 mM) evoked an increase of dialysate levels of Glu, Asp, Gly and Tau. A chromatogram obtained with a dialysate sample collected between 40 and 45 min after discontinuing perfusion of 2.5 mM MPP^+ (Figure 5:02C) illustrates the effects of MPP^+ perfusion on dialysate levels of Glu, Asp, Gly and Tau. Thus, MPP^+ evoked a delayed (compared to the biogenic amines discussed in Chapter Two) efflux of Glu, Asp, Gly and Tau that, after attaining maximal values, declined back towards basal levels

Table 5:01 and Figures 5:03-10 depict the maximum efflux (% of basal levels on corresponding day) of Glu, Asp, Gly and Tau after 30 min perfusions of various (0.7, 1.3, 2.5 and 10.0 mM) concentrations of MPP^+ (in the presence and absence of 1.0 mM ACV) on day 1 and 24 hours later after an identical perfusion. The time dependent efflux levels are presented for each amino acid at each concentration of MPP^+ perfused in the presence and absence of 1.0 mM ACV in Figures 5:11-42.

Table 5:01. Maximum efflux levels of Glu, Asp, Gly and Tau on day 1 and day 2 in the absence and presence of ACV (% of basal levels on corresponding day ± SEM, n = 4).

Amino Acid	MPP^+ [mM]	Absence of ACV		Presence of ACV	
		Day 1	Day 2	Day 1	Day 2
Glu	0.7	100 ± 22	100 ± 10	100 ± 12	116 ± 23
	1.3	173 ± 33 (x)	100 ± 14 (#)	215 ± 71	100 ± 6
	2.5	8876 ± 953 (**, xx)	129 ± 15 (x, ##)	7889 ± 897 (**, xx)	127 ± 35 (##)
	10.0	16786 ± 3198 (**, x)	129 ± 34 (##)	17481 ± 3984 (*, x)	103 ± 16 (#)
Asp	0.7	175 ± 58	132 ± 29	134 ± 16	127 ± 31
	1.3	299 ± 98	100 ± 13	461 ± 149	100 ± 14 (#)
	2.5	3824 ± 783 (**, x)	164 ± 28 (x, ##)	2240 ± 340 (**, xx)	129 ± 12 (x, ##)
	10.0	9310 ± 1245 (**, xx)	113 ± 19 (##)	6409 ± 1099 (**, x)	100 ± 11 (x, ##)
Gly	0.7	146 ± 44	111 ± 9	129 ± 18	122 ± 9
	1.3	125 ± 28	100 ± 5	281 ± 60 (x, +)	100 ± 14 (#)
	2.5	366 ± 100 (*)	113 ± 15 (#)	288 ± 38 (*)	107 ± 22 (##)
	10.0	1103 ± 230 (*, x)	124 ± 26 (#)	510 ± 83 (*, x, +)	113 ± 19 (##)
Tau	0.7	162 ± 47	141 ± 33	295 ± 101	164 ± 16
	1.3	291 ± 82	106 ± 14	1236 ± 322 (*, x)	160 ± 21 (#)
	2.5	1558 ± 359 (*, x)	118 ± 33 (#)	1456 ± 508 (*)	112 ± 27 (#)
	10.0	4701 ± 657 (**, xx)	113 ± 33 (##)	7965 ± 699 (***, xxx, +)	118 ± 23 (###)

(*) = significant difference vs. basal level on the same day.
(x) = significant difference vs. the previously lower MPP^+ concentration perfused.
(#) = significant difference between day 2 and day 1.
(+) = significant difference between the presence and absence of ACV.
$^1p < 0.05$, $^2p < 0.01$, $^3p < 0.001$.

Perfusion of 0.7 mM MPP^+ (with and without ACV) and 1.3 mM MPP^+ (alone) did not evoke any statistically significant changes in the efflux of Glu, Asp, Gly or Tau (Figures 5:11-13, 19-21, 27-29 and 35-37). However, perfusion of 1.3 mM MPP^+ (with 1.0 mM ACV) evoked slight elevations in Glu, Asp, and Gly (Figures 5:14, 22, and 30), but these were not statistically significant changes from basal levels. The same perfusion (1.3 mM MPP^+ with 1.0 mM ACV) did evoke an increase ($p < 0.05$) in Tau efflux of 1236% of basal levels (Figure 5:10), reaching maximum efflux levels 60 min after perfusion of MPP^+ was discontinued (Figure 5:38).

Substantial changes in efflux levels were observed when the MPP^+ concentration was increased to 2.5 and 10.0 mM. All four amino acids monitored exhibited an increase in efflux levels that was significantly greater than basal levels both with and without coperfusion of ACV (Table 5:01 and Figures 5:03-10, 15-18, 23-26, 31-34, and 39-42). When perfusing 2.5 or 10.0 mM MPP^+ in the absence of ACV, Glu levels rose to 8876 and 16786% of basal levels and in the presence of ACV to 7889 and 17481% of basal levels, respectively. Maximum Asp efflux levels were 3824 and 9310% of basal level in the absence of ACV, and 2240 and 6409% of basal level in the presence of ACV when 2.5 and 10.0 mM, respectively MPP^+ were perfused (Table 5:01). The maximum efflux levels for Glu and Asp (with and without ACV) occurred at 20-30 min after MPP^+

perfusions were discontinued (at both 2.5 and 10.0 mM concentrations of MPP^+; Figures 5:15-18 and 23-26). For both Glu and Asp, as the concentration of MPP^+ ($\geq$ 1.3 mM) increased, the maximum efflux increased (Figures 5:03-06). This same concentration dependence occurred for Gly (Figures 5:07 and 08) and Tau (Figures 5:09 and 10) but was not observed until the perfused MPP^+ concentration was $\geq$ 2.5 mM, except for one situation where statistically significant increases in maximum efflux levels of Tau began when $\geq$ 1.3 mM MPP^+ (in the presense of ACV) was perfused (Figures 5:10 and 37).

Twenty-four hours after day 1 experiments, identical microdialysis experiments were conducted where the same concentration of MPP^+ (with or without ACV) was perfused as on day 1. Interestingly, on day 2 at all concentrations of MPP^+ perfused, both in the presence and absence of ACV, there was no significant change in efflux levels compared to basal levels for any of the amino acids studied (Table 5:01 and Figures 5:03-10). The concentration dependence observed for biogenic amines (Chapter Two), where the maximum efflux on day 2 was inversely proportional to the concentration of MPP^+ perfused on day 1, was not observed for the four amino acids studied here.

An interesting trend is depicted in Table 5:02, which presents the percentage change of day 2 basal levels compared to those on day 1. It appears that day 2 basal levels are potentiated in proportion to the concentration of MPP^+ perfused on day 1 (both in the absence and presence of ACV). This observation is apparent for both Glu and Asp at all MPP^+ concentrations perfused, both with and without ACV. This trend is not observable for Gly and Tau when perfused MPP^+ concentration were $\leq$ 1.3 mM, but becomes so, when the perfused concentration of MPP^+ was $\geq$ 2.5 mM. For some reason basal amino acid levels measured in groups of animals at the same concentration of MPP^+

perfused differed substantially from group to group. Therefore, statistical comparisons for the changes in basal levels were not possible. Nevertheless, the trend that day 2 basal levels are potentiated in proportion to the concentration of MPP^+ perfused on day 1 is apparent and should probably not be ignored. Additionally, immunohistochemical results presented in Chapter Six suggest an explanation for this trend.

Table 5:02. Amino acid basal levels on day 2 (24 hours after 30 min perfusion of various concentrations of MPP^+ with or without 1.0 mM ACV) percent change from day 1 basal levels (n = 4).

	Amino Acids			
[MPP^+]	**Glu**	**Asp**	**Gly**	**Tau**
0.7	71.9	78.0	137.2	138.8
1.3	106.0	126.7	122.9	140.6
2.5	397.5	159.6	193.3	136.2
10.0	837.4	280.0	541.8	697.1
0.7 w/ACV	81.6	92.0	103.6	140.0
1.3 w/ACV	112.5	114.6	122.1	153.8
2.5 w/ACV	302.0	167.2	159.2	155.7
10.0 w/ACV	1096.2	252.1	389.6	280.4

D. Discussion

Initially, the primary purpose of these investigations was to determine the effect of ACV on extracellular concentrations of Glu and Gly evoked by MPP^+ in the rat striatum. ACV was expected to block the hydrolysis (*in vivo*) of GSH to Glu, Gly and Cys. Indeed, coperfusion of MPP^+ and 1.0 mM ACV caused extracellular levels of Cys to become virtually undetectable, whereas, extracellular levels of GSH increased (Figure 1:06).[215] Furthermore, the maximum efflux of GSH was much greater in the presence of ACV than in its absence. Additionally, the decline of GSH from maximum efflux levels (when coperfusing ACV) was much slower compared to when MPP^+ was perfused alone, in which case GSH declined rather rapidly after reaching maximum efflux levels. The results from these previous experiments suggested that ACV blocked the hydrolysis of extracellular GSH to Cys and changed the time-dependent efflux behavior of GSH by its inhibitory effect on the γ-GT-induced degradation of GSH. However, the results presented here reveal that ACV fails to attenuate the rise of extracellular Glu or Gly (Table 5:01, and Figures 5:03, 04, 07, and 08). Statistically, there was no significant difference in any of the maximum efflux levels nor time-dependent concentration changes of Glu or Gly (Figures 5:11-18, and 27-34) when perfusions of MPP^+ alone were compared to results from co-perfusions of MPP^+ with ACV. However, while it is clear that extracellular Cys is derived from GSH under these circumstances, microdialysis experiments indicate that neither Glu nor Gly are derived from GSH. Additionally, Asp and Tau maximum effluxes (Figures 5:05, 06, 09 and 10), and time dependent extracellular concentration behaviors (Figures 5:19-26 and 35-42) evoked by MPP^+ perfusion were not significantly affected by coperfusion of ACV.

Changes in extracellular levels of Glu, Asp and Gly (which have binding sites on the NMDA receptor) together with the MPP^+-induced removal of the Mg^{2+} blockade of the calcium channel of the NMDA receptor leads to an influx of Ca^{2+}. The term "excitotoxicity" has been coined to refer to the neurotoxicity resulting from excessive stimulation of Glu receptors and the ensuing influx of Ca^{2+} which activates numerous Ca^{2+}-dependent enzymes, including phospholipases A_2 and C, protein kinase C, Ca^{2+}/calmodulin dependent protein kinase II, nitric oxide synthase, and various proteases and nucleases. These enzymes are involved in metabolism of proteins, phospholipids, and nucleic acids, and when activated can lead to cell death by various mechanisms including excessive ROS generation.[330]

All striatal neurons[160,161] and dopaminergic SN_{pc} cells[162-165] express NMDA and AMPA receptors. When stimulated, NMDA and many AMPA receptors open Ca^{2+} channels. Recent studies indicate that AMPA receptor antagonists protect striatal neurons against MPTP/MPP^+-induced neurotoxicity[166] and NMDA receptor antagonists protect SN_c neurons.[167,168] NMDA and/or AMPA receptor antagonists also attenuate the dopaminergic neurotoxicity of MA.[334,335] However, definitive results are lacking from the studies employing various Glu receptor antagonists, with conflicting results sometimes reported.[336] For example, in two other studies systemic administration to mice[171,337]and rats[337] of MK-801 (an NMDA receptor antagonist) did not afford protection from MPTP/MPP^+-induced neurodegeneration.[338]

When relatively low concentrations of MPP^+ ($\leq$ 1.3 mM) were perfused on day 1 there was little or no change in dialysate levels of Glu, Asp or Gly (Figures 5:03-08). However, the large energy impairment induced by MPP^+ should permit even basal levels

of EAAs to activate NMDA[201,202] and AMPA receptors,[339,340] and possibly mediate excitotoxicity. Gly is a coagonist on the NMDA receptor and, therefore, is important to the neurotoxicity invoked by Ca^{2+}-induced cell death. Blockade of the NMDA receptor by a non-competitive Gly-site inhibitor protects cerebellar granule cell cultures from the MPP^+-induced cell death by blocking the influx of Ca^{2+}.[341] In a similar study where mice were treated with MPTP, a NMDA receptor Gly-site antagonist attenuated MPTP-induced depletion of striatal DA and the degeneration of TH-positive SN_{pc} neurons.[342]

From studies presented here, it is clear that the source of Glu and Gly observed following perfusion of $\geq$ 2.5 mM MPP^+ is not derived from the γ-GT degradation of GSH. Astrocytes are well characterized as having a functional role in clearing excess extracellular Glu and, by the action of glutamine synthetase, converting it into glutamine.[343] Also, MPP^+ mediates intraastrocytic ROS generation and inactivation of glutamine synthetase and, thus intracellular Glu levels become elevated.[344] However, several lines of evidence point to astrocytes as a possible source of Glu export. The mechanisms leading to release of Glu from astrocytes remain to be determined, but several potential pathways have been suggested.[345] These include: (1) reversal of the GLT-1 under conditions of energy impairment induced consequent to MPP^+ entry into astrocytes,[346,347] (2) astrocytic swelling, (which may also cause release of Asp and Tau),[348] and (3) calcium-dependent release from putative vesicles.[349-352] In recent studies it has been suggested that, unlike DA, extracellular levels of Glu measured by microdialysis techniques do not reflect synaptic release. Glu can arise from neurons and particularly astrocytes that are not necessarily in the immediate vicinity of the microdialysis probe (extracellular transmission).[353]

From previous studies, the role of Tau in the CNS remains speculative but its function has been associated with osmoregulation, inhibitory neuromodulation, membrane stabilization, and even as an antioxidant.[333] It has been proposed that Tau may serve as neurochemical marker of generalized cell loss and is reported to be localized in both neurons and glia.[354] The role of Tau as an antioxidant is supported by a recent study where Tau inhibited oxidative damage caused by iron-stimulated DA oxidation, and therefore, served a neuroprotective role.[355] Tau exhibited neurotransmitter characteristics in a previous study where it was shown (in rats) to be released from the terminals of nigrostriatal neurons by stimulation of AMPA/kainate receptors in the striatum.[356]

Tau levels measured in CSF of PD patients are conflicting,[326] having been reported to be decreased,[332] increased,[357] and even unchanged[358] compared to Tau levels measured in similar age group controls. Additionally, there have been studies conducted to determine the effect of aging on Tau levels and the results also appear to be contradictory.[359,360] Thus, Tau levels in CSF have been reported to be increased,[361] decreased,[333] and unchanged[362] with advancing age. Interestingly, there appears to be some groups (especially those who previously reported decreased levels of Tau in PD patients) that propose a correlation between Tau levels and the loss of DA neurons. These conflicting results are not surprising since age-related and PD studies are difficult to correlate due to the inherent variables that are often uncontrollable in human studies.

In the present studies, MPP^+ perfusions at concentrations $\geq$ 1.3 mM evoke an increase in the efflux of Tau (Figures 5:09, 10). The source of Tau in the striatum may also be from astrocytes, although supporting evidence has not been established. In fact, previous studies (similar to those conducted here with perfusion of MPP^+ into the rat

striatum) in which Tau dialysate levels were measured have not previously been reported. Whether Tau serves a neuroprotective function or contributes to the neurotoxicity of MPP^+ or neither, remains to be determined.

E. Conclusion

Contrary to expectations, the coperfusion of 1.0 mM ACV with apparent neurotoxic concentrations of MPP^+ did not attenuate the release of Glu and/or Gly when compared to MPP^+ perfusions in the absence of ACV. Thus, the rise of extracellular Glu and Gly after MPP^+ perfusions are discontinued must originate from a source other than GSH. None of the four amino acids (Glu, Asp, Gly and Tau) displayed a significant change in dialysate levels until the concentration of perfused MPP^+ was $\geq$ 2.5 mM. In Chapter Two, perfusion of 1.3 (and to a lesser extent, 0.7) mM concentrations of MPP^+ on day 1 attenuated the release of DA on day 2, an apparent sign of MPP^+-induced dopaminergic neurotoxicity on day 1. Immunohistochemical analyses conducted 24 hours after day 1 microdialysis (presented in Chapter Six), confirms the degeneration of DA terminals at these lower concentrations ($\leq$ 1.3 mM) of perfused MPP^+. However, in results presented here, there was no detectable release of Glu, Asp, Gly and Tau on day 1. Therefore, elevated amino acid release (specifically, Glu release) does not appear to be necessary for MPP^+-evoked neurotoxicity. Indeed, analysis of recent literature suggests that dopaminergic neurodegeneration is not the direct result of Glu-induced excitotoxicity, but may be exacerbated by increased levels of Glu.[330] It is tempting to speculate, that at low concentrations of perfused MPP^+ ($\leq$ 1.3 mM), there are mechanisms (possibly mediated through volume transmission) which enable the extracellular

environment to maintain constant apparent extracellular levels of these amino acids, hence, minimal fluctuations in amino acid levels are not detectable by microdialysis. At higher concentrations of perfused MPP^+ ($\geq$ 2.5 mM), these protective mechanisms are overwhelmed, consequently the elevated extracellular amino acid concentrations are observed, leading to additional damage from excitotoxicity.

If Glu, Asp, Gly and Tau are all released from astrocytes (which appear to be destroyed by MPP^+; as presented in Chapter Six), this could explain the lack of release on day 2 of any of the amino acids at any of the MPP^+ concentrations perfused. Day 2 amino acid basal levels are elevated and proportional to both the concentration of MPP^+ perfused on day 1 and the area lacking astrocytes. This supports other studies indicating that astrocytes are required to maintain basal amino acid levels under normal conditions.[84,353,363-365]

Chapter Five Figures

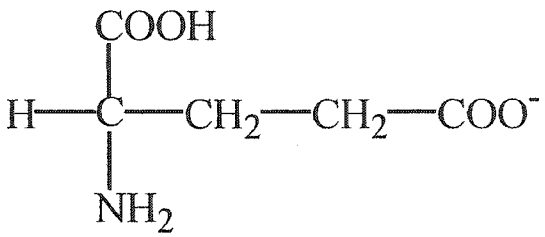

Glutamate
(GLU)

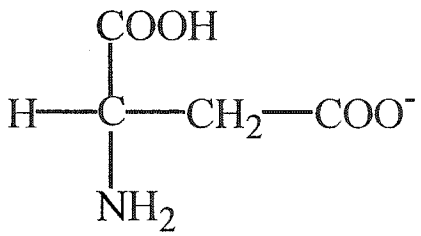

Aspartate
(ASP)

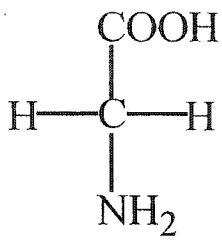

Glycine
(GLY)

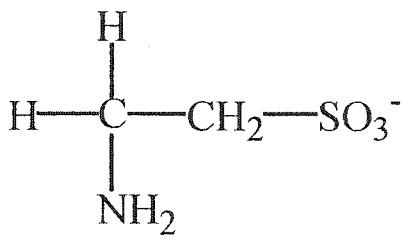

Taurine
(Tau)

Figure 5:01. Amino acids: Glutamate (Glu), Aspartate (Asp), Glycine (Gly) and Taurine (Tau).

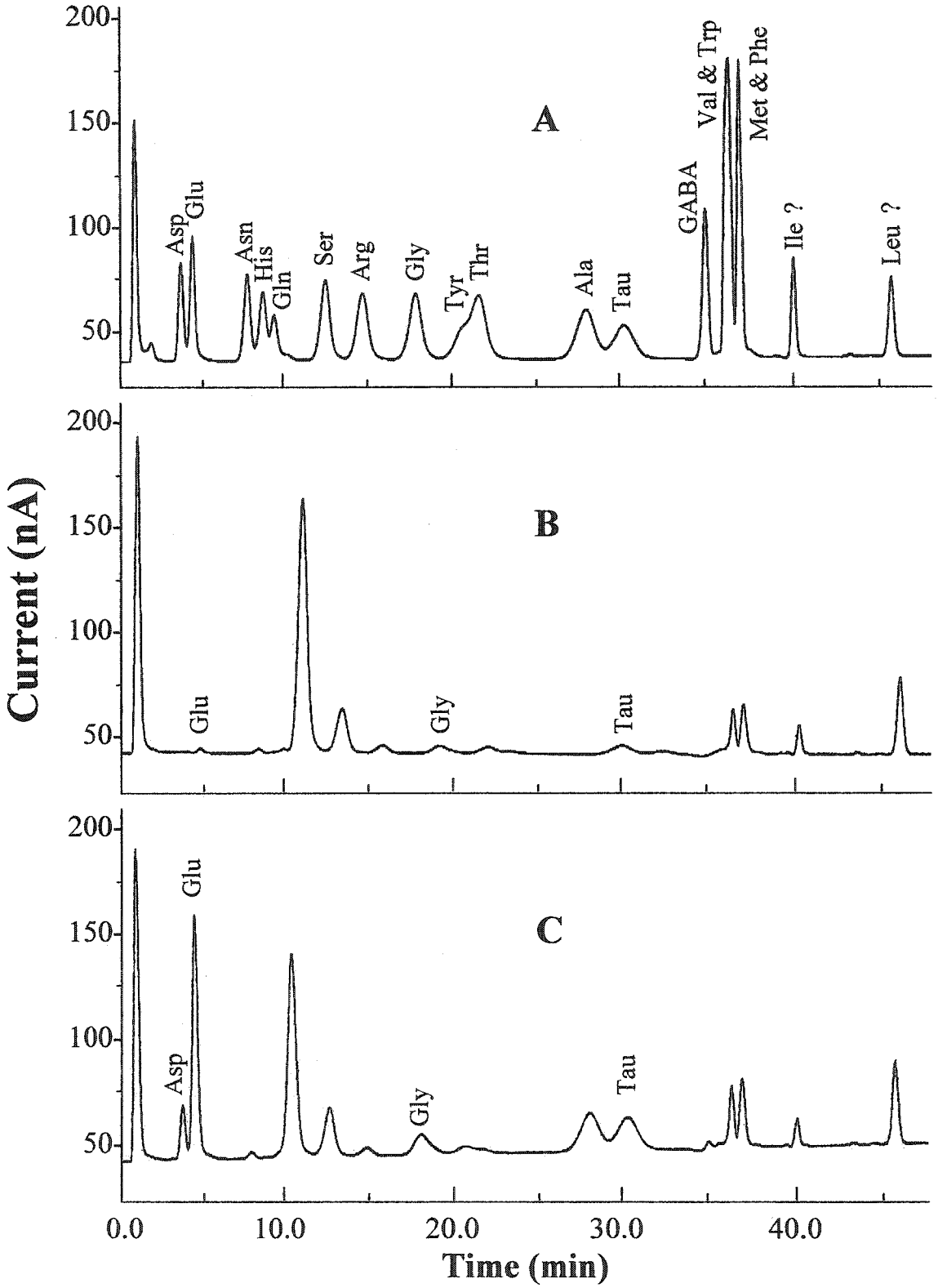

Figure 5:02. HPLC-EC chromatograms of: (A) standard mixture of 20 amino acids; (B) rat striatal dialysate collected prior to MPP^+ perfusion: and (C) rat striatal dialysate collected from 40-45 min after 2.5 mM MPP^+ perfusion was terminated.

Chapter Five Figures (cont.)

Figures 5:03-5:10. Maximum efflux of Glu, Asp Gly and Tau evoked by 30 min perfusions of MPP^+ (0.7-10.0 mM) in the absence and presence of continuous perfusion of 1.0 mM ACV into the striatum of awake rat on day 1 and day 2. A significant difference between Glu, Asp, Gly and Tau efflux versus basal efflux is indicated by $^*p < 0.05$; $^{**}p < 0.01$; $^{***}p < 0.001$. A significant difference between Glu, Asp, Gly and Tau efflux on day 1 or day 2 compared to that evoked by the immediate lower concentration is indicated by $^{x}p < 0.05$; $^{xx}p < 0.01$. A significant difference between the day 2 and day 1 efflux is indicated by $^{\#}p < 0.05$; $^{\#\#}p < 0.01$; $^{\#\#\#}p < 0.001$. A significant difference between Glu, Asp, Gly and Tau efflux on day 1 or day 2 when 1.0 mM ACV was perfused before, during and after (0.7-10.0 mM) MPP^+ versus an identical perfusion in the absence of ACV is indicated by $^{+}p < 0.05$; $^{++}p < 0.01$. Data are mean ± SEM (n = 4).

Figures 5:11-5:42. Time-dependent effects of a 30 min perfusion of MPP^+ (0.7-10.0 mM) in the absence and presence of continuous perfusion of 1.0 mM ACV into striatum of awake rat on dialysate levels of Glu, Asp, Gly and Tau on day 1 and an identical perfusion on day 2. The horizontal black bar shows the period during which MPP^+ entered the brain. $^*p < 0.05$; $^{**}p < 0.01$ compared to basal levels measured on day 1 or day 2. $^{\#}p < 0.05$ when basal dialysate concentration on day 2 was compared to day 1. Data are mean ± SEM (n = 4).

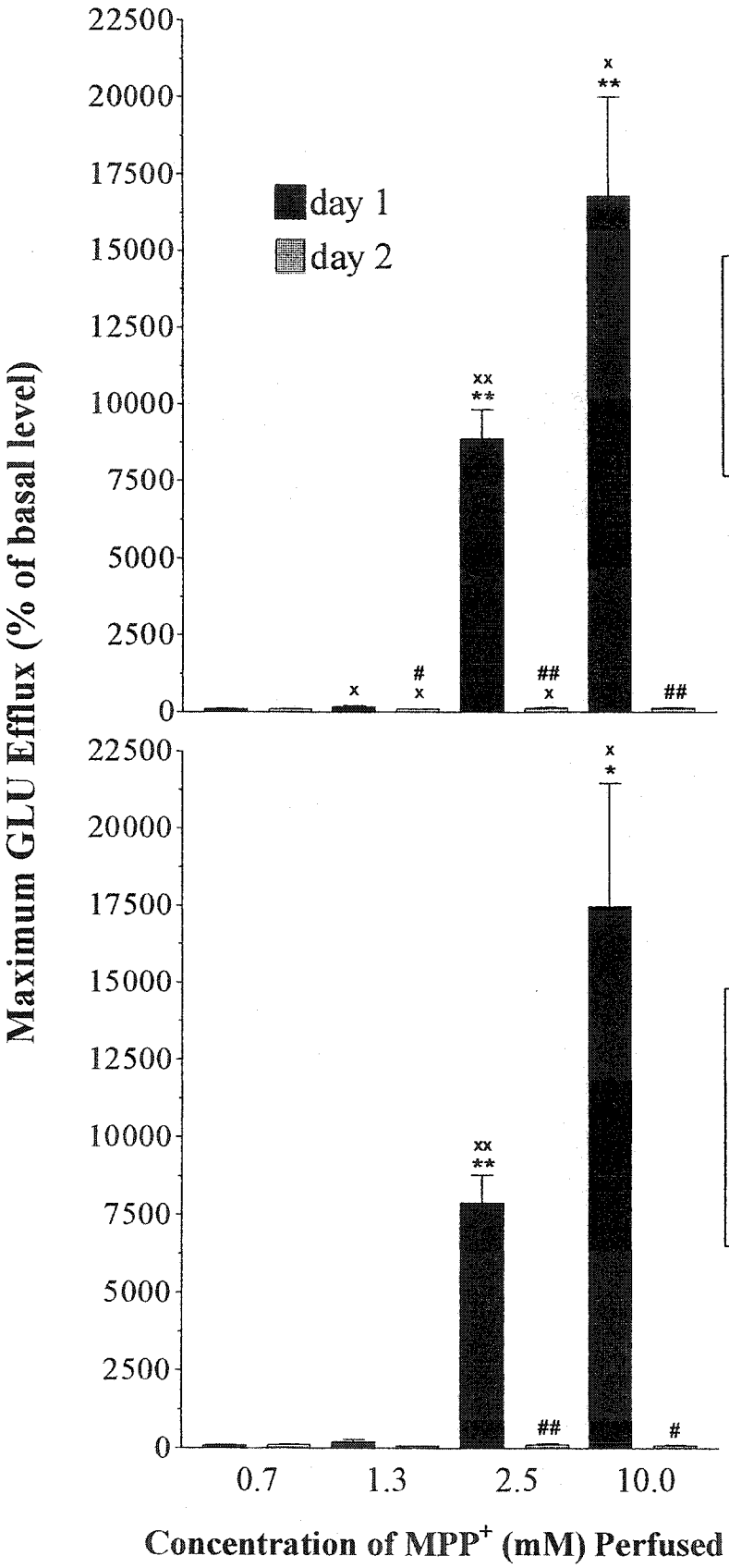

Figure 5:03.
GLU maximum efflux (% basal) at each MPP^+ concentration perfused, n = 4 for each concentration

Figure 5:04.
GLU maximum efflux (% basal) at each MPP^+ concentration perfused with 1.0 mM ACV, n = 4 for each concentration

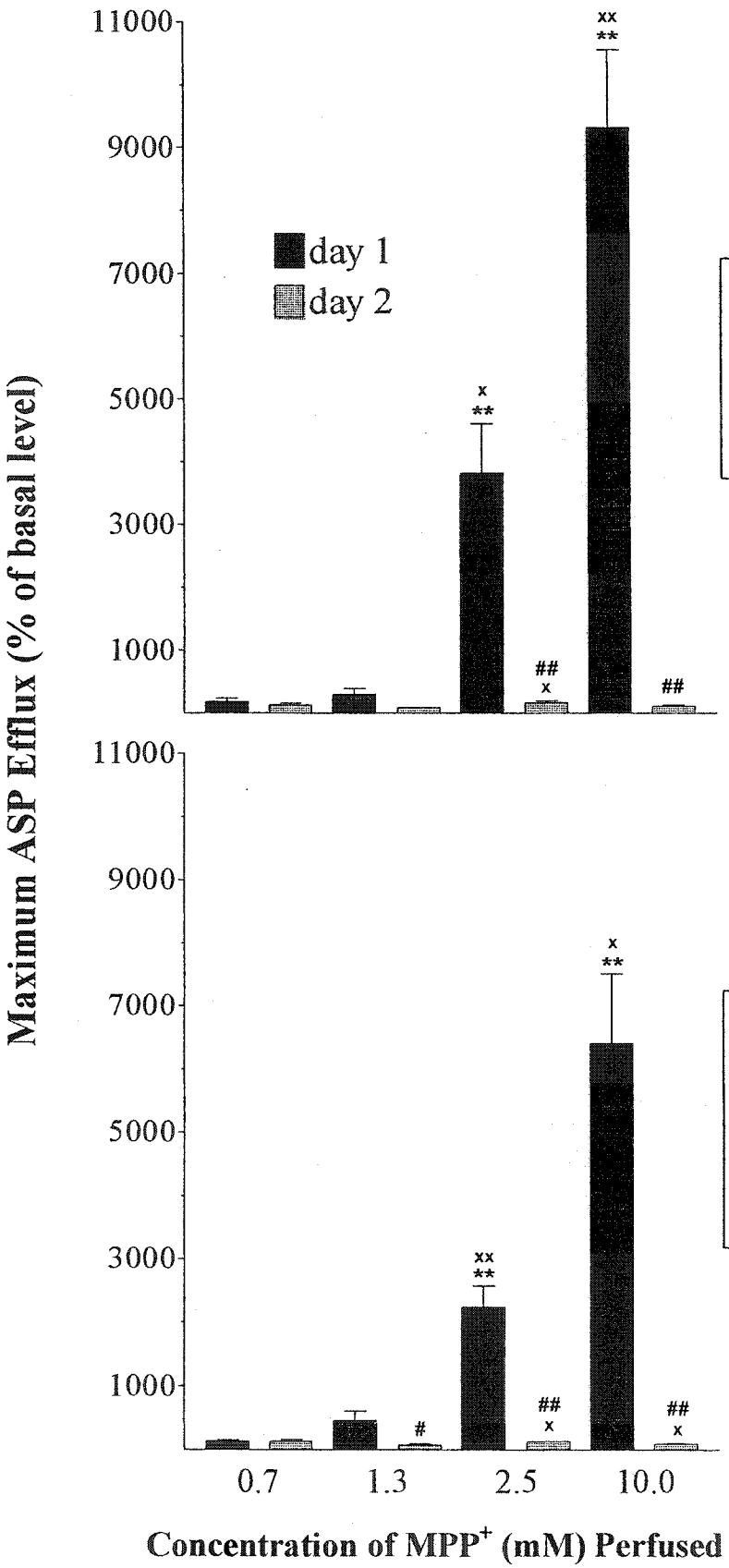

Figure 5:05.
ASP maximum efflux (% basal) at each MPP^+ concentration perfused, n = 4 for each concentration

Figure 5:06.
ASP maximum efflux (% basal) at each MPP^+ concentration perfused with 1.0 mM ACV, n = 4 for each concentration

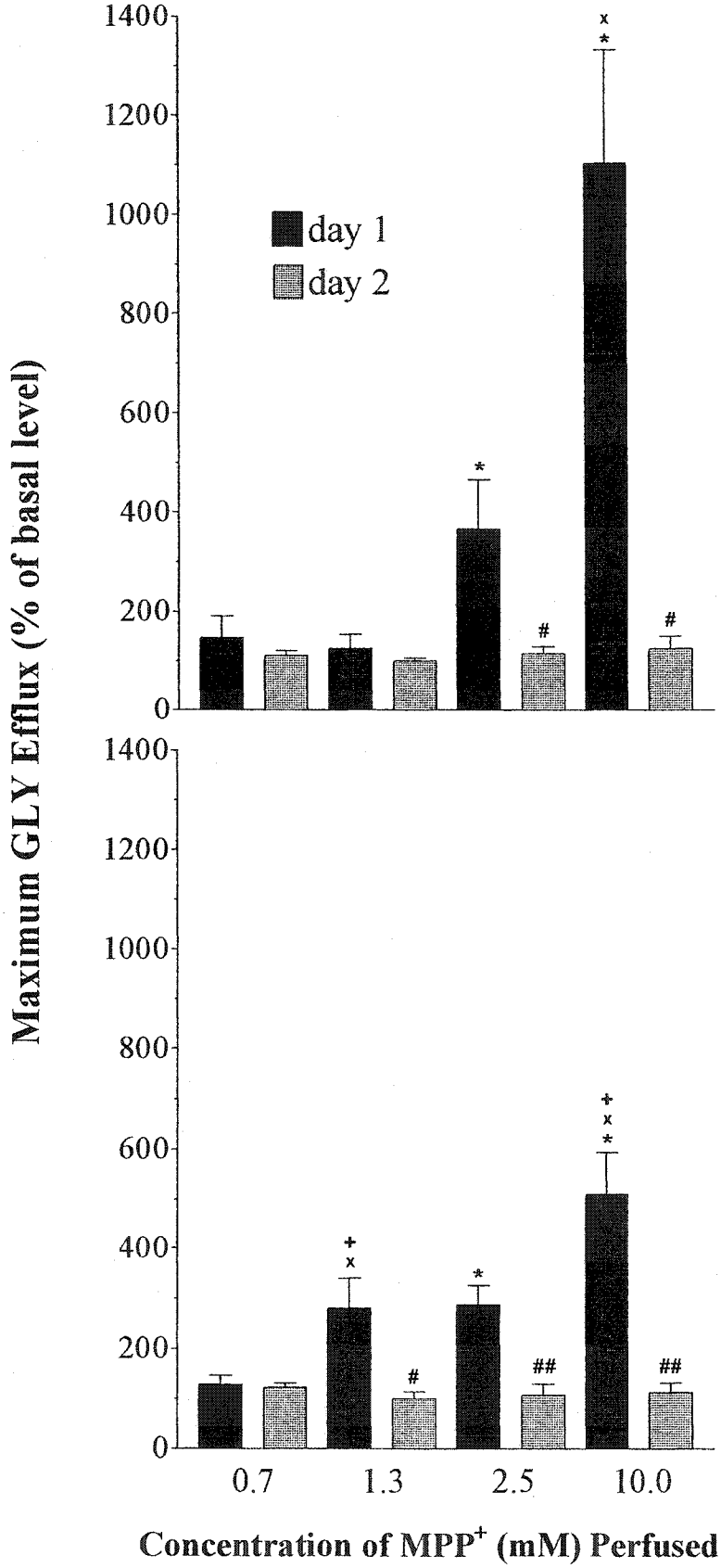

Figure 5:07.
GLY maximum efflux (% basal) at each MPP^+ concentration perfused, n = 4 for each concentration

Figure 5:08.
GLY maximum efflux (% basal) at each MPP^+ concentration perfused with 1.0 mM ACV, n = 4 for each concentration

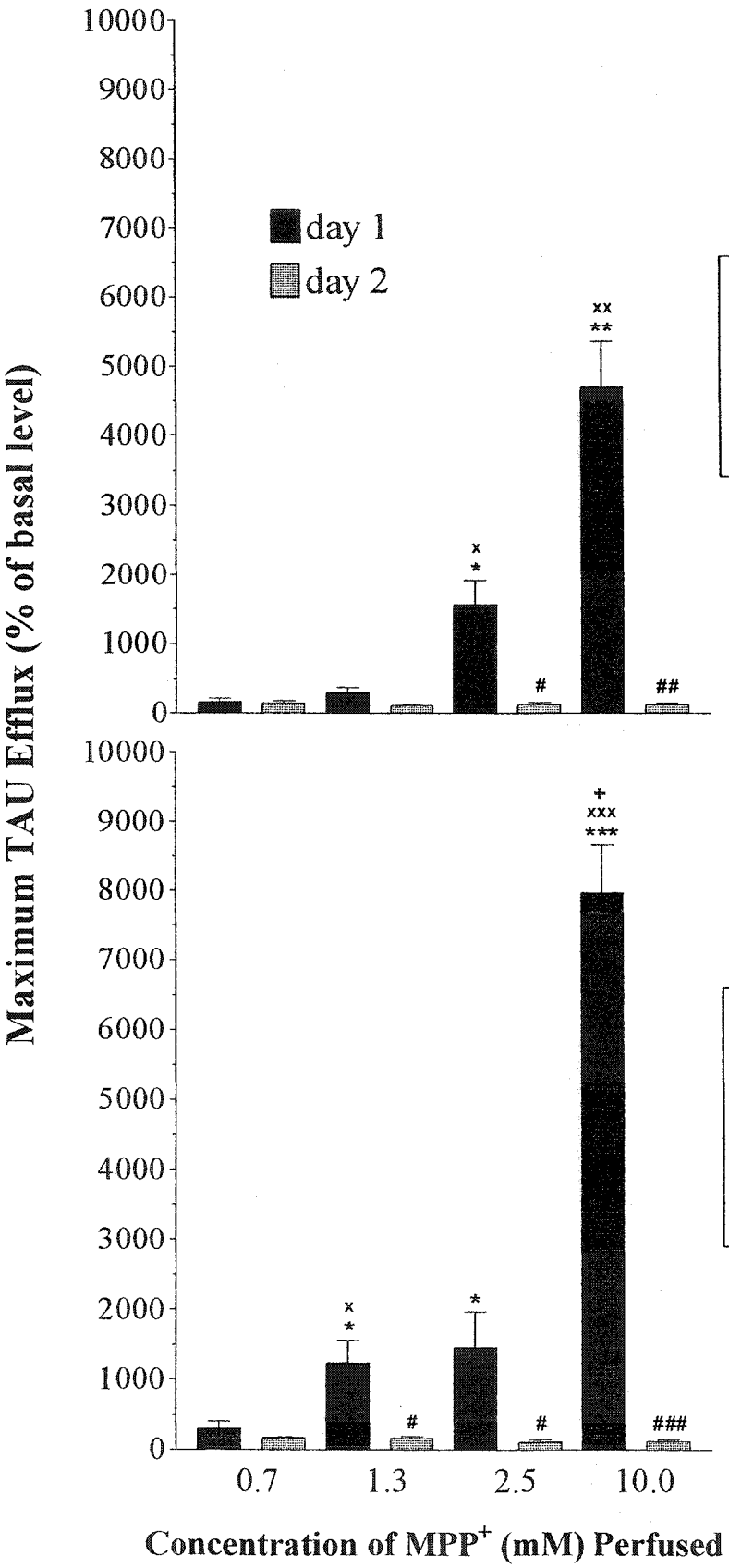

Figure 5:09.
TAU maximum efflux (% basal) at each MPP^+ concentration perfused, n = 4 for each concentration

Figure 5:10.
TAU maximum efflux (% basal) at each MPP^+ concentration perfused with 1.0 mM ACV, n = 4 for each concentration

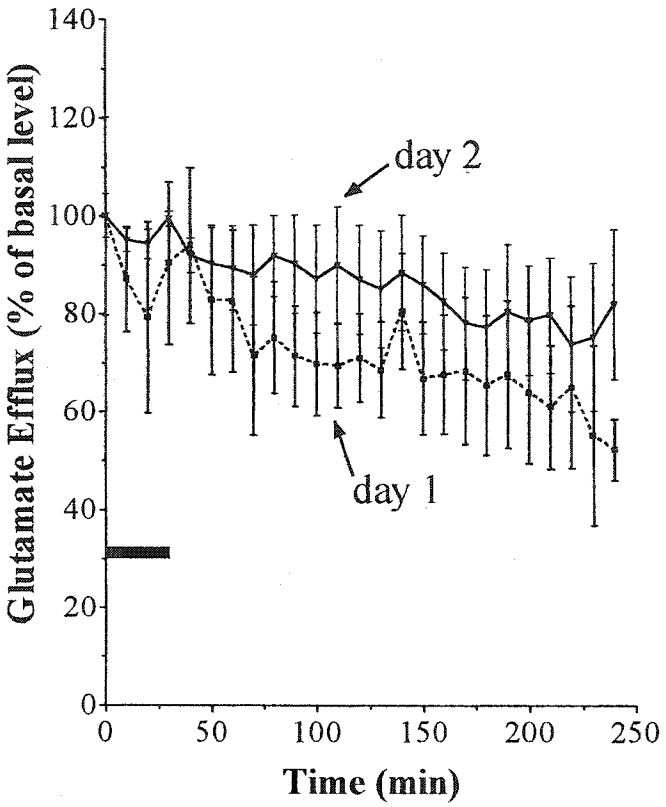

Figure 5:11.
0.7 mM MPP^+;
Glutamate Efflux (% basal)
vs. Time (min), n = 4.

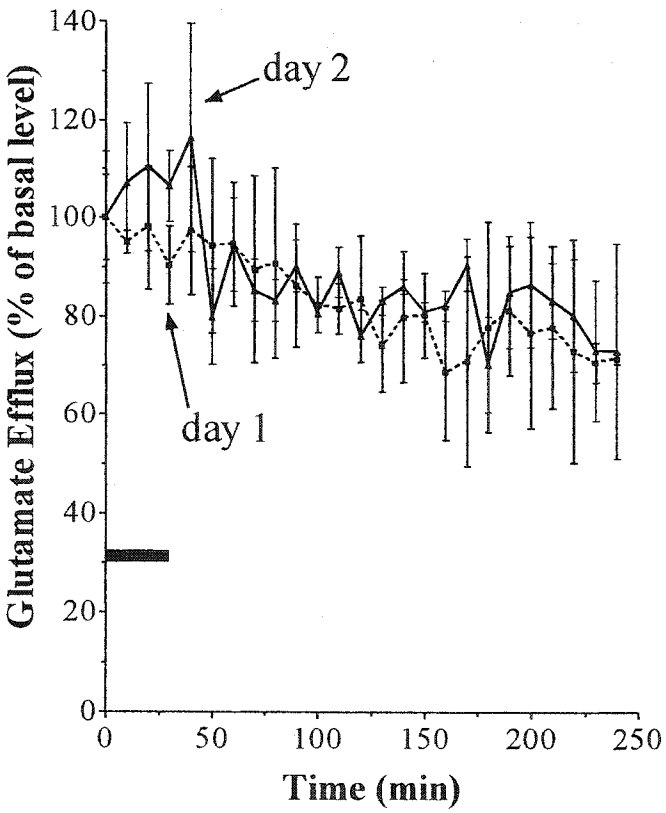

Figure 5:12.
0.7 mM MPP^+ with
1.0 mM ACV;
Glutamate Efflux (% basal)
vs. Time (min), n = 4.

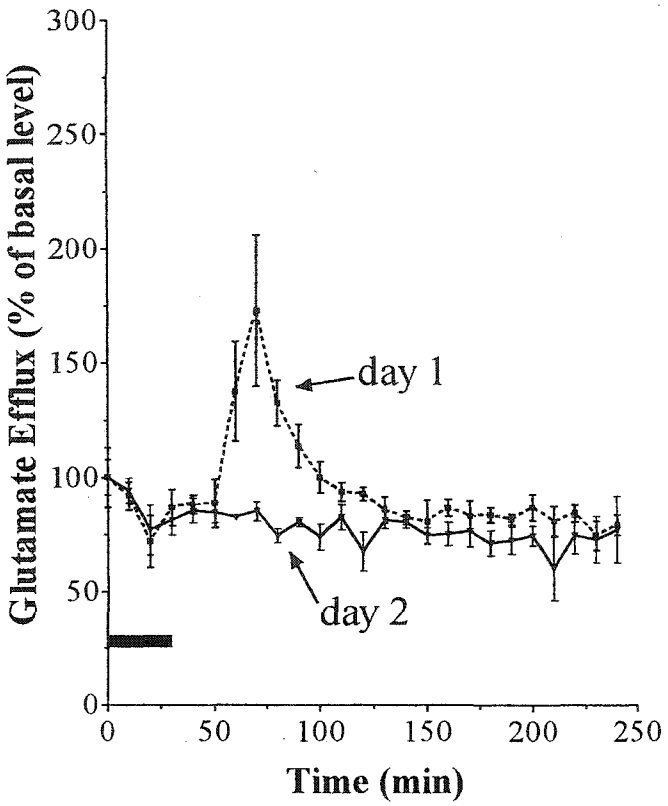

Figure 5:13.
1.3 mM MPP^+;
Glutamate Efflux (% basal)
vs. Time (min), n = 4.

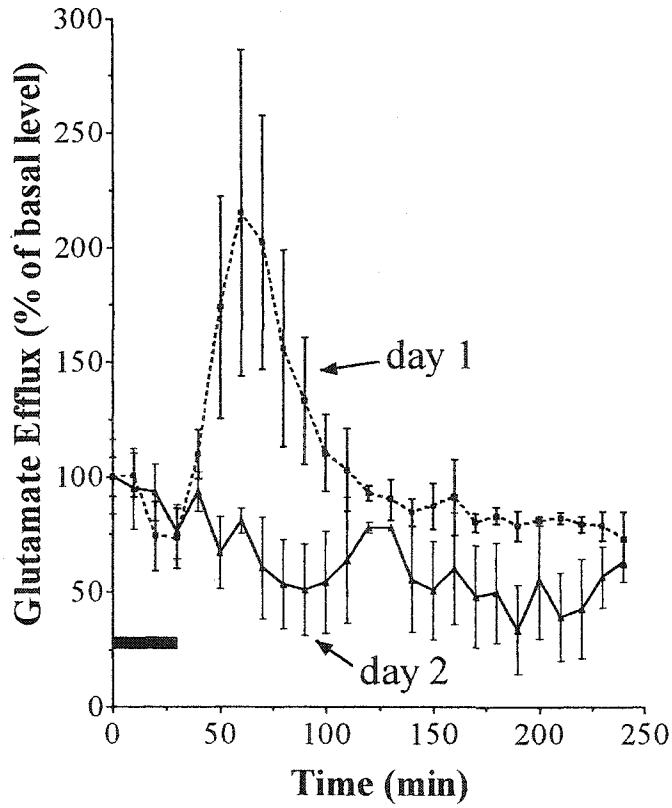

Figure 5:14.
1.3 mM MPP^+ with
1.0 mM ACV;
Glutamate Efflux (% basal)
vs. Time (min), n = 4.

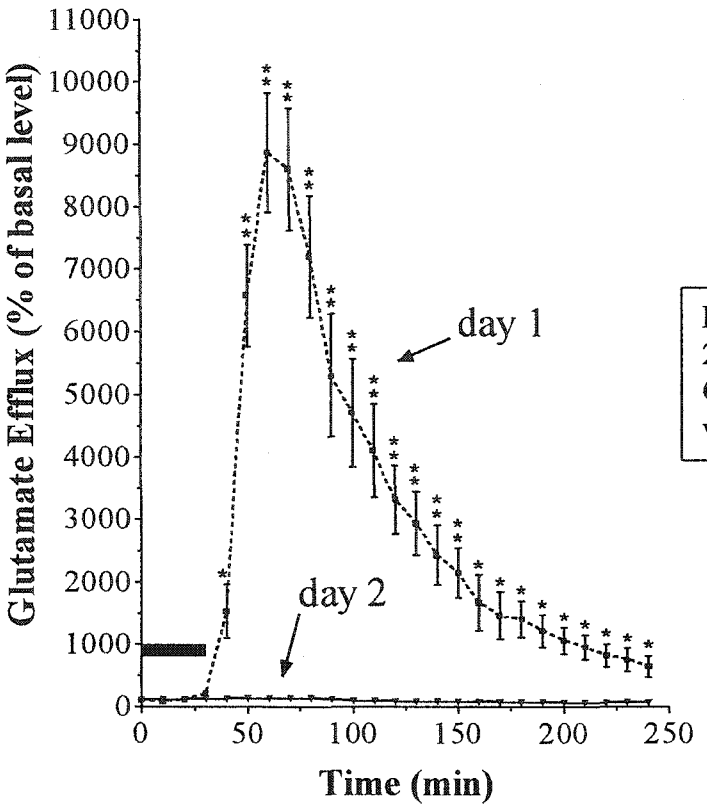

Figure 5:15.
2.5 mM MPP^+;
Glutamate Efflux (% basal)
vs. Time (min), n = 4.

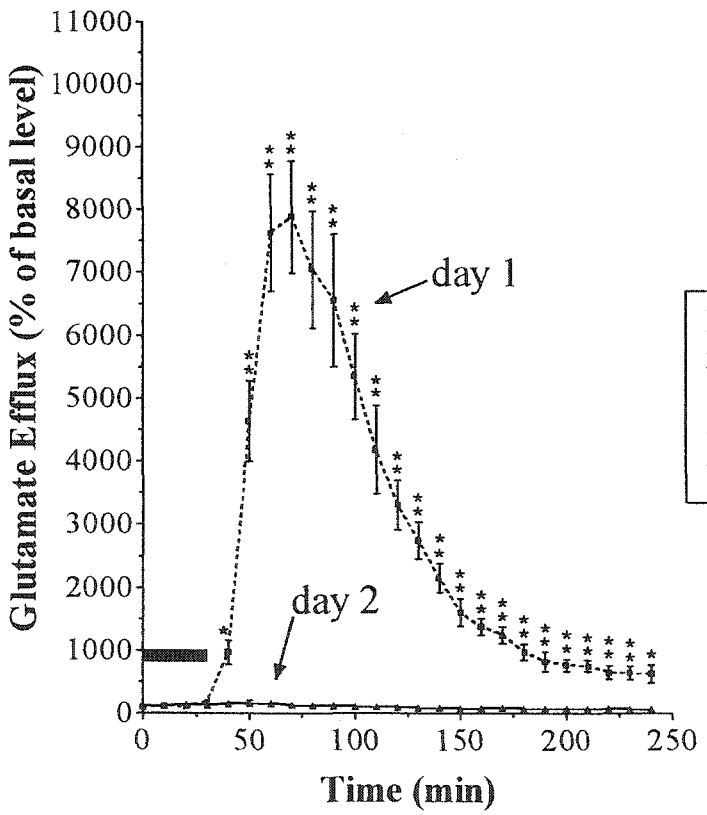

Figure 5:16.
2.5 mM MPP^+ with
1.0 mM ACV;
Glutamate Efflux (% basal)
vs. Time (min), n = 4.

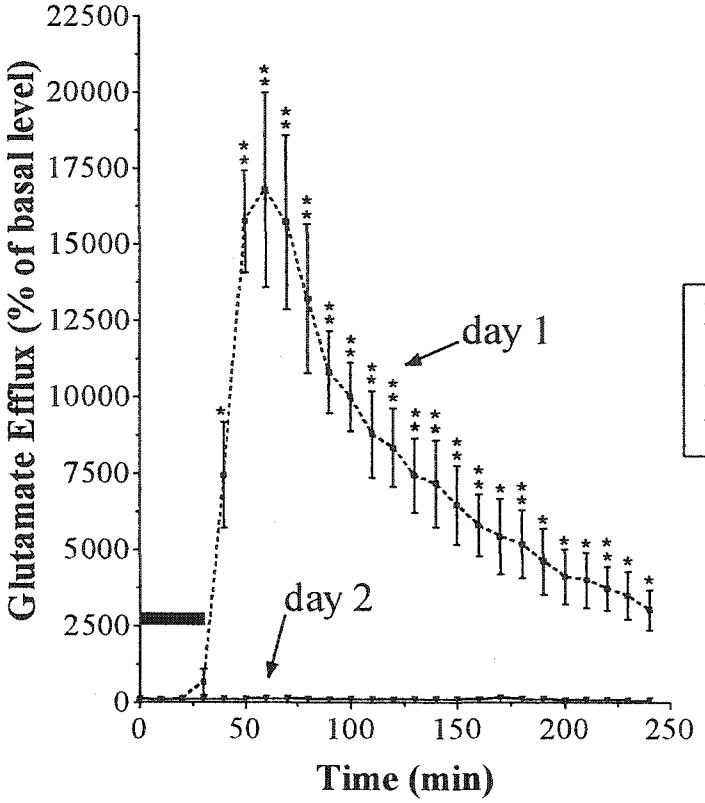

Figure 5:17.
10.0 mM MPP^+;
Glutamate Efflux (% basal)
vs. Time (min), n = 4.

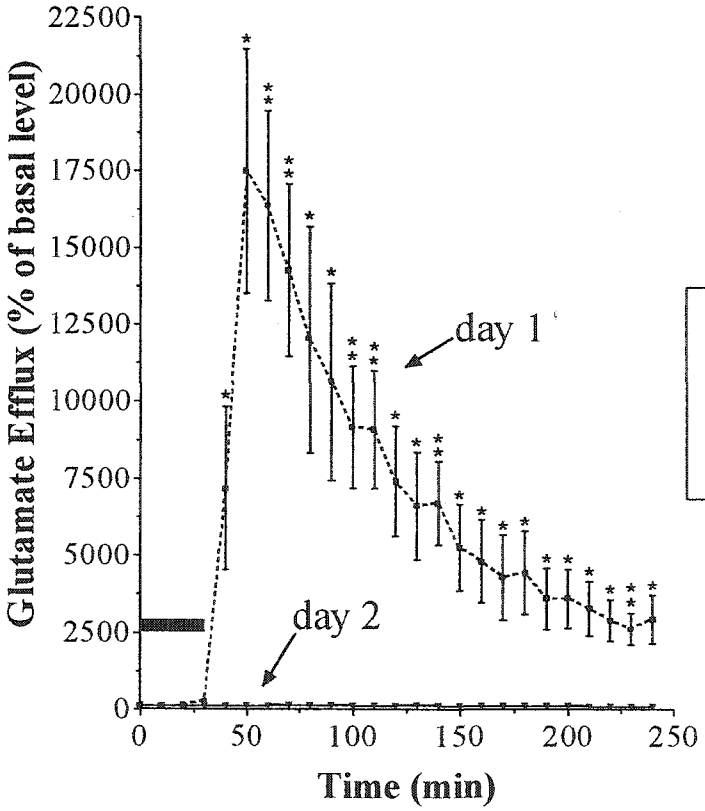

Figure 5:18.
10.0 mM MPP^+ with
1.0 mM ACV;
Glutamate Efflux (% basal)
vs. Time (min), n = 4.

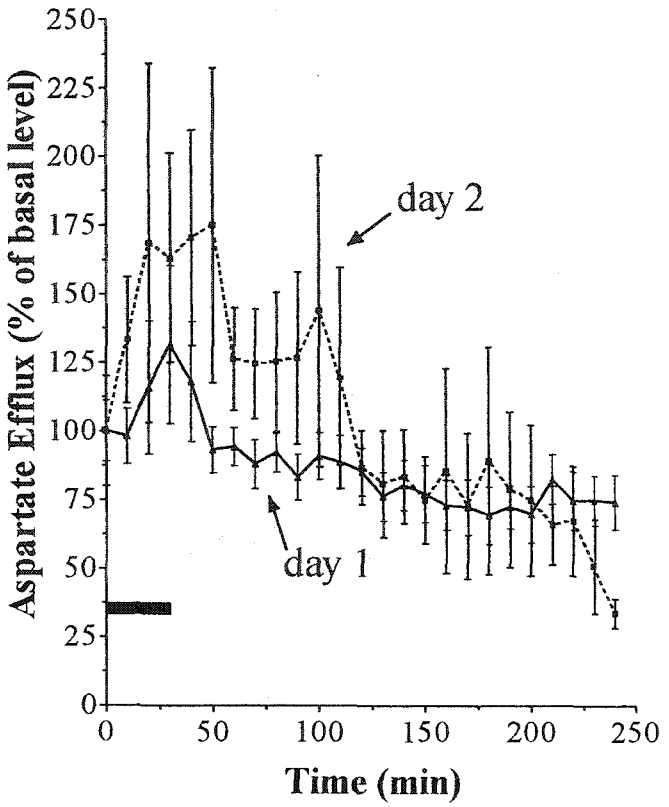

Figure 5:19.
0.7 mM MPP^+;
Aspartate Efflux (% basal)
vs. Time (min), n = 4.

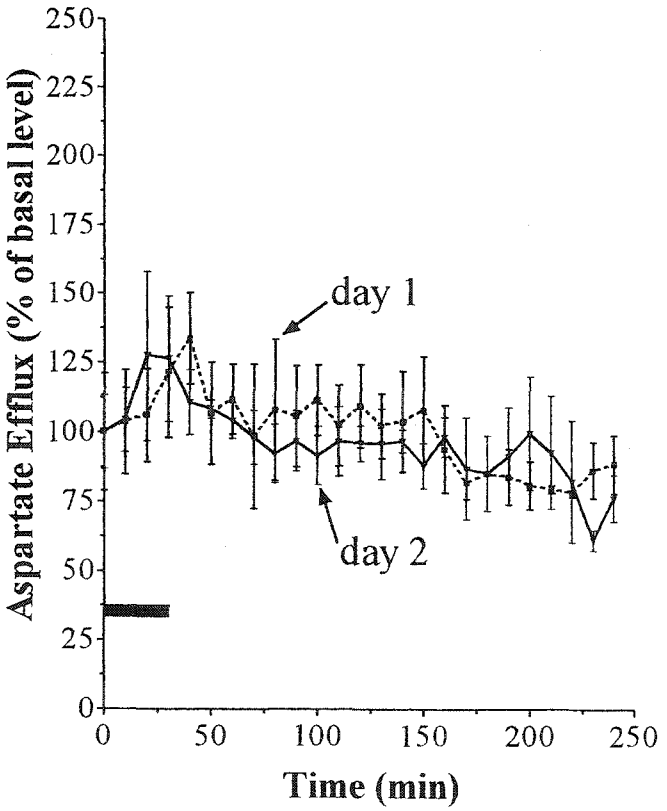

Figure 5:20.
0.7 mM MPP^+ with
1.0 mM ACV;
Aspartate Efflux (% basal)
vs. Time (min), n = 4.

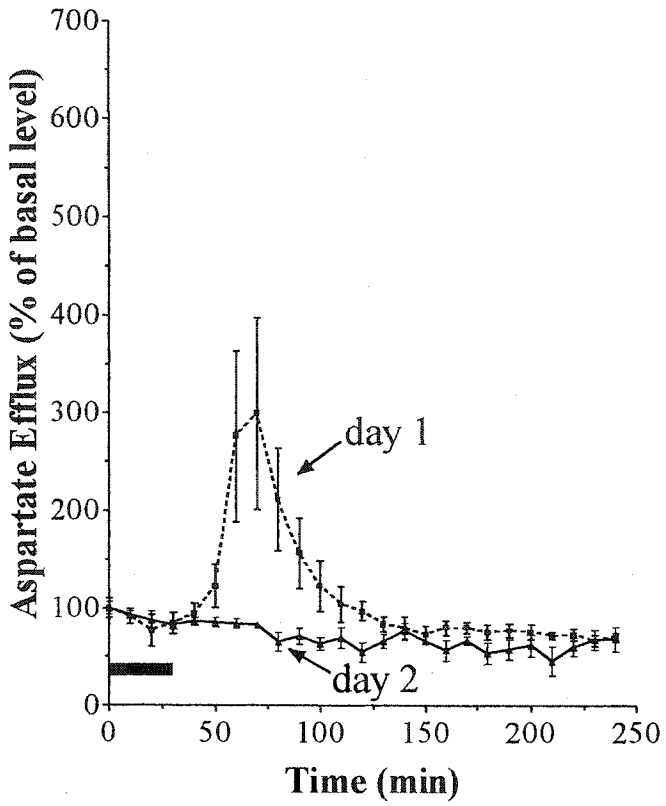

Figure 5:21.
1.3 mM MPP^+;
Aspartate Efflux (% basal)
vs. Time (min), n = 4.

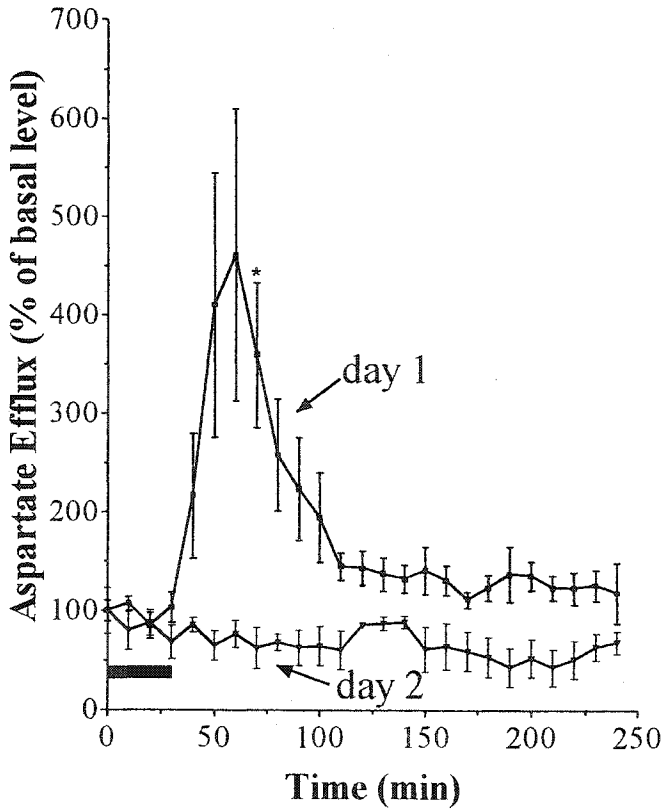

Figure 5:22.
1.3 mM MPP^+ with
1.0 mM ACV;
Aspartate Efflux (% basal)
vs. Time (min), n = 4.

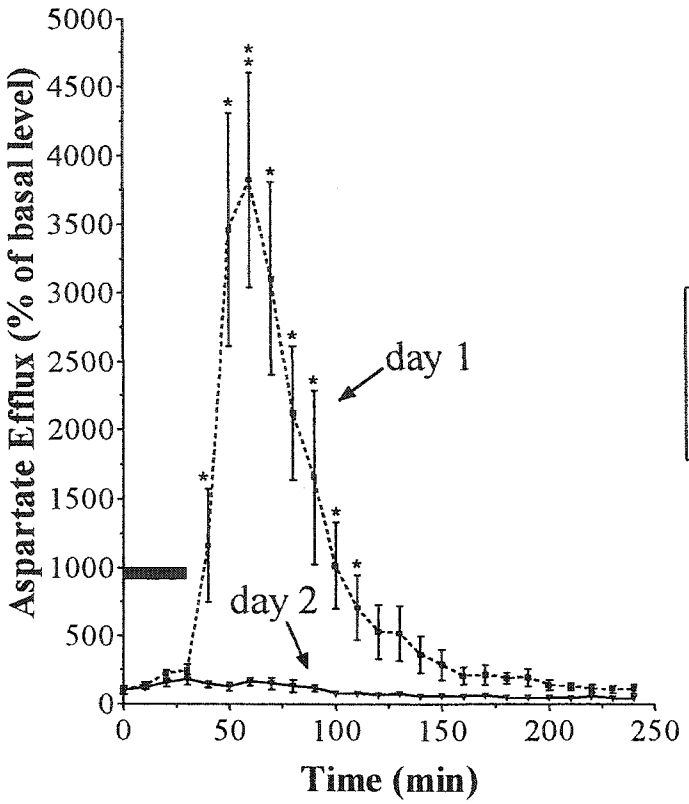

Figure 5:23.
2.5 mM MPP^+;
Aspartate Efflux (% basal)
vs. Time (min), n = 4.

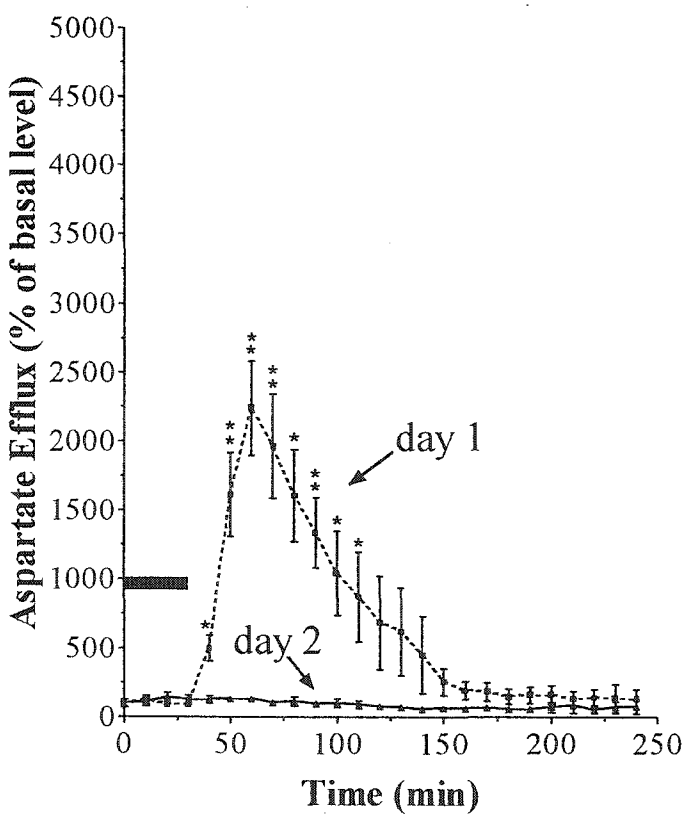

Figure 5:24.
2.5 mM MPP^+ with
1.0 mM ACV;
Aspartate Efflux (% basal)
vs. Time (min), n = 4.

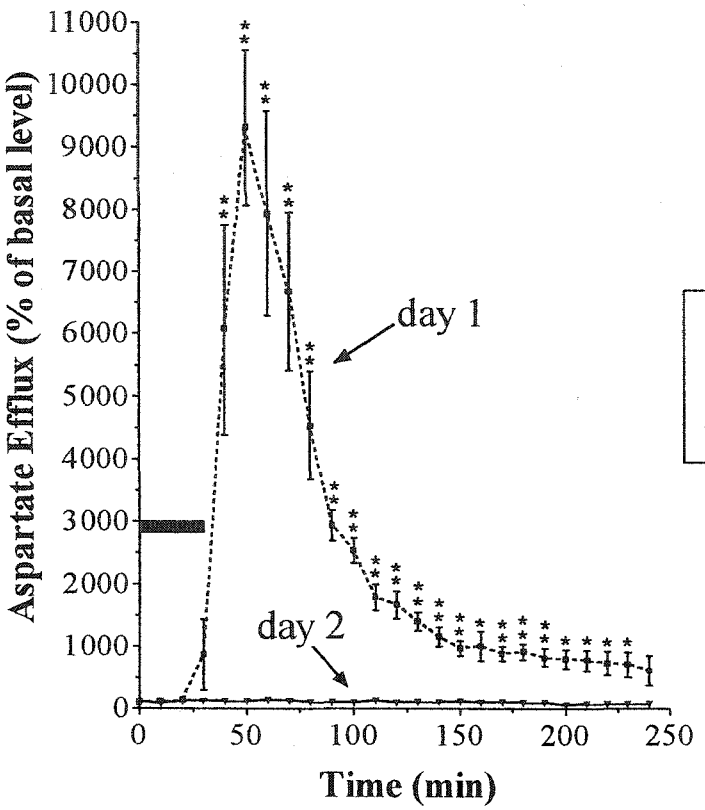

Figure 5:25.
10.0 mM MPP^+;
Aspartate Efflux (% basal)
vs. Time (min), n = 4.

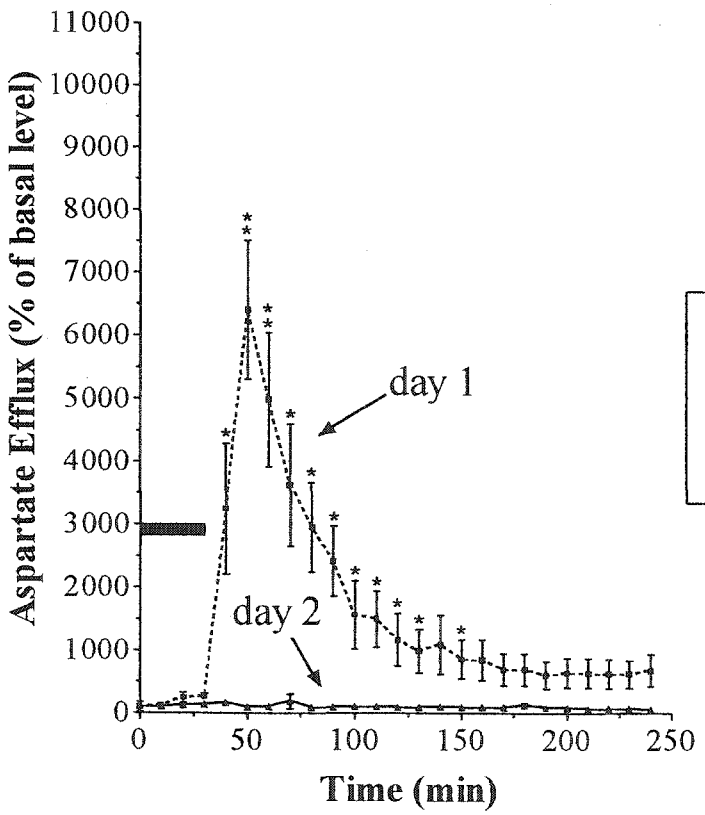

Figure 5:26.
10.0 mM MPP^+ with
1.0 mM ACV;
Aspartate Efflux (% basal)
vs. Time (min), n = 4.

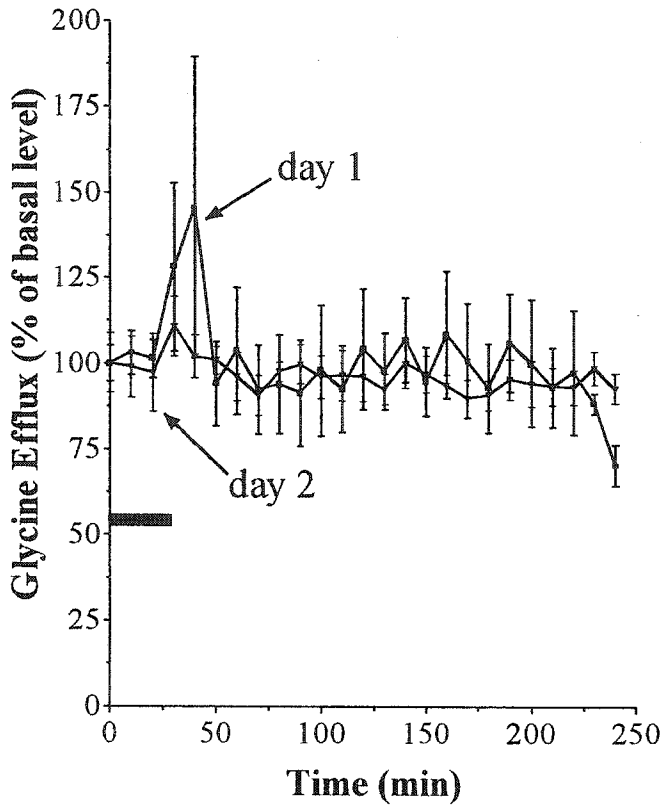

Figure 5:27.
0.7 mM MPP^+;
Glycine Efflux (% basal)
vs. Time (min), n = 4.

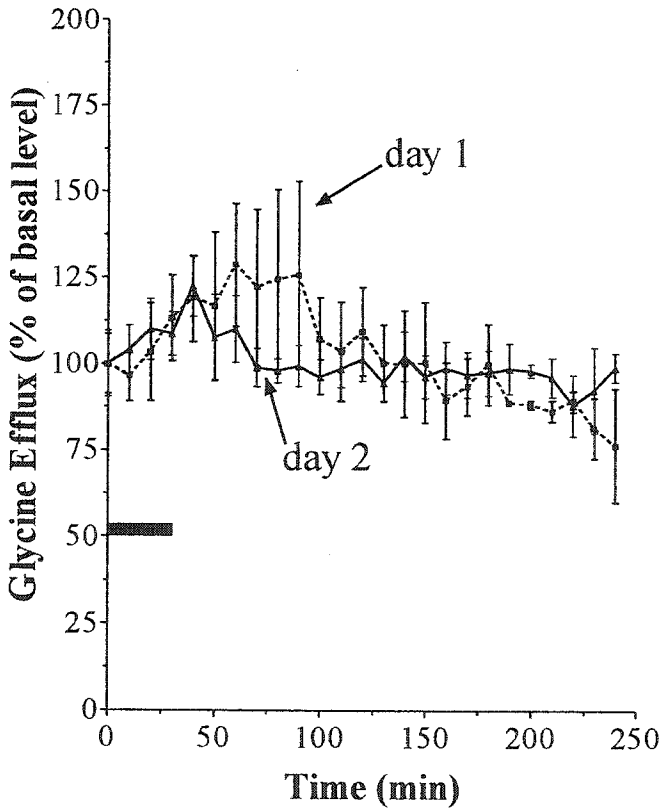

Figure 5:28.
0.7 mM MPP^+ with
1.0 mM ACV;
Glycine Efflux (% basal)
vs. Time (min), n = 4.

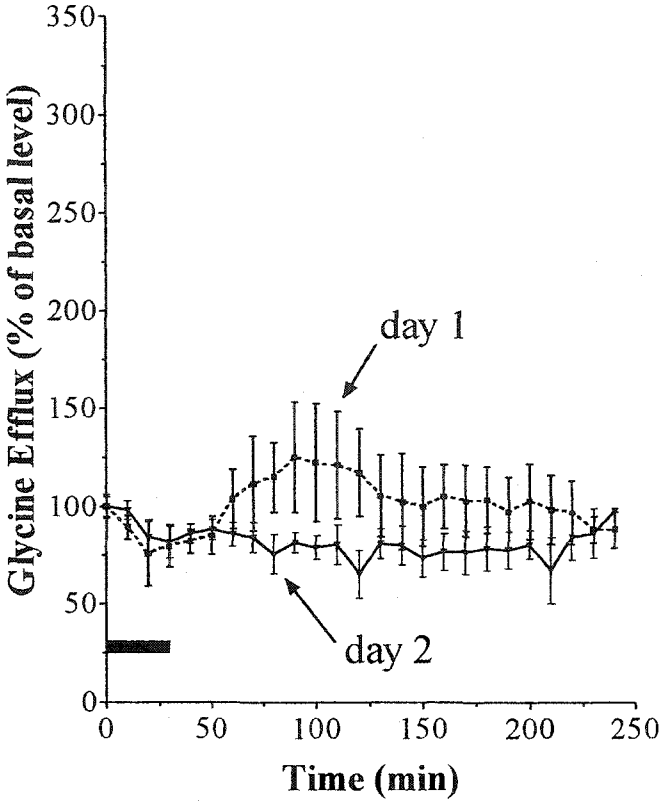

Figure 5:29.
1.3 mM MPP^+;
Glycine Efflux (% basal)
vs. Time (min), n = 4.

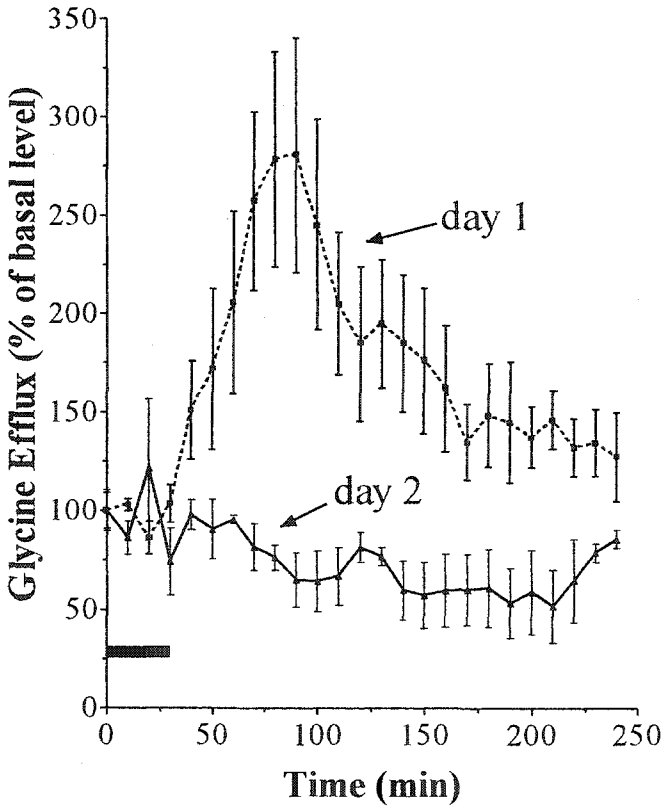

Figure 5:30.
1.3 mM MPP^+ with
1.0 mM ACV;
Glycine Efflux (% basal)
vs. Time (min), n = 4.

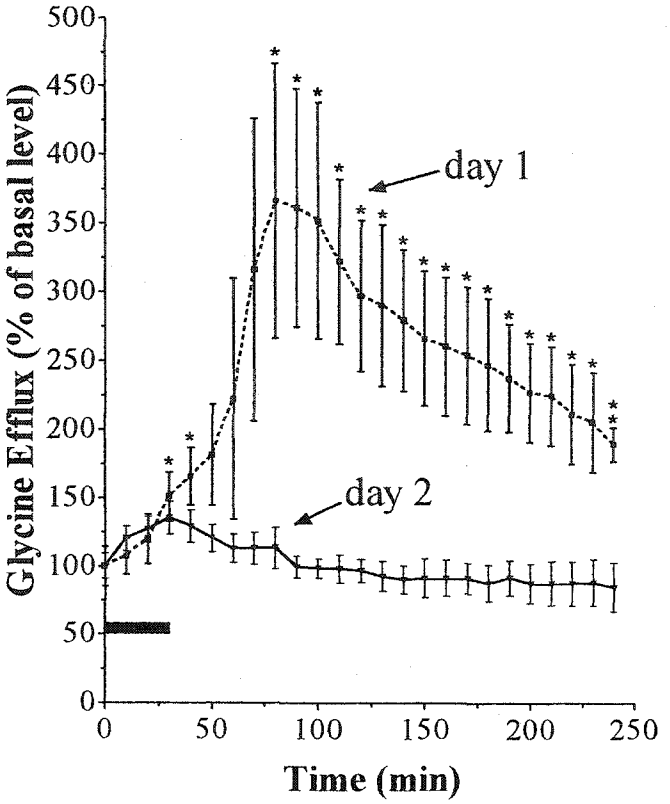

Figure 5:31.
2.5 mM MPP^+;
Glycine Efflux (% basal)
vs. Time (min), n = 4.

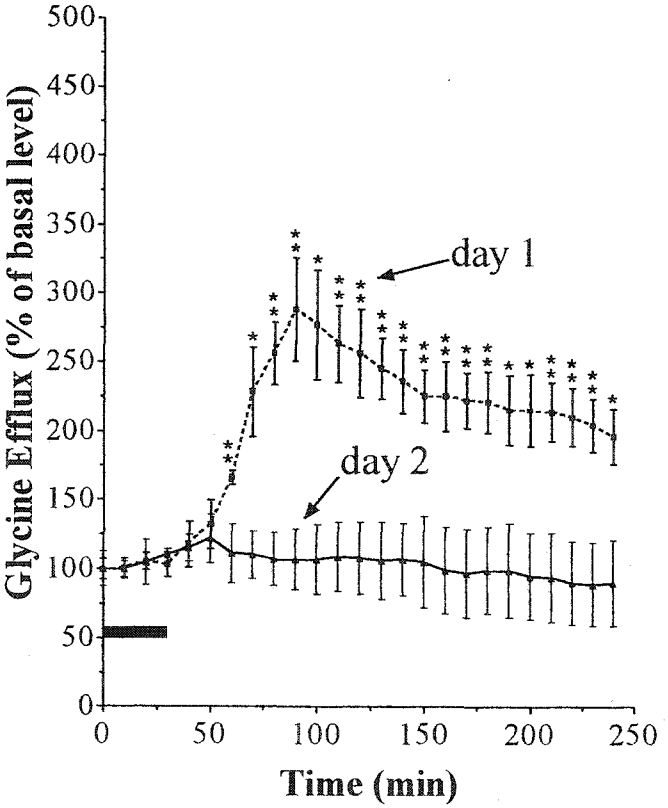

Figure 5:32.
2.5 mM MPP^+ with
1.0 mM ACV;
Glycine Efflux (% basal)
vs. Time (min), n = 4.

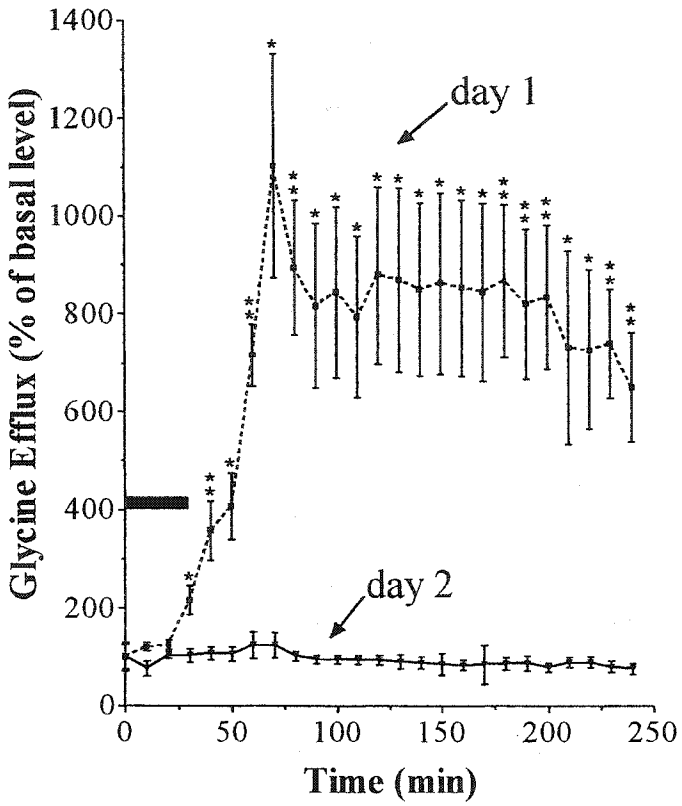

Figure 5:33.
10.0 mM MPP^+;
Glycine Efflux (% basal)
vs. Time (min), n = 4.

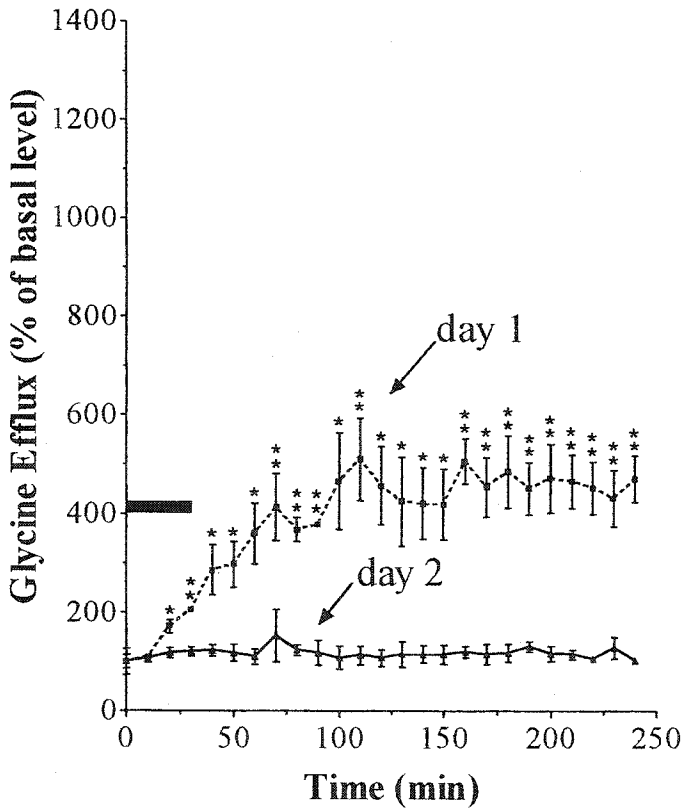

Figure 5:34.
10.0 mM MPP^+ with
1.0 mM ACV;
Glycine Efflux (% basal)
vs. Time (min), n = 4.

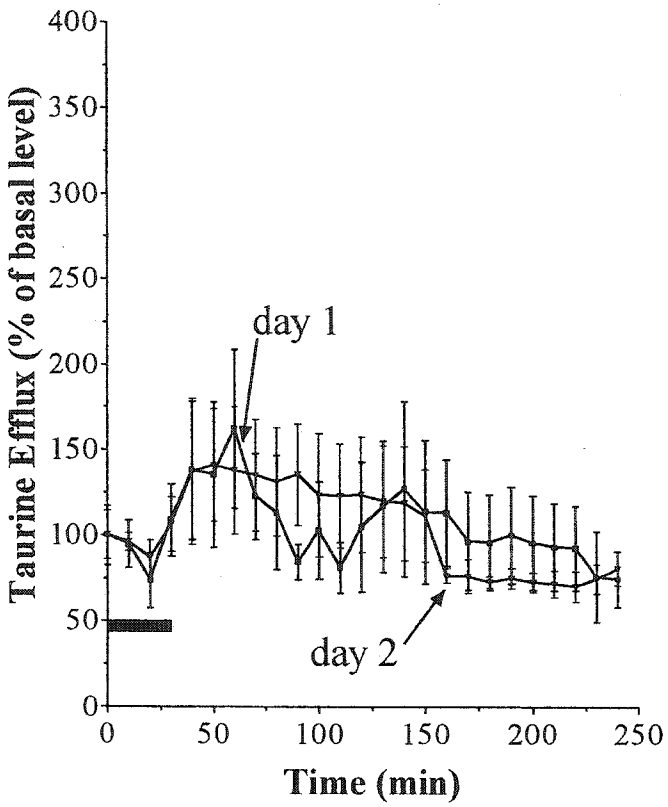

Figure 5:35.
0.7 mM MPP^+;
Taurine Efflux (% basal)
vs. Time (min), n = 4.

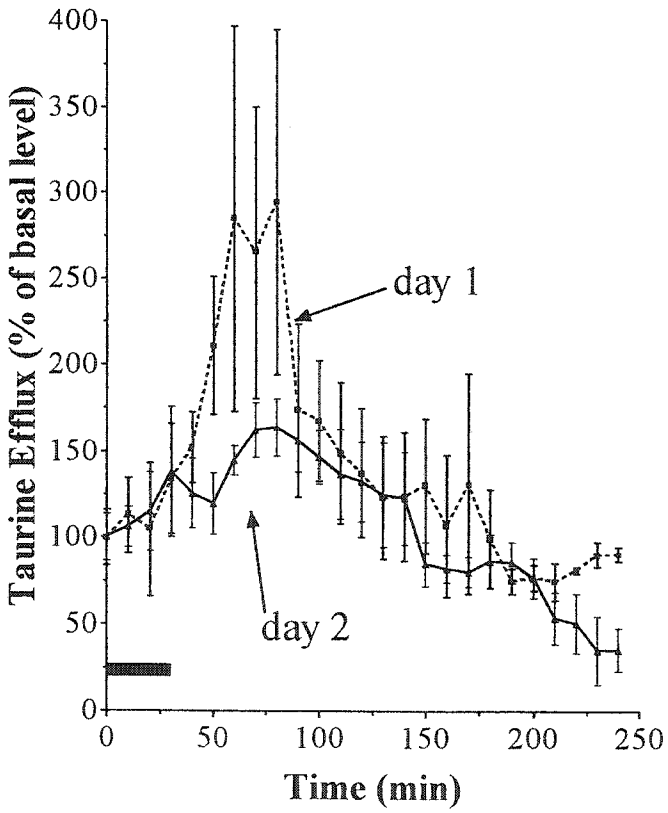

Figure 5:36.
0.7 mM MPP^+ with
1.0 mM ACV;
Taurine Efflux (% basal)
vs. Time (min), n = 4.

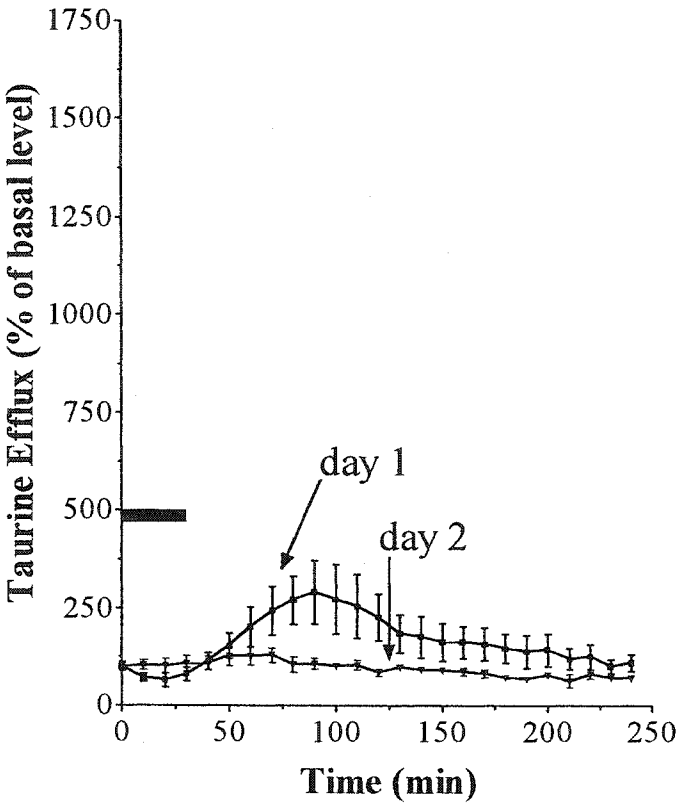

Figure 5:37.
1.3 mM MPP^+;
Taurine Efflux (% basal)
vs. Time (min), n = 4.

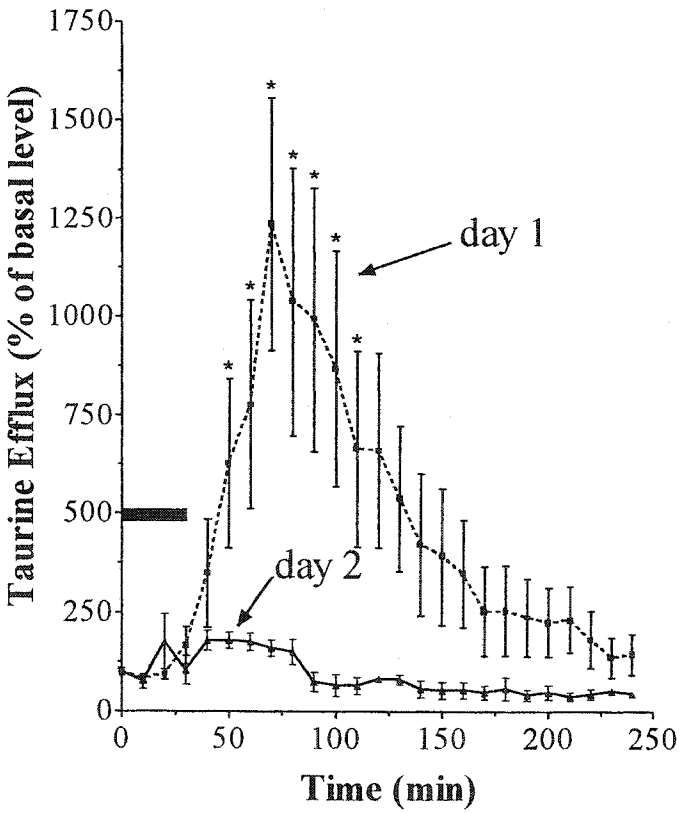

Figure 5:38.
1.3 mM MPP^+ with
1.0 mM ACV;
Taurine Efflux (% basal)
vs. Time (min), n = 4.

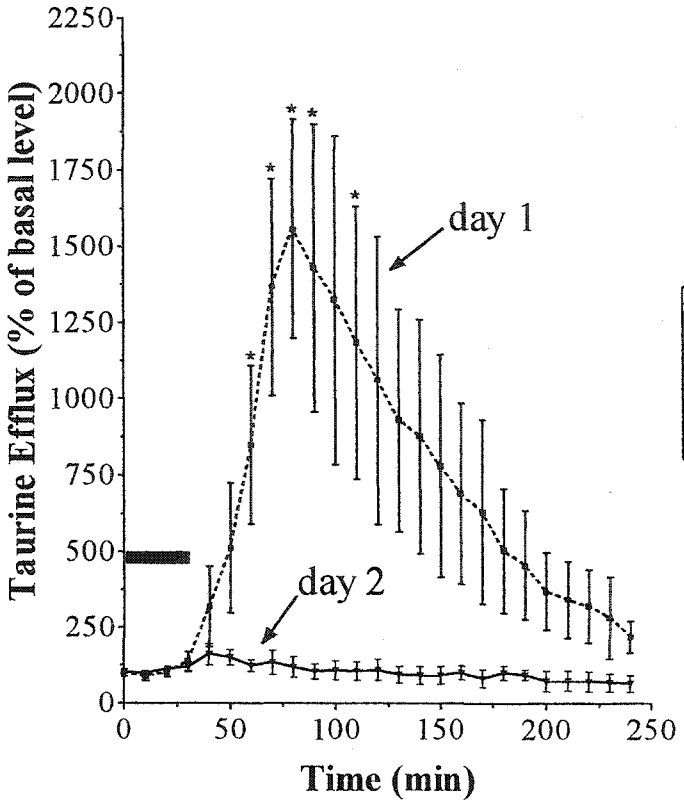

Figure 5:39.
2.5 mM MPP^+;
Taurine Efflux (% basal)
vs. Time (min), n = 4.

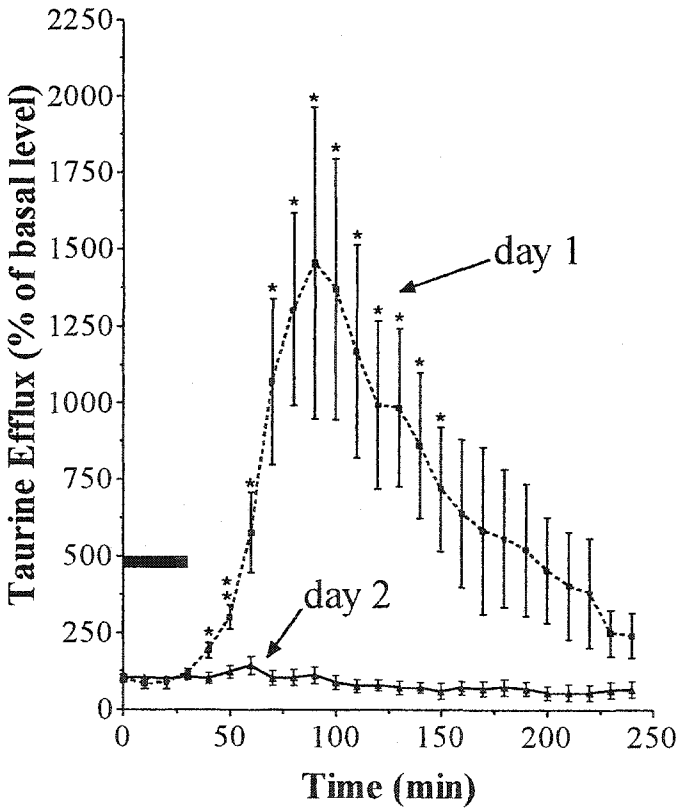

Figure 5:40.
2.5 mM MPP^+ with
1.0 mM ACV;
Taurine Efflux (% basal)
vs. Time (min), n = 4.

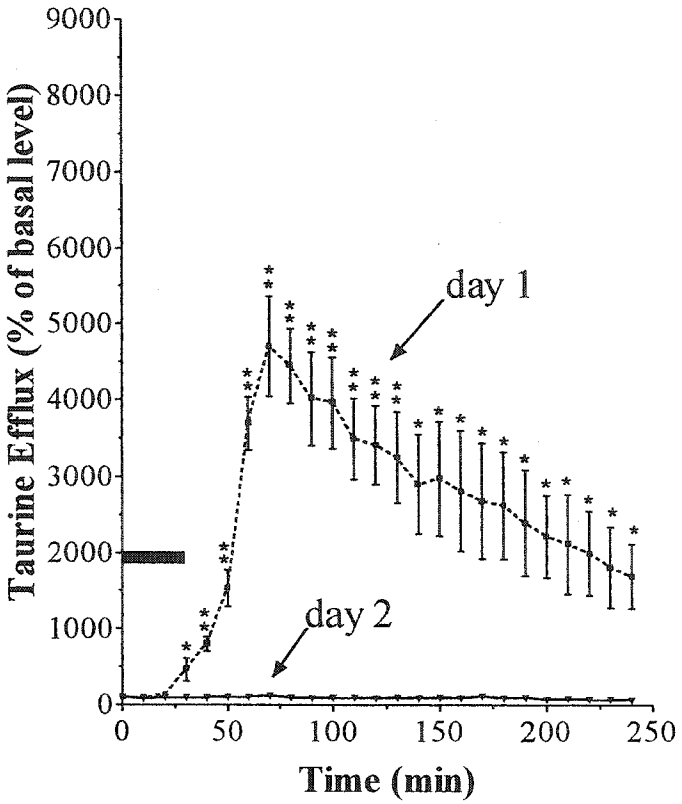

Figure 5:41.
10.0 mM MPP^+;
Taurine Efflux (% basal)
vs. Time (min), n = 4.

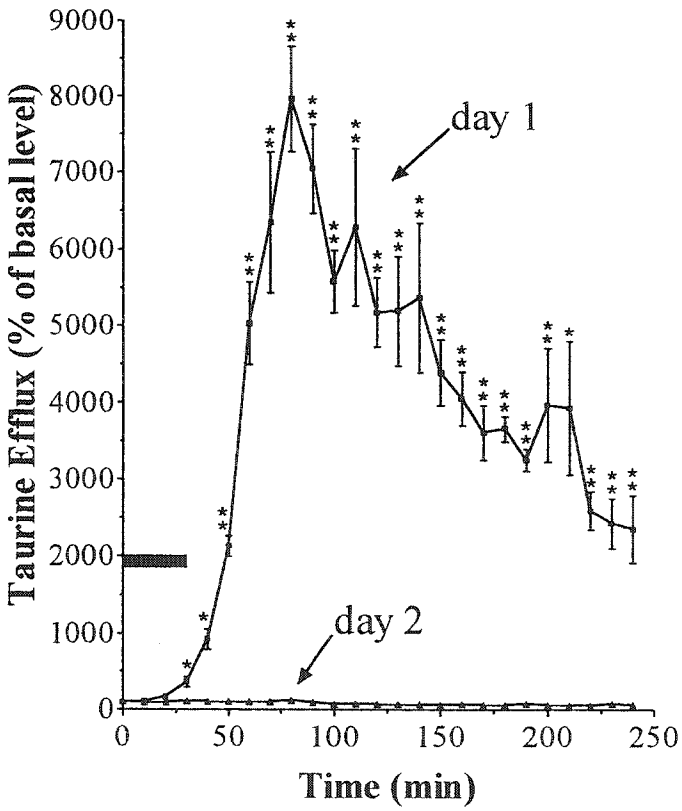

Figure 5:42.
10.0 mM MPP^+ with
1.0 mM ACV;
Taurine Efflux (% basal)
vs. Time (min), n = 4.

Chapter Six

Immunohistochemistry

A. Introduction

In microdialysis experiments presented in Chapter Two and by others,[151,152,227,239,327,366,367] perfusion of ≥ 0.7 mM concentrations of MPP^+ into the striatum of rats on day 1 evoked a massive release of DA. The greater the release of DA on day 1, the smaller the release caused by the day 2 perfusion of MPP^+. These observations suggest that the day 1 perfusion of MPP^+ caused DA neurotoxicity. In this chapter, experiments are described that were designed to examine tissue changes that occurred in response to MPP^+, using various immunohistochemical analyses in rat brain. Thus on day 1 animals were perfused for 30 min with aCSF or one of four concentrations of MPP^+ (0.7, 1.3, 2.5, 10.0 mM). Twenty-four hours after the day 1 perfusion rats were sacrificed and brain tissue in the vicinity of the microdialysis probe was examined immunohistochemically using: (1) TH-immunoreactivity (-IR), an indication of DA terminal degeneration; (2) GFAP-IR, a structural protein indicative of reactive astrocytes; (3) OX-42-IR, an indication of reactive microglia; and (4) Nissl staining with thionin, a tinctorial cellular stain for neuronal cell bodies.

B. Experimental

1. Chemicals and Drugs

Pentobarbital (sodium salt), sucrose, H_2O_2 (30%), 3,3'-diaminobenzidine tetrahydrochloride (DAB), Trizma (hydrochloride salt), fetal bovine serum (FBS), bovine serum albumin (BSA), polyvinylpyrrolidone (PVP), Triton X-100, thionin acetate stain, goat anti-rabbit IgG biotinylated secondary antibody (normal goat serum, NGS) and horse anti-mouse IgG biotinylated secondary antibody (normal horse serum, NHS) were obtained from Sigma. Permount®, paraformaldehyde and xylenes were obtained from Fisher. Potassium phosphate (KH_2PO_4) was obtained from EM Science. Sodium phosphate (Na_2HPO_4) and sodium chloride (NaCl) were obtained from Mallinckrodt. Hemosol (polyvinylchloride) was obtained from Aldrich. Rabbit anti-TH primary antiserum was obtained from Chemicon (Temecula, CA). Rabbit anti-GFAP primary antiserum was obtained from DakoCytomation (Carpinteria, CA). Mouse anti-OX-42 primary antiserum was obtained from Serotec (Oxford, England). The Vectastain avidin-biotin-peroxidase complex (ABC) kit was obtained from Vector Labs (Burlingame, CA). Tissue-Tek O.C.T. Compound was obtained from IMEB, Inc. (San Marcos, CA). The sources of all other chemicals have been described previously.

2. Animals and Surgery

Details of rats and surgical procedures have been described in Chapter Two. For all immunohistological experiments, only one probe was implanted.

3. Microdialysis and HPLC

Microdialysis experiments were identical to those described in Chapters Two and Five, except the day 2 microdialysis was not carried out. Dialysates from day 1 experiments were analyzed for biogenic amines employing HPLC-EC method I as described in Chapter Two.

4. Immunohistochemistry

Twenty-four hours after the day 1 MPP^+ perfusions, Nissl staining and TH, GFAP and OX-42 immunohistochemistry were conducted on horizontal striatal tissue slices using a modification of the methods described by Matarredona et al.[327] The following solutions were made in preparation for immunohistochemical experiments.

a. Solutions

(1) 8% Paraformaldehyde Stock Solution was prepared by dissolving 80 g of paraformaldehyde in 900 mL of deionized water. The solution was heated to 55 > 60°C under ventilation, removed from the heat and 2 M NaOH was added until the solution became clear (approximately 5 mL). The solution was filtered (Whatman #1 filter paper), diluted to 1000 mL with deionized water, stored at 4°C and was not used beyond 10 days storage.

(2) Sorenson's Phosphate Buffer Stock Solution (0.2 M, pH 7.2) was prepared by dissolving 8.06 g KH_2PO_4 and 20.0 g Na_2HPO_4 in 900 mL of deionized water. The pH was adjusted to 7.2 with 1 M HCl or 1 M NaOH (whichever was

necessary), the volume diluted to 1000 mL with additional deionized water, and stored at ambient temperature (23 ± 1°C).

(3) 0.9% Saline Solution was prepared by dissolving 9.0 g of NaCl in 1000 mL of deionized water and stored at ambient temperature (23 ± 1°C).

(4) 20% Sucrose Solution was prepared by dissolving 50.0 g sucrose in 250 mL of 0.1 M Sorenson's phosphate buffer. This was stored at 4°C and was not used beyond 7 days storage.

(5) Perfusion Solution was prepared by combining equal volumes of 8% paraformaldehyde solution and 0.2 M (pH 7.2) Sorenson's buffer stock solution. This solution was prepared immediately prior to use.

(6) Phosphate Buffered Saline (PBS) was prepared by dissolving 13.4 g $Na_2HPO_4 \cdot 7H_2O$ and 8.0 g NaCl in 1 L of deionized water. The pH was adjusted to 7.2 with 1 M NaOH and stored at ambient temperature (23 ± 1°C).

(7) Tris-Saline was prepared by dissolving 7.45 g Trizma in 1 L of 0.9% saline solution. The pH was adjusted to 7.4 (with 0.1 M NaOH or 0.1 M HCl, as appropriate) and stored at 4°C.

(8) Phosphate Buffered Saline/Triton Solution (PBS-T) was prepared by adding 3 mL of Triton X-100 to 997 mL of PBS. This solution was stored at 4°C.

(9) Thionin Stain was made by slowly adding and dissolving 2.5 g thionin acetate (while stirring) in 1 L of a solution of 36 mM NaOH and 0.2 M acetic acid at 60°C. After the thionin had dissolved, the solution was covered and boiled (60°C) for 45 min. The solution was filtered (Whatman #2 filter paper), stored in a brown bottle

(to protect from light) at ambient temperature (23 ± 1°C) and used within 4 months.

b. Procedures

i. General

On day 2, (24 hours after the day 1 microdialysis experiment) rats (330-360 g) were perfused through the heart under sodium pentobarbitol anesthesia (50 mg/mL i.v. of 5% w/v sodium pentobarbitol solution, *ca.* 1.0 mL) with 200 mL of 0.9% saline solution followed by 470 mL of Perfusion Solution. Brains were removed and then serially cryoprotected (at 4°C), first in Perfusion Solution for 24 h and then in 20% sucrose solution for 1-2 days or until they sank. The brains were then frozen in O.C.T. Compound at -15°C, and 30 μm horizontal striatal cross-sections were cut at -20°C on a cryostat (Reichert Histostat, Germany). Tissue was mounted on gelatine-coated slides (4/slide) and placed on a slide warmer (37°C) for 30-60 min.

Once tissue was placed in solution (rehydrated) it was never left out of solution for more than 15 sec during ensuing immunohistochemical processing. In subsequent procedures, tissue sections were always rinsed at ambient temperature (23 ± 1°C) in plastic slide-holders (Lab Scientific; Livingston, NJ) on a Bio-Shaker (Midwest Scientific; St. Louis, MO) at speed #4 unless noted otherwise. For each animal there were approximately 20 slides (*ca.* 4 tissue sections per slide). One slide-holder with 5 slides was set aside for Nissl staining (description below).

ii. Immunohistochemistry

The remaining slide-mounted tissue (*ca.* 15 per animal) was placed in slide-holders (5 slides/holder) and rinsed in PBS for 10 min. Endogenous peroxidases were blocked by incubating tissue in a solution of 3% H_2O_2 in 10% MeOH for 5 min. Tissue sections were then rinsed twice (10 min each time) in PBS, followed by incubation in a solution containing 10% NGS, 10% NHS, 10% FBS, 1% BSA and 1% PVP in 21 mL PBS-T for 60 min.

The slide-mounted tissue in each of the three holders was incubated with one of the following primary antibodies (diluted in PBS-T) for 72 h at 4°C: (1) rabbit anti-TH, 1:1000; (2) rabbit anti-GFAP, 1:2000; or (3) mouse anti-OX-42, 1:1000. Tissue sections were drained and rinsed three times (10 min each) in PBS. Tissue sections were drained, taken out of holders and laid flat. TH and GFAP sections were incubated with biotinylated goat anti-rabbit IgG secondary antibody diluted 1:740 with PBS-T. OX-42 sections were incubated with biotinylated horse anti-mouse IgG secondary antibody diluted 1:715 with PBS-T. Each slide received 200 µL of diluted secondary antibody, was covered with another glass slide and incubated (not on the shaker), at ambient temperature for 90 min. Sections were then placed back in their respective holders and rinsed three times (10 min each) with PBS. Tissue sections were then drained and incubated for 90 min with Vectastain® ABC reagent (diluted 1:50 in PBS), followed by three 10 min rinses (two times in PBS and one time in Tris-Saline).

The peroxidase bound to the secondary antibody was visualized by incubating tissue in a DAB solution (made immediately prior to use by combining 15 mg DAB and 300 µL of 0.3% H_2O_2 with 30 mL Tris-saline). The reaction was terminated after 5-30

min (depending on efficiency of tissue staining as periodically monitored on a light microscope) by rinsing tissue three times (10 min each) with PBS. Tissue was dehydrated with the following schedule (5 min each): 70% EtOH, 95% EtOH, 95% EtOH, 100% EtOH, 100% EtOH, hemosol, xylenes, and xylenes.

iii. Nissl staining

For Nissl staining with thionin the slide-holder was rehydrated with PBS for 2 min. Tissue sections were drained and incubated in thionin solution for 8 min followed by PBS and rinsing three times (5 min each) to stop the reaction. Tissue was dehydrated with the following schedule: 95% EtOH (1 min), 100% EtOH (1 min), 100% EtOH (1 min), 1:1 solution of 100% EtOH:xylenes (3 min), xylenes (5 min), xylenes (5 min).

iv. Dehydration and visualization

Cover slips were applied to all slide-mounted tissue sections with Permount. Visual analysis was conducted employing a Olympus Provis light microscope with SPOT imaging software® (Diagnostic Instruments; version 3.5.7 for Windows) and photographs were taken with a SPOT digital camera.

C. Results

1. TH-IR

Figures 6:01A-F show the changes in TH-IR visualized from cross-sections of striatal tissue fixed 24 hours after day 1 perfusion of aCSF or 0.7, 1.3, 2.5 or 10.0 mM concentrations of MPP^+ (Figures 6:01A-F, respectively). The normal pattern of TH-IR in

the striatum (shown in Figure 6:01A) consists of punctate staining in the cellular neuropil surrounding numerous fiber bundles. Around the microdialysis probe, a small dark area of punctate TH-IR was observed (Figure 6:01A).

In the tissue from rats which received 0.7 mM MPP^+ (Figure 6:01B), the TH-IR pattern was slightly disrupted around the microdialysis probe. In this area, TH-IR was decreased except for swollen punctate TH-immunoreactive profiles. Outside of this halo TH-IR appeared normal. In tissue from animals which received 1.3 (Figure 6:01C) and 2.5 (Figure 6:01D) mM MPP^+, the halo of disrupted TH-IR increased. Within this area, large swollen varicose fibers are observed. In the tissue from the 2.5 mM MPP^+-treated rats, a dark amorphous area appears around the microdialysis probe. In the tissue from the 10.0 mM MPP^+-treated rats (Figure 6:01E) this same amorphous area extended outward from the microdialysis probe to the edge of the striatum. Little to no characteristic TH-IR occurred in this area. Figure 6:01F is a photograph of tissue from a 10.0 mM MPP^+-treated rat which shows the outlying area of the striatum. The edge of the striatum reveals what appears to be early stage distal axonopathy (antereograde terminal die-back).

Overall, it appears that the decrease in normally-appearing TH-IR in dopaminergic terminals is proportional to the amount of DA efflux on day 2, 24 hours after day 1 MPP^+ perfusion. However, at MPP^+ concentrations $\geq$ 2.5 mM, there is an increasing area outwards from the microdialysis probe track that is heavily stained for TH-IR, but which lacks any structural morphology and is probably not indicative of surviving DA terminals.

2. Nissl Staining

Thionin was employed to stain for Nissl substance in all cell bodies in tissue sections. Figures 6:02A-E depict the changes in cell bodies with Nissl staining, conducted 24 hours after day 1 perfusion of aCSF or 0.7, 1.3, 2.5 or 10.0 mM MPP^+. There is an apparent decrease in cell staining density proportional to the concentration of MPP^+ perfused on day 1. Additionally, there are morphological changes when only aCSF was perfused (Figure 6:02A). In this figure, there is a densely staining area immediately surrounding the probe location. These are probably signs of neuronal necrosis induced by the placement of the microdialysis probe (i.e., mechanical damage). In day 2 tissue obtained following 0.7 mM MPP^+ perfusion on day 1 (Figure 6:02B) there is an apparent decrease in Nissl staining probably due to karyorrhesis (fragmentation and breakdown of the nuclei) and especially, karyolysis (total dissolution and disappearance of the nuclei).

In tissue obtained after 1.3 mM MPP^+ was perfused on day 1 (Figure 6:02C), further changes in the Nissl staining are indicated. There is an increased area (inside the dashed line) showing a generalized decrease in staining. Additionally, the dark-staining area around the probe observed in tissue following perfusion of 0.7 mM MPP^+ or aCSF alone has virtually disappeared. In tissue obtained following perfusion of 2.5 mM MPP^+ on day 1 (Figure 6:02D), almost the entire field of view shows a decrease in the density of cellular staining. Obvious signs of karyolysis are prominent in some areas around the probe track. In this photograph the necrotic tissue from the probe hole has remained virtually intact. This is not necessarily apparent in all tissue from this concentration of MPP^+, and therefore, is probably not relevant to MPP^+-dependent changes. The last of

these photographs (Figure 6:02E, tissue after 10.0 mM MPP^+ was perfused on day 1) depicts an enormous field of decreased cellular staining. The few cells remaining in this area are very small in size. Note especially the apparent transition that occurs when ≥ 2.5 mM MPP^+ was perfused on day 1. Thus, there is a dramatic increase in karyolysis compared to that caused by lower MPP^+ concentrations where the visible remnants of necrosis can still be observed as signs of pyknosis (condensation and shrinking of the cell nucleus) and karyorrhesis.

3. GFAP-IR

Anti-GFAP monoclonal antibody was used to detect astrocytes on day 2 in cross-sections of striatal tissue. Figures 6:03A-F show the effect of day 1 perfusion of aCSF (6:03A) and 0.7 (6:03B), 1.3 (6:03C), 2.5 (6:03D), and 10.0 (6:03E, F) mM MPP^+ on astrocytes as indicated by GFAP-IR. In Figure 6:03A, only aCSF was perfused on day 1, yet there is a small distance projecting from the probe track in which GFAP immunoreactivity is absent. The insert of Figure 6:03A, shows a typical resting astrocyte from the area outside the dashed line. Note the minimal processes and narrow cell body. At the lowest level of MPP^+ perfused on day 1 (0.7 mM) GFAP-IR shows an increased area void of GFAP-IR extending radially from the probe location (Figure 6:03B). The insert in Figure 6:03B is a typical astrocyte from the area immediately outside the dashed circle showing a swollen cell body, an early sign of reactive astrocytosis. With 1.3 mM MPP^+ (Figure 6:03C) the area lacking GFAP-IR astrocytes increased from the previous concentration of perfused MPP^+. Additionally, there is a change in the morphology of the GFAP-IR astrocytes outside the dashed circle, indicative of advanced astrocytosis

with a swollen cell body and numerous enlarged stellar processes (insert of Figure 6:03C).

With 2.5 mM MPP^+, an area radial from the probe contains broken GFAP immunoreactive cellular elements (Figure 6:03D). This area is followed (outward) by a zone absent of GFAP-IR which is enlarged from the previous concentration of MPP^+. The insert of Figure 6:03D shows a characteristic astrocyte in the area outside the dashed line. This photograph shows fragmentation of the astrocytes, with stellar processes separated from swollen cell bodies.

Figure 6:03E shows GFAP-IR after 10.0 mM MPP^+ perfusion. The entire field of view contains very little GFAP-IR. At a higher magnification (Figure 6:03 F and insert) GFAP-IR appears but only in widely dispersed astrocytes with fragmented cell bodies and processes. Some of the astrocytic cell bodies appear swollen, whereas, others are the size of normal resting astrocytes.

4. OX-42 (microglia-IR)

OX-42 is an antibody that is directed against the type-3 complement receptor (CR-3) and recognizes microglial cells. This antibody was used to detect microglia on day 2 in cross-sections of striatal tissue. Specific terminology will be used to relate various stages of microglial activation as described by Matarredona et al.[327] There are basically three different stages of activation that will be differentiated as: (1) "ramified" microglia are in the resting state and are characterized by a small cell body with several emanating processes; (2) "activated" microglia have a swollen cell body with thicker processes; (3) "reactive" microglia have become macrophages with a pseudopodic to

globular-shape, without processes. In some of the photographs these will be pointed out with a (1) box, ramified; (2) solid circle, activated; (3) dashed circle, reactive. The Figures 6:04A-L show the effect of aCSF perfusion (6:04A, B) and of 0.7 (6:04C, D), 1.3 (6:04E, F), 2.5 (6:04G, H), and 10.0 (6:04I - L) mM MPP^+ on microglia as indicated by OX-42 immunohistology.

In Figure 6:04A, B the effects of day one perfusion of aCSF are shown. In the area around the probe, some reactive microglia are observed. A magnification of the area around the probe (Figure 6:04B) shows all three stages of microglia, with the ramified microglia farthest away from the probe track. The effects of 0.7 mM MPP^+ are shown in Figures 6:04C, D. There are more reactive microglia in the area around the probe compared to when only aCSF was perfused. Magnification of the area around the probe (Figure 6:04D) reveals that all three stages of microglia are still present. When the concentration of MPP^+ was increased to 1.3 mM, (Figures 6:04E, F) there are lightly staining reactive microglia (insert of Figure 6:04E) with sparse clusters of more intensely staining reactive microglia (Figure 6:04E). Away from the probe, in an area outside the field of view of Figure 6:04E, both activated and ramified microglia can still be observed (Figure 6:04F).

The OX-42 immunoreactivity dramatically changes as the concentration of perfused MPP^+ was increased to 2.5 mM (Figures 6:04G, H). The area around the probe (Figure 6:04G and insert) depicts a dense area of reactive microglia. Outside this field of view (Figure 6:04H) at the edge of the striatum there are darkly staining clusters of reactive microglia, and near the edge of the striatum (top of photograph) some activated microglia are still visible. Figures 6:04I - L shown the destructive effects of 10.0 mM

MPP^+. In Figure 6:04I the entire field of view exhibits intense nonspecific staining. Even the texture of the tissue appears corrugated and this effect extends almost to the edge of the striatum. Magnification of this area (Figures 6:04J, K) show large clusters of reactive microglia. In Figures 6:04J, L the area outside this intensely staining non-specific region, shows sparse and barely visible activated microglia.

D. Discussion

Numerous microdialysis studies have shown that perfusion of millimolar concentrations of MPP^+ into the rat striatum produces a massive increase in DA efflux.[151,152,227,239,327,366,367] In some of these microdialysis studies, the same or a similar concentration of MPP^+ was perfused on day 2 (24 hours after day 1 perfusion), resulting in an attenuated release (maximum efflux) of DA. This attenuated release of DA on day 2 has been proposed[151,152,227,368-370] to be an indication of dopaminergic terminal damage. That is, the amount of DA efflux on day 2 is proposed to reflect the number of dopaminergic terminals remaining in the striatum. While this is not an indication of dopaminergic neuronal cell body loss, it has been shown that the loss of TH-IR (indicative of dopaminergic terminal damage) results in eventual dopaminergic neuronal cell body loss in the SN_{pc} due to the retrograde axonal transport of MPP^+.[371-373] The present immunohistochemical analysis was conducted only on striatal tissue. In fact, the DA neuronal cell loss in the SN_{pc} is believed to be a much slower process, taking several days (after perfusion of MPP^+) to occur.[374] The TH-IR changes shown in Figures 6:01C-F provide good evidence for distal axonopathy (dying-back axonal degeneration) and may be an indication of Wallerian degeneration (axon and myelin sheath degeneration

when disconnected from the cell body).[375] The present study indicates that the maximum DA efflux on day 2 is: (1) inversely proportional to the amount of TH-IR and (2) proportional to the quantity of remaining DA terminals in the striatum.

Cell bodies containing Nissl substance were stained with thionin as presented in 6:02A-F. Dopaminergic neuronal cell bodies are not present in the striatum and, hence, Nissl staining (or lack of) is not an indication of their presence or loss. The Nissl staining in the present study was conducted to obtain insight into the effects of MPP^+ on all neurons located in the striatum. While low concentrations of MPTP/MPP^+ may be selective to dopaminergic neurons,[5,77,134] we now provide some evidence that as the concentration of MPP^+ perfused (or the total quantity of MPP^+ perfused) is increased, MPP^+ becomes non-selective, apparently indiscriminately destroying many neurons along with astrocytes and perhaps microglia.[376] Therefore, while MPP^+ may be selective to DA degeneration at low concentrations, with increasing concentrations it becomes an indiscriminate cellular toxin. The results from the present study indicate that at MPP^+ concentrations $\leq$ 1.3 mM (Figures 6:02A - C) cellular loss is minimal as characterized by the density of Nissl staining. However, at MPP^+ concentrations $\geq$ 2.5 mM (Figures 6:02D, E) there is widespread destruction of many if not all cell types in the vicinity of the probe. This effect is apparent in Figure 6:02E, when 10.0 mM MPP^+ was perfused on day 1. There is very little Nissl staining in the striatal area shown, indicative of rampant karyolysis.

At all MPP^+ concentrations perfused there appears to be signs of neuronal cell loss, the extent of which is proportional to the MPP^+ concentration perfused on day 1. The proposition that at $\geq$ 2.5 mM MPP^+ becomes non-selectively toxic is supported by

the general signs of karyolysis depicted by Nissl staining experiments, and the darkened appearance of non-structurally morphologic patterns of TH-IR, GFAP-IR and microglia immunoreactivity (Figures 6:01E, F, 6:03E, F, and 6:04G-L, respectively). In fact when 10.0 mM MPP^+ was perfused on day 1 enormous generalized toxic destruction of a majority of the cells in the striatum was observed radiating outward from the probe.

In the present study, examination of the response of astrocytes to MPP^+ using GFAP immunohistochemistry on day 2 was also conducted. As the concentration of perfused MPP^+ on day 1 was increased, there was a corresponding increase in the area (radiating outward from the probe) which was void of astrocytes as indicated by a complete lack of GFAP-IR (Figures 6:03A-F). This area corresponds to the same area where there was no TH-IR (Figures 6:01C-E). Additionally this same area corresponds to the area in the Nissl stained tissue sections where there were clear cellular signs of necrosis indicated by karyorrhesis and karyolysis (Figures 6:02 C-E). Indeed, the GFAP-IR relationship to TH-IR is clearly apparent (Figures 6:03D, E and 6:01D, E, respectively) when the concentration of MPP^+ perfused on day 1 was $\geq$ 2.5 mM. A darkened area extending radially, outward from the probe (similar to TH-IR at the same concentration) which upon closer magnifications (Figure 6:03F) shows the remnants of astrocytes. Many of these remnants appear to be normal sized astrocytes. This suggests that MPP^+, at concentrations $\geq$ 2.5 mM, is astrocytoxic and the toxic response is so rapid that astrocytes died before becoming reactive. This appears to be substantiated by the earlier findings with Nissl staining where there appears to be a generalized loss of all cell types at these concentrations of MPP^+ perfused on day 1 (2.5 and 10.0 mM).

Interestingly, ≥ 2.5 mM MPP^+ perfusions cause a substantial delayed elevation in Glu efflux (Chapter Five).

The inserts in Figures 6:03A-D, F show magnifications of astrocytes (at each concentration of perfused MPP^+) in the initial area away from the probe track where there is GFAP-IR (i.e., just outside the dashed line). As the concentration of MPP^+ perfused on day 1 increases there are characteristic changes in the morphology of these astrocytes. A resting astrocyte is shown in the insert of Figure 6:03A in tissue perfused with aCSF alone. At 0.7 mM MPP^+ (insert of Figure 6:03B) astrocytes exhibit an enlarged cell body, while at 1.3 mM MPP^+ (insert of Figure 6:03C) astrocytes exhibit both an enlarged cell body and stellar processes. Corresponding with the idea that at higher concentrations (≥ 2.5 mM) MPP^+ becomes a non-selective toxin, the inserts from Figures 6:03D, F show disruption of astrocytes and signs of cellular destruction.

Day 1 perfusions of MPP^+ resulted in a dose-dependent microglial response as shown by OX-42 immunoreactivity. When aCSF (Figures 6:04A, B) and 0.7 mM MPP^+ (Figures 6:04C, D) were perfused there were clearly visible signs of reactive microglia in the area around the probe. Activated and then ramified microglia appear as the distance from the probe increases. With tissue from when 1.3 mM MPP^+ was perfused the reactive microglia became darker and sparse (Figure 6:04E, F). In the 2.5 (Figures 6:04G, H) and 10.0 mM (Figure 6:04I-L) MPP^+ animals the intense OX-42-IR corresponded to that showing decreased TH-IR (Figures 6:01D-F) and GFAP-IR (Figures 6:03D-F) at these same concentrations of MPP^+. Close examination showed heavily stained OX-42 immunoreactive microglia. An additional dose-dependent change observed with OX-42-IR was an increase in the distance from the probe where activated

and ramified microglia were detected. At 2.5 mM MPP^+ activated microglia are only visible at the peripheral area of the striatum (Figure 6:04H). Close examination of Figure 6:04L (a magnification of the edge of the striatum) shows lightly staining ramified and activated microglia. The toxic insult from MPP^+ may have been so rapid that the microglia died before entering the reactive phase, similar to that seen with GFAP-IR at the same concentration (Figure 6:03E, F).

The functions of astrocytes and microglia in the normal and diseased brain are not well understood and represent an area of active investigation. In the normal brain, astrocytes are considered largely beneficial by releasing trophic factors, scavenging ROS and controlling extracellular Glu levels.[377-381] While astrocytes are thought to have a supportive role for neurons, microglia may exert deleterious effects in the PD brain and in MPTP/MPP^+-treated animals.[382] Many previous studies have reported a glial response (gliosis) which occurs as a result of MPTP/MPP^+ administration.[175,383,384] In addition, post-mortem analysis of PD brain tissue shows elevated microglial immunoreactivity.[385-388] Gliosis was originally believed to evoke similar effects as other macrophages, i.e., removal of cellular debris.[380-382] However, in the PD brain and in MPTP/MPP^+-treated animals, microglia may exert a deleterious effect by producing ROS, RNS, proinflammatory prostaglandins and cytokines.[382] ROS and RNS production can lead to neuronal cell death.[36,173,257,389,390] Prostaglandin E_2 (PGE_2) and its synthesizing enzyme cyclooxygenase type-2 (Cox-2) expression is increased during gliosis associated with inflammation.[391,392] Elevated levels of Cox-2 and PGE_2 have been detected in the SN_{pc} of post-mortem PD brains[393] and inhibition of Cox-2 attenuates MPTP neurotoxicity in mice.[394] Of the cytokines, tumor necrosis factor-α (TNF-α) and interleukin-1β (IL-1β)

have both been implicated in PD neurotoxicity having been found at elevated levels in the SN_{pc} of post-mortem PD brains and in the CSF of living PD patients.[395-397] These cytokines are produced by microglia, which can stimulate other microglia and, hence, amplify neuronal damage.[382] Interestingly, activation of microglia can occur before astrocytosis and, most importantly, before significant dopaminergic neurodegeneration has occurred.[175]

E. Conclusion

Analysis of rat striatal tissue analyzed 24 hr after perfusion of 0.0 - 10.0 MPP^+ show MPP^+-induced concentration dependent changes in TH-IR, GFAP-IR, OX-42-microgial-IR and Nissl staining. The present study indicates that the maximum DA efflux on day 2 is: (1) inversely proportional to the amount of TH-IR and (2) proportional to the quantity of remaining DA terminals in the striatum. GFAP-IR shows that as MPP^+ concentrations perfused on day 1 are increased there is an increase in the distance from the probe track that is absent astrocytes indicated by a lack of GFAP-IR. With OX-42-IR, the microglia morphology change is apparent with an increase in reactive microglia with increasing concentrations of MPP^+ having been perfused on day 1. There is a dramatic decrease in the amount of Nissl staining with increasing concentration of perfused MPP^+ especially, at MPP^+ concentrations $\geq$ 2.5 mM, obvoius signs of cellular destruction. Taken together, the results of the immunohistochemical experiments suggest that MPP^+ concentrations $\geq$ 2.5 mM induce non-specific neurotoxicity (i.e., not limited to DA and 5-HT neurons) destroying astrocytes, microglia and other striatal neurons.

Chapter Six Figures

Figures 6:01A-F. Horizontal tissue sections (30 μm) through the striatum on day 2 depicting TH immunoreactivity. The striata were perfused on day 1 with aCSF (A) or various millimolar concentrations of MPP^+ for 30 min: 0.7 (B), 1.3 (C), 2.5 (D) and 10.0 (E, F). The area inside the dashed line depicts an absence of TH-immunoreactivity, which increases outwards from the probe proportional to the concentration of MPP^+ perfused on day 1. The asterisk depicts the approximate center of the probe hole.

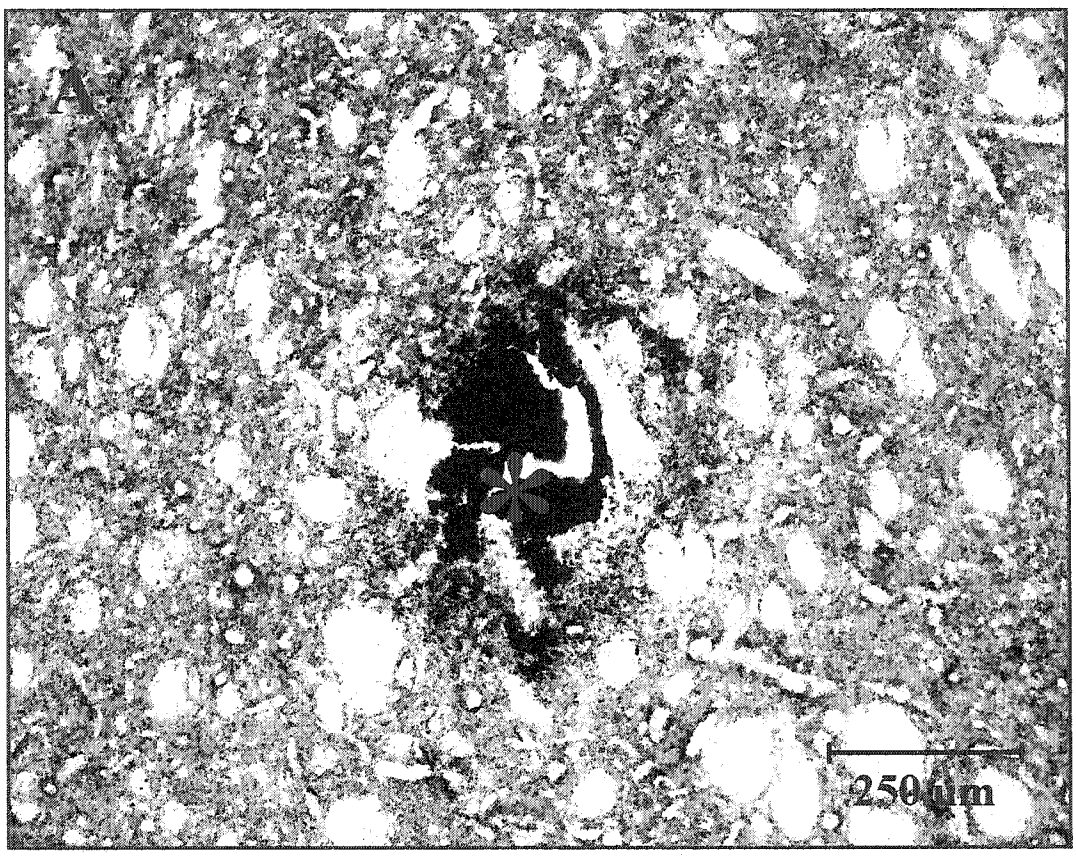
250 um

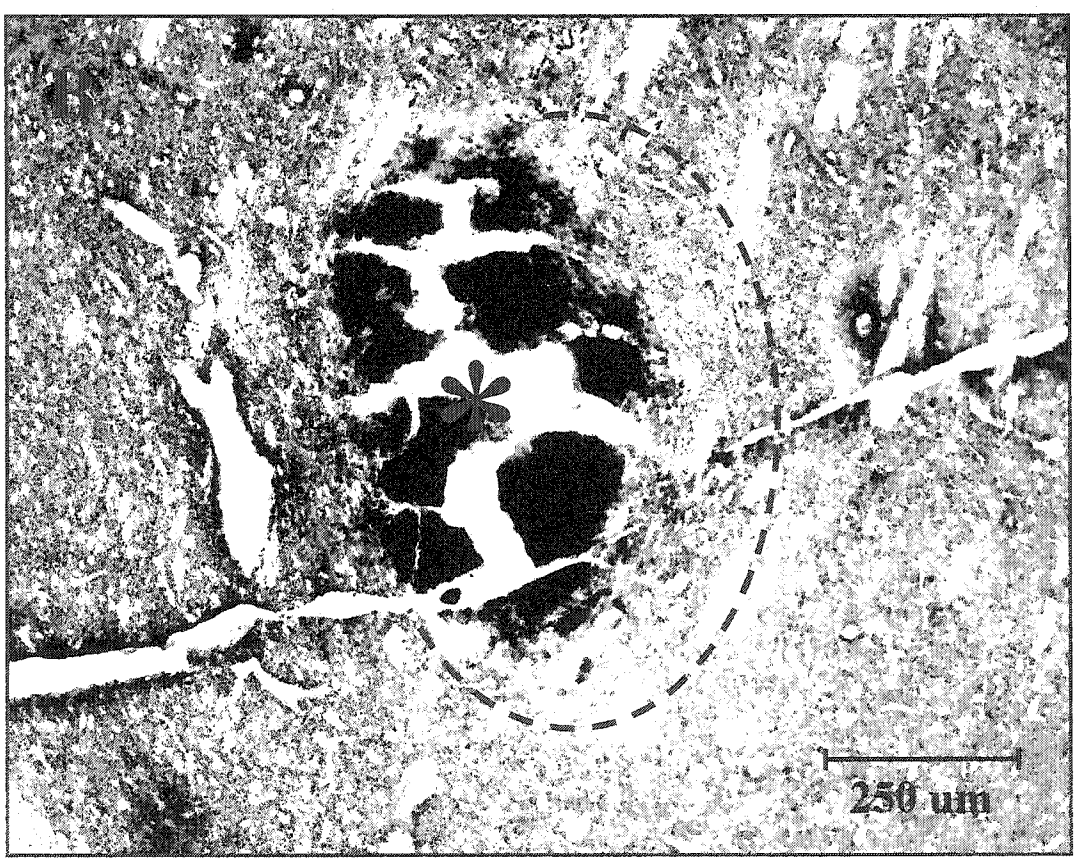
250 um

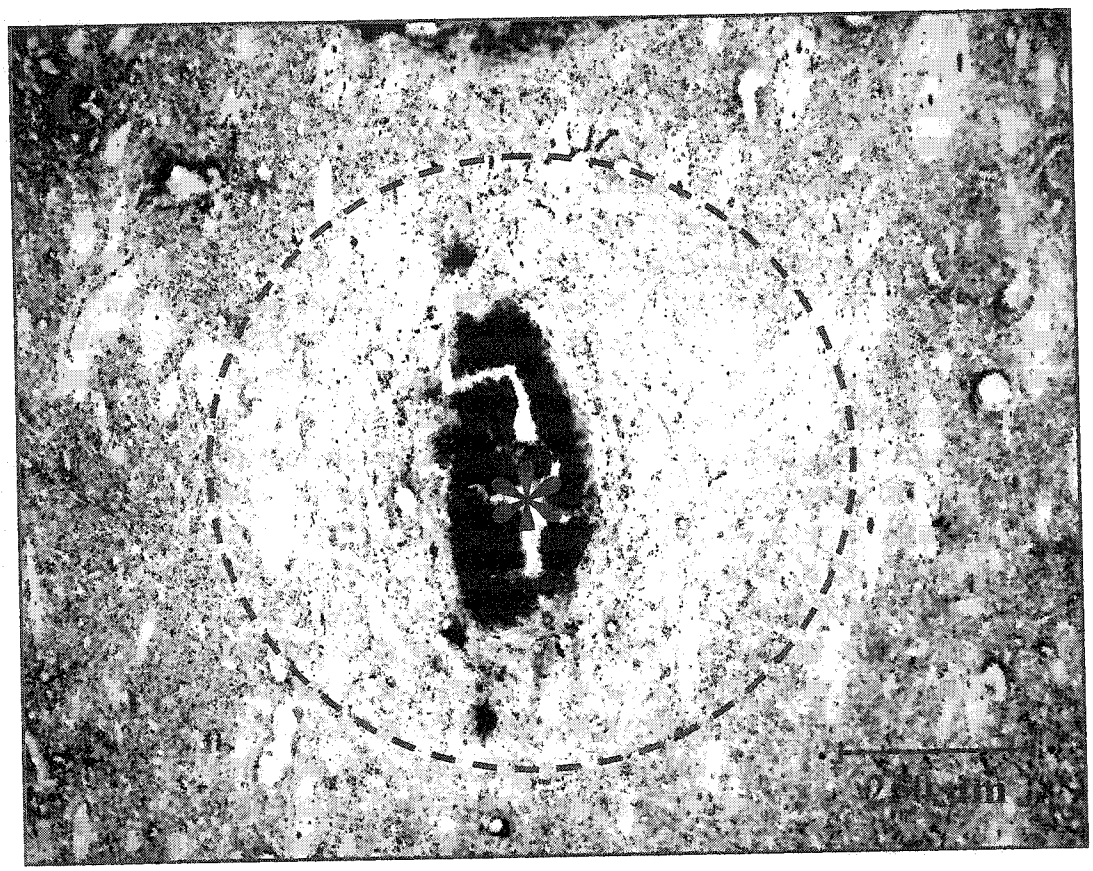
250 µm

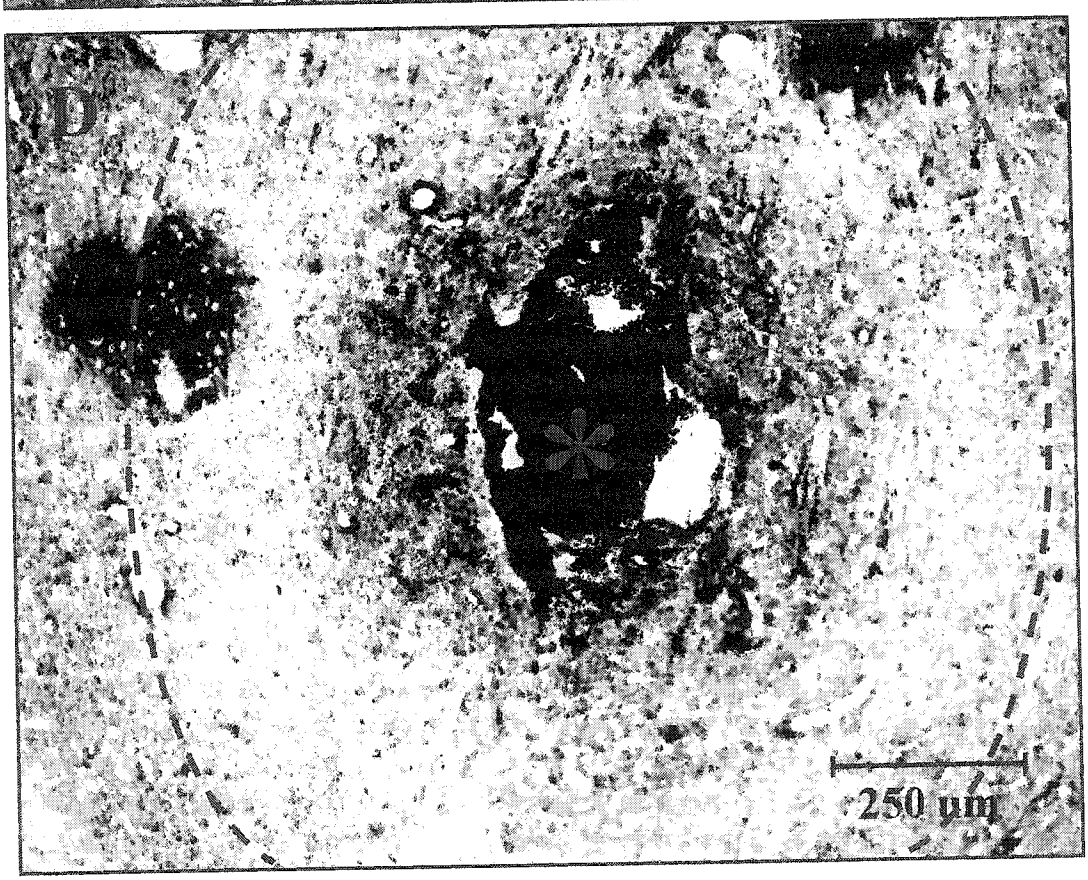
250 µm

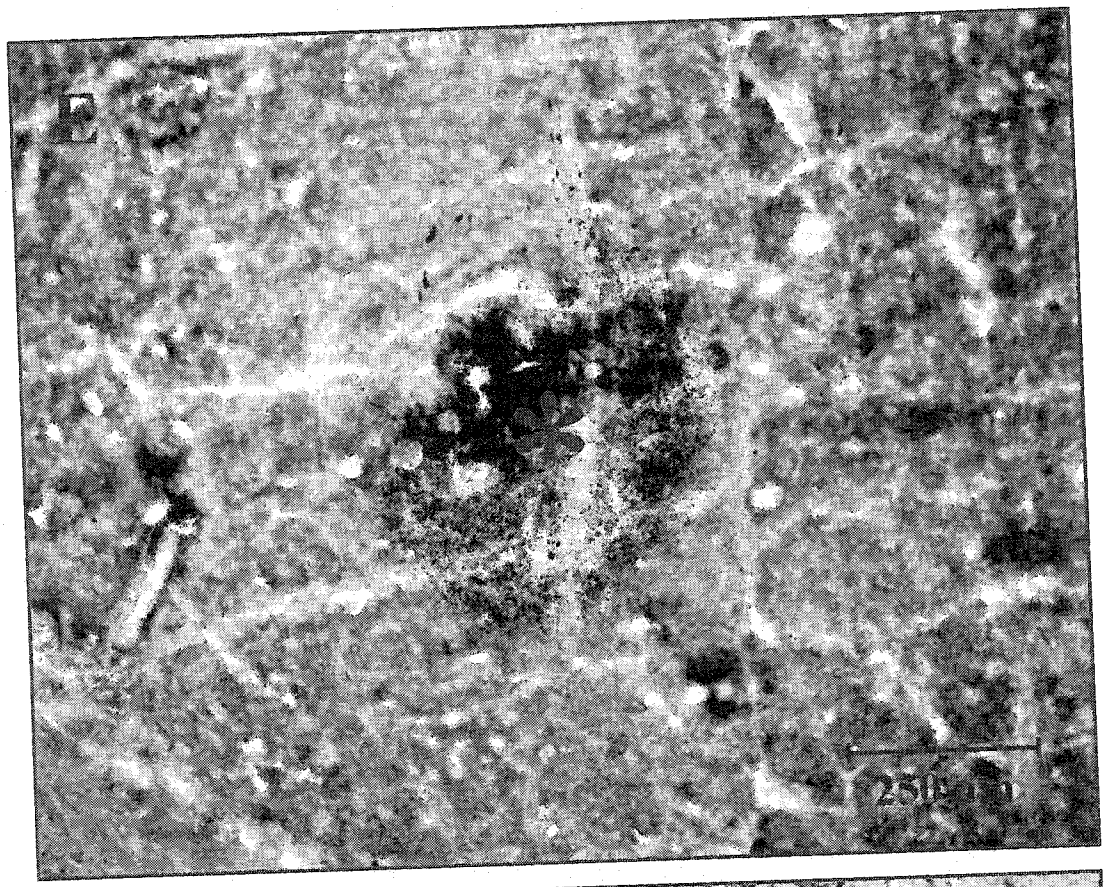
E

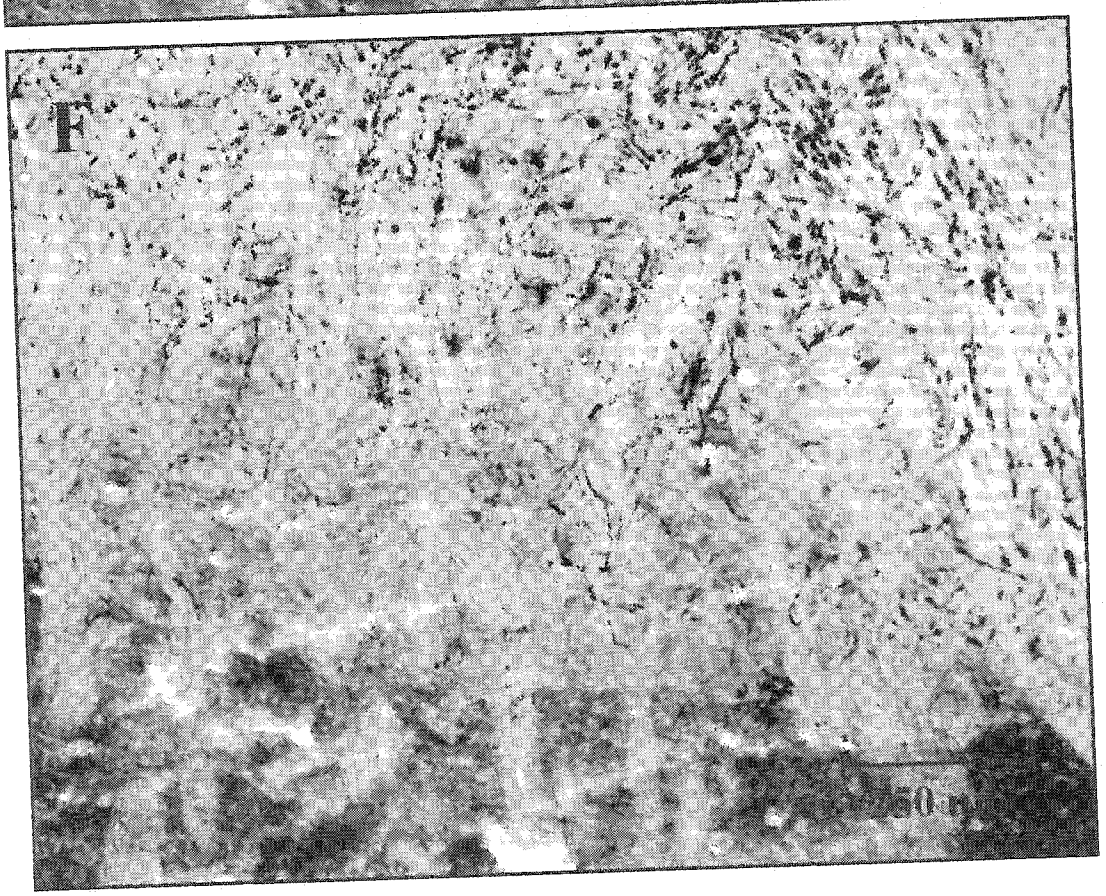
F

Figures 6:02A-E. Horizontal tissue sections (30 μm) through the striatum on day 2 depicting Nissl staining. The striata were perfused on day 1 with aCSF (A) or various millimolar concentrations of MPP^+ for 30 min: 0.7 (B), 1.3 (C), 2.5 (D) and 10.0 (E). Note the decrease in density of Nissl stained cell bodies proportional to the increasing concentrations of MPP^+ (perfused on day 1), especially at $\geq$ 2.5 mM MPP^+. The asterisk depicts the approximate center of the probe hole.

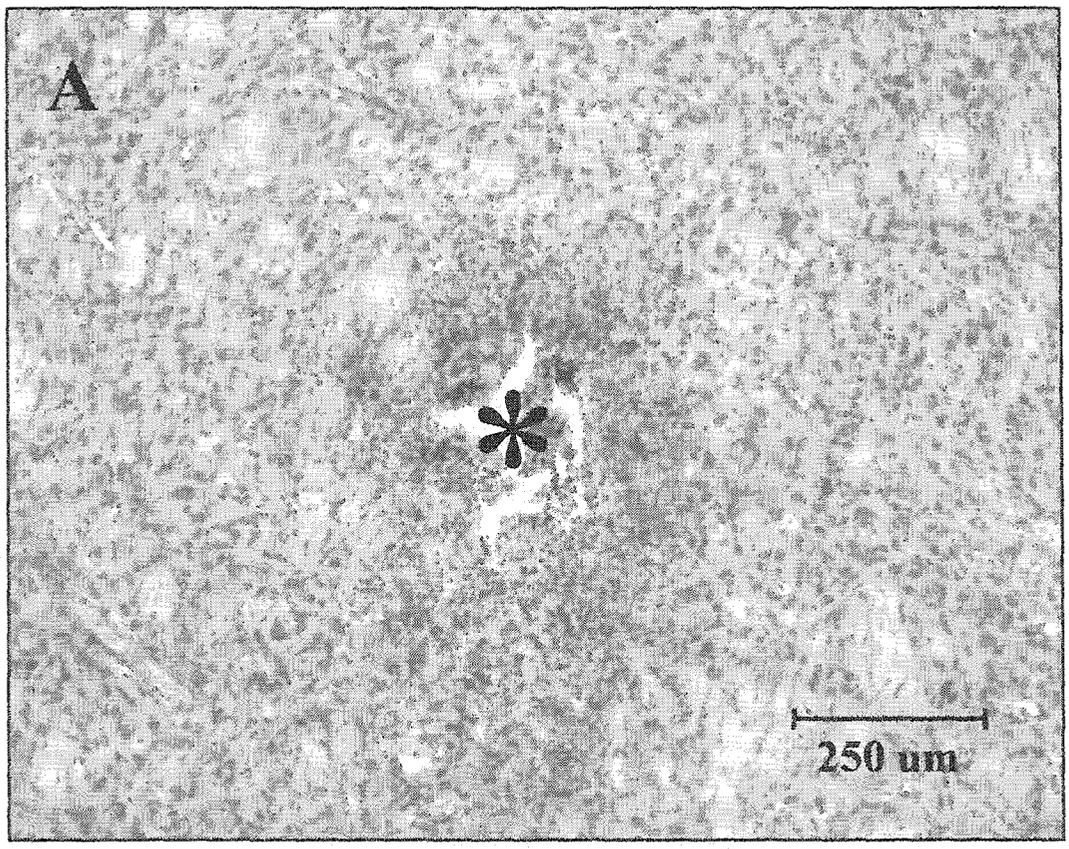
A
250 um

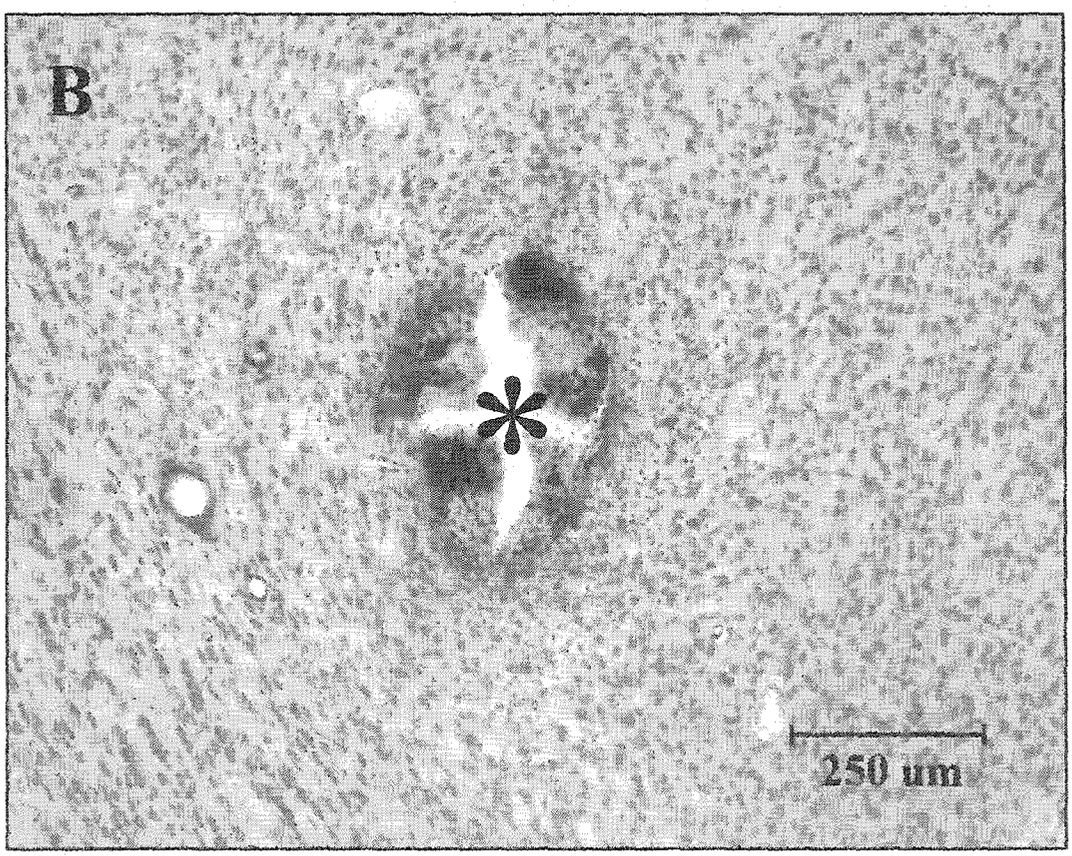
B
250 um

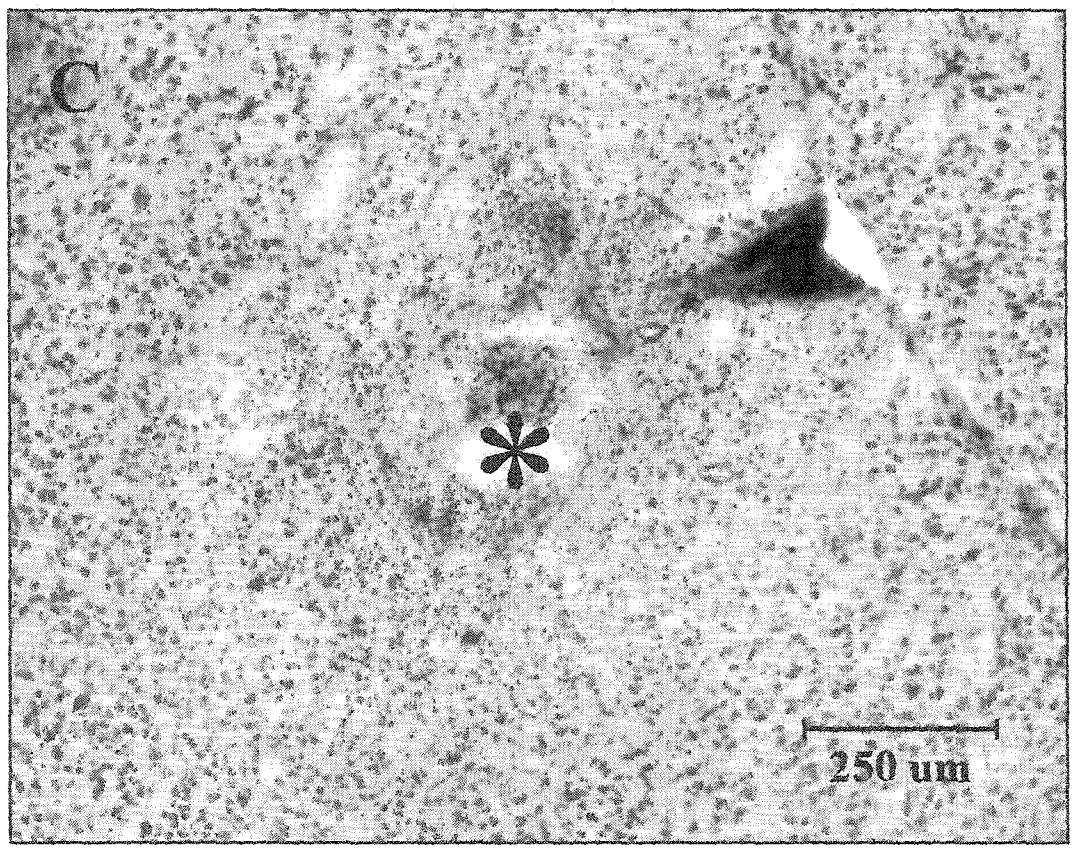
C
250 um

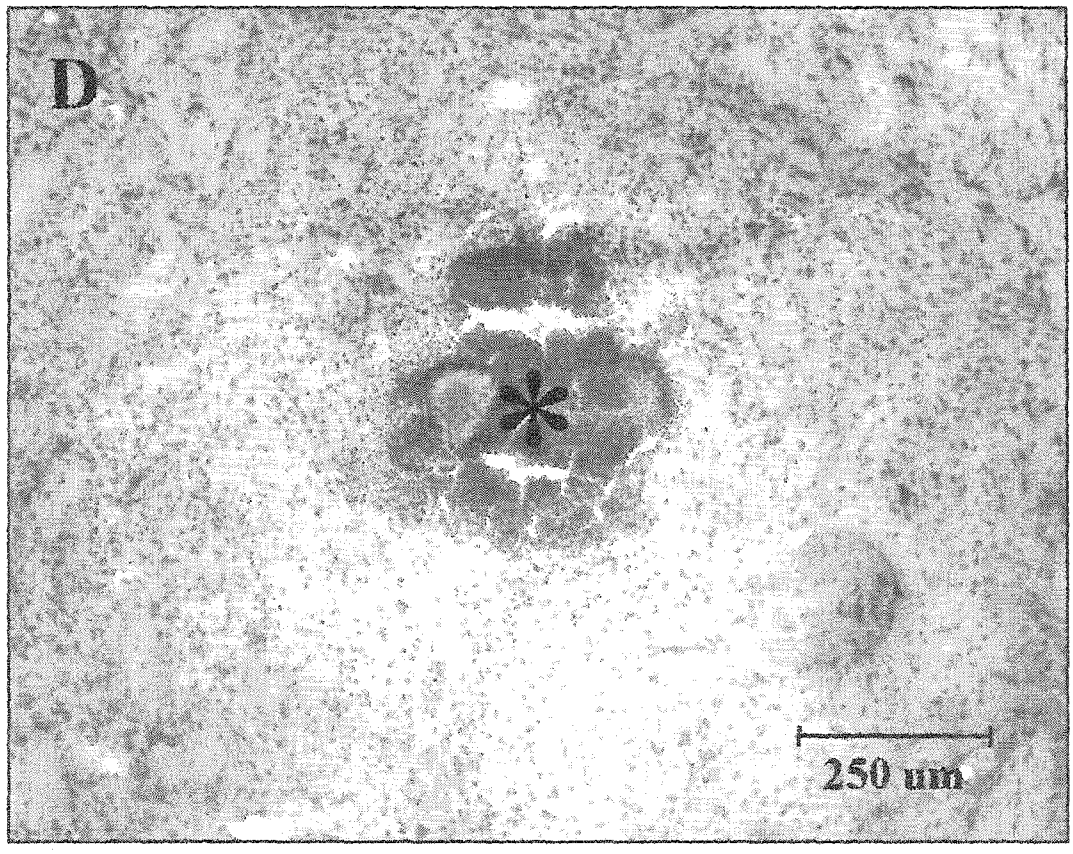
D
250 um

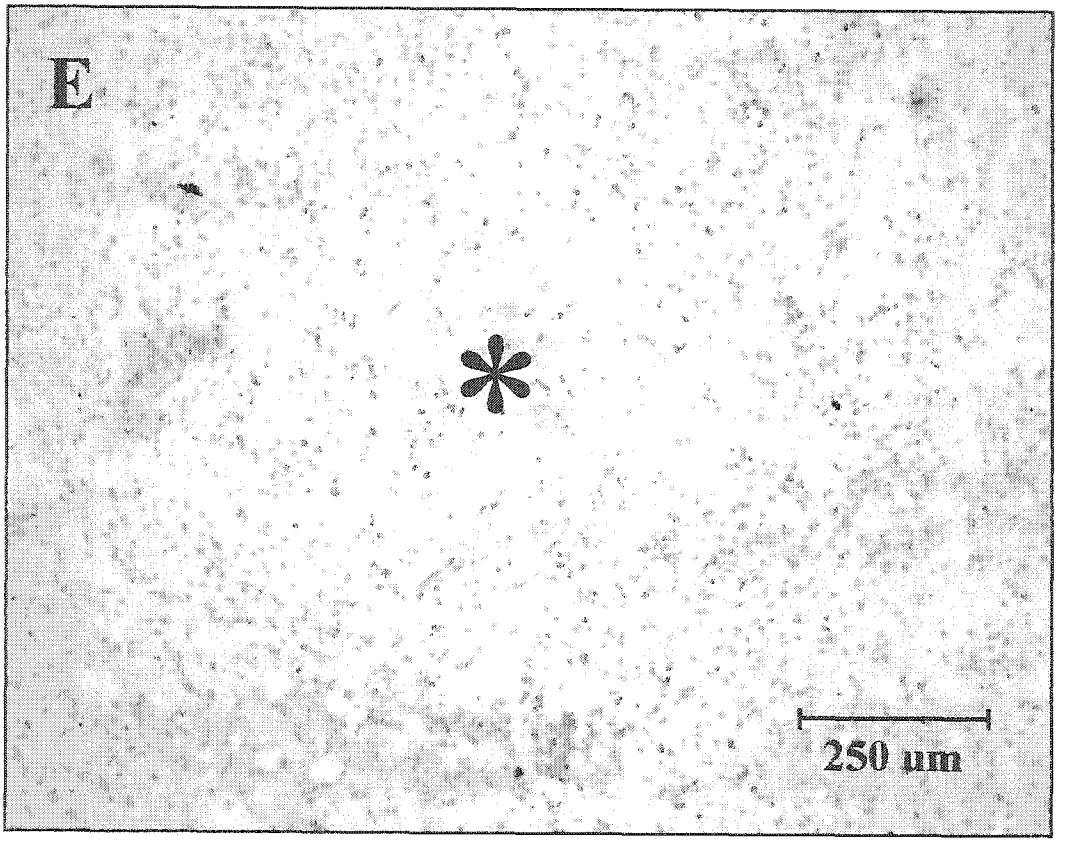
E
250 µm

Figures 6:03A-F. Horizontal tissue sections (30 μm) through the striatum on day 2 depicting GFAP immunoreactivity. The striata were perfused on day 1 with aCSF (A) or various millimolar concentrations of MPP^+ for 30 min: 0.7 (B), 1.3 (C), 2.5 (D) and 10.0 (E, F). The area inside the dashed line depicts an absence of GFAP-staining astrocytes which increases outwards from the probe proportional to the concentration of MPP^+ perfused on day 1. Note the complete lack of reactive astrocytes and the change in tissue contrast and texture in (E), which begins to appear in (D). This tissue is depicted in (F) at higher magnification revealing what may be the remnants of necrotic glia. The asterisk depicts the approximate center of the probe hole.

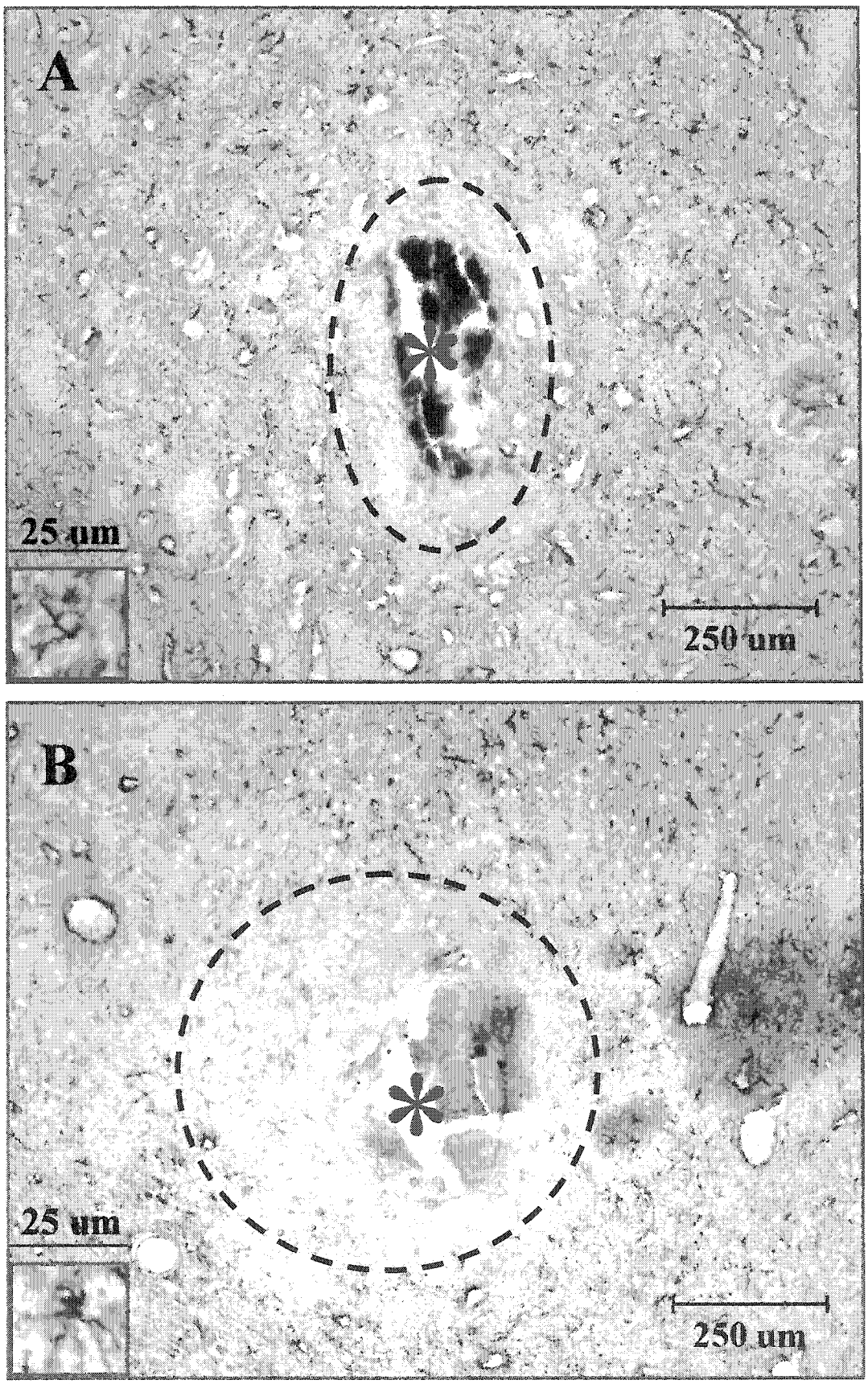
A
25 um
250 um
B
25 um
250 um

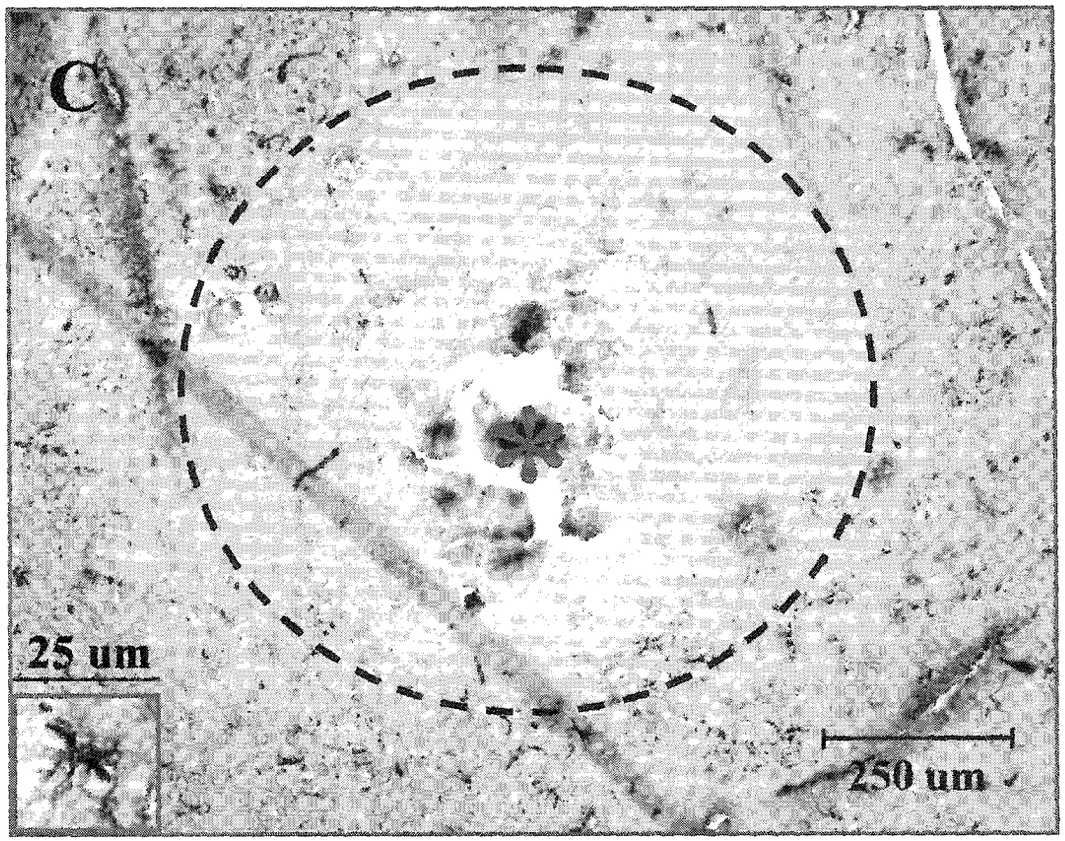
C
25 um
250 um

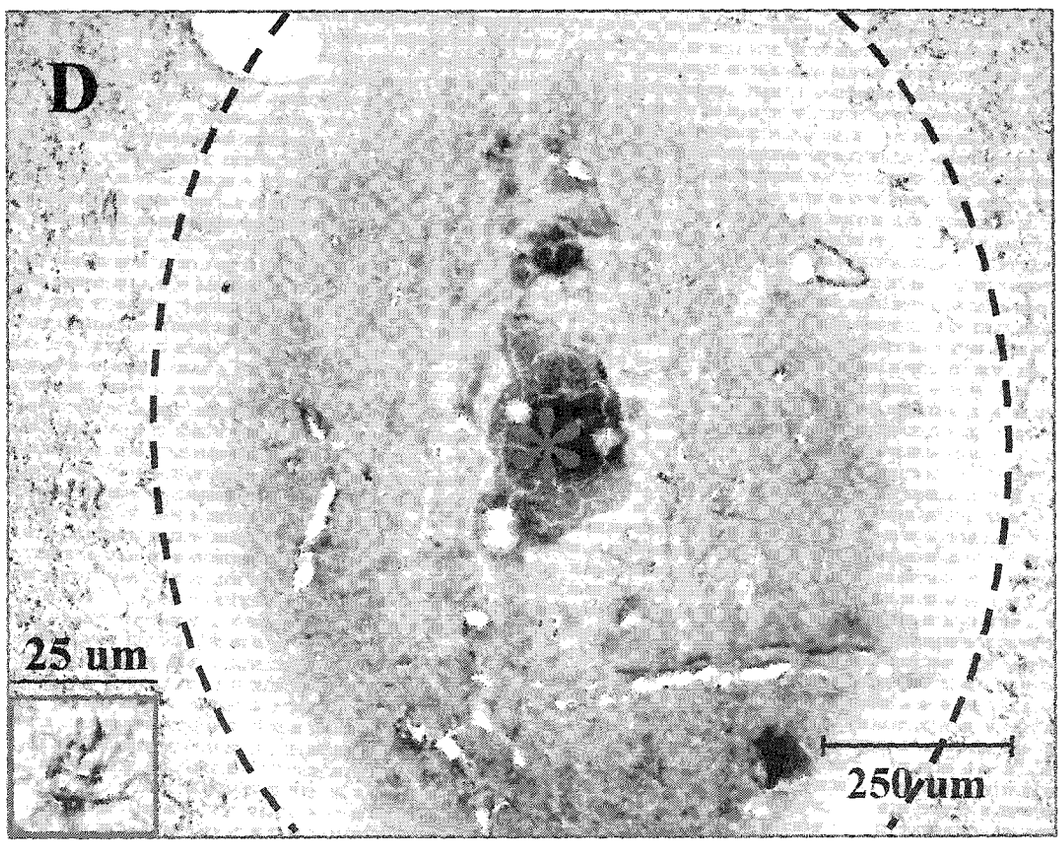
D
25 um
250 um

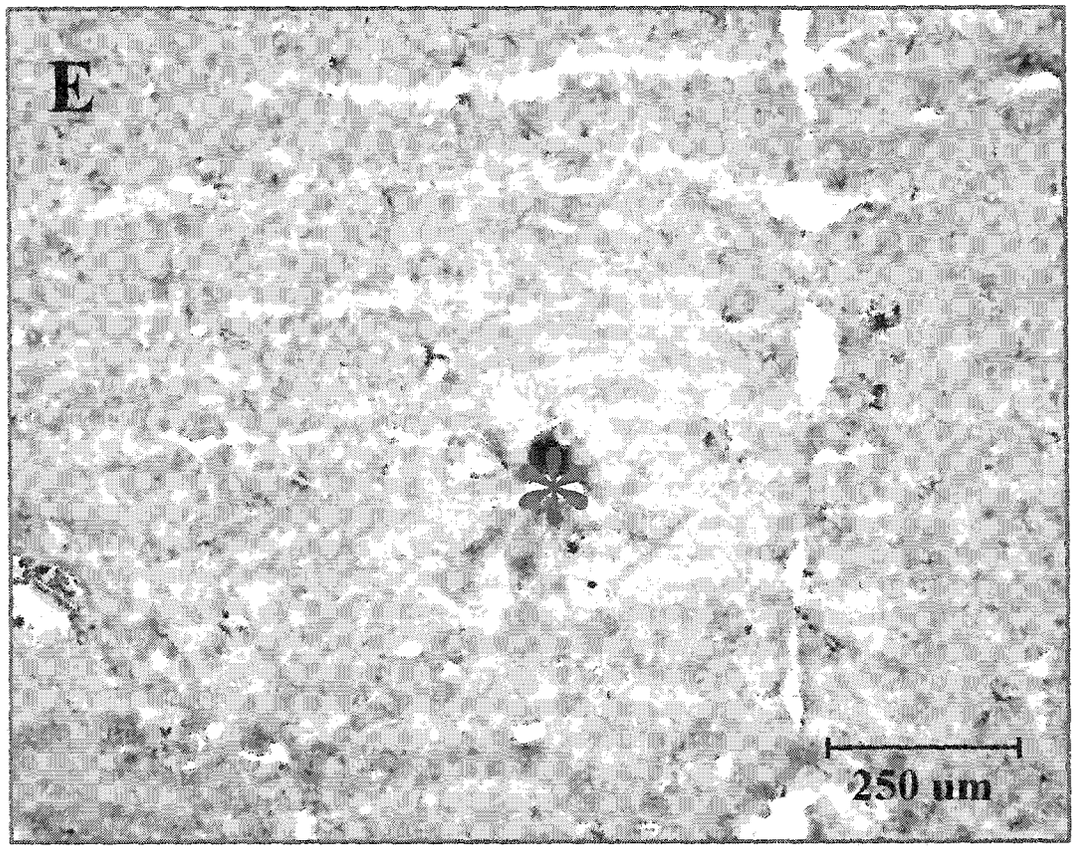
E
250 um

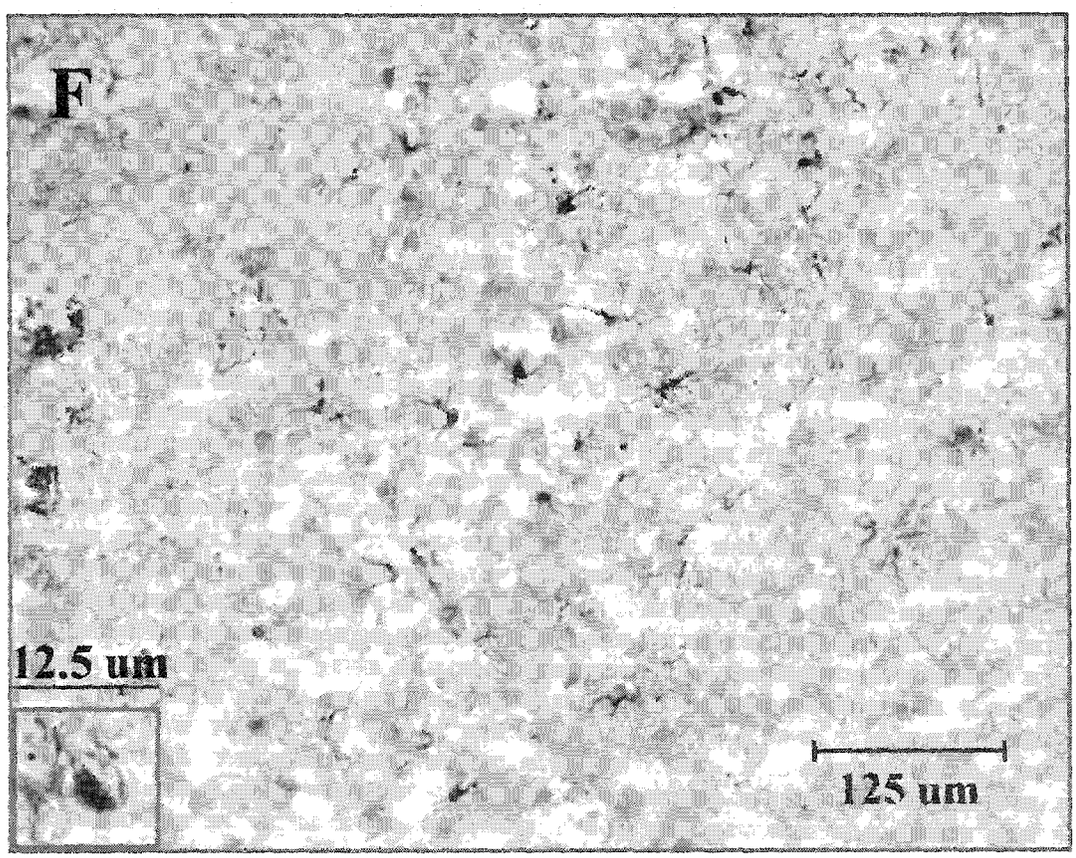
F
12.5 um
125 um

Figures 6:04A-L. Horizontal tissue sections (30 μm) through the striatum on day 2 depicting OX-42 (specific for microglia) immunoreactivity. The striata were perfused on day 1 with aCSF (A, B) or various millimolar concentrations of MPP^+ for 30 min: 0.7 (C, D), 1.3 (E, F), 2.5 (G, H) and 10.0 (I-L). There are basically three different stages of activation that are differentiated as: (1) "ramified" microglia are in the resting state and are characterized by a small cell body with several emanating processes; (2) "activated" microglia have a swollen cell body with thicker processes; (3) "reactive" microglia have become macrophages with a pseudopodic to globular-shape, without processes. In some of the photographs these will be pointed out with a (1) box, ramified; (2) solid circle, activated; (3) dashed circle, reactive. The asterisk depicts the approximate center of the probe hole.

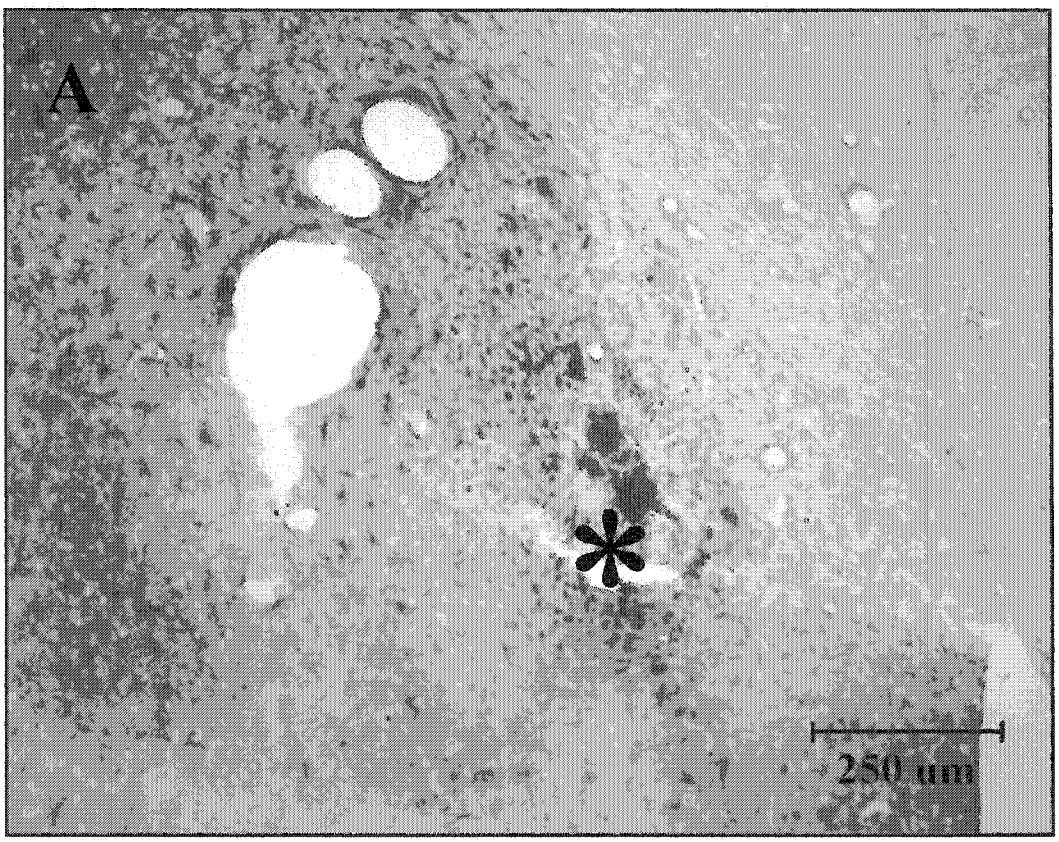
A
250 um

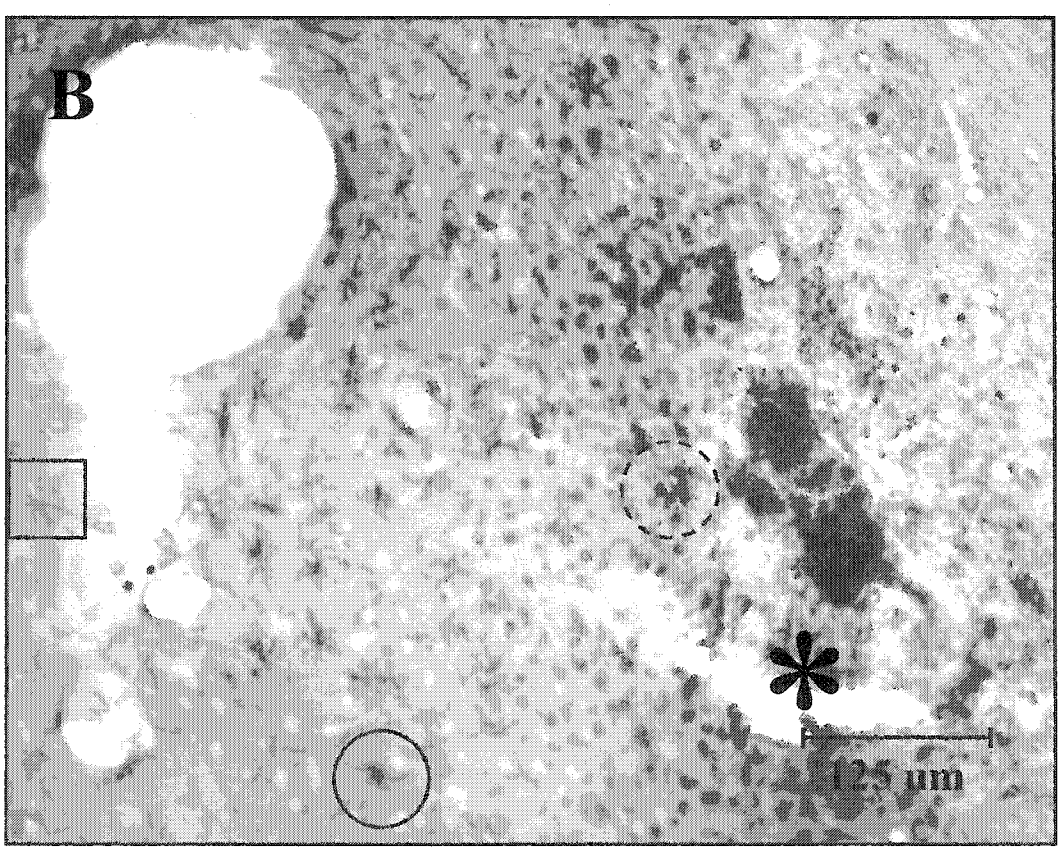
B
125 um

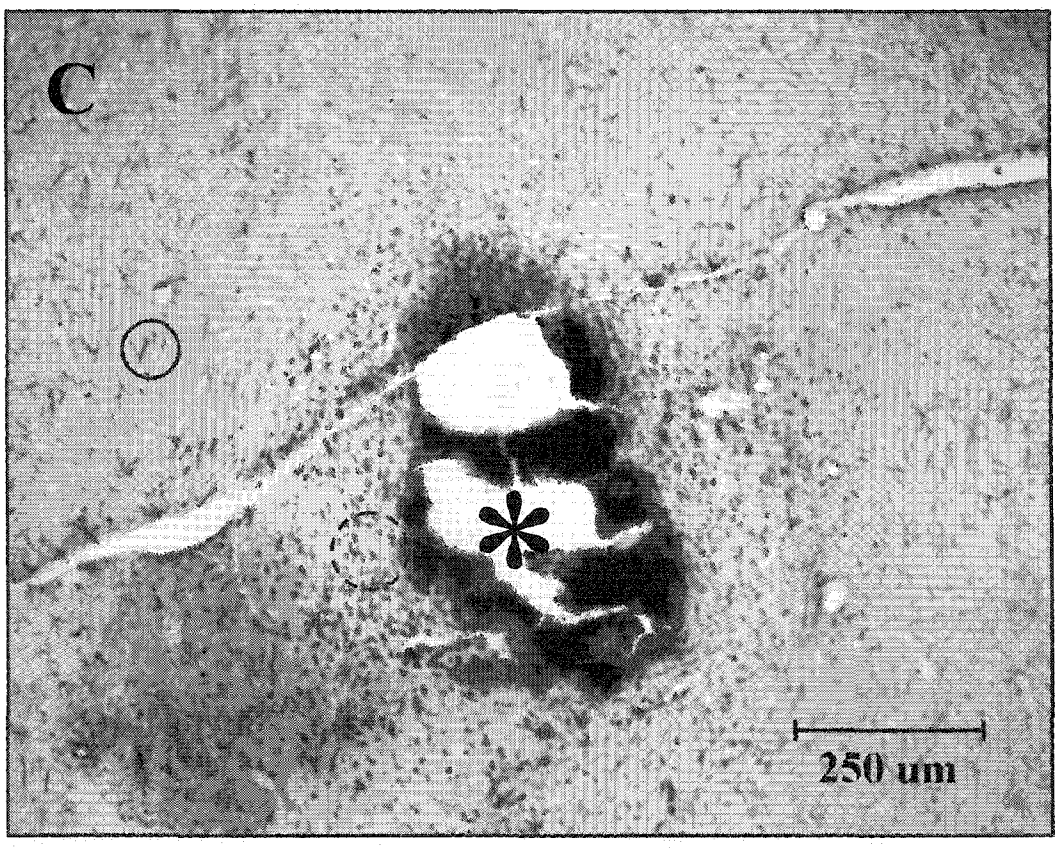
C
250 um

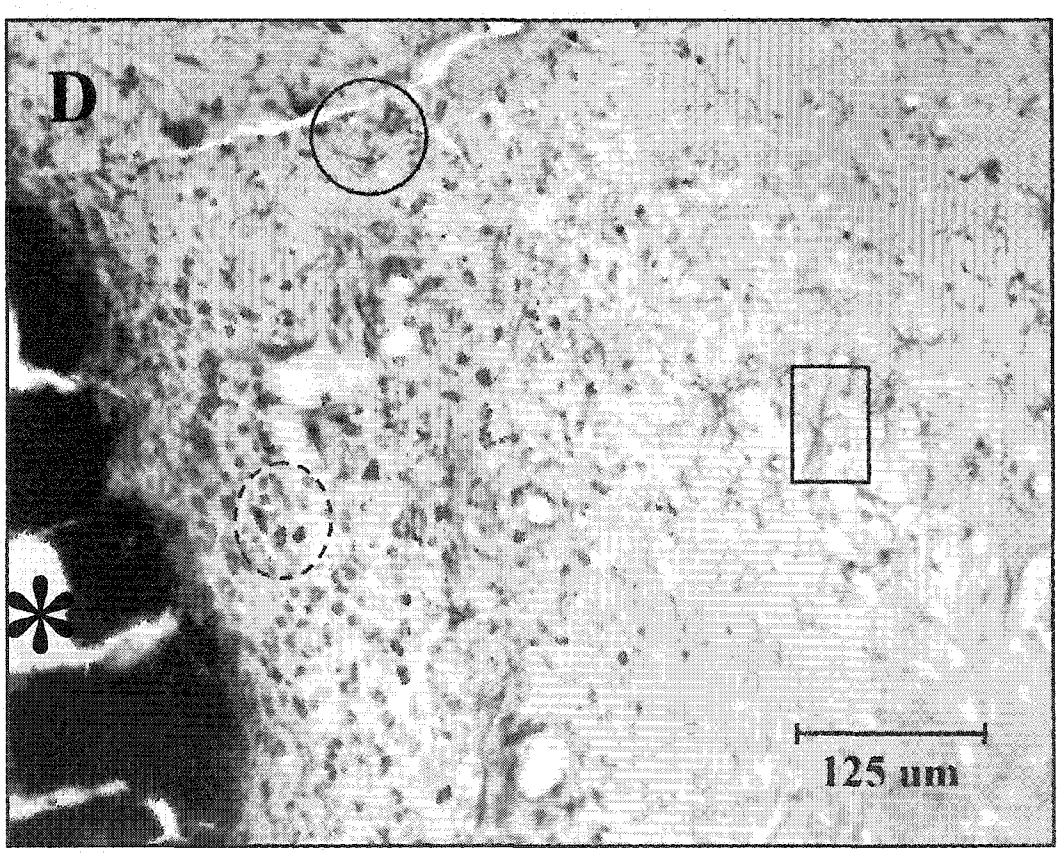
D
125 um

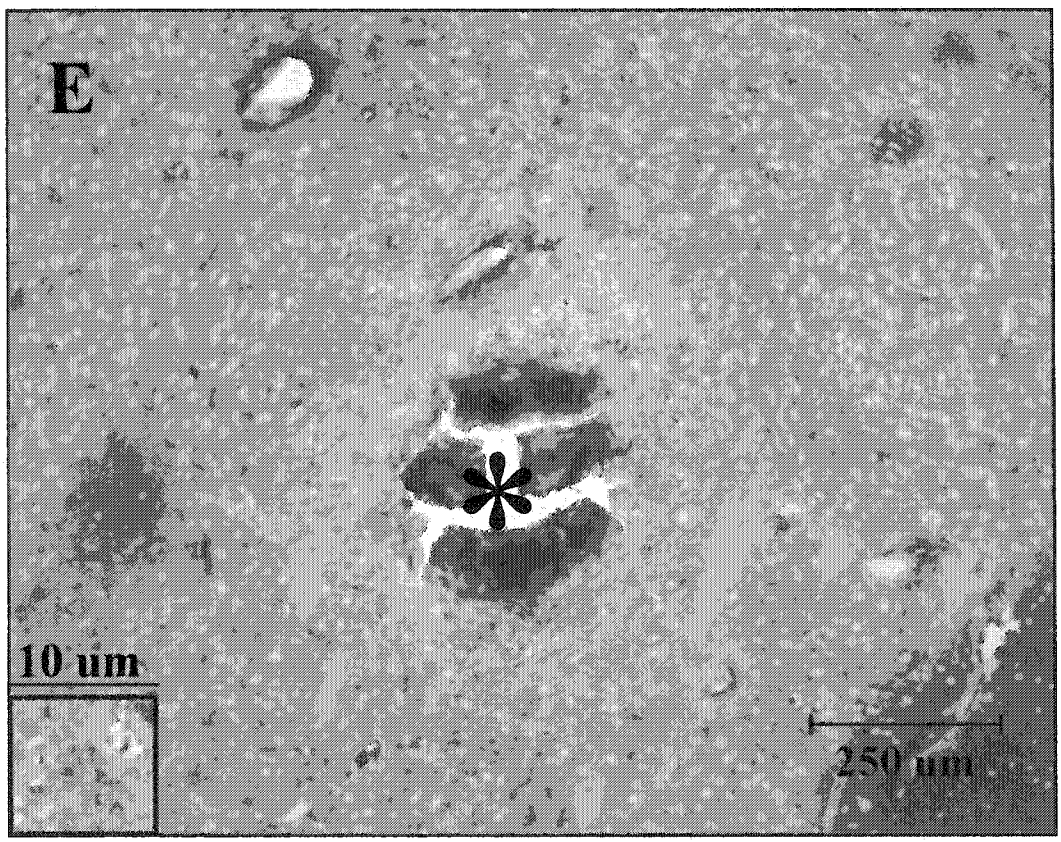
E
10 um
250 um

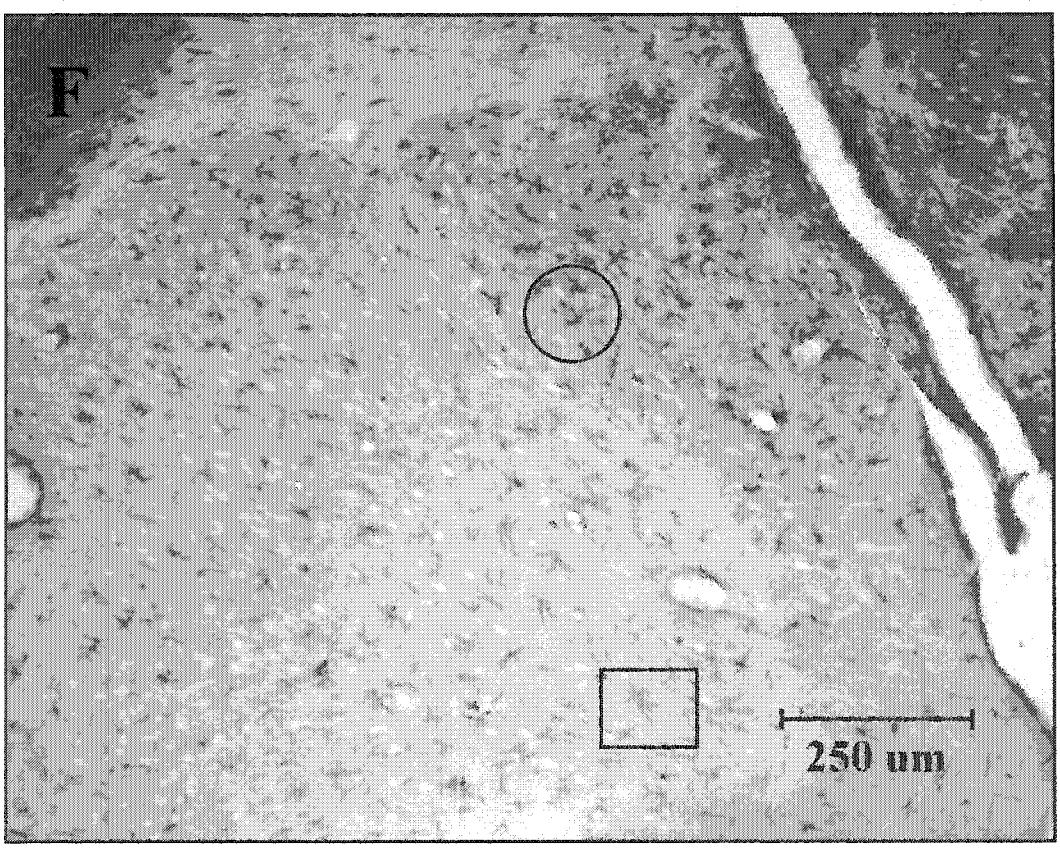
F
250 um

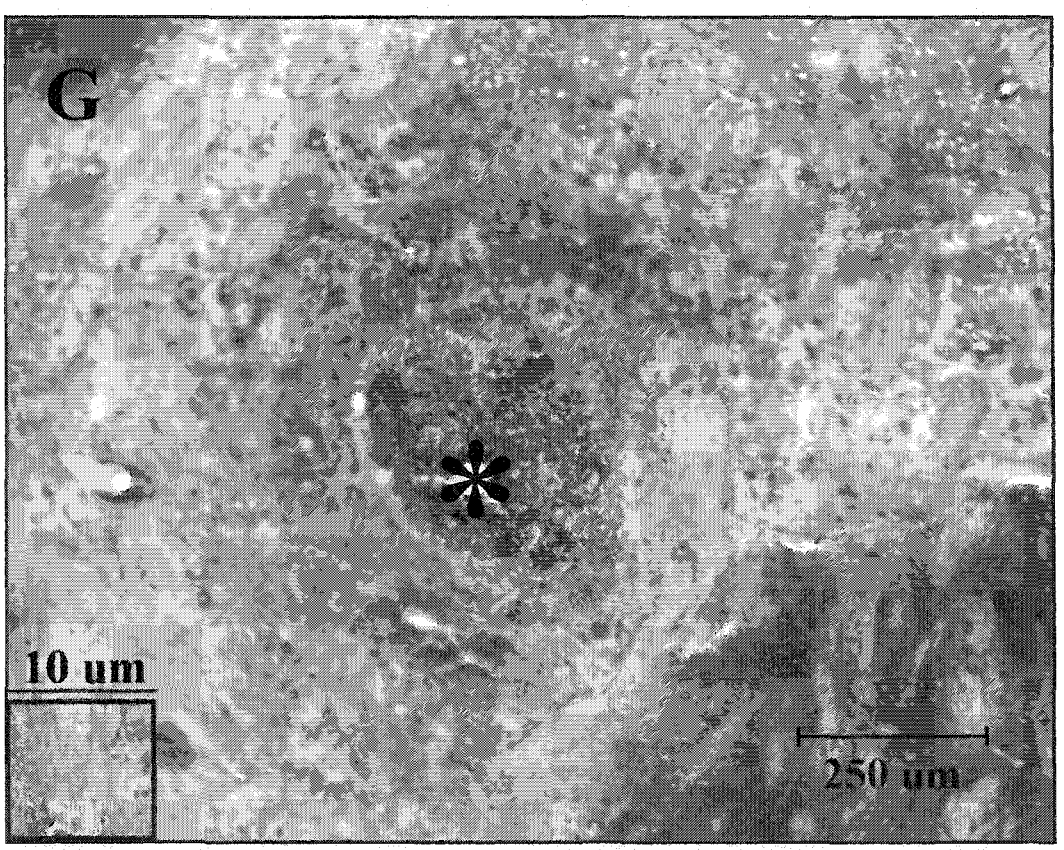
G
10 um
250 um

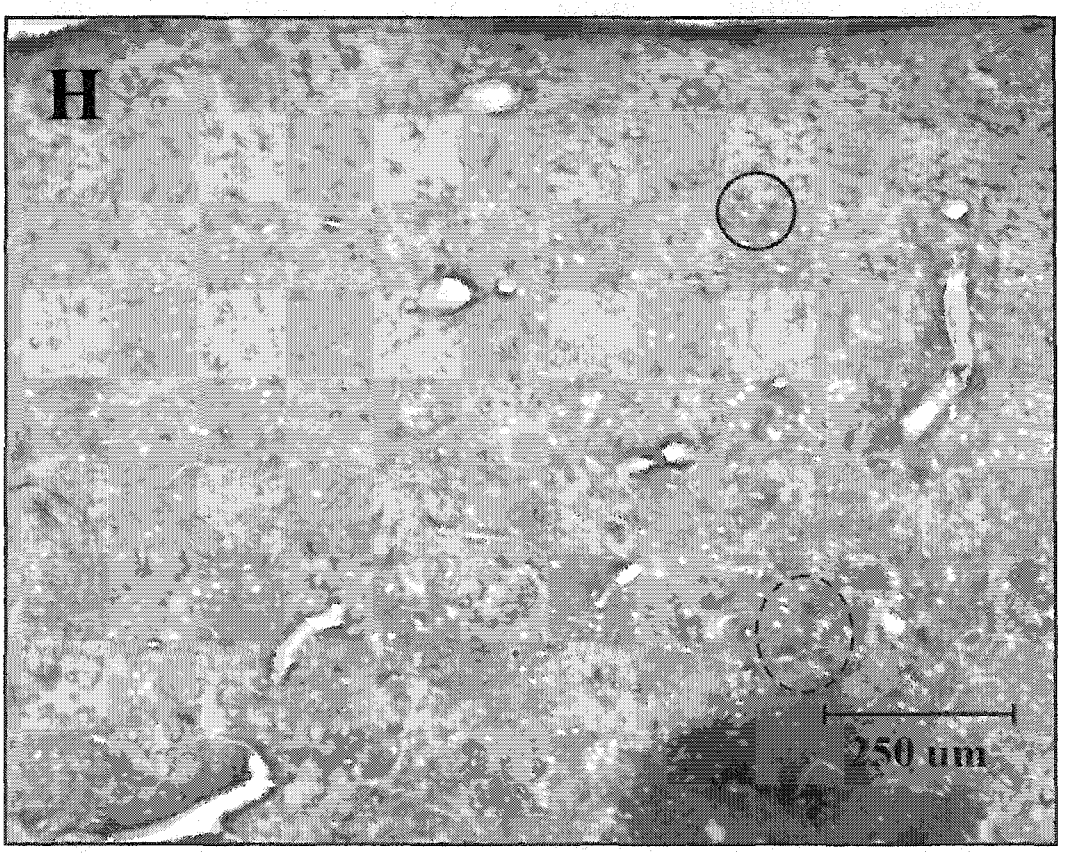
H
250 um

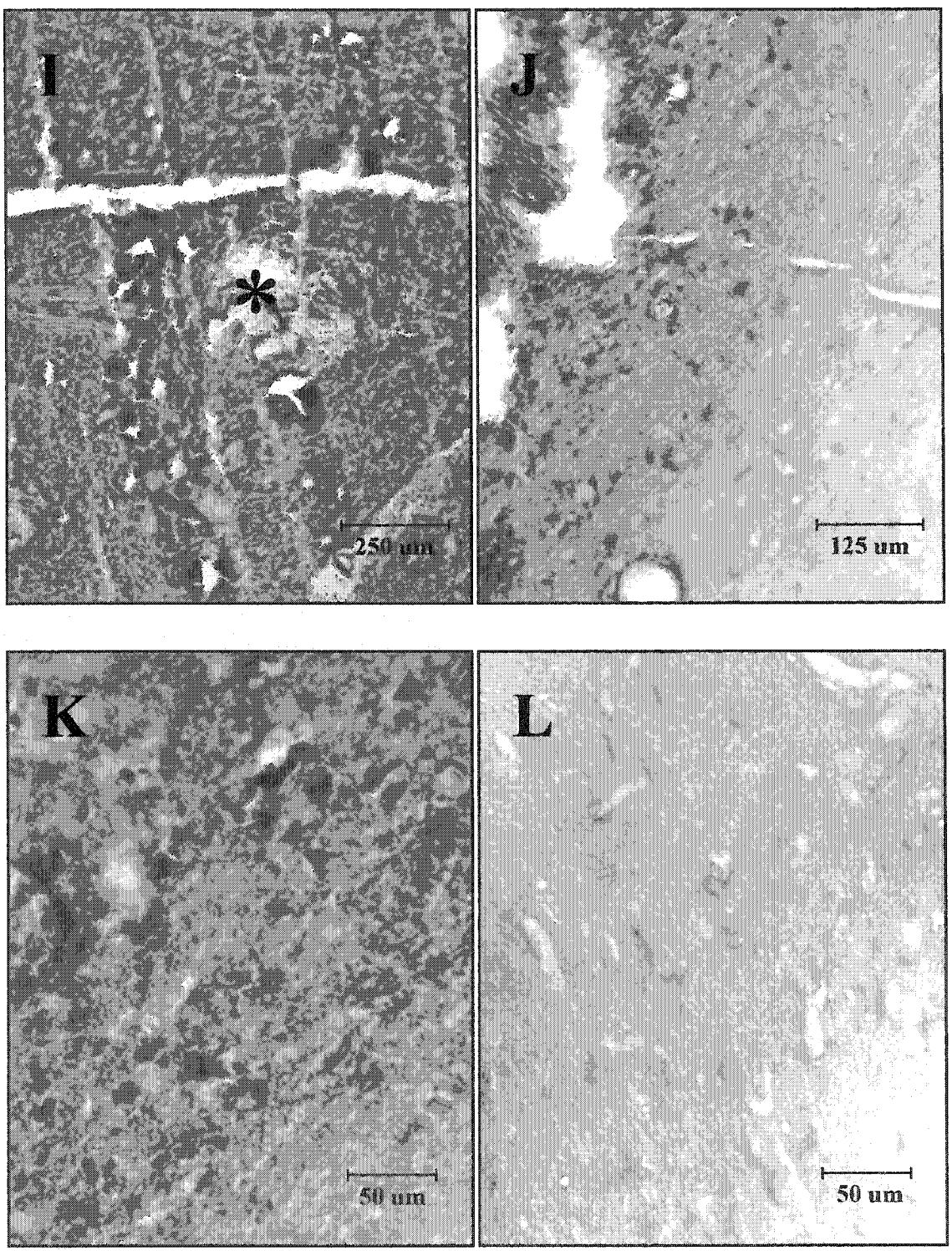
I
250 um
J
125 um
K
50 um
L
50 um

Chapter Seven

Conclusions and Future Directions

During a MPP^+-induced energy impairment DA is massively released from neurons[150-152] (Figures 2:13-20). Shortly after this DA release (once MPP^+ perfusions are discontinued) there is a massive release of GSH (Figure 1:05) into the extracellular space.[97-104,215] This dopaminergic energy impairment presumably allows basal extracellular Glu[202,203] to activate NMDA receptors[199,200] which results in an influx of Ca^{2+} mediating intraneuronal $O_2^{-\cdot}$ generation[203-205] and activation of nNOS[173,176,179,180] with consequent $NO\cdot$,[206] and finally $ONOO^-$ generation.[207-209]

During the early years of this project it was proposed that extracellular $HO\cdot$ and/or $ONOO^-$ would oxidize released GSH and DA to radicals and eventually form glutathionyl conjugates of DA (Figure 1:02). Additionally, it was proposed that released GSH (both from neurons and glia) would be degraded by γ-GT/ApN to Cys, Gly and Glu. Some Cys and DA would be oxidized to cysteinyl conjugates of DA. Some DA would be metabolized to DOPAC and thus glutathionyl and cysteinyl conjugates of DOPAC would be expected.

As the dopaminergic energy impairment subsides it was proposed that Cys would be transported into neurons, where it is the rate-limiting substrate for GSH synthesis.[83,84,95,96] During this period DA reuptake into neurons would scavenge intraneuronal $ONOO^-$ and hence block extracelluar generation of $HO\cdot$. During the period

of recovery but still reduced ATP production, elevated levels of Glu (from the γ-GT degradation of GSH) would continue NMDA receptor activation and hence intraneuronal $ONOO^-$ production. This $ONOO^-$ would oxidize DA to DAQ some of which would bind to active site cysteinyl residues of TH invoking irreversible inhibition of this enzyme.[219] However, most of the DAQ would react with translocated Cys forming cysteinyl conjugates of DA which are further oxidized to DHBT and BT metabolites. These metabolites were proposed to be responsible *in vivo* for the ensuing DA cell death. Indeed, *in vitro* experiments conducted in our laboratory showed that DHBTs and BTs are accumulated by brain mitochondria and evoke a time-dependent irreversible inhibition of mt complex I and α-KGDH.[224-226]

So according to this hypothesis, the role of γ-GT was perceived as crucial for the degradation of GSH to Glu, Cys and Gly. Elevated levels of Glu would continue activation of NMDA receptors and, hence, intraneuronal production of $HO^{\cdot}$ and/or $ONOO^-$ that would oxidize DA to DAQ. The latter reacting with transported Cys to form 5-*S*-Cys-DA and eventually DHBT/BTs. Microdialysis experiments were designed to examine the effects of γ-GT inhibition by ACV. Under these conditions several differences should have been observed. GSH would not be degraded to Cys, Gly and Glu. Microdialysis experiments would probably only detect glutathionyl conjugates of DA and DOPAC. Decreased levels of Glu and Gly would be seen in these experiments. Cys would not be available for translocation into dopaminergic neurons. Therefore, cysteinyl conjugates of DA would not be formed intraneuronally which would block formation of DHBTs and BTs. Most importantly, extracellular levels of Glu would be attenuated, NMDA receptors would not remain activated as neuronal ATP production

increased. Therefore, DA, as it re-enters neurons would not be oxidized to DAQ, which the latter is neurotoxic itself. DA neurons would survive and, hence, ACV inhibition of γ-GT would afford neuroprotection.

The results presented in Chapter Two did not support many of the proposed ideas. Glutathionyl and cysteinyl conjugates of DA and/or DOPAC were never detected before, during or after perfusion of MPP^+ in the presence or absence of ACV. Perfusion of 1.0 mM ACV before, during and after a 30 min perfusion of 0.7-10.0 mM MPP^+ was not neuroprotective. This was indicated by an attenuated release of DA in an identical microdialysis experiment with MPP^+ conducted 24 hours after day 1 MPP^+ perfusions (Figures 2:13-20) and a loss of TH-IR 24 h after day 1 MPP^+ perfusions. There was minimal (if any) difference in the maximum extracellular concentrations of L-DOPA, DA, 5-HT and their metabolites in microdialysis experiments where MPP^+ was perfused in the absence or presence of ACV (Figures 2:61-74). In fact, coperfusion of ACV may have resulted in more destruction of DA neurons, as seen by an attenuated maximal release on day 2 microdialysis experiments compare to similar experiments conducted in the absence of ACV.

In Chapter Five, results were presented from analysis of amino acids present in dialysate collected from the same microdialysis experiments employing MPP^+ as those presented in Chapter Two. Coperfusion of ACV with aCSF did not change the MPP^+-induced time-dependent release or maximum efflux of Glu (Figures 5:03, 04, 11-18) or any of the other amino acids (Figures 5:06-11, 20-43) when compared to identical microdialysis experiments conducted in the absence of ACV. This was particularly surprising since previous microdialysis experiments conducted in our laboratory had

shown that coperfusion of ACV blocked MPP^+-mediated Cys efflux and potentiated GSH efflux (Figure1:06).[215] The results from experiments presented in Chapter Five led to the conclusion that Glu and Gly do not originate from the γ-GT hydrolysis of GSH when millimolar concentrations of MPP^+ are perfused. It currently appears that MPP^+ probably induces release of Glu, Gly, Asp and Tau from astrocytes. Experiments are currently underway in our laboratory to examine the source of Glu. If Glu is released from astrocytes by MPP^+-induced reversal of the Glu transporter then pharmacologic inhibition of these transporters should result in an attenuated release of Glu. Inhibitors of DAT on DA neurons will also be used to determine if MPP^+-induced Glu release is originating from astrocytes. However, these experiments may not identify the source of Glu, since the latter may be released from astrocytes by other routes (as discussed in Chapter Five).[345,348-352] Interestingly, at lower MPP^+ concentrations that resulted in dopaminergic (0.7 and 1.3 mM; Figures 2:13-16) and apparent serotonergic (1.3 mM; Figures 2:31, 32) neurotoxicity, there was minimal if any detectable release of Glu (Figures 5:11-14). It was not until when MPP^+ concentrations ≥ 2.5 mM were perfused that a substantial release of Glu was observed (Figures 5:15-18). This indicates that elevated release of Glu is not required for dopaminergic and serotonergic neurotoxicity. However, during conditions of attenuated ATP production (induced by MPP^+) even basal levels of Glu can activate NMDA receptors,[201] and, thus, continued generation of intraneuronal $HO^{\cdot}$ and/or $ONOO^-$ which can oxidize DA to neurotoxic DAQ.[202] Also, it is reasonable to suspect, at MPP^+ concentrations ≥ 2.5 mM when there is a substantial release of Glu (Figures 5:03, 04, 15-18), additional damage is induced by excitotoxic mechanisms.

It seems improbable that in an HO·-enriched extracellular environment that DA, DOPAC, GSH, and Cys could escape oxidation. However, in the results presented in Chapter Three, it appears that there may be minimal extracellular levels of HO· and $ONOO^-$ which is supported by several observations. Constant perfusion of 2.5 mM SA before, during and after a 30 min perfusion of 10.0 mM MPP^+ did result in the formation of 2,3-DHBA, however, not until MPP^+ perfusions were discontinued (Figure 3:08). During the period when MPP^+ was being perfused in these experiments GSSG, cystine and sulfinic and sulfonic acids were not detected which would be expected if there was generation of extracellular HO· and/or $ONOO^-$.[245] In previous experiments conducted in our laboratory GSH release was similarly delayed[215] as was the formation of 2,3-DHBA. Therefore, it may be that once the antioxidant GSH is released from neurons, SA (if present intracellularly) is hydroxylated by $ONOO^-$ and/or HO·, resulting in formation of 2,3-DHBA. Coperfusion of MPP^+ and SA failed to attenuate the apparent dopaminergic (Figure 3:02) and serotonergic (Figure 3:04) neurotoxicity of MPP^+ (Table 3:01). Thus, it seems likely that intracellular concentrations of SA do not reach sufficiently high levels for it to act as a neuroprotective HO·/$ONOO^-$ scavenger.

Perhaps the most significant observation from all the experiments conducted in the present study was the MPP^+-induced dose-dependent release of L-DOPA (Figures 2:05-12, 61, 62). Many experiments were designed and conducted to confirm the identity of this compound and ascertain insight into why it was present in dialysates. In fact, during analysis of early microdialysis experiments, this compound was thought to be 2,5,6-tri-*S*-GSH-DA (Figure 2:04). Using HPLC-EC method I, the then putative 2,5,6-tri-*S*-GSH-DA had the same t_R and coeluted with standard 2,5,6-tri-*S*-GSH-DA (Table

2:02). However, employing HPLC-EC method II the putative 2,5,6-tri-*S*-GSH-DA did not have the same t_R as standard 2,5,6-tri-*S*-GSH-DA and did not coelute with added standard 2,5,6-tri-*S*-GSH-DA (Table 2:02). Another system was developed (HPLC-EC method III) which provided the same chromatographic results as HPLC-EC method II (Table 2:02). Instead the unknown compound was found to be L-(D-)DOPA based on matching t_R and coelution with standard L-DOPA employing HPLC-EC methods I-IV (Table 2:02).

A series of experiments were designed to provide insight into the mode of formation of the neurotransmitter-like release of putative L-(D-)DOPA. Two antioxidants, mannitol and SA were coperfused before, during and after perfusion of 10.0 mM MPP^+. In the event that Tyr was being hydroxylated by $HO\cdot$ and/or $ONOO^-$, these antioxidants should attenuate the formation of putative DOPA. Mannitol is believed to be an extracellular antioxidant,[248] and the site of SA's antioxidation could be both extracellularly and intracellularly, although this is not clearly established. There was no difference in the putative L-DOPA time-dependent behavior (Figures 3:01, 09) or the maximum efflux (Table 3:01) when MPP^+ was perfused in the absence or presence of SA or mannitol. These observations suggest that $HO\cdot$ and/or $ONOO^-$ (if generated intracellularly or extracellularly) do not hydroxylate Tyr to form L-DOPA.

A generous gift from Professor Carla Borri-Voltatorrini of purified DDC enabled the design of a series of *in vitro* and *in vivo* experiments to observe the activity of DDC. HPLC-EC method IV was developed to conduct *in vitro* experiments with DDC. This was the fourth system which chromatographically confirmed the identity of L-(D-)DOPA based on matching t_R and coelution with added standard L-DOPA (Table 2:02).

Observations from *in vitro* experiments found no inhibition of DDC from the addition of 15.0 mM MPP^+ to an incubation mixture where L-DOPA was quantitatively decarboxylated to DA. Dialysate collected at the time of maximum putative L-DOPA release from experiments where rats received 10.0 mM MPP^+ was analyzed in assays with DDC. The results from the latter experiments showed that DDC converted the putative L-DOPA to DA. Thus, since DDC decarboxylates L-DOPA not D-DOPA, these experiments confirmed the identity of L-DOPA (Figure 3:17). HPLC-EC method V was developed to be employed in the analysis of rat brain striatal tissue for the *in vivo* activity of DDC. Analysis of tissue in the area around the probe obtained when L-DOPA was at maximum concentration, revealed a MPP^+-induced inhibition of DDC (Figure 3:16). More importantly, these experiments provided a rational explanation for the formation/release of L-DOPA. The possible reasons for the inhibition of DDC remain to be determined. Some of the possibilities are described at the end of Chapter Three. Future experiments are being designed to examine modifications of residues contained in DDC which could result in decreased activity of this enzyme.

The discovery that MPP^+ induces a dose dependent release of L-DOPA and the rapid inhibition of DDC was certainly an exciting observation. However, why these effects have escaped observations in other laboratories seemed surprising. Several factors may have contributed to the ability to detect L-DOPA in our experiments, when others had not. HPLC-EC method I employed a very unconventional mobile phase that resulted in an EC response for the biogenic amines observed that is approximately 2.5 times greater than traditional mobile phases that are composed of SOS, citric acid, EDTA, DEA, MeOH and MeCN. Additionally, the short t_R usually observed with L-

DOPA, often causes it to coelute with the solvent front. Another important difference in the design of the microdialysis experiments presented in this work, was the 5 min collection intervals. Most microdialysis experiments described in the literature[152,227,239-241] and previously conducted in our laboratory[215] collected dialysate fractions at much longer time intervals. The shorter time intervals allow rapid changes in neurochemicals to be observed more easily.

Since these MPP^+ microdialysis experiments induce dopaminergic neurotoxicity and are considered animal models of PD, the possibility that L-DOPA release might occur with another dopaminergic neurotoxin and animal model of PD was explored by conducting similar experiments with MA.[5] In experiments employing MA (i.p.) injections, there was a similar release of L-DOPA and DA (Figures 4:04, 05, respectively) as seen in microdialysis experiments where MPP^+ was perfused. This was significant because it shows that the neurotransmitter-like release of L-DOPA was not limited to MPP^+, and indeed might be an early event which occurs in PD. Additionally, the maximum extracellular concentration of DA induced by MA was attenuated compared to experiments with low concentrations (0.7 mM) of MPP^+, supporting previous suggestions that MA inhibits the DAT.[322] An additional animal model of neurodegeneration, MDMA, which is known to result in serotonergic degeneration and minimal dopaminergic degeneration (in rats) was then employed.[291] Administration of MDMA also resulted in the release of L-DOPA and DA (Figures 4:12, 13, respectively). The delayed MDMA-induced release of DA (compared to the MPP^+ and MA-induced release of DA) supports previous suggestions that MDMA is a substrate for SERT but not for the DAT (both MPP^+ and MA are substrates for DAT) and must passively diffuse into

DA neurons. Experiments have not been conducted to determine if MA and MDMA induce similar inhibition of DDC (as that mediated by MPP^+). Certainly in the near future, experiments should be conducted to examine such a possibility. Additionally, experiments need to examine the time-dependent inhibition of DDC when perfusing MPP^+.

The significance of the inhibition of DDC with consequent neurotransmitter-like release of L-DOPA remains to be determined. *In vitro* studies have demonstrated possible L-DOPA neurotoxicity,[274,283,398-400] especially its ability to induce oxidative stress.[401-403] However, *in vivo* evidence is still lacking. On the other hand, some reports propose a neuroprotective role for L-DOPA by its ability *in vitro* to upregulate GSH[404,405] and exert neurotrophic effects.[19,406] Amazingly, despite almost forty years of being used to treat PD, L-DOPA just recently (1998) entered clinical drug trials. However, the preliminary results of these studies appear conflicting.[289] Nevertheless, L-DOPA/ carbidopa remains the most often prescribed and is considered the best treatment currently available to PD patients, despite the numerous side effects, eventual wearing-off problems and the possibility that it may potentiate DA neuronal damage.[19,262,290]

In microdialysis experiments with perfusions of millimolar concentrations of MPP^+, dialysate was analyzed by HPLC-PDA to search for possible hydroxylation and nitration products of Tyr and Phe and glutathionyl and cysteinyl conjugates of DA and DOPAC. The possibility that MPP^+ might mediate the formation of 3-nitro-Tyr, 4-nitro-Phe, *o*- and *m*-Tyr was suggested by previous studies that reported markers of RNS/ ROS,[319] protein-bound 3-nitro-Tyr in animal models of MPTP/MPP^+[257] and elevated levels of 3-nitro-Tyr in the autopsied brains of PD patients.[35] None of the suspected

markers of ROS/RNS (i.e., 3-nitro-Tyr, 4-nitro-Phe, *o*- and *m*-Tyr), glutathionyl and cysteinyl conjugates of DA and/or DOPAC, or any unknown compounds were ever detected in our experiments employing the PDA. However, the full potential of this instrument remains to be utilized. Indeed, future experiments are being designed to employ this PDA detector in search of possible metabolites of MDMA, which may be formed during administration of the parent compound.

The results from the immunohistochemical studies showed: (1) a decrease in TH-IR, (2) a lack of GFAP-IR with increasing distance from the probe track, (3) an increase in reactive microglia, and (4) a decrease in Nissl staining that were all four in proportion to the MPP^+-induced attenuated release of DA observed in microdialysis experiments conducted 24 hours after an identical concentration of MPP^+ had been perfused. Therefore, these immunohistochemical experiments show that increasing concentrations of MPP^+ perfused on day 1 mediate increasing levels of: (1) DA terminal damage, (2) astrocytic destruction, (3) reactive microglia, and (4) non-specific cellular death.

Animal models provide us with valuable insight into many neurodegenerative processes. Without them, no or minimal progress would be made in the search to understand PD and other neurodegenerative diseases. This project presented numerous challenges which were at times difficult, but were always intellectually challenging. The inherent nature of this kind of interdisciplinary research requires a continuous quest to venture into areas that are not familiar. However, without an attempt to understand what researchers are doing in other fields and how this relates to ones own individual efforts, limits the conclusions that each individual field can contribute to a further understanding of the entire neurodegenerative process. It is certainly disappointing to observe the

competition for funding often competes with researchers' ability to share results and ideas. It may sound a bit idealistic, but if all the various disciplines could find a way to work together, answers would come sooner and the people we are trying to help would certainly benefit. After all, is not the reason why one investigates neurodegenerative processes, to possibly make a difference in someone's life. This is quite certainly what motivates me. It is my hope that the research presented here and that which I may conduct in the future will provide valuable insight into any aspect of neurodegeneration, especially Parkinson's disease.

Literature Cited

1. Fahn S. and Przedborski S. (2000) Parkinsonism., in *Merritt's Neurology.* (Rowland L. P., ed.), pp. 679-693. Wilkins, New York.

2. Parkinson J. (1817) *An Essay on the Shaking Palsy*, Sherwood, Neely, and Jones., London.

3. Hornykiewicz O. and Kish S. J. (1986) Biochemical pathophysiology of Parkinson's disease. *Adv. Neurol.* **45,** 19-34.

4. Kish S. J., Shannak K., and Hornykiewicz O. (1988) Uneven pattern of dopamine loss in the striatum of patients with idiopathic Parkinson's disease: pathophysiologic and clinical implications. *N. Eng. J. Med.* **318,** 876-880.

5. Gerlach M. and Riederer P. (1996) Animal models of Parkinson's disease: an empirical comparison with the phenomenology of the disease in man. *J. Neural Transm.* **103,** 987-1041.

6. Bernheimer H., Birkmayer W., Hornykiewicz O., Jellinger K., and Seitelberger F. (1973) Brain dopamine and the syndromes of Parkinson and Huntington. Clinical, morphological and neurochemical correlations. *J. Neurol. Sci.* **20,** 415-455.

7. Spillantini M. G., Schmidt M. L., Lee V. M., Trojanowski J. Q., Jakes R., and Guedert M. (1997) α-Synuclein in Lewy bodies. *Nature* **388,** 839-840.

8. Mezey E., Dehejia A., Harta G., Papp M. I., Polmeropoulos M. H., and Brownstein M. J. (1998) α-Synuclein in neurodegenerative disorders: murderer or accomplice? *Nature Med.* **4,** 755-757.

9. Nishiyama K., Murayama S., Shimizu J., Ohya Y., Kwak Y., Asayama K., and Kanazawa I. (1995) Cu/Zn superoxide dismutase-like immunoreactivity is present in Lewy bodies from Parkinson's disease: a light and electron microscopic immunocytochemical study. *Acta Neuropath. (Berlin)* **89,** 471-474.

10. D'Amato R. J., Zweig R. M., Whitehouse P. J., Wenk G. L., Singer H. S., Mayeux R., and Price D. L. S. S. H. (1987) Aminergic systems in Alzheimer's disease and Parkinson's disease. *Ann. Neurol.* **22,** 229-236.

11. Jellinger K. (1990) New developments in the pathology of Parkinson's disease. *Adv. Neurol.* **53,** 1-16.

12. Gerlach M., Jellinger K., and Riederer P. (1994) The possible role of noradrenergic deficits in selected signs of Parkinson's disease., in *Noradrenergic Mechanisms in Parkinson's Disease.* (Briley M. and Marien M., eds.), CRC Press, Boca Raton.

13. Whitehouse P. J., Hedreen J. C., White C. L., and Price D. L. (1983) Basal forebrain in the dementia of Parkinson's disease. *Ann. Neurol.* **13,** 243-248.

14. Jellinger K. (1988) Pathology of Parkinson's syndrome., in *Handbook of Experimental Pharmacology* (Calne D. B., ed.), pp. 47-112. Springer-Verlag, Berlin.

15. Chui H. C., Mortimer J. A., Slager U., Zarow C., Bondareff W., and Webster D. D. (1986) Pathologic correlates of dementia in Parkinson's disease. *Arch. Neurol.* **43,** 991-995.

16. Gaspar P., Duyckaerts C., Alvarez C., Javoy-Agid F., and Berger B. (1991) Alterations of dopaminergic and noradrenergic innervations in motor cortex in Parkinson's disease. *Ann. Neurol.* **30,** 365-374.

17. Stocchi F., Bonamartini A., Vacca L., and Rugieri S. (1996) Motor fluctuations in levodopa treatment: clinical pharmacology. *Eur. Neurol.* **36,** 38-42.

18. Chase T. N., Engber T. M., and Mouradian M. M. (1996) Contribution of dopaminergic and glutamatergic mechanisms to the pathogenesis of motor response complications in Parkinson's disease. *Adv. Neurol.* **69,** 497-501.

19. Jenner P. G. and Brin M. F. (1998) Levodopa neurotoxicity: Experimental studies versus clinical relevance. *Neurology* **50,** S39-S43.

20. Jenner P. and Olanow C. W. (1996) Pathological evidence for oxidative stress in Parkinson's disease and related disorders., in *Neurodegeneration and Neuroprotection in Parkinson's Disease.* (Olanow C. W., Jenner P., and Youdim M., eds.), Academic Press, New York.

21. Hornykiewicz O. (1974) The mechanisms of action of L-dopa in Parkinson's disease. *Life Sci.* **15,** 1249-1259.

22. Elbaz A., Bower J. H., Peterson B. J., Maraganore D. M., McDonnell S. K., Ahlskog J. E., Schaid D. J., and Rocca W. A. (2003) Survival study of Parkinson's disease in Olmsted county, Minnesota. *Arch. Neurol.* **60,** 91-96.

23. Fahn S. (2003) Description of Parkinson's disease as a clinical syndrome. *Ann. N.Y. Acad. Sci.* **991,** 1-14.

24. Mizuno Y., Matuda S., Yoshino H., Mori H., Hattori N., and Ikebe S. J. (1994) An immunohistochemical study on α-ketoglutarate dehydrogenase complex in Parkinson's disease. *Ann. Neurol.* **35,** 204-210.

25. Shapira A. H. V., Cooper J., Dexter D., Clark J. B., Jenner P., and Marsden C. D. (1990) Mitochondrial complex I deficiency in Parkinson's disease. *J. Neurochem.* **54,** 823-827.

26. Dexter D. T., Carter C. J., Wells F. R., Javoy-Agid F., Lees A. J., Jenner P., and Marsden C. D. (1989) Basal lipid peroxidation in substantia nigra is increased in Parkinson's disease. *J. Neurochem.* **52,** 381-389.

27. Alam Z. I., Daniel S. E., Lees A. J., Marsden C. D., Jenner P., and Halliwell B. (1997) A generalized increase in protein carbonyls in the brain in Parkinson's but not incidental Lewy body disease. *J. Neurochem.* **69,** 1326-1329.

28. Zhang J., Perry G., Smith M. A., Robertson D., Olson S. J., Graham D. G., and Montine T. J. (1999) Parkinson's disease is associated with oxidative damage to cytoplasmic DNA and RNA in substantia nigra neurons. *Am. J. Pathol.* **154,** 1423-1429.

29. Ceballos I., Lafon M., Javoy-Agid F., Hirsch E., Nicole A., Sinet P. M., and Agid Y. (1990) Superoxide dismutase and Parkinson's disease. *Lancet* **335,** 1035-1036.

30. Riederer P., Sofic E., Rausch W. D., Schmidt B., Reynolds G. P., Jellinger K., and Youdim M. B. (1989) Transition metals, ferritin, glutathione, and ascorbic acid in parkinsonian brains. *J. Neurochem.* **52,** 515-520.

31. Sofic E., Lange K. W., Jellinger K., and Riederer P. (1992) Reduced and oxidized glutathione in the substantia nigra of patients with Parkinson's disease. *Neurosci. Lett.* **142,** 128-130.

32. Sian J., Dexter D., Lees A., Daniel S., Agid Y., Javoy-Agid F., Jenner P., and Marsden C. D. (1994) Alterations in glutathione levels in Parkinson's disease and other neurodegenerative disorders affecting the basal ganglia. *Ann. Neurol.* **36,** 348-355.

33. Tohgi H., Abe T., Saheki M., Hamato F., Sasaki K., and Takahashi S. (1995) Reduced and oxidized forms of glutathione and α-tocopherol in the cerebrospinal fluid of parkinsonian patients comparison between, before and after L-dopa treatment. *Neurosci. Lett.* **184,** 21-24.

34. Halliwell B. and Gutteridge J. M. C. (1999) *Free Radicals in Biology and Medicine*, Oxford University Press, Oxford, N.Y.

35. Good P. F., Hsu A., Werner D. P., Perl P., and Olanow C. W. (1996) Protein nitration in Parkinson's disease. *J. Neuropathol. Exp. Neurol.* **57,** 338-342.

36. Przedborski S., Jackson-Lewis V., Yokoyama R., Shibata T., Dawson V. L., and Dawson T. M. (1996) Role of neuronal nitric oxide in MPTP (1-methyl-4-phenyl-1,2,3,6-tetrahydropyridine)-induced dopaminergic neurotoxicity. *Proc. Natl. Acad. Sci. U.S.A.* **93,** 4565-4571.

37. Spencer J. P., Wong J., Jenner A., Aruma O. I., Cross C. E., and Halliwell B. (1996) Base modifications and strand breakage in isolated calf thymus DNA and in DNA from human skin epidermal keratinocytes exposed to peroxynitrite or 3-morpholinosydnonimine. *Chem. Res. Toxicol.* **9,** 1152-1158.

38. Radi R., Beckman J. S., Bush K. M., and Freeman B. A. (1991) Peroxynitrite-induced membrane lipid peroxidation: the cytotoxic potential of superoxide and nitric oxide. *Arch. Biochem. Biophys.* **288,** 481-487.

39. Greenacre S. A. and Ischiropoulos H. (2001) Tyrosine nitration: localization, quantification, consequences for protein function and signal transduction. *Free Radic. Res.* **34,** 541-581.

40. Sian J., Gerlach M., Youdim M. B. H., and Riederer P. (1999) Parkinson's disease: a major hypokinetic basal ganglia disorder. *J. Neural Transm.* **106,** 443-476.

41. Hoyer S. (1990) Brain glucose and energy metabolism during normal aging. *Aging* **2,** 245-248.

42. Sastre J., Pallardo F. V., and Vina J. (2000) Mitochondrial oxidative stress plays a key role in aging and apoptosis. *IUBMB Life* **49,** 427-435.

43. Tian L., Cai Q., and Wei H. (1998) Alterations of antioxidant enzymes and oxidative damage to macromolecules in different organs of rats during aging. *Free Rad. Biol. Med.* **24,** 1477-1484.

44. Desai V. G., Feuers R. J., Hart R. W., and Ali S. F. (1996) MPP^+-induced neurotoxicity in mouse is age-dependent: evidenced by the selective inhibition of complexes of electron transport. *Brain Res.* **715,** 1-8.

45. Beal M. F. (1995) *Mitochondrial Dysfunction and Oxidative Damage in Neurodegenerative Diseases.*, R. G. Landes Co., Austin, TX.

46. Landfield P. W., Thibault O., Massanti M. L., Porter N. M., and Kerr D. S. (1992) Mechanisms of neuronal death in brain aging and Alzheimer's disease: role of endocrine-mediated calcium dyshomeostasis. *J. Neurobiol.* **23,** 1247-1260.

47. Gibson G. E. and Peterson C. (1987) Calcium and the aging nervous system. *Neurobiol. Aging* **8,** 329-343.

48. Stadman E. R. (1988) Protein modification in aging. *J. Gerontol.* **43,** B112-B120.

49. Rodgers A. D. and Curzon G. (1975) Melanin formation by human brain in vitro. *J. Neurochem.* **24,** 1123-1129.

50. Graham D. G. (1978) Oxidation pathways for catecholamines in the genesis of neuromelanin and cytotoxic quinones. *Mol. Pharmacol.* **14,** 633-643.

51. Van Woert M. H. and Ambani L. M. (1974) Biochemistry of neuromelanin. *Adv. Neurol.* **5,** 215-223.

52. Hastings T. G. (1995) Enzymatic oxidation of dopamine: the role of prostaglandin H synthase. *J. Neurochem.* **64,** 919-924.

53. McGeer P. L., McGeer E. G., and Suzuki J. S. (1976) Aging and extrapyrimidal function. *Arch. Neurol.* **34,** 33-35.

54. Fearnley J. M. and Lees A. J. (1991) Ageing and Parkinson's disease: substantia nigra regional selectivity. *Brain* **114,** 2283-2301.

55. Damier P., Hirsch E. C., Agid Y., and Graybiel A. M. (1999) The substantia nigra of the human brain: II. Patterns of loss of dopamine-containing neurons in Parkinson's disease. *Brain* **122,** 1437-1448.

56. Kish S. J., Shannak K., Rajput A., Deck J. H., and Hornykiewicz O. (1992) Aging produces a specific pattern of striatal dopamine loss: implications for the etiology of idiopathic Parkinson's disease. *J. Neurochem.* **58,** 642-648.

57. Le Couteur D. G., McLean A. J., Taylor M. C., Woodham B. L., and Board P. G. (1999) Pesticides and Parkinson's disease. *Biomed. Pharmacother.* **53,** 122-130.

58. Shahi G. S. and Das S. M. (1990) Parkinson's disease and cytochrome P450: a possible link? *Med. Hypotheses* **32,** 277-282.

59. Le Couteur D. G. and McClean A. J. (1998) The ageing liver: drug clearance and an oxygen diffusion barrier hypothesis. *Clin. Pharmacokinetics* **34,** 359-373.

60. Semchuk K. M., Love E. J., and Lee R. G. (1992) Parkinson's disease and exposure to agricultural work and pesticide chemicals. *Neurology* **42,** 1328-1335.

61. Barbeau A., Roy M., Bernier G., Campanella G., and Paris S. (1987) Ecogenetics of Parkinson's disease: prevalence and environmental aspects in rural areas. *Can. J. Neurol. Sci.* **14,** 36-41.

62. Hubble J. P., Cao T., Hassanein R. E., Neuberger J. S., and Koller W. C. (1993) Risk factors for Parkinson's disease. *Neurology* **43,** 1693-1697.

63. Veldman B. A., Wijn A. M., Knoers N., Praamstra P., and Horstink M. W. (1998) Genetic and environmental risk factors in Parkinson's disease. *Clin. Neurol. Neurosurg.* **100,** 15-26.

64. Fleming L., Mann J. B., Bean J., Briggle T., and Sanchez-Ramos J. R. (1994) Parkinson's disease and brain levels of organochlorine pesticides. *Ann. Neurol.* **36,** 100-103.

65. Corrigan F. M., Wienburg C. L., Shore R. F., Daniel S. E., and Mann D. (2000) Organochlorine insecticides in substantia nigra in Parkinson's disease. *J. Toxicol. Environ. Health* **59,** 229-234.

66. Guehl D., Bezard E., Dovero S., Boraud T., Bioulac B., and Gross C. (1999) Trichloroethylene and parkinsonism: a human and experimental observation. *Eur. J. Neurol.* **6,** 609-611.

67. Masalha R., Herishanu Y., Alfahel-Kakunda A., and Silverman W. F. (1997) Selective dopamine neurotoxicity by an industrial chemical: an environmental cause of Parkinson's disease? *Brain Res.* **774,** 260-264.

68. Carella F., Grassi M. P., Savoiardo M., Contri P., Rapuzzi B., and Mangoni A. (1988) Dystonic-parkinsonian syndrome after cyanide poisoning: clinical and MRI findings. *J. Neurol. Neurosurg. Psychiatry* **51,** 1345-1348.

69. Gorell J. M., Johnson C. C., Rybicki B. A., Peterson E. L., Kortsha G. X., Brown G. G., and Richardson R. J. (1999) Occupational exposure to manganese, copper, lead, iron, mercury and zinc and the risk of Parkinson's disease. *Neurotoxicol.* **20,** 239-247.

70. Kanthasamy A. G., Borowitz J. L., Pavlakovic G., and Isom G. E. (1994) Dopaminergic neurotoxicity of cyanide: neurochemical, histological, and behavioral characterization. *Toxicol. Appl. Pharmacol.* **126,** 156-163.

71. Sengstock G. J., Olanow C. W., Menzies R. A., Dunn A. J., and Arandash G. W. (1993) Infusion of iron into rat substantia nigra: nigral pathology and dose-dependent loss of striatal markers. *J. Neurosci. Res.* **35,** 76-82.

72. Lash L. H., Xu Y., Elfarra A. A., Duescher R. J., and Parker J. C. (1995) Glutathione-dependent metabolism of tricloroethylene in isolated liver and kidney cells of rats and its role in mitochondrial and cellular toxicity. *Drug Metab. Dispos.* **23,** 846-853.

73. Moduh E. U., Borowitz J. L., and Isom G. E. (1991) Cyanide-induced alteration of the adenylate energy pool in a rat neurosecretary cell line. *J. Appl. Toxicol.* **11,** 97-101.

74. Bergen W. G. (1971) The in vitro effect of dieldrin on respiration of rat liver mitochondria. *Proc. Soc. Exp. Biol. Med.* **136,** 732-735.

75. Cooper J. M. and Shapira A. H. V. (1997) Mitochondrial dysfunction in neurodegeneration. *J. Bioenerg. Biomembranes* **29,** 175-183.

76. Heikkila R. E., Nicklas W. J., Vyas I., and Duvoisin R. C. (1985) Dopaminergic toxicity of rotenone and the 1-methyl-4-phenylpyridinium ion after stereotaxic administration to rats: implications for the mechanism of 1-methyl-4-phenyl-1,2,3,6-tetrahydropyridine toxicity. *Neurosci. Lett.* **62,** 389-394.

77. Gerlach M., Riederer P., Przuntek H., and Youdim M. B. H. (1991) MPTP mechanisms of neurotoxicity and their implications for Parkinson's disease. *Eur. J. Pharmacol.* **208,** 273-286.

78. Burrows K. B., Gudelsky G., and Yamamoto B. K. (2000) Rapid and transient inhibition of mitochondrial function following methamphetamine or 3,4-methylenedioxymethamphetamine administration. *Eur. J. Pharmacol.* **398,** 11-18.

79. Vaccari A. and Saba P. (1995) The tyramine-labelled vesicular transporter for dopamine: a putative target of pesticides and neurotoxins. *Eur. J. Pharmacol.* **292,** 309-314.

80. Vaccari A. (1993) The tyramine binding site in the central nervous system: an overview. *Neurochem. Res.* **18,** 861-868.

81. Brown J. M., Hanson G. R., and Fleckenstein A. E. (2000) Methamphetamine rapidly decreases vesicular dopamine uptake. *J. Neurochem.* **74,** 2221-2223.

82. Miller G. W., Kirby M. L., Levey A. I., and Bloomquist J. R. (1999) Heptaclor alters expression and function of dopamine transporters. *Neurotoxicology* **20,** 631-637.

83. Sagara J., Miura K., and Bannai S. (1993) Maintenance of neuronal glutathione by glial cells. *J. Neurochem.* **61,** 1672-1676.

84. Wang X. F. and Cynader M. S. (2000) Astrocytes provide cysteine to neurons by releasing glutathione. *J. Neurochem.* **74,** 1434-1442.

85. Cooper A. J. and Kristal B. S. (1997) Multiple roles of glutathione in the central nervous system. *Biol. Chem.* **378,** 793-802.

86. Drukarch B., Schepens E., Jongenelen C. A. M., Stoof J. C., and Langeveld C. H. (1997) Astrocyte-mediated enhancement of neuronal survival is abolished by glutathione deficiency. *Brai Res.* **770,** 123-130.

87. Desagher S., Glowinski J., and Premont J. (1996) Astrocytes protect neurons from hydrogen peroxide toxicity. *J. Neurosci.* **16,** 2553-2562.

88. Langeveld C., Jongenelen C. A. M., Schepens E., Stuof J. C., Bast A., and Drukarch B. (1995) Cultured rat striatal and cortical astrocytes protect mesencephalic dopaminergic neurons against hydrogen peroxide toxicity independent of their effect on neuronal development. *Neurosci. Lett.* **192,** 13-16.

89. Hirrlinger J., Schukz J. B., and Dringen R. (2002) Glutathione release from cultured brain cells: multidrug resistance protein 1 mediates the release of GSH from rat astroglial cells. *J. Neurosci. Res.* **69,** 318-326.

90. Reyes E. and Palmer G. C. (1976) Biochemical localization of γ-glutamyl transpeptidase within cellular elements of the rat cerebral cortex. *Commun. Chem. Pathol. Pharmacol.* **14,** 759-762.

91. Dringen R., Gutterer J. M., Gros C., and Hirrlinger J. (2001) Aminopeptidase N mediates the utilization of the GSH precursor CysGly by cultured neurons. *J. Neurosci. Res.* **66,** 1003-1008.

92. Utsunomiya-Tate N., Endou H., and Kanai Y. (1996) Cloning and functional characterization of a system ASC-like Na^+-dependent neutral amino acid transport. *J. Biol. Chem* **271,** 14883-14890.

93. Shafqat S., Tamarappoo B. K., Kilberg M. S., Puranam R. S., McNamara J. O., Guadano-Ferraz A., and Fremeau R. T. (1993) Cloning and expression of a novel Na^+-dependent neutral amino acid transporter structurally related to mammalian Na^+ glutamate cotransporters. *J. Biol. Chem.* **268,** 15351-15355.

94. Arriza J. L., Kavanaugh M. P., Fairman W. A., Wu Y. N., Murdoch G. H., North R. A., and Amara S. G. (1993) Cloning and expression of a human neutral amino acid transporter with structural similarity to the glutamate gene family. *J. Biol. Chem.* **268,** 15329-15332.

95. Tate S. S. and Meister A. (1985) γ-Glutamyl transpeptidase from kidney. *Meth. Enzymol.* **113,** 400-437.

96. Kranich O., Hamprecht B., and Dringen R. (1996) Differential preferences in the utilization of amino acids for glutathione synthesis in cultured neurons and astroglial cells dervived from rat brain. *Neurosci. Lett.* **219,** 211-214.

97. Mitöfer K., Sandy M. S., Smith M. T., and Di Monte D. (1992) Mitochondrial poisons cause depletion of glutathione in isolated hepatocytes. *Arch. Bioch. Biophys.* **295,** 132-136.

98. Zängerle L., Cuenod M., Winterhalter K. H., and Do K. Q. (1992) Screening of thiol compounds: depolarization-induced release of glutathione and cysteine from rat brain slices. *J. Neurochem.* **59,** 181-189.

99. Khan S. and O'Brien P. J. (1997) Rapid and specific efflux of glutathione before hepatocyte injury induced by hypoxia. *Biochem. Biophys. Res. Commun.* **238,** 320-322.

100. Kurosawa K., Hayashi N., Sato N., Kamada T., and Tagawa K. (1990) Transport of glutathione across the mitochondrial membranes. *Biochem. Biophys. Res. Commun.* **167,** 367-372.

101. Savage M. K., Jones D. P., and Reed D. J. (1991) Calcium- and phosphate-dependent release and loading of glutathione by liver mitochondria. *Arch. Biochem. Biophys.* **290,** 51-56.

102. Rigobello M. P. and Bindoli A. (1993) Effect of pyruvate on rat thiol status during ischemia and hypoxia followed by reperfusion. *Mol. Cell. Biochem.* **122,** 93-100.

103. Reed D. J. and Savage M. K. (1995) Influence of metabolic inhibitors on mitochondrial permeability transition and glutathione status. *Biochem. Biophys. Acta* **1271,** 43-50.

104. Zeevalk G. D., Bernard L. P., Sinha C., Ehrhart J., and Nicklas W. J. (1998) Excitotoxicity and oxidative stress during inhibition of energy metabolism. *Dev. Neurosci.* **20,** 444-453.

105. Sian J., Dexter D. T., Lees A. J., Daniel S., Jenner P., and Marsden C. D. (1994) Glutathione-related enzymes in brain in Parkinson's disease. *Ann. Neurol.* **36,** 356-361.

106. Pearce R. K. B., Owen A., Daniel S., Jenner P., and Marsden C. D. (1997) Alterations in the distribution of glutathione in the substantia nigra of Parkinson's disease. *J. Neural Transm.* **104,** 661-677.

107. Fornstedt B., Brun A., Rosengren E., and Carlsson A. (1989) The apparent autoxidation rate of catechols in dopamine-rich regions of human brains increases with the degree of depigmentation. *J. Neural Transm. Park. Dis. Dement. Sect.* **1,** 279-295.

108. Spencer J. P. E., Jenner P., Daniel S. E., Lees A. J., Marsden D. C., and Halliwell B. (1998) Conjugates of catecholamines with cysteine and GSH in Parkinson's disease. Possible mechanisms of formation involving reactive oxygen species. *J. Neurochem.* **71,** 2112-2122.

109. Kerry N. and Rice-Evans C. (1999) Inhibition of peroxynitrite-mediated oxidation of dopamine by flavonoid and phenolic antioxidants and their structural relationships. *J. Neurochem.* **73,** 247-253.

110. Daveu C., Servy C., Dendane M., Marin P., and Docrocq C. (1997) Oxidation and nitration of catecholamines by nitrogen oxides derived from nitric oxide. *Nitric Oxide* **1,** 234-243.

111. Cooper A. J. L. (1998) Role of astrocytes in maintaining cerebral glutathione homeostasis and protecting the brain against xenobiotics and oxidative stress., in *Glutathione in the Nervous System.* (Shaw C. A., ed.), pp. 91-115. Taylor and Francis, Washington, D.C.

112. Betarbet R., Sherer T. B., and Greenamyre J. T. (2002) Animal models of Parkinson's disease. *BioEssays* **24,** 308-318.

113. Perese D. A., Ulman J., Viola J., Ewing S. E., and Bankiewicz K. S. (1989) A 6-hydroxydopamine-induced selective parkinsonian rat model. *Brain Res.* **494,** 285-293.

114. Przedborski S., Levivier M., Jiang H., Ferreira M., Jackson-Lewis V., Donaldson D., and Togasaki D. M. (1995) Dose-dependent lesions of the dopaminergic nigrostriatal pathway induced by intrastriatal injection of 6-hydroxydopamine. *Neuroscience* **67,** 631-647.

115. Schwarting R. K. and Huston J. P. (1996) Unilateral 6-hydroxydopamine lesions of meso-striatal dopamine neurons and their physiological sequelae. *Prog. Neurobiol.* **49,** 215-266.

116. Fauli R. L. and Laverty R. (1969) Changes in dopamine levels in the corpus striatum following lesions in the substantia nigra. *Exp. Neurol.* **23,** 332-340.

117. Ungerstedt U. (1968) 6-Hydroxy-dopamine induced degeneration of central-monoamine neurons. *Eur. J. Pharmacol.* **5,** 107-110.

118. Perumal A. S., Gopal V. B., Tordzro W. K., Cooper T. B., and Cadet J. L. (1992) Vitamin E attenuates the toxic effects of 6-hydroxydopamine on free radical scavenging systems in rat brain. *Brain Res. Bul.* **29,** 699-701.

119. Glinka Y. Y. and Youdim M. B. H. (1995) Inhibition of mitochondrial complex I and IV by 6-hydroxydopamine. *Eur. J. Pharmacol.* **292,** 329-332.

120. Cappon G. D., Pu C., and Vorhees C. V. (2000) Time-course of methamphetamine-induced neurotoxicity in rat caudate-putamen after single dose treatment. *Brain Res.* **863,** 106-111.

121. O'Dell S. J., Weihmuller F. B., and Marshall J. F. (1991) Multiple methamphetamine injections induce marked increases in extracellular dopamine which correlate with subsequent neurotoxicity. *Brain Res.* **564,** 256-260.

122. Fukumura M., Cappon G. D., Pu C., Broening H. W., and Vorhees C. V. (1998) A single dose model of methamphetamine-induced neurotoxicity in rats: effects on neostriatal monamines and glial fibrillary acidic protein. *Brain Res.* **806,** 1-7.

123. Nash J. F. and Yamamoto B. K. (1992) Methamphetamine neurotoxicity and striatal glutamate release: comparison to 3,4-methylenedioxymethamphetamine. *Brain Res.* **581,** 237-243.

124. Haughey H. M., Fleckenstein A. E., and Hanson G. R. (1999) Differential regional effects of methamphetamine on the activities of tryptophan and tyrosine hydroxylase. *J. Neurochem.* **72,** 661-668.

125. Sharp T., Zetterström T., and Ungerstedt U. (1986) An *in vivo* study of dopamine release and metabolism in rat brain regions using intracerebral dialysis. *J. Neurochem.* **47,** 113-121.

126. Itzhak Y. and Ali S. F. (1996) The neuronal nitric oxide synthase inhibitor, 7-nitroindazole, protects against methamphatamine neurotoxicity *in vivo*. *J. Neurochem.* **67,** 1770-1773.

127. Haughey H. M., Fleckenstein A. E., Metzger R. R., and Hanson G. R. (2000) The effects of methamphetamine on serotonin transporter activity: role of dopamine and hyperthermia. *J. Neurochem.* **75,** 1608-1617.

128. Ryan L. J., Linder J. C., Martone M. E., and Groves P. M. (1990) Histological and ultrastructural evidence that *d*-amphetamine causes degeneration in neo-striatum and frontal cortex of rats. *Brain Res.* **518,** 67-77.

129. Fukui K., Nakajima T., Kariyama H., Kashiba A., Kato N., and Tohyama I. K. H. (1989) Selective reduction of serotonin immunoreactivity in some forebrain regions of rats induced by acute methamphetamine treatment: quantitative morphometric analysis by serotonin immunocytochemistry. *Brain Res.* **482,** 198-203.

130. Fleckenstein A. E., Wilkins D. G., Gibb J. W., and Hanson G. R. (1997) Interaction between hyperthermia and oxygen radical formation in the 5-hydroxy-tryptaminergic response to a single methamphetamine administration. *J. Pharmacol. Exp. Ther.* **283,** 281-285.

131. Kalant H. and Kalant O. J. (1975) Death in amphetamine users: causes and rates. *J. Can. Med. Assoc.* **112,** 299-304.

132. Betarbet R., Sherer T. B., MacKenzie G., Garcia-Osuna M., Panov A. V., and Greenamyre J. T. (2000) Chronic systemic pesticide exposure reproduces features of Parkinson's disease. *Nat. Neurosci.* **3,** 1301-1306.

133. Langston J. W., Ballard P., Tetrud J. W., and Irwin I. (1983) Chronic parkinsonism in humans is due to a product of meperidine-analog synthesis. *Science* **219,** 979-980.

134. Tipton K. and Singer T. P. (1993) Advances in our understanding of the mechanisms of the neurotoxicity of MPTP and related compounds. *J. Neurochem.* **61,** 1191-1206.

135. Ferraro T. N., Golden G. T., De Mattei M., Hare T. A., and Fariello R. G. (1986) Effect of 1-methyl-4-phenyl-1,2,3,6-tetrahydropyridine (MPTP) on levels of glutathione in the extrapyramidal system of the mouse. *Neuropharmacology* **25,** 1071-1074.

136. Yong V. W., Perry T. L., and Krisman A. A. (1986) Depletion of glutathione in brainstem of mice caused by *N*-methyl-4-phenyl-1,2,3,6-tetrahydropyridine is prevented by antioxidant pretreatment. *Neurosci. Lett.* **63,** 56-60.

137. Oishi T., Hasegawa E., and Murai Y. (1993) Sulfhydral drugs reduce neurotoxicity of 1-methyl-4-phenyl-1,2,3,6-tetrahydropyridine (MPTP) in the mouse. *J. Neural Transm. Park. Dis. Dementia Sect.* **6,** 45-52.

138. Sriram K., Pai K. S., Boyd M. R., and Ravindranath V. (1997) Evidence for generation of oxidative stress in brain by MPTP: in vitro and in vivo studies in mice. *Brain Res.* **749,** 44-52.

139. Forno L. S., Langston J. W., DeLanney L. E., and Irwin I. (1988) An electron microscopic study of MPTP-induced inclusion bodies in an old monkey. *Brain Res.* **448,** 150-157.

140. Kowell N. W., Hantraye P., Brouillet E., Beal M. F., McKee A. C., and Ferrante R. J. (2000) MPTP induces α-synuclein aggregation in the substantia nigra of baboons. *Neuroreport* **11,** 211-213.

141. Ransom B. R., Kunis D. M., Irwin I., and Langston J. W. (1987) Astrocytes convert the parkinsonism inducing neurotoxin, MPTP to its active metabolite, MPP^+. *Neurosci. Lett.* **75,** 323-328.

142. Javitch J. A., D'Amato R. J., Strittmatter S. M., and Snyder S. H. (1985) Parkinsonian-inducing neurotoxin, N-methyl-4-phenyl-1,2,3,6-tetrahydropyridine: uptake of the metabolite N-methyl-4-phenylpyridine by dopamine neurons explains selective toxicity. *Proc. Natl. Acad. Sci. U.S.A.* **82,** 2173-2177.

143. Ramsay R. R., Dadgar J., Trevor A., and Singer T. P. (1986) Energy driven uptake of N-methyl-4-phenylpyridine by brain mitochondria mediates the neurotoxicity of MPTP. *Life Science* **39,** 581-588.

144. Mizuno Y., Saitoh T., and Sone N. (1987) Inhibition of mitochondrial α-ketoglutarate dehydrogenase by 1-methyl-4-phenylpyridinium ion. *Biochem. Biophys. Res. Commun.* **143,** 971-976.

145. Cosi C. and Marien M. (1999) Implication of poly(ADP-ribose)polymerase (PARP) in neurodegeneration and brain energy metabolism. Decreases in mouse NAD^+ and ATP caused by MPTP are prevented by the PARP inhibitor benzamide. *Ann. N.Y. Acad. Sci.* **890,** 227-239.

146. Mandir A. S., Przedborski S., Jackson-Lewis V., Wang K. Q., Simbulan-Rosenthal C. M., Smulson M. E., Hoffman B. E., Guastella D. B., Dawson V. L., and Dawson T. M. (1999) Poly(ADP-ribose)polymerase activation mediates 1-methyl-4-phenyl-1,2,3,6-tetrahydropyridine. *Proc. Nat. Acad. Sci. U.S.A.* **96,** 5774-5779.

147. Cosi C. and Marien M. (1998) Decreases in mouse brain NAD^+ and ATP by 1-methyl-4-phenyl-1,2,3,6-tetrahydropyridine (MPTP): prevention by the poly (ADP-ribose)polymerase inhibitor, benzamide. *Brain Res.* **809**.

148. Cosi C., Colpaert F., Koek W., Degryse A., and Marien M. (1996) Poly(ADP-ribose)polymerase inhibitors protect against MPTP-induced depletions of striatal dopamine and cortical noradrenaline in C57B1/6 mice. *Brain Res.* **729,** 264-269.

149. Chan P., Delanney L. E., Irwin I., Langston J. W., and Di Monte D. (1991) Rapid ATP loss caused by MPTP in mouse brain. *J. Neurochem.* **57,** 348-351.

150. Rollema H., Damsma G., Horn A. S., De Vries J. B., and Westerink B. H. C. (1986) Brain dialysis in conscious rats reveals an instantaneous massive release of striatal dopamine in response to MPP^+. *Eur. J. Pharmacol.* **126,** 345-346.

151. Matarredona E. R., Santiago M., Machado A., and Cano J. (1997) Lack of involvement of glutamate-induced excitotoxicity in MPP^+ toxicity in striatal dopaminergic terminals: possible involvement of ascorbate. *Br. J. Pharmacol.* **12,** 1038-1044.

152. Giovanni A., Sonsalla P. K., and Heikkila R. E. (1994) Studies on species sensitivity to the dopaminergic neurotoxin 1-methyl-4-phenyl-1,2,3,6-tetrahydropyridine. Part 2: central administration of 1-methyl-4-phenylpyridinium. *J. Pharmacol. Exp. Ther.* **270,** 1008-1014.

153. Greene J. G. and Greenamyre J. T. (1996) Bioenergetics and excitotoxicity: the weak excitotoxic hypothesis, in *Neurodegeneration and Neuroprotection in Parkinson's Disease* (Olanow C. W., Jenner P., and Youdim M., eds.), pp. 125-142. Academic Press, New York.

154. Chiueh C. C. and Huang S. J. (1991) MPP^+ enhances potassium evoked striatal dopamine release through an Ω-conotoxin-insensitive, tetrodotoxin- and nimodipine-sensitive calcium dependent mechanism. *Ann. N.Y. Acad. Sci.* **635,** 393-396.

155. Lotharius J. and O'Malley K. L. (2000) The parkinsonism-inducing drug 1-methyl-4-phenylpyridinium triggers intracellular dopamine oxidation. A novel mechanism of toxicity. *J. Biol. Chem.* **275,** 38581-38588.

156. Cao C. J., Eldefrawi A. T., and Eldefrawi M. E. (1990) ATP-regulated neuronal catecholamine uptake: a new mechanism. *Life Sci.* **47,** 655-667.

157. Carboni S., Melis F., Pani L., Hadjiconstantinou M., and Rossetti Z. L. (1990) The non-competative NMDA-receptor antagonist MK-801 prevents the massive release of glutamate and aspartate from rat striatum induced by 1-methyl-4-pyridinium (MPP^+). *Neurosci. Lett.* **117,** 129-133.

158. Benazzouz A., Boraud T., Dubet P., Boireau A., Stutzmann J. M., and Cross C. (1995) Riluzole prevents MPTP-induced parkinsonism in the rhesus monkey: a pilot study. *Eur. J. Pharmacol.* **284,** 299-307.

159. Schmidt C. J., Matsuda L. A., and Gibb J. W. (1984) In vitro release of titrated monoamines from rat CNS tissue by the neurotoxic compound 1-methyl-4-phenyl-1,2,3,6-tetrahydropyridine. *Eur. J. Pharmacol.* **103,** 255-260.

160. Standaert D. G., Friberg I. K., Landwehrmeyer G. B., Young A. B., and Penney J. B. (1999) Expression of NMDA glutamate receptor subunit mRNAs in neurochemically identified projection and interneurons in the striatum of the rat. *Brain Res. Mol. Brain Res.* **64,** 11-23.

161. Bernard V. and Bolam J. P. (1998) Subcellular and subsynaptic distribution of the NRI subunit of the NMDA receptor in the neostriatum and globus pallidus of the rat: co-localization at synapses with the GluR2/3 subunit of the AMPA receptor. *Eur. J. Neurosci.* **10,** 3721-3736.

162. Yung K. K. (1998) Localization of ionotropic and metabotropic glutamate receptors in distinct neuronal elements of the rat substantia nigra. *Neurochem. Int.* **33,** 313-326.

163. Counihan T. J., Landwehrmeyer G. B., Standaert D. G., Kosinski C. M., Scherzer C. R., Daggett L. P., Velicelebi G., Young A. B., and Penney J. B. (1998) Expression of N-methyl-D-aspartate receptor subunit mRNA in the human brain: mesencephalic dopaminergic neurons. *J. Comp. Neurol.* **390,** 91-101.

164. Paquet M., Tremblay M., Soghomonian J. J., and Smith Y. (1997) AMPA and NMDA glutamate receptor subunits in midbrain dopaminergic neurons in the squirrel monkey: an immunohistochemical and in situ hybridization study. *J. Neurosci.* **17,** 1377-1396.

165. Albers D. S., Weiss S. W., Iadarola M. J., and Standaert D. G. (1999) Immunohistochemical localization of N-methyl-D-aspartate and α-amino-3-hydroxy-5-methyl-4-isoxazolepropionate receptor subunits in the substantia nigra pars compacta of the rat. *Neurosci.* **89,** 209-220.

166. Merino M., Vizuete M. L., Cano L., and Machado A. (1999) The non-NMDA glutamate receptor antagonists 6-cyano-7-nitroquinoxaline-2,3-dione and 2,3-dihydroxy-6-nitrosulfamoyl-benzo(*f*)quinoxaline, but not NMDA antagonists, block the intrastriatal neurotoxic effect of MPP^+. *J. Neurochem.* **73,** 750-757.

167. Zeevalk G. D. and Manzino L. S. P. K. (2000) NMDA receptors modulate dopamine loss due to energy impairment in the substantia nigra but not striatum. *Exp. Neurol.* **161,** 638-646.

168. Loschmann P. A., Lange K. W., Wachtel H., and Turski L. (1994) MPTP-induced degeneration: interference with glutamatergic toxicity. *J. Neural Transm.* **43,** 133-143.

169. Przedborski S., Jackson-Lewis V., Kostic V., Carlson E., Epstein C. J., and Cadet J. L. (1992) Superoxide dismutase, catalase, and glutathione peroxidase activities in copper/zinc-superoxide dismutase transgenic mice. *J. Neurochem.* **58,** 1760-1767.

170. Przedborski S., Kostic V., Jackson-Lewis V., Naini A. B., Simoneltá S., Fah S., Carlson E., Epstein C. J., and Cadet J. L. (1992) Transgenic mice with increased Cu/Zn superoxide dismutase activity are resistant to N-methyl-4-phenyl-1,2,3,6-tetrahydropyridine-induced neurotoxicity. *J. Neurosci.* **12,** 1658-1667.

171. Kupsch A., Löschmann P. A., Sauer H., Arnold G., Renner P., Pufal D., Burg M., Wachtel H., ten Bruggencate G., and Oertel W. H. (1992) Do NMDA receptor antagonists protect against MPTP-toxicity? Biochemical and immunocytochemical analyses in black mice. *Brain Res.* **592,** 74-83.

172. Akekawa T., Ohmori T., and Koyama T. (1994) Effects of repeated administration of a high dose of methamphetamine on dopamine and glutamate release in the rat striatum and nucleus accumbens. *Brain Res.* **643,** 276-281.

173. Ara J., Przedborski S., Naini A. B., Jackson-Lewis V., Trifiletti R. R., and Horwitz J. I. H. (1998) Inactivation of tyrosine hydroxylase by nitration following exposure to peroxynitrite and 1-methyl-4-phenyl-1,2,3,6-tetrahydropyridine. *Proc. Natl. Acad. Sci. U.S.A.* **95,** 7659-7663.

174. Matthews R. T., Beal M. F., Fallon J., Fedorchak K., Huang P. L., Fishman M. C., and Hyman B. T. (1997) MPP^+ induced substantia nigra degeneration is attenuated in nNOS knockout mice. *Neurobiol. Dis.* **4,** 114-121.

175. Liberatore G. T., Jackson-Lewis V., Vukosavic S., Mandir A. S., Vila M., McAuliffe W. G., Dawson V. L., Dawson T. M., and Przedborski S. (1999) Inducible nitric oxide synthase stimulates dopaminergic neurodegeneration in the MPTP model of Parkinson's disease. *Nat. Med.* **5,** 1403-1409.

176. Klivenyi P., Andreassen O. A., Ferrante R. J., Lancelot E., Reif D., and Beal M. F. (2000) Inhibition of neuronal nitric oxide synthase protects against MPTP toxicity. *Neuroreport* **11,** 1265-1268.

177. Bredt D. S., Glatt C. E., Hwang P. M., Fotuhi M., Dawson T. M., and Snyder S. H. (1991) Nitric oxide synthase protein and mRNA are discretely localized in neuronal populations of the mammalian CNS together with NADPH diaphorase. *Neuron* **7,** 615-624.

178. Xia Y. and Zweier J. L. (1997) Superoxide and peroxynitrite generation from inducible nitric oxide synthase in macrophages. *Proc. Natl. Acad. Sci. U.S.A.* **94,** 6954-6958.

179. Ferrante R. J., Hantraye P., Brouillet E., and Beal M. F. (1999) Increased nitro-tyrosine immunoreactivity in substantia nigra neurons in MPTP treated baboons is blocked by inhibition of neuronal nitric oxide synthase. *Brain Res.* **823,** 177-182.

180. Schulz J. B., Matthews R. T., Klockgether T., Dichgans J., and Beal M. F. (1997) The role of mitochondrial dysfunction and neuronal nitric oxide in animal models of neurodegenerative diseases. *Mol. Cell. Biochem.* **174,** 193-197.

181. Chiueh C. C., Wu R. M., Mohanaakumar K. P., Sternberger L. M., Krishna G., Obata T., and Murphy D. L. (1994) *In vivo* generation of hydroxyl radicals and MPTP-induced dopaminergic toxicity in the basal ganglia. *Ann. N.Y. Acad. Sci.* **738,** 25-36.

182. Martin F. R., Sanchez-Ramos J., and Rosenthal M. (1991) Selective and non-selective effects of MPTP on oxygen consumption in rat striatal and hippo-campal slices. *J. Neurochem.* **57,** 1340-1346.

183. Melamed E., Rosenthal J., Globus M., Cohen O., and Uzzan A. (1985) Suppression of MPTP-induced dopaminergic neurotoxicity in mice by nomifensine and L-dopa. *Brain Res.* **342,** 401-404.

184. Bezard E., Gross C. E., Fournier M. C., Dovero S., Bloch B., and Jaber M. (1999) Absence of MPTP-induced neuronal death in mice lacking the dopamine transporter. *Exp. Neurol.* **155,** 268-273.

185. Gainetdinov R. R., Fumagalli F., Wang Y. M., Jones S. R., Levey A. I., Miller G. W., and Cardon M. G. (1998) Increased MPTP neurotoxicity in vesicular monoamine transporter 2 heterozygote knockout mice. *J. Neurochem.* **70,** 1973-1978.

186. Sanghera M. K., Manaye K., McMahon A., Sonsalla P. K., and German D. C. (1997) Dopamine transporter mRNA levels are high in midbrain neurons vunerable to MPTP. *Neuroreport* **8,** 3327-3331.

187. Edwards R. H. (1993) Neural degeneration and the transport of neurotransmitters. *Ann. Neurol.* **34,** 638-645.

188. Hoyt K. R., Reynolds I. J., and Hastings T. G. (1997) Mechanisms of dopamine-induced cell death in cultured rat forebrain neurons: interactions with and differences from glutamate-induced cell death. *Exp. Neurol.* **143,** 269-281.

189. Sanchez-Ramos J., Facca A., Basit A., and Song S. (1998) Toxicity of dieldrin for dopaminergic neurons in mesencephalic cultures. *Exp. Neurol.* **150,** 263-271.

190. Gopalaswamy U. V. and Aiyer A. S. (1984) Effects of lindane on liver mitochondrial function in the rat. *Bull. Environ. Contam. Toxicol.* **33,** 106-113.

191. Bachurin S. O., Shevtzova E. P., Lermontova N. N., Serkova T. P., and Ramsay R. R. (1996) The effect of dithiocarbamates on neurotoxic action of 1-methyl-4-phenyl-1,2,3,6-tetrahydropyridine (MPTP) and on mitochondrial respiration. *Neurotoxicology* **17,** 897-903.

192. Tawara T., Fukushima T., Hojo N., Isobe A., Shiwaku K., Setogawa T., and Yamane Y. (1996) Effects of paraquat on mitochondrial electron transport system and catecholamine contents in rat brain. *Arch. Toxicol.* **70,** 585-589.

193. Gassner B., Wuthrich A., Scholtysik G., and Solioz M. (1997) The pyrethroids perfethin and cyhalothrin are potent inhibitors of the mitochondrial complex I. *J. Pharmacol. Exp. Therap.* **281,** 855-860.

194. Wood N. (1997) Genes and parkinsonism. *J. Neurol. Neurosurg. Psychiatry* **62,** 305-309.

195. Tanner C. M. (1989) The role of environmental toxins in the etiology of Parkinson's disease. *Trends Neurosci.* **12,** 49-54.

196. de Silva H. R., Khan N. L., and Wood N. W. (2000) The genetics of Parkinson's disease. *Curr. Opin. Genet. Dev.* **10,** 292-298.

197. Tanner C. M., Ottman R., Goldman S. M., Ellenberg J. C. P., Mayeux R., and Langston J. W. (1999) Parkinson's disease in twins: an etiologic study. *J. Am. Med. Assoc.* **281,** 341-346.

198. Bougria M., Vitorica J., Cano J., and Machado A. (1995) Implications of dopamine transporter system on 1-methyl-4-phenylpyridinium and rotenone effect in striatal synaptosomes. *Eur. J. Pharmacol.* **291,** 407-415.

199. Nowak L., Bregestovski P., Ascher P., Herbet A., and Prochiantz A. (1984) Magnesium gates glutamate-activated channels in mouse central neurons. *Nature* **307,** 462-465.

200. Mayer M. L., Westbrooke G. L., and Guthrie P. B. (1984) Voltage-dependent block by Mg^{2+} of NMDA responses in spinal cord neurons. *Nature* **309,** 261-263.

201. Novelli R., Reilly J. A., Lysko P. G., and Henneberry R. C. (1988) Glutamate becomes neurotoxic when intracellular energy levels are reduced. *Brain Res.* **451,** 205-212.

202. Zeevalk G. D. and Nicklas W. J. (1991) Mechanisms underlying initiation of excitotoxicity associated with metabolic inhibition. *J. Pharmacol. Exp. Therap.* **257,** 870-878.

203. Lafon-Cazal M., Pletri S., Culcasi M., and Bockaert J. (1993) NMDA-dependent superoxide production and neurotoxicity. *Nature* **364,** 535-537.

204. Sensi S. L., Yin H. Z., Carriedo S. G., Rao S. S., and Weiss J. H. (1999) Preferential Zn^{2+} influx through Ca^{2+} permeable AMPA/kainate channels triggers prolonged mitochondrial superoxide production. *Proc. Nat. Acad. Sci. U.S.A.* **96,** 2414-2419.

205. Klivenyi P., Beal M. F., Ferrante R. J., Andreassen O. A., Wermer M., Chin M. R., and Bonventre J. V. (1998) Mice deficient in group IV cytosolic phospholipase A2 are resistent to MPTP neurotoxicity. *J. Neurochem.* **71,** 2634-2637.

206. Quijano C., Alvarez B., Gatti R. M., Augusto O., and Radi R. (1997) Pathways of peroxynitrite oxidation of thiol groups. *Biochem. J.* **322** , 167-173.

207. Gunasekar P. G., Kanthasamy A. G., Borowitz J. L., and Isom G. E. (1995) NMDA receptor activation produces concurrent generation of nitric oxide and reactive oxygen species: implications for cell death. *J. Neurochem.* **65,** 2016-2021.

208. Beal M. F. (1996) Therapeutic effects of nitric oxide synthase inhibition in neuronal injury., in *Neurodegeneration and Neuroprotection in Parkinson's Disease.* (Olanow C. W., Jenner P., and Youdim M., eds.), pp. 91-101. Academic Press, New York.

209. Marin P., Quignard J. F., Lafon-Cazal M., and Bockaert J. (1993) Non-classical glutamate receptors, blocked by both NMDA and non-NMDA antagonists, stimulate nitric oxide production in neurons. *Neuropharmacology* **32,** 29-36.

210. Gutteridge J. M. C. (1996) Hydroxyl radicals, iron, oxidative stress, and neurodegeneration. *Ann. N.Y. Acad. Sci.* **738,** 201-213.

211. Lan J. and Jiang D. H. (1997) Desferrioxamine and vitamin E protect against iron and MPTP-induced neurodegeneration in mice. *J. Neural Transm.* **104,** 469-481.

212. Zhang F. and Dryhurst G. (1995) Influence of glutathione on the oxidation chemistry of the catecholaminergic neurotransmitter dopamine. *J. Electroanal. Chem.* **398,** 117-128.

213. Kachur A. V., Koch C. J., and Biaglow J. E. (1999) Mechanism of copper-catalyzed autoxidation of cysteine. *Free Rad. Res.* **31,** 23-34.

214. Sagara J., Makino N., and Bannai S. (1996) Glutathione efflux from cultured astrocytes. *J. Neurochem.* **66,** 1876-1881.

215. Han J., Cheng F.-C., Zhaoliang Y., and Dryhurst G. (1999) Inhibitors of mitochondrial respiration, iron (II), and hydroxyl radical evoke release and extracellular hydrolysis of glutathione in rat striatum and substantia nigra: potential implications to Parkinson's disease. *J. Neurochem.* **73,** 1683-1695.

216. Hosli E. and Hosli L. (1997) Autoradiographic studies on the uptake of ^{3}H-dopamine by neurons and astrocytes in explant and primary culture of rat CNS: effects of uptake inhibitors. *Int. J. Dev. Neurosci.* **15,** 45-53.

217. Inazu M., Kuboto N., Zhang J., Kiuchi J., Oguchi K., and Matsumiya T. (1999) Pharmacological characterization of dopamine transport in cultured rat astrocytes. *Life Sci.* **64,** 2239-2245.

218. Semenoff D. and Kimelberg H. K. (1985) Autoradiography of high affinity uptake of catecholamines by primary astrocyte cultures. *Brain Res.* **348,** 125-136.

219. Kuhn D. M., Arthur R. E., Thomas D. M., and Elferink L. A. (1999) Tyrosine hydroxylase is inactivated by catechol-quinones and converted to a redox-cycling quinoprotein: possible relevance to Parkinson's disaese. *J. Neurochem.* **73,** 1309-1317.

220. Zhang F. and Drhurst G. (1994) Effects of L-cysteine on the oxidation chemistry of dopamine: new reaction pathways of potential relevance to idiopathic Parkinson's disease. *J. Med. Chem.* **37,** 1084-1098.

221. Shen X. M. and Dryhurst G. (1996) Further insights into the influence of L-cysteine on the oxidation chemistry of dopamine: reaction pathways of potential relevance to Parkinson's disease. *Chem. Res. Toxicol.* **9,** 751-763.

222. Shen X. M. and Dryhurst G. (1998) Iron- and manganese-catalyzed autoxidation of dopamine in the presence of L-cysteine: possible insights into iron- and manganese-mediated dopaminergic neurotoxicity. *Chem. Res. Toxicol.* **11,** 824-837.

223. Shen X. M., Zhang F., and Dryhurst G. (1997) Oxidation of dopamine in the presence of cysteine: characterization of new toxic products. *Chem. Res. Toxicol.* **10,** 147-155.

224. Li H. and Dryhurst G. (1997) Irreversible inhibition of mitochondrial complex I by 7-(2-aminoethyl)-3,4-dihydro-5-hydroxy-2*H*-1,4-benzothiazine-3-carboxylic acid (DHBT-1): a putative nigral endotoxin of relevance to Parkinson's disease. *J. Neurochem.* **69,** 1530-1541.

225. Li H., Shen X. M., and Dryhurst G. (1998) Brain mitochondria catalyze the oxidation of 7-(2-aminoethyl)-3,4-dihydro-5-hydroxy-2*H*-1,4-benzothiazine-3-carboxylic acid to intermediates that irreversibly inhibit complex I and scavenge glutathione: potential relevance to the pathogenesis of Parkinson's disease. *J. Neurochem.* **71,** 2049-2062.

226. Shen X. M., Li H., and Dryhurst G. (2000) Oxidative metabolites of 5-*S*-cysteinyldopamine inhibit the α-ketoglutarate dehydrogenase complex: relevance to the pathogenesis of Parkinson's disease. *J. Neural Transm.* **107,** 959-978.

227. Santiago M., Machado A., and Cano J. (2001) Validity of a quantitative technique to study striatal dopaminergic neurodegeneration by in vivo microdialysis. *J. Neurosci. Meth.* **108,** 181-187.

228. Berman S. B. and Hastings T. G. (1999) Dopamine oxidation alters mitochondrial respiration and induces permeabilty transition in brain mitochondria: implications for Parkinson's disease. *J. Neurochem.* **73,** 1127-1137.

229. Christian G. D. and Purdy W. C. (1962) The residual current in orthophosphate medium. *J. Electroanal. Chem. Interfacial Electrochem.* **3,** 363-367.

230. Paxinos G. and Watson C. (1986) *The Rat Brain in Stereotaxic Coordinates.*, Academic Press, New York.

231. Santiago M., Granero L., Machado A., and Cano J. (1995) Complex I inhibitor effect on the nigral and striatal release of dopamine in the presence and absence of nomifensine. *Eur. J. Pharmacol.* **280,** 251-256.

232. Shen X. M., Xia B., Wrona M. Z., and Dryhurst G. (1996) Synthesis, redox properties, in vivo formation and neurobehavioral effects of *N*-acetylcysteinyl conjugates of dopamine: possible metabolites of relevance to Parkinson's disease. *Chem. Res. Toxicol.* **9,** 1117-1126.

233. Bergquist J. and Silberring J. (1998) Identification of catecholamines in the immune system by electrospray ionization mass spectrometry. *Rapid Commun. Mass Spectrom.* **12,** 683-688.

234. Kerwin J. L. (1996) Negative ion electrospray mass spectrometry of polyphenols, catecholamines and their oxidation products. *J. Mass Spectrom.* **31,** 1429-1439.

235. Hammermeister D. E., Serrano J., Schmieder P., and Kuchl D. (2000) Characterization of dansylated glutathione disulfide, cysteine and cystine by narrow bore chromatograph/electrospray ionization mass spectrometry. *Rapid Commun. Mass Spectrom.* **14,** 503-508.

236. Boismenu D., Mamer O., Ste-Marie L., Vachon L., and Montgomery J. (1996) *In vivo* hydroxylation of the neurotoxin, 1-methyl-4-phenylpyridinium, and the effects of monoamine oxidase inhibitors: electrospray-MS analysis of intrastriatal microdialysates. *J. Mass Spectrom.* **31,** 1101-1108.

237. Smyth W. F. (1999) The use of electrospray mass spectrometry in the detection and determination of molecules of biological significance. *Trends Anal. Chem.* **18,** 335-346.

238. Chen S., Li Q., Carvey P. M., and Li K. (1999) Analysis of 9-fluorenylmethyloxycarbonyl derivatives of catecholanmines by high performance liquid chromatography, liquid chromatography/mass spectrometry and tandem mass spectrometry. *Rapid Commun. Mass Spectrom.* **13,** 1869-1877.

239. Obata T. and Chiueh C. C. (1992) In vivo trapping of hydroxyl free radicals in the striatum utilizing intracranial microdialysis perfusion of salicylate: effects of MPTP, $MPDP^+$, and MPP^+. *J. Neural Transm.* **89,** 139-145.

240. Smith T. S., Swerdlow R. H., Parker W. D., and Bennett J. P. (1994) Reduction of MPP^+-induced hydroxyl radical formation and nigrostriatal MPTP toxicity by nitric oxide synthase. *Neuroreport* **5,** 2598-2600.

241. Rose S., Hindmarsh J. G., and Jenner P. (1999) Neuronal nitric oxide synthase inhibition reduces MPP^+-evoked hydroxyl radical formation but not dopamine efflux in rat striatum. *J. Neural Transm.* **106,** 477-486.

242. Youngster S. K., McKeown K. A., Jin Y. Z., Ramsay R. R., Heikkila R. E., and Singer T. P. (1989) Oxidation of analogs of 1-methyl-4-phenyl-1,2,3,6-tetrahydropyridine by monoamine oxidases A and B and the inhibition of monoamine oxidases by the oxidation products. *J. Neurochem.* **53,** 1837-1842.

243. Ramsay R. R., Krueger M. J., Youngster S. K., Gluck M. R., Casida J. E., and Singer T. P. (1991) Interaction of 1-methyl-4-phenylpyridinium (MPP^+) and its analogs with the rotenone/piericidin binding site of NADH dehydrogenase. *J. Neurochem.* **56,** 1184-1190.

244. Pérez-Otaño I., Herrero M. T., Oset C., de Ceballos M. L., Luquin M. L., Obeso J. A., and Del R'o J. (1991) Extensive loss of brain dopamine and serotonin induced by chronic administration of MPTP in the marmoset. *Brain Res.* **567,** 127-132.

245. Foster S. B., Wrona M. Z., Han J., and Dryhurst G. (2003) The parkinsonian neurotoxin 1-methyl-4-phenylpyridinium (MPP^+) mediates release of L-3,4-dihydroxyphenylalanine (L-DOPA) and inhibition of L-DOPA decarboxylase in the rat striatum: a microdialysis study. *Chem. Res. Toxicol.* **16,** 1372-1384.

246. Hadjiconstantinou M., Wemlinger T. A., Sylvia C. P., Hubble J. P., and Neff N. H. (1993) Aromatic L-amino acid decarboxylase activity of mouse striatum is modulated via dopamine receptors. *J. Neurochem.* **60,** 2175-2180.

247. Halliwell B., Kaur H., and Ingelman-Sundberg M. (1991) Hydroxylation of salicylate as an assay for hydroxyl radicals: A cautionary note. *Free Rad. Biol. Med.* **10,** 439-441.

248. Zimmer L. K. E., Guilloteau D., Garreau L., Besnard J. C., and Chalon S. (2000) Microdialysis as a tool for in vivo study of dopamine transporter function in rat brains. *J. Neurosci. Meth.* **103,** 137-144.

249. Ozaki N., Nakahara D., Mogi M., Harada M., Kiuchi K., Kaneda N., Miura Y., Kasahara Y., and Nagatsu T. (1988) Inactivation of tyrosine hydroxylase in rat striatum by 1-methyl-4-phenylpyridinium (MPP^+). *Neurosci. Lett.* **85,** 228-232.

250. Yee R. E., Huang S. C., Stout D. B., Irwin I., Shoghi-Jadid K., Togaski D. M., DeLanney L. E., Langston J. W., Satyamurthy N., Farahani K. F., Phelps M. E., and Barrio J. R. (2000) Nigrostriatal reduction of aromatic L-amino acid decarboxylase activity in MPTP-treated squirrel monkeys: in vivo and in vitro investigations. *J. Neurochem.* **74,** 1147-1157.

251. Naoi M., Takahashi T., Ichinose H., and Nagatsu T. (1988) Inhibition of aromatic L-amino acid decarboxylase in clonal pheochromocytoma PC12h cells by N-methyl-4-phenylpyridinium ion (MPP^+). *Biochem. Biophys. Res. Commun.* **152,** 15-21.

252. Siow Y. L. and Dakshinamurti K. (1986) Effect of 1-methyl-4-phenyl-1,2,3,6-tetrahydropyridine and 1-methyl-4-phenylpyridinium on aromatic L-amino acid decarboxylase in rat brain. *Biochem. Pharmacol.* **35,** 2640-2641.

253. Burkhard P., Dominici P., Borri-Voltattorni C., Jansonius J. N., and Malashkevich V. N. (2001) Structural insight into Parkinson's disease treatment from drug-induced DOPA decarboxylase. *Nat. Struct. Biol.* **8,** 963-967.

254. Siow Y. L. and Dakshinamurti K. (1990) Neuronal dopa decarboxylase. *Ann. N.Y. Acad. Sci.* **585,** 173-188.

255. Neff N. H. and Hadjiconstantinou M. (1995) Aromatic L-amino acid decarboxylase modulation and Parkinson's disease. *Prog. Brain Res.* **106,** 91-97.

256. Kuwabara H., Cumming P., Yasuhara Y., Léger G. C., Guttman M., Diksic M., Evans A. C., and Gjedde A. (1995) Regional striatal DOPA transport and decarboxylase activity in Parkinson's disease. *J. Nucl. Med.* **36,** 1226-1231.

257. Pennathur S., Jackson-Lewis V., Przedborski S., and Heinecke J. W. (1999) Mass spectrometric quantification of 3-nitrotyrosine, *ortho*-tyrosine, and *o,o'*-dityrosine in brain tissue of 1-methyl-4-phenyl-1,2,3,6-tetrahydropyridine-treated mice, a model of oxidative stress in Parkinson's disease. *J. Biol. Chem.* **274,** 34621-34628.

258. Blanchard-Fillion B., Souza J. M., Friel T., Jiang G. C. T., Vrana K., Sharov V., Barrón L., Schöneich C., Quijano C., Alvarez B., Radi R., Przedborski S., Fernando G. S., Horitz J., and Ischiropoulos H. (2001) Nitration and inactivation of tyrosine hydroxylase by peroxynitrite. *J. Biol. Chem.* **276,** 46017-46023.

259. Tanaka T., Horio Y., Taketoshi M., Imamura I., Ando-Yamamoto M., Kangawa K., Matsuo H., Kurodo M., and Wada H. (1989) Molecular cloning and sequencing of a cDNA of rat dopa decarboxylase: partial amino acid homologies with other enzymes synthesizing catecholamines. *Proc. Natl. Acad. Sci. U.S.A.* **86,** 8142-8146.

260. Ishii S., Mizuguchi H., Nishino J., Hayashi H., and Kagamiyama H. (1996) Functionally important residues of aromatic L-amino acid decarboxylase probed by sequence alignment and site-directed mutagenesis. *J. Biochem. (Tokyo)* **120,** 369-376.

261. Kuhn D. M. and Arthur R. (1998) Dopamine inactivates tryptophan hydroxylase and forms a redox-cycling quinoprotein: possible endogenous toxin to serotonin neurons. *J. Neurosci.* **18,** 7111-7117.

262. Tolosa E., Marti M. J., Valldeoriola F., and Molinuevo J. L. (1998) History of levodopa and dopamine agonists in Parkinson's disease treatment. *Neurology* **50,** S2-S10.

263. Birkmayer W. and Hornykiewicz O. (1961) Der L-3,4-dihydroxyphenylalanin (=DOPA) effekt bei der Pakinson-akinese. *Wein. Klin. Wochenschr.* **73,** 787-788.

264. Cotzias G. C., Van Woert M. H., and Schiffer L. M. (1967) Aromatic amino acids and modification of parkinsonism. *N. Engl. J. Med.* **276,** 374-379.

265. Tolosa E. (1993) Levodopa arrives in New York: the work of George Cotzias., in *Twenty Years of Madopar: New Avenues.* (Poewe W. and Lees A. J., eds.), pp. 29-42. Editiones Roche, Basel.

266. Cotzias G. C., Papavasiliou P. S., and Gellene R. (1969) Modification of parkinsonism: chronic treatment with L-dopa. *N. Engl. J. Med.* **280,** 337-345.

267. Basma R. B., Morris E. J., Niklas W. J., and Geller M. H. (1995) L-DOPA cytotoxicity to PC12 cells in culture is via its autoxidation. *J. Neurochem.* **64,** 825-832.

268. Opacka-Juffry J. and Brooks D. J. (1995) L-Dihydroxyphenylalanine and its decarboxylase: new ideas on their neuroregulatory roles. *Mov. Disord.* **10,** 241-249.

269. Hornykiewicz O. (2002) L-DOPA: from a biologically inactive amino acid to a successful therapeutic agent. *Amino Acids* **23,** 65-70.

270. Goshima Y., Kubo T., and Misu Y. (1988) Transmitter-like release of endogenous 3,4-dihydroxyphenylalanine from rat striatal slices. *J. Neurochem.* **50,** 1725-1730.

271. Tison F., Mons N., Rouet-Karama S., Geffard M., and Henry P. (1989) Endogenous L-DOPA in the rat dorsal vagal complex; an immunocytochemical study by light and electron microscopy. *Brain Res.* **497,** 260-270.

272. Sugaya Y., Sasaki Y., Goshima Y., Kitahama K., Kusakabe T., Miyamae T., Kato T., and Misu Y. (2001) Autoradiographic studies using L-[14C]DOPA and L-DOPA reveal regional Na^+-dependent uptake of the neurotransmitter candidate L-DOPA in the CNS. *Neuroscience* **104,** 1-14.

273. Olney J. W., Zorumski C. F., Stewart G. R., Price M. T., Wang. G., and Labruyere J. (1990) Excitotoxicity of L-DOPA and 6-OH-DOPA: implications for Parkinson's and Huntington's disease. *Exp. Neurol.* **108,** 269-272.

274. Goshima Y., Ohno K., Nakamura S., Miyamae T., Misu Y., and Akaike A. (1993) L-DOPA induces Ca^{2+}-dependent and tetradotoxin-sensitive release of endogenous glutamate from rat striatal slices. *Brain Res.* **617,** 167-170.

275. Furukawa N., Arai N., Goshima Y., Miyamae T., Ohshima E., Suziki F., Fujita K., and Misu Y. (2001) Endogenously released DOPA is a causal factor for glutamate release and resultant delayed neuronal cell death by transient ischemia in rat striata. *J. Neurochem.* **76,** 815-824.

276. Ishida Y., Hashiguchi H., Todaka K., Ishizuka Y., and Mitsuyama Y. (2000) Repeated administration of high dose levodopa enhances hydroxyl radical production in the rat striatum denervated with 6-hydroxydopamine. *Neurosci. Lett.* **290,** 33-36.

277. Smith T. S., Parker Jr. W. D., and Bennett Jr. J. P. (1994) L-DOPA increases nigral production of hydroxyl radicals *in vivo*: potential L-DOPA toxicity. *Neuroreport* **5,** 1009-1011.

278. Przedborski S., Jackson-Lewis V., Muthane U., Jiang H., Ferreira M., Naini A. B., and Fahn S. (1993) Chronic levodopa administration alters cerebral mitochondrial respiratory chain activity. *Ann. Neurol.* **34,** 715-723.

279. Schapira A. H. V., Cooper J., Dexter D., Clark J. B., Jenner P., and Marsden C. D. (1990) Mitochondrial complex I deficiency in Parkinson's disease. *J. Neurochem.* **54,** 823-827.

280. Schapira A. H. V., Mann V. M., Cooper J. M., Dexter D., Daniel S. E., Jenner P., Clark J. B., and Marsden C. D. (1990) Anatomic and disease specificity of NADH-CoQ_1 reductase (complex I) deficiency in Parkinson's disease. *J. Neurochem.* **55,** 2142-2145.

281. Janetsky B., Hauck S., Youdim M. B., Riederer P., Jellinger K., Pantucek F., Zochling R., Boissl K. W., and Reichmann H. (1994) Unaltered aconitase activity, but decreased complex I activity in substantia nigra pars compacta of patients with Parkinson's disease. *Neurosci. Lett.* **169,** 126-128.

282. Cheng N. N., Maeda T., Kume T., Kaneko S., Kochiyama H., Akaike A., Goshima Y., and Misu Y. (1996) Differential neurotoxicity induced by L-DOPA and dopamine in cultured striatal neurons. *Brain Res.* **743,** 278-283.

283. Ziv I., Zilkha-Falb R., Offen D., Shirvan A., Barzilai A., and Melamed E. (1997) Levodopa induces apoptosis in cultured neuronal cells: a possible accelerator of nigrostriatal degeneration in Parkinson's disease. *Mov. Disord.* **12,** 17-23.

284. Hefti F., Melamed E., Bhawan J., and Wurtman R. J. (1981) Long-term administration of levodopa does not damage dopaminergic neurons in the mouse. *Neurology* **31,** 1194-1195.

285. Reches A. and Fahn S. (1982) Chronic dopa feeding of mice. *Neurology* **32,** 684-685.

286. Rajput A. H., Fenton M. E., Birdi S., and Macaulay R. (1997) Is levodopa toxic to human substantia nigra? *Mov. Disord.* **12,** 634-638.

287. Rajput A. H., Fenton M. E., and Dhand A. (1996) Is levodopa toxic to nondegenerating substantia nigra cells? Clinical evidence. *Neurology* **46,** A371-A373.

288. Blunt S. B., Jenner P., and Marsden C. D. (1993) Suppressive effect of L-DOPA on dopamine cells remaining in the ventral tegmental area of rats previously exposed to the neurotoxin 6-hydroxydopamine. *Mov. Disord.* **8,** 129-133.

289. Romano C. J. (2003) Levodopa and Parkinson's disease progression-contradictory results from the ELLDOPA study. *Neurology Reviews.com* **11**. Accessed 11/15/2003. http://www.neurologyreviews.com/jun03/jun03-ELLDOPA.html.

290. Fahn S. (1999) Parkinson's disease, the effect of Levodopa, and the ELLDOPA trial. *Arch. Neurol.* **56,** 529-535.

291. Huether G., Zhou D., and Rüther E. (1997) Causes and consequences of the loss of serotonergic presynapses elicited by the consumption of 3,4-methylenedioxymethamphetamine. *J. Neural Transm.* **104,** 771-794.

292. Colado M. I., O'Shea E., Granados R., Esteban B., and Martin A. B. (1999) Studies on the role of dopamine in the degeneration of 5-HT nerve endings in the brain of Dark Agouti rats following 3,4-methylenedioxymethamphetamine (MDMA or 'ecstasy') administration. *Br. J. Pharmacol.* **126,** 911-924.

293. Davidson C., Gow A. J., Lee T. H., and Ellinwood E. H. (2001) Methamphetamine neurotoxicity: necrotic and apoptotic mechanisms and relevance to human abuse and treatment. *Brain Res. Brain Res. Rev.* **36,** 1-22.

294. Bowyer J. F. and Holson R. R. (1995) Methamphetamine and amphetamine neurotoxicity, in *Handbook of Neurotoxicology* (Chang L. W. and Dryer R. S., eds.), pp. 845-870. Marcel Dekker, New York.

295. Green A. R., Cross A. J., and Goodwin G. M. (1995) Review of the pharmacology and clinical pharmacology of 3,4-methylenedioxymethamphetamine (MDMA or "Ecstasy"). *Psychopharmacology* **119,** 247-260.

296. Lyles J. and Cadet J. T. (2003) Methylenedioxymethamphetamine (MDMA, Ecstasy) neurotoxicity: cellular and molecular mechanisms. *Brain Res. Brain Res. Rev.* **42,** 155-168.

297. Aubin N., Curet O., Deffois A., and Carter C. (1998) Aspirin and salicylate protect against MPTP-induced dopamine depletion in mice. *J. Neurochem.* **71,** 1635-1642.

298. Cadet J. L., Sheng P., Ali S., Rothman R., Carlson E., and Epstein C. (1994) Attenuation of methamphetamine-induced neurotoxicity in copper/zinc superoxide dismutase transgenic mice. *J. Neurochem.* **62,** 380-383.

299. Ali S. F. and Itzhak Y. (1998) Effects of 7-nitroindazole, an nNOS inhibitor, on methamphetamine-induced dopaminergic and serotonergic neurotoxicity in mice. *Ann. N. Y. Acad. Sci.* **844,** 122-130.

300. Shankaran M., Yamamoto B. K., and Gudelsky G. A. (1999) Involvement of the serotonin transporter in the formation of hydroxyl radicals induced by 3,4-methylenedioxymethamphetamine. *Eur. J. Pharmacol.* **385,** 103-110.

301. Przedborski S. and Jackson-Lewis V. (1998) Experimental developments in movement disorders: update on proposed free radical mechanisms. *Curr. Opin. Neurol.* **11,** 335-339.

302. Kemp, P. Neurotoxicity of Methamphetamine. Invited lecturer. Neurotoxicology (PHSC 6453) Graduate Course at OUHSC 2000.

303. Teter C. J. and Guthrie S. K. (2001) A comprehensive review of MDMA and GHB: two common club drugs. *Pharmacotherapy* **21,** 1486-1513.

304. Gartside S. E., McQuade R., and Sharp T. (1996) Effects of repeated administration of 3,4-methylenedioxymethamphetamine on 5-hydroxytryptamine neuronal activity and release in the rat brain *in vivo. J. Pharmacol. Exp. Ther.* **279,** 277-283.

305. Ricaurte G. A., Bryan G., Strauss L., Seiden L., and Schuster C. (1985) Hallucinogenic amphetamin selectively destroys brain serotonin terminals. *Science* **229,** 986-988.

306. Koch S. and Galloway M. P. (1997) MDMA induced dopamine release in vivo: role of endogenous serotonin. *J. Neural Transm.* **104,** 135-146.

307. Ricaurte G. A., Yuan J., and McCann U. D. (2000) (±) 3,4-Methylenedioxymethamphetamine ('ecstasy')-induced serotonin neurotoxicity: studies in animals. *Neuropsychobiology* **42,** 5-10.

308. O'Hearn E., Battaglia G., DeSouza B., Kuhar M. J., and Molliver M. E. (1988) Methylenedioxyamphetamine (MDA) and 3,4-methylenedioxymethamphetamine (MDMA) cause selective ablation of serotonergic axon terminals in forebrain: immunocytochemical evidence for neurotoxicity. *J. Neurosci.* **8,** 2788-2803.

309. Battaglia G. S., Yeh S. Y., O' Hearn E., Molliver M. C., Kuhar M. J., and DeSouza E. B. (1987) 3,4-methylenedioxymethamphetamine and 3,4-methylenedioxyamphetamine destroy serotonin terminals in rat brain: quantitation of neurodegeneration by measurement of [^{3}H]-paroxetine-labeled serotonin uptake sites. *J. Pharmacol. Exp. Ther.* **242,** 911-916.

310. Hansen J. P., Riddle E. L., Sandoval V., Brown J., Gibb J. W., Hanson G. R., and Fleckenstein A. E. (2002) Methylenedioxymethamphetamine decreases plasmalemmal and vesicular dopamine transport: mechanisms and implications for neurotoxicity. *J. Pharmacol. Exp. Ther.* **300,** 1093-1100.

311. Ricaurte G. A. (1989) Studies on MDMA-induced neurotoxicity in nonhuman primates: a basis for evaluating long-term effects in humans. *NIDA Res. Monogr.* **94,** 306-322.

312. Gordon C. J., Watkinson W. P., O'Callaghan J. P., and Miller D. B. (1991) Effects of 3,4-methylenedioxymethamphetamine on autonomic thermoregulatory responses of the rat. *Pharmacol. Biochem. Behav.* **38,** 339-344.

313. Cadet J. L., Thiriet N., and Jayanthi S. (2001) Involvement of free radicals in MDMA-induced neurotoxicity in mice. *Ann. Med. Inter.* **152,** 1857-1859.

314. Camarero J., Sanchez V., O'Shea E., Green A. R., and Colado M. I. (2002) Studies, using *in vivo* microdialysis, on the effect of the dopamine uptake inhibitor GBR 12909 on 3,4-methylenedioxymethamphetamine ('ecstasy')-induced dopamine release and free radical formation in the mouse striatum. *J. Neurochem.* **81,** 961-972.

315. Hensley K., Williamson K. S., and Floyd R. A. (2000) Measurement of 3-nitrotyrosine and 5-nitro-gamma-tocopherol by high-performance liquid chromatography with electrochemical detection. *Free Radic. Biol. Med.* **28,** 520-528.

316. Hensley K., Maidt M. L., Pye Q. N., Stewart C. A., Wack M., Tabatabaie T., and Floyd R. A. (1997) Quantitation of protein-bound 3-nitrotyrosine and 3,4-dihydroxyphenylalanine by high-performance liquid chromatography with electrochemical detection. *Anal. Biochem.* **251,** 187-195.

317. Cadet J. L. and Brannock C. (1998) Free radicals and the pathobiology of brain dopamine systems. *Neurochem. Int.* **32,** 117-131.

318. Bhardwaj A., Northington F. J., Ichord R. N., Hanley D. F., Traystman R. J., and Koehler R. C. (1997) Characterization of ionotropic glutamate receptor-mediated nitric oxide production in vivo in rats. *Stroke* **28**.

319. Ferger B., Themann C., Rose S., Halliwell B., and Jenner P. (2001) 6-Hydroxydopamine increases the hydroxylation and nitration of phenylalanine *in vivo*: implication of peroxynitrite formation. *J. Neurochem* **78,** 509-514.

320. Zhang Y.-Y. and Loscalzo J. (1996) Nitrosation of Proteins, in *Nitric Oxide Synthase: Characterization and Functional Analysis* (Maines M. D., ed.), pp. 41-46. Academic Press, San Diego.

321. Williams D. L. H. (1999) The chemistry of S-nitrosothiols. *Acc. Chem. Res.* **32,** 869-876.

322. Sandoval V., Riddle E. V., Hanson G. R., and Fleckenstein A. E. (2003) Methylphenidate alters vesicular monoamine transport and prevents methamphetamine-induced dopaminergic deficits. *J. Pharmacol. Exp. Ther.* **304,** 1181-1187.

323. Ossowska K. (1994) The role of excitatory amino acids in experimental models of Parkinson's disease. *J. Neural Transm. Park. Dis. Dement. Sect.* **8,** 39-71.

324. Götz M. E., Künig G., Riederer P., and Youdim M. B. H. (1994) Oxidative stress: free radical production in neural degeneration. *Pharmacol. Ther.* **63,** 37-122.

325. Fornai F., Vaglini F., Maggio R., Bonuccelli U., and Corsini G. U. (1997) Species differences in the role of excitatory amino acids in experimental parkinsonism. *Neurosci. Biobehav. Rev.* **21,** 401-415.

326. Engelborghs S., Marescau B., and De Deyn P. P. (2003) Amino acids and biogenic amines in cerebrospinal fluid of patients with Parkinson's disease. *Neurochem. Res.* **28,** 1145-1150.

327. Matarredona E. P., Santiago M., Venero J. L., Cano J., and Machado A. (2001) Group II metabotropic glutamate receptor activation protects striatal dopaminergic nerve terminals against MPP^+-induced neurotoxicity along with brain-derived neurotrophic factor induction. *J. Neurochem.* **76,** 351-360.

328. Gołembiowska K., Konieczny J., Ossowska K., and Wolfarth S. (2002) The role of striatal metabotropic glutamate receptors in degeneration of dopamine neurons: review article. *Amino Acids* **23,** 199-205.

329. Marino M. J., Awad H., Poisik O., Wittmann M., and Conn P. J. (2002) Localization and physiological roles of metabotropic glutamate receptors in the direct and indirect pathways of the basal ganglia. *Amino Acids* **23,** 185-191.

330. Blandini F., Porter R. H. P., and Greenamyre J. T. (1996) Glutamate and Parkinson's Disease. *Mol. Neurobio.* **12,** 73-94.

331. Schmidt W. J. and Kretschmer B. D. (1997) Behavioural pharmacology of glutamate receptors in the basal gaglia. *Neurosci. Biobehav. Rev.* **21,** 381-392.

332. Molina J. A., Jiménez-Jiménez F. J., Gómez P., Vargas C., Navarro J. A., Ortí-Pareja M., Gasalla T., Benito-León J., Bermejo F., and Arenas J. (1997) Decreased cerebrospinal fluid levels of neutral and basic amino acids in patients with Parkinson's disease. *J. Neurol. Sci.* **150,** 123-127.

333. Dawson Jr. R., Pelleymounter M. A., Cullen M. J., Gollub M., and Liu S. (1999) An age-related decline in striatal taurine is correlated with a loss of dopaminergic markers. *Brain Res. Bull.* **48,** 319-324.

334. Sonsalla P. K., Nicklas W. J., and Heikkila R. E. (1989) Roles for excitatory amino acids in methamphetamine-induced nigrostriatal dopaminergic toxicity. *Science* **243,** 398-400.

335. Johnson M., Hanson G. R., and Gibb J. W. (1989) Effect of MK-801 on the decrease in tryptophan hydroxylase induced methamphetamine and its methylenedioxy analog. *Eur. J. Pharmacol.* **165,** 315-318.

336. Starr M. S., Starr B. S., and Kaur S. (1997) Stimulation of basal and L-DOPA-induced motor activity by glutamate antagonists in animal models of Parkinson's disease. *Neurosci. Biobehav. Rev.* **21,** 437-446.

337. Sonsalla P. K., Zeevalk G. D., Manzino L., Giovanni A., and Nicklas W. J. (1992) MK-801 fails to protect against the dopaminergic neuropathology produced by systemic 1-methyl-4-phenyl-1,2,3,6-tetrahydropyridine in mice or intranigral 1-methyl-4-phenylpyridinium in rats. *J. Neurochem.* **58,** 1979-1982.

338. Doble A. (1995) Excitatory amino acid receptors and neurodegeneration. *Therapie* **50,** 319-337.

339. Greene J. G. and Greenamyre T. (1995) Exacerbation of NMDA, AMPA, and L-glutamate excitotoxicity by the succinate dehydrogenase inhibitor malonate. *J. Neurochem.* **64,** 2332-2338.

340. Cebers G., Cebere A., and Liljequist S. (1998) Metabolic inhibition potentiates AMPA-induced Ca^{2+} fluxes and neurotoxicity in rat cerebellar granule cells. *Brain Res.* **779,** 194-204.

341. Leist M., Volbracht C., Fava E., and Nicotera P. (1998) 1-Methyl-4-phenylpyridinium induces autocrine excitotoxicity, protease activation, and neuronal apoptosis. *Mol. Pharmacol.* **54,** 789-801.

342. Kanthasamy A. G., Kanthasamy A., Matsumoto R. R., Vu T. Q., and Truong D. D. (1997) Neuroprotective effects of the strychnine-insensitive glycine site NMDA antagonist (R)-HA-966 in an experimental model of Parkinson's disease. *Brain Res.* **759,** 1-8.

343. Anderson C. M. and Swanson R. A. (2000) Astrocyte glutamate transport: review of properties, regulation, and physiological functions. *Glia* **32,** 1-14.

344. Ambrosia S., Espino A., Cutillas B., and Bartrons R. (1996) MPP^+ toxicity in rat striatal slices: relationship between nonselective effects and free radical production. *Neurochem. Res.* **21,** 73-78.

345. Araque A., Carmignoto G., and Haydon P. G. (2001) Dynamic signaling between astrocytes and neurons. *Annu. Rev. Physiol.* **63,** 795-813.

346. Szatkowski M., Barbour B., and Attwell D. (1990) Non-vesicular release of glutamate from glial cells by reversed electrogenic glutamate uptake. *Nature* **348,** 443-446.

347. Hazell A. S., Itzhak Y., Liu H., and Norenburg M. D. (1997) 1-methyl-4-phenyl-1,2,3,6-tetrahydropyridine (MPTP) decreases glutamate uptake in cultured astrocytes. *J. Neurochem.* **68,** 2216-2219.

348. Kimelburg H. K., Goderie S. K., Higman S., Pang S., and Waniewski R. A. (1990) Swelling induced release of glutamate, aspartate, and taurine from astrocyte cultures. *J. Neurosci.* **10,** 1583-1591.

349. Girod R., Povov S., Alder J., Zheng J. Q., Lohof A., and Poo M. M. (1995) Spontaneous quantal transmitter secretion from myocytes and fibroblasts: comparison with neuronal secretion. *J. Neurosci.* **15,** 2826-2838.

350. Morimoto T., Popov S., and Buckley K. M. (1995) Calcium-dependent transmitter secretion from fibroblasts: modulation by synaptotagmin. *Neuron* **15,** 689-696.

351. Maienschein V., Marxen M., Volknandt W., and Zimmermann H. (1999) A plethora of presynaptic proteins associated with ATP-storing organelles in cultured astrocytes. *Glia* **26,** 233-244.

352. Jeftinija S. D., Jeftinija K. V., and Stefanovic G. (1997) Cultured astrocytes express proteins involved in vesicular glutamate release. *Brain Res.* **750,** 41-47.

353. Del Arco A., Segovia G., Fuxe K., and Mora F. (2003) Changes in dialysate concentrations of glutamate and GABA in the brain: an index of volume transmission mediated actions? *J. Neurochem.* **85,** 23-33.

354. Della Corte L., Clarke D. J., Bolam J. P., and Smith A. D. (1987) Uptake, localization and release of taurine in the rat basal ganglia. in *The Biology of Taurine.* (Huxtable R. J., Franconi F., and and Giotti A., eds.), pp. 285-294. Plenum, New York.

355. Dawson R., Tang E., Shih D., Hern H., Hu M., Baker D., and Eppler B. (1998) Taurine inhibition of iron-stimulated catecholamine oxidation., in *Taurine 3* (Lombardi J.B., Schaffer S., and Huxtable R.J., eds.), pp. 155-162. Plenum, New York.

356. Bianchi L., Bolam J. P., Galeffi F., Frosini M., Palmi M., Sgaragli G., and Della Corte L. (1996) In vivo release of taurine from rat neostriatum and substantia nigra. *Adv. Exp. Med. Biol.* **403,** 427-433.

357. Lakke J. P., Teelken A. W., van der Vloet H., and Wolthers B. G. (1987) Amino acid abnormalities in cerebrospinal fluid and blood serum of patients with Parkinson's disease, other heredodegenerative disorders and head injuries. *Adv. Neurol.* **45,** 243-247.

358. Hare T. A., Beasley B. L., Chambers R. A., Boehme D. H., and Vogel W. H. (1973) DOPA and amino acid levels in plasma and cerebrospinal fluid of patients with Parkinson's disease before and during treatment with L-DOPA. *Clin. Chim. Acta* **45.**

359. Goodnick P. J., Evans H. E., Dunner D. L., and Fieve R. R. (1980) Amino acid concentrations in cerebrospinal fluid: effects of aging, depression and probenecid. *Biol. Psychiatry* **15,** 557-563.

360. McGale E. H. F., Pye I. F., Stonier C., Hutchinson E. C., and Aber G. M. (1977) Studies of the interrelationship between cerebrospinal fluid and plasma amino acid concentrations in normal individuals. *J. Neurochem.* **29,** 291-297.

361. Tohgi H., Takahashi S., and Abe T. (1993) The effect of age on concentrations of monamines, amino acids, and their related substances in the cerebrospinal fluid. *J. Neural Transm. Park. Dis. Dement. Sect.* **5,** 215-226.

362. Ferraro T. N. and Hare T. A. (1985) Free and conjugated amino acids in human CSF: influence of sex and age. *Brain Res.* **338,** 53-60.

363. Attwell A., Barbour B., and Szatkowski M. (1993) Nonvesicular release of neurotransmitter. *Neuron* **11,** 401-407.

364. Snyder S. H. and Kim P. M. (2000) D-amino acids as putative neurotransmitters: focus on D-serine. *Neurochem. Res.* **25,** 553-560.

365. Magistretti P. and Pellerin L. (2000) The astrocyte-mediated coupling between synaptic activity and energy metabolism operates through volume transmission., in *Volume Transmission Revisited* (Agnati L. F., Fuxe K., Nicholson C., and Syková E., eds.), pp. 229-240. Elsevier Science BV, Amsterdam.

366. Santiago M., Machado A., and Cano J. (1994) Effect of L-arginine/nitric oxide pathway on MPP^+-induced cell injury in the striatum of rats. *Br. J. Pharmacol.* **111,** 837-842.

367. Rollema H., Kuhr W. G., Franeborg G., De Vries J., and Van Den Berg C. (1988) MPP^+-induced efflux of dopamine and lactate from rat striatum have similar time courses as shown by *in vivo* brain dialysis. *J. Pharmacol. Exp. Ther.* **245,** 858-863.

368. Booth R. G., Castagnoli N. Jr., and Rollema H. (1989) Intracerebral microdialysis studies of quinoline and isoquinoline derivatives related to MPTP/MPP^+. *J. Neurosci. Meth.* **100,** 306-312.

369. Rollema H., Skolnik M., D' Engelbronner J., Igarashi K., Usuki E., and Castagnoli N. Jr. (1994) MPP^+-like neurotoxicity of a pyridinium metabolite derived from haloperidol: in vivo microdialysis and in vitro mitochondrial studies. *J. Pharmacol. Exp. Ther.* **268,** 380-387.

370. Santiago M., Matarredona E. R., Granero L., Cano J., and Machado A. (1997) Neuroprotective effect of the iron chelator desferrioxamine against MPP^+ toxicity on striatal dopaminergic terminals. *J. Neurochem.* **68,** 732-738.

371. Heikkila R. E., Sieber B. A., Manzino L., and Sonsalla P. K. (1989) Some features of the nigrostriatal dopaminergic neurotoxin 1-methyl-4-phenyl-1,2,3,6-tetrahydropyridine (MPTP) in the mouse. *Mol. Chemic. Neuropathol.* **10,** 171-183.

372. Seniuk N. A., Tatton W. G., and Greenwood C. E. (1990) Dose-dependent destruction of the coeruleus-cortical and nigral-striatal projections by MPTP. *Brain Res.* **527,** 7-20.

373. Muthane U., Ramsay K. A., Jiang H., Jackson-Lewis V., Donaldson D., Fernando S., Ferreira M., and Przedborski S. (1994) Differences in nigral neuron number and sensitivity to 1-methyl-4-phenyl-1,2,3,6-tetrahydropyridine in C57/bl and CD-1-mice. *Exp. Neurol.* **126,** 195-204.

374. Jackson-Lewis V., Jakowec M., Burle R. E., and Przedborski S. (1995) Time course and morphology of dopaminergic neuronal death caused by the neurotoxin 1-methyl-4-phenyl-1,2,3,6-tetrahydropyridine. *Neurodegeneration* **4,** 257-269.

375. Chang L. W. (1992) Basic histopathological alterations in the central and peripheral nervous systems: classification, identification, approaches, and techniques., in *Neurotoxicology* (Abou-Donia M. B., ed.), pp. 223-252. CRC Press, Boca Raton.

376. Ter Horst G. J., Knigge M. F., and Van der Wal A. (1992) Neurochemical lesioning in the rat brain with iontophoretic injection of the 1-methyl-4-phenyl-pyridinium ion (MPP^+). *Neurosci. Lett.* **141,** 203-207.

377. Michael D. and Norenburg M. D. (1994) Astrocyte responses to CNS injury. *J. Neuropathol. Exp. Neurol.* **53,** 213-220.

378. Eddleston M. and Mucke L. (1993) Molecular profile of reactive astrocytes: implications for their role in neurologic disease. *Neuroscience* **54,** 15-36.

379. Müller H. W., Junghans U., and Keppler J. (1995) Astroglial neurotrophic and neurite-promoting factors. *Pharmacol. Ther.* **65,** 1-18.

380. Wilken G. P. and Knott C. (1999) Glia: a curtain raiser. *Adv. Neurol.* **80,** 3-7.

381. Gehrmann J., Matsumoto Y., and Kreutzberg G. W. (1995) Microglia: intrinsic immuneffector cell of the brain. *Brain Res. Rev.* **20,** 269-287.

382. Wu D. C., Ties K., Cohen O., Choi D. K., Vila M., Jackson-Lewis V., Teismann P., and Przedborski S. (2002) Glial cell response: a pathogenic factor in Parkinson's disease. *J. Neurovirol.* **8,** 551-558.

383. Czlonkowska A., Kohutnicka M., Kurkowska-Jastrzebska I., and Czlonkowski A. (1996) Microglia reaction in MPTP (1-methyl-4-phenyl-1,2,3,6-tetrahydropyridine) induced Parkinson's disease mice model. *Neurodegeneration* **5,** 137-143.

384. Kohutnicka M., Lewandowska E., Kurowska-Jastrzebska I., Czlonkowski A., and Czlonkowska A. (1998) Microglial and astrocytic involvement in a murine model of Parkinson's disease induced by 1-methyl-4-phenyl-1,2,3,6-tetrahydropyridine (MPTP). *Immunopharmacology* **39,** 167-180.

385. McGeer P. L., Itagaki S., Boyes B. E., and McGeer E. R. (1988) Reactive microglia are positive for HLA-DR in the substantia nigra of Parkinson's and Alzheimer's disease brains. *Neurology* **38,** 1285-1291.

386. Forno L. S., Delanney L. E., Irwin I., Di Monte D., and Langston J. W. (1992) Astrocytes and Parkinson's disease. *Prog. Brain Res.* **94,** 429-436.

387. Banati R. B., Daniel S. E., and Blunt S. B. (1998) Glial pathology but absence of apoptotic nigral neurons in long-standing Parkinson's disease. *Mov. Disord.* **13,** 221-227.

388. Mirza B., Hadberg H., Thomsen P., and Moos T. (2000) The absence of reactive astrocytosis is indicative of a unique inflammatory process in Parkinson's disease. *Neuroscience* **95,** 425-432.

389. Giasson B. I., Duda J. E., Murray I. V., Chen Q., Souza J. M., Hurtig H. I., Ischiropoulos H., Trojanowski J. Q., and Lee V. M. (2000) Oxidative damage linked to neurodegeneration by selective alpha-synuclein nitration in synucleinopathy lesions. *Science* **290,** 285-289.

390. Przedborski S., Chen Q., Vila M., Giasson B. I., Djaldatti R., Vukosavic S., Souza J. M., Jackson-Lewis V., Lee V. M., and Ischiropoulos H. (2001) Oxidative post-translational modifications of alpha-synuclein in the 1-methyl-4-phenyl-1,2,3,6-tetrahydropyridine (MPTP) mouse model of Parkinson's disease. *J. Neurochem.* **76,** 637-640.

391. Seibert K., Masferrer J., Zhang Y., Gregory S., Olson G., Hauser S., Leahy K., Perkins W., and Isakson P. (1995) Mediation of inflammation by cyclooxygenase-2. *Agents Actions Suppl.* **46,** 41-50.

392. O'Banion M. K. (1999) Cyclooxygenase-2: molecular biology, pharmacology, and neurobiology. *Crit. Rev. Neurobiol.* **13,** 45-82.

393. Knott C., Stern G., and Wilken G. P. (2000) Inflammatory regulators in Parkinson's disease: iNOS, lipocortin-1, and cyclooxygenase-1 and -2. *Mol. Cell. Neurosci.* **16,** 724-739.

394. Teismann P. and Ferger B. (2001) Inhibition of the cyclooxygenase isoenzymes COX-1 and COX-2 provide neuroprotection in the MPTP-mouse model of Parkinson's disease. *Synapse* **39,** 167-174.

395. Mogi M., Harada M., Riederer P., Narabayashi H., Fujita K., and Nagatsu T. (1994) Tumor necrosis factor-alpha (TNF-alpha) increases both in the brain and in the cerebrospinal fluid from parkinsonian patients. *Neurosci. Lett.* **165,** 208-210.

396. Mogi M., Harada M., Narabayashi H., Inagaki H., Minami M., and Nagatsu T. (1996) Interleukin (IL)-1beta, IL-2, IL-4, IL-6 and transforming growth factor-alpha levels are elevated in ventricular cerebrospinal fluid in juvenile parkinsonism and Parkinson's disease. *Neurosci. Lett.* **221,** 13-16.

397. Mogi M., Togari A., Kondo T., Mizuno Y., Komure O., Kuno S., Ichinose H., and Nagatsu T. (2000) Caspase activities and tumor necrosis factor receptor R1 (p55) level are elevated in the substantia nigra from parkinsonian brain. *J. Neural Transm.* **107,** 335-341.

398. Wick M. M., Byers L., and Frei E. (1977) L-DOPA: selective toxicity for melanoma cells in vitro. *Science* **197,** 468-469.

399. Mena M. A., Pardo B., Casarejos M. J., Fahn S., and de Yébenes J. G. (1992) Neurotoxicity of levodopa on catecholamine-rich neurons. *Mov. Disord.* 7, 23-31.

400. Walkinshaw G. and Waters C. M. (1995) Induction of apoptosis in catecholaminergic PC12 cells by L-DOPA: implications for the treatment of Parkinson's disease. *J. Clin. Invest.* **95,** 2458-2464.

401. Mena M. A., Pardo B., Paino C. L., and de Yébenes J. G. (1993) Levodopa toxicity in foetal rat midbrain neurones in culture: modulation by ascorbic acid. *Neuroreport* **4,** 438-440.

402. Pardo B., Mena M. A., Fahn S., and de Yébenes J. G. (1993) Ascorbic acid protects against levodopa-induced neurotoxicity on a catecholamine-rich human neuroblastoma cell line. *Mov. Disord.* **8,** 278-284.

403. Offen D., Ziv I., Sternin H., Melamed E., and Hochman A. (1996) Prevention of dopamine-induced cell death by thiol antioxidants: possible implications for treatment of Parkinson's disease. *Exp. Neurol.* **141,** 32-39.

404. Mytilineou C., Han S. K., and Cohen G. (1993) Toxic and protective effects of L-DOPA on mesencephalic cell cultures. *J. Neurochem.* **61,** 1470-1478.

405. Han S. K., Mytilineou C., and Cohen G. (1996) L-DOPA up-regulates glutathione and protects mesencephalic cultures against oxidative stress. *J. Neurochem.* **66,** 501-510.

406. Mena M. A., Davila V., and Sulzer D. (1997) Neurotrophic effects of L-DOPA in postnatal midbrain dopamine neuron/cortical astrocyte co-cultures. *J. Neurochem.* **69,** 1398-1408.